1991

The Stratigraphy And Sedimentology Of The Upper Cretaceous Cardium Formation In Northwestern Alberta And Adjacent British Columbia (volumes I And Ii)

Bruce Samuel Hart

THE STRATIGRAPHY AND SEDIMENTOLOGY OF THE UPPER CRETACEOUS CARDIUM FORMATION IN NORTHWESTERN ALBERTA AND ADJACENT BRITISH COLUMBIA

VOLUME I

by

Bruce S. Hart

Department of Geology

Submitted in partial fulfilment
of the requirements for the degree of
Doctor of Philosophy

Faculty of Graduate Studies
The University of Western Ontario
London, Ontario
August 1990

ISBN 0-315-64273-4

ABSTRACT

The Upper Cretaceous Cardium Formation developed along the western margin of the Western Interior Seaway. The cyclic sedimentation style represented in the formation (consisting of a hierarchial array of shallowing upward cycles capped by transgression surfaces) developed in response to regressions and transgressions occurring on differing temporal scales. Shoreline progradation was generally to the northeast. The two main packages probably developed in response to eustatic third order sea level falls in the mid-Turonian and lower Coniacian. Superimposed on those cycles were fourth order relative sea level fluctuations (each cycle of about 10^5 years duration) which were responsible for the development of individual allomembers in the Cardium Formation. Possible evidence for higher (fifth) order cyclicity is represented by few-meter thick sandier upward successions in offshore deposits, and punctuated shoreline progradation of the Kakwa Member.

The Kakwa Member represents the preserved shoreface portions of the lowest 3 progradational packages. It consists essentially of two stacked sandstone bodies, with the contact between the lower and upper portions being originally a near-horizontal (ravinement) surface developed during the E3 transgression. The sandstones above and below this surface can be distinguished on the basis of

sedimentary structures, grain size and diagenetic history.

Conglomerates are locally present in the Kakwa Member, generally representing shoreface or beach deposits. A well-exposed section near Bay Tree (Alberta) suggests that wave-reworked gravels from shorefaces dominated by longshore transport are likely to be clast-supported, horizontally stratified and generally massive in appearance. Comparison of this section with other conglomeratic sections in the formation suggests that (in agreement with previous workers) bed lenticularity increases and clast segregation decreases in sections as the influence of fluvial depositional processes becomes greater.

This study suggests that basement tectonic elements had a greater influence on the pattern of deposition and erosion during Cardium time than previously recognised, controlling the position of bevels on the E5 and E7 surfaces, and the position of the basinward edge of the Kakwa Member. There is some evidence that structural elements may also have been important elsewhere in the basin at this time.

ACKNOWLEDGEMENTS

I like reading the Acknowledgements of other peoples' theses. I always find that its fairly easy to spot the people the author *wants* to thank, and those that he/she *needs* to thank. In the present case, I'd like to thank everybody, but can't - without making the "Credits" of the *Star Wars* films look like a short list. So, if you think your name should be here but isn't, *Sorry but....*

First, I'd like to thank my Supervisor, Mentor and (especially) my Friend, Dr. A. Guy Plint for offering the project in the first place, then following up with (in no particular order) encouragement, friendship, generosity, good curries, advice, constructive criticism and *patience* (hey - I didn't even know what a *Vail Curve* was when I started this). I learned a lot, and had a lot of fun doing it. Thanks, I hope I haven't been a disappointment.

Mike Risk (who will never see this), Professor with the Geology Department at McMaster (my *alma mater*), suggested that I contact Guy in the first place - and my M.Sc. supervisor now that I think of it. Thanks to his tips, I'm still in geology, and have spent the last 6 years doing something *worthwhile* from every possible perspective.

I could never have completed this project without the support of "Industry People" in Calgary. Home Oil Co. Ltd. allowed me to use their facilities to copy the well logs used in this study. Sid Leggett, Senior Geologist at Home, went out of his way to provide me with base maps, computer print-outs, and various other forms of technical assistance. Above all, Sid reminded me how much fun it can be to fly a kite. I wish that I could have seen him more frequently.

Several companies, including Canadian Hunter Exploration Ltd., Texaco Canada Resources (R.I.P.), Esso Canada Resources Ltd. and Unocal (thanks to Mick Portigal for pointing out the Horseshoe Mountain outcrop site) paid for chopper time, and so got me to parts of the world most people don't know exist. The folks at Canadian Hunter were especially generous, and their man in Grande Prairie, Lorne Hunter, provided tips about access to several key locations. Speaking of helicopters, Brian Tozo, Phil Hocking (both with Highland Helicopters) and Mike Belamy flew the machines which got our crew to and from the remote outcrops. Their considerable abilities did not go unnoticed (Foothills weather being what it is...).

Dr. R.W. Arnott (that is to say, *Cowboy*), formerly of Texaco and now with Esso, provided accommodation, transport, nourishment, drink (hic), advice, a bathing suit, "thoughtful discussion" and various and sundry forms of encouragement and technical supplies. Who'd have thought, almost twenty (ouch!) years ago sitting around the Jimmy Thompson pool, that one day....... There may be a better friend to be had somewhere in this world, but I doubt it.

Darryl Reiter and Rick Vantfoort took great notes, acted as scale bars, pointed out all (well...most) of the mistakes I made measuring sections, endured my ill winds, attended to domestic chores and pretended to laugh at my bad jokes - all without complaining (well...). *Muchos gracias amigos*! Darryl showed me how to "chimney" up (or down) crevices, a great technique employed in the sections near Dawson Creek. Rick helped me to do some things on steep shaley slopes by making *me* be the responsible one (except when Guy was around...).

Fred Longstaffe generously provided facilities, advice and encouragement in the siderite study. He beat me 3 out of 5 games (in the 5th game, in overtime) in ping pong in the spring of 1988 - I still want a rematch. Paul Middlestead very patiently showed me what to do in the isotope extraction lab, and analysed the gasses with the Mass-Spec. *Merci bonhomme!*

Many grad students, undergrads, staff and faculty helped in a variety of ways, providing advice and encouragement, showing an interest, passing the puck. or just laughing and having a beer. Notable contributors to this last activity include Brett Norris and Barry Larson. Greg Browne taught me the joys of Aussie-bashing, and gave me a can of oil for my bike chain. I wish that I could have spent much more time with all of them. Photographic assistance was always cheerfully supplied by Ian Craig.

Finally, my thanks to the little girl who joined my family just over a year ago, and to the big girl who made that possible. It can't be easy to have a husband/daddy who's never there, or can never take the time off to do anything fun. Life hasn't been easy at times, but through it all they've made me understand what the truly important things in life are all about. To Mallorie Ann Hart and Aline Falardeau, with much love, I dedicate this work. Daddy will be able to take (most) weekends off now.

TABLE OF CONTENTS

LIST OF FIGURES

LIST OF TABLES

LIST OF APPENDICES

Il nous faut non seulement comprendre comment s'est faite une découverte, mais aussi pourquoi une découverte qui nous semble aujourd'hui familière ou simple ne s'est pas faite plus tôt. Cet effort nous prouve qu'en dépit de l'accroissement constant de nos connasissances, nous nous trouvons dans une situation semblable à celle de nos prédécesseurs, encore aveugles devant une multitude de phénomènes inconnus. Ce type de connaissance nous fait mieux ouvrir les yeux sur la nature pour la découvrir, il nous donne l'audace réfléchie qui chasse le conformisme.

Frédéric Joliot, 1946

CHAPTER 1

INTRODUCTION

1.1 Introduction

The Cardium Formation of western Canada is a major oil and gas producer, and as such it has received considerable attention, both from industry and academia. The formation has formed the object of stratigraphic studies in outcrop and subsurface (e.g. Harding 1955; Stott 1963, 1967; Krause and Nelson 1984; Duke 1985; Plint, Walker and Bergman 1986; Plint, Walker and Duke 1988), diagenetic studies (e.g. Machemer and Hutcheon 1988; Staley 1988), studies of the reservoir characteristics (Krause *et al.* 1987), ichnology (Pemberton and Frey 1984; Vossler and Pemberton 1988) and numerous other studies of the sedimentology of the formation (e.g. Beach 1955; Michaelis and Dixon 1969; Bergman and Walker 1987; Walker 1983; Plint 1988). Due to the number and diversity of these previous studies, a comprehensive survey of all published work on the Cardium is beyond the scope of the present dissertation.

In the early 1980's, Roger Walker and co-workers at McMaster University began a systematic dissection of the Cardium. Parallel to this, was the development of the sequence stratigraphy paradigm for understanding the depositional history of rock units. The marriage of the McMaster Cardium Group's work with sequence stratigraphic principles lead to the proposal of an event stratigraphy for the formation (Plint *et al.* 1986, 1987, 1988). The area north of Township 65 in Alberta has received little attention from that group, and it is that region which forms the object of the present study.

1.2 Cardium Stratigraphy

The first use of the word "Cardium" in a lithostratigraphic sense was by Dr. James Hector, geologist and medical doctor for the Palliser Expedition in the mid 1800's. He reported that marine beds of Cretaceous age exposed along the Bow River contained fossils of the genus Cardium (Whiteaves 1895). Later, Cairnes (1907) restricted the name "Cardium" to a succession of sandy units within the dominantly shaley Cretaceous section on the Bow river. Rutherford (1927) raised the Cardium to formational rank. About this time, Malloch (1911), working further to the north, applied the name "Bighorn" to a package of shales, sandstones and conglomerates in the Bighorn Basin west of Nordegg. The Bighorn and Cardium were subsequently shown to be correlative, and it was suggested that the name Cardium, having precedence, should be applied to all these strata (Harding 1955). Stott (1963) designated Malloch's (1911) section on Wapiabi Creek as the type section of the Cardium Formation.

Based on his work in the south and central Foothills, Stott (1963) divided the formation into 6 members. From bottom to top, these are the Ram, Moosehound, Kiska, Cardinal, Leyland and Sturrock members. Stott (1963, p.61) reported that the Cardium is "characterised by sandstone, but in many places contains a large percentage of shale". He noted that the entire Alberta Group (to which the Cardium belongs) can be divided into a sequence of nested cycles of different magnitudes. Each of the cycles was interpreted to represent an oscillatory movement of the palaeoshoreline position, with minor transgressions and regressions superimposed on more major, longer period shoreline movements.

Duke (1985) re-examined outcrops of the Cardium Formation in the south and central Foothills. He rejected Stott's (1963) outcrop nomenclature, noting that Stott's member division cut across cycle boundaries. Although Duke's (1985) member division was later abandoned, his work provided the basis for the most recent outcrop to subsurface correlation of the Cardium (Plint *et al.* 1988).

Despite the economic importance of the Cardium, the details of the subsurface stratigraphy have, until recently, remained obscure (at least in the public domain). The terms Cardium "A" and "B" Sands have been employed for stratigraphically separated units in individual fields, although correlation between fields was not necessarily established (Walker 1983). A well log marker at the top of the "Cardium Zone" has been used to define the top of the formation in subsurface (e.g. Krause and Nelson 1984).

Walker (1983) investigated the sedimentology and stratigraphy of the Cardium in the Garrington - Caroline area. His Raven River and Burnstick members were later incorporated into the more general stratigraphic division of Plint *et al.* (1986). These authors proposed an "event stratigraphy" for the Cardium, based on the recognition of 6 major coarsening or sandier-upward sequences. Each of these was capped by an erosion surface ("E" surface), and some of these were overlain by a pebble veneer which, when traced laterally, could "swell" into major conglomerate bodies up to 20 m thick. Overlying the pebble veneer or conglomerate was a transgression ("T") surface which separated the conglomerate from the overlying sequence. In places the erosion and transgression surfaces are in contact, producing an E/T surface. This concept was first proposed by Michaelis (1957) for the Cardium, but received little acceptance.

In the Plint *et al.* (1986) system, the members are, in the majority, defined by their relation to the erosion and transgression surfaces. Sandier-upwards sequences bounded by E/T surfaces were given member status, as were the thick conglomerates and correlative pebble veneers. Later, Plint *et al.* (1988) correlated the subsurface work with the outcrop data of Duke (1985) and proposed that the subsurface names be extended to outcrop.

The most recent stratigraphic cross-section of the Cardium Formation (Plint *et al.* 1988) is reproduced in Figure 1.1a, along with a modified cross-section based on the present work (Fig. 1.1b; see Chapter 6). In the Plint *et al.* (1988) stratigraphy (Fig. 1a), it can be seen that the shoreface sandstones of the Kakwa Member to the southwest are considered the lateral equivalents of the Nosehill, Bickerdike and Hornbeck allomembers[1] to the northeast. Plint *et al.* (1986) originally labelled three separate portions of the Kakwa Member as (N), (B) and (H) to indicate their equivalence to the three coarsening-upward successions. The Waskahigan and Burnstick allomembers represent conglomeratic units associated with the E3/T3 and E4/T4 surfaces respectively. The Musreau Member (equivalent to the Moosehound Member of Stott 1963, 1967) consists of generally fine-grained non-marine sediments with isolated sandstone channel bodies, conformably overlying the Kakwa Member. The Raven River Allomember represents another broadly coarsening-upward succession which is composed of several stacked minor successions at Willesden Green (Walker and Eyles 1988). Westward, the Raven River Allomember successively overlies the Hornbeck, Burnstick, Kakwa and

---

[1] The stratigraphic framework of Plint et al. (1986, 1987, and 1988) includes both *members* (defined by lithology) and *allomembers* (defined by bounding discontinuities; see NACSN 1983). Although the latter are generally also labelled as "members" by those workers, in this work I have chosen to name them "allomembers".

Figure 1.1. Comparison of existing and proposed stratigraphic framework for the Cardium Formation. 1.1a) Based on Plint *et al.* (1988); 1.1b) Based on this study (see Chapter 6). W - Waskahigan Allomember; B - Burnstick Allomember

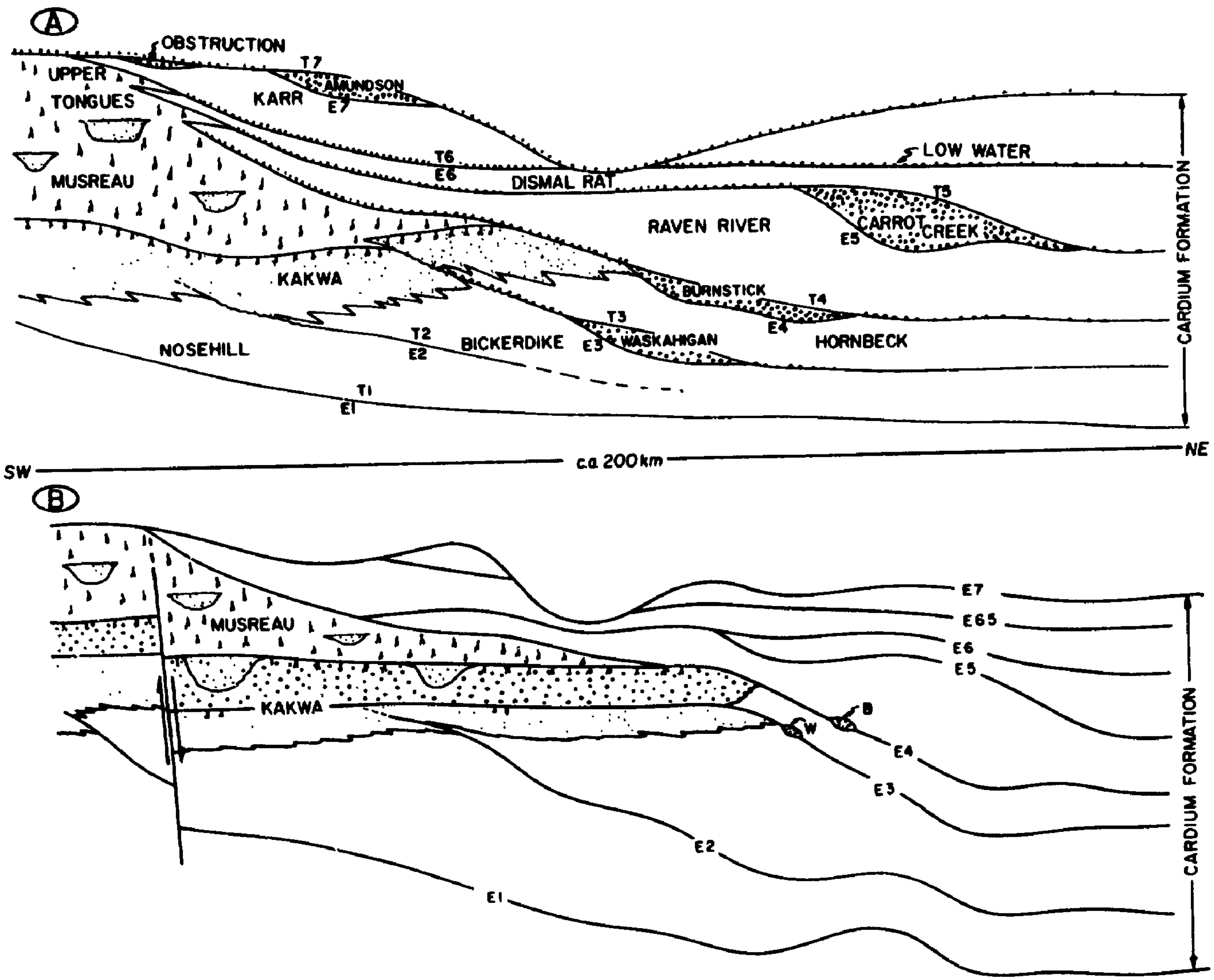
A
OBSTRUCTION
T7
AMUNDSON
E7
UPPER
TONGUES
KARR
MUSREAU
T6
E6
DISMAL RAT
LOW WATER
RAVEN RIVER
T5
CARROT CREEK
E5
KAKWA
BURNSTICK
T4
E4
T3
E3
WASKAHIGAN
HORNBECK
T2
E2
BICKERDIKE
NOSEHILL
T1
E1
CARDIUM FORMATION
SW
ca 200 km
NE
B
MUSREAU
KAKWA
E7
E65
E6
E5
B
W
E4
E3
E2
E1
CARDIUM FORMATION

Musreau (allo)members. The Carrot Creek Allomember consists of the conglomeratic units between E5 and T5. The Dismal Rat and Karr allomembers represent the upper two coarsening-upward cycles, and are separated by the Low Water Allomember, the conglomerate associated with the E6/T6 surface. Overlying the Karr is a thin non-marine unit (Obstruction Allomember) and the conglomerates/pebble veneers of the Amundson Allomember at the very top of the formation. Following the outcrop work of Duke (1985), Plint *et al.* (1988) felt that the Musreau Member interfingers with the upper three coarsening-upward cycles, giving rise to two "upper Musreau tongues". Significantly however, this relationship was not observed in the subsurface (Plint *et al.* 1988, p. 174).

Like Michaelis (1957), Stott (1963), and Duke (1985) before them, Plint *et al.* (1986, 1988) attributed the cyclic style of sedimentation observed in the Cardium to a sequence of transgressions and regressions, suggesting that each of the coarsening-upward successions represented a period of shoreline progradation. The erosion surfaces capping the coarsening-upward successions were initiated during relative sea level fall and continued to develop during sea level lowstands. The linear but asymmetric "bevels" which host the conglomerates of the Waskahigan, Burnstick,Carrot Creek and Amundson allomembers were cut as lowstand incised shorefaces (Bergman and Walker 1987; Pattison 1988; Plint

1988). The conglomerates of these members are interpreted as shoreface sediments, emplaced after the bevels were cut, while the thin pebble veneers represent lag deposits left as the shoreline transgressed.

In the Pembina/Carrot Creek area, it has been suggested that marine transgressive erosion following emplacement of the Carrot Creek shoreface conglomerates must have removed all trace of subaerial conditions developed landward of the lowstand paleoshoreline (Bergman and Walker 1987, 1988). As a result, the top of the Raven River Allomember, where not overlain by Carrot Creek conglomerates, represents a ravinement ("T") surface without preservation of the subaerial erosion ("E") surface. This relationship appears applicable to other allomembers of the Cardium as well

Rine, Helmold and Bartlett (1987) and Hayes and Smith (1987) criticised the initial stratigraphic subdivision and interpretations of Plint *et al.* (1986). Although many of the criticisms were made without supporting evidence, Hayes and Smith (1987) rightly pointed out that the terminology of Plint *et al.* (1986) - using "Formation" and "Member" to describe units which cut across lithologic boundaries - was inappropriate. This was later acknowledged by Plint *et al.* (1987, 1988).

1.3 Previous Work in the present study area

The Cardium Formation forms part of the Smoky Group in northwestern Alberta (Fig. 1.2), a name applied by Dawson

Figure 1.2. Stratigraphy of the Smoky Group in the study area, based on Stott (1967), as modified by Plint *et al.* (1990) and Plint and Hart (in prep.). 1st W. Sp. - First White Speckled Shale; 2nd W. Sp. - Second White Speckled Shale.

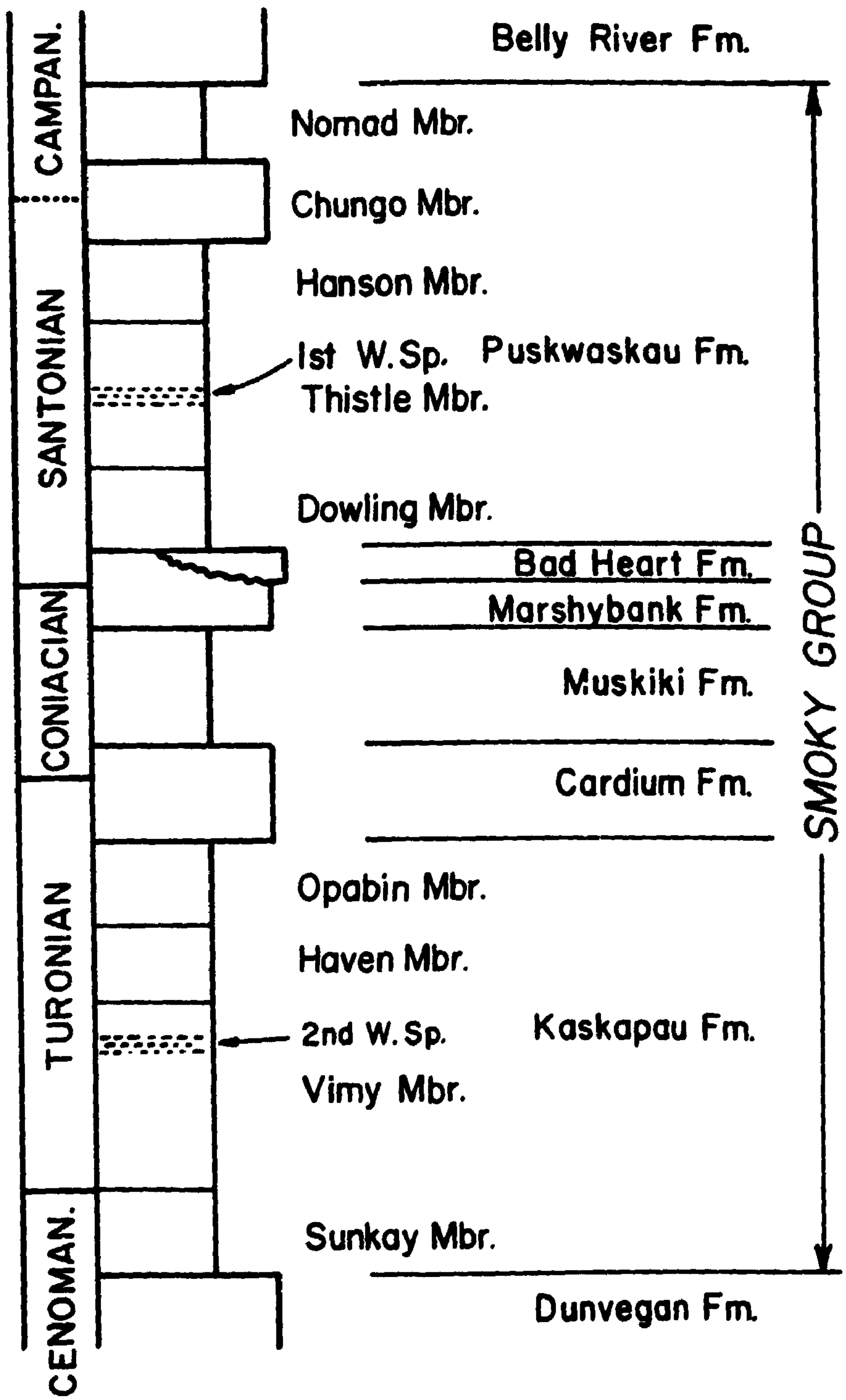
CAMPAN.
SANTONIAN
CONIACIAN
TURONIAN
CENOMAN.
Belly River Fm.
Nomad Mbr.
Chungo Mbr.
Hanson Mbr.
Ist W.Sp.
Puskwaskau Fm.
Thistle Mbr.
Dowling Mbr.
Bad Heart Fm.
Marshybank Fm.
Muskiki Fm.
Cardium Fm.
Opabin Mbr.
Haven Mbr.
2nd W.Sp.
Kaskapau Fm.
Vimy Mbr.
Sunkay Mbr.
Dunvegan Fm.
SMOKY GROUP

(1881) for "upper dark shales" exposed on the Smoky River of the northern Plains. Later, McLearn (1918) distinguished 3 members, a lower shale, a middle sandstone (the Bad Heart), and an upper shale. The name Smoky was subsequently raised to Group status, and the units re-named as Kaskapau, Bad Heart, and Upper Shale formations (McLearn and Henderson 1944).

For some time, the Bad Heart sandstones were considered as lateral equivalents of the Cardium, and the two were mapped together, often under the name of the Bighorn Formation (McLearn and Henderson 1944; Crickmay 1944; Gleddie 1949; McLearn and Kindle 1950). Later, it became evident that the Cardium and Bad Heart sandstones of the plains were not equivalent (Stelck 1955; Harding 1955) although another sandstone stratigraphically above the Cardium in the northern Foothills was still included in the Cardium as an "upper sandstone" (e.g. Stelck 1955; Harding 1955). These "upper" and "lower" sandstones were apparently considered as equivalents of the subsurface "A" and "B" sands. MacDonald (1957) correlated the "upper sandstone" with the Bad Heart Formation, separating it from the Cardium. This has been generally accepted by later workers (Stott 1961, 1963, 1967; Burk 1963; Jones 1966). Norris (1989) has since shown that the Bad Heart of the plains is not laterally equivalent to the Foothills sandstones, and Plint, Norris and Donaldson (1990) proposed the name

Marshybank Formation be applied to these latter units.

A conglomeratic unit of uncertain stratigraphic affinities in the Dawson Creek area was named the Baytree Member by Stelck (in Gleddie 1949), after the locality (Bay Tree[2], Alberta) north of the type section. Stelck (1955) reported that the Baytree Conglomerate comprised up to 11 m (37 feet) of massive black chert and quartzite conglomerate, the lowermost portion of which contained cross-bedded lenses of coarse sandstone and fine conglomerate with scattered coaly fragments. This particular outcrop (Sec. 25, Twp 78 13W6) was destroyed by mining of the conglomerates for aggregate (Jones 1966, p.31), and another outcrop in Sections 12 and 13, Twp 78, 13W6 was designated as the type locality by Stott (1967).

Stelck (1955) felt that the Baytree Member was correlative with the "upper Cardium sandstone" found near Huguenot Creek. As mentioned previously, that sandstone was later shown to be the Marshybank Formation (Plint *et al.* 1990). Stelck (1955) believed the Baytree Member to be in large part a basal conglomerate to the Wapiabi flooding, based on observations on Tupper Creek, southeast of the town of Dawson Creek. There, he reported observing a transitional contact between the conglomerate and the overlying Wapiabi shales. Gleddie (1949) reported finding

---

[2] Note the difference in spelling between the *Baytree* Member and the *Bay Tree* locality

a chert pebble bed about 0.3 m (1 foot) thick in silty shales about 3 m (10 feet) above the main conglomerate, also on Tupper Creek. Stott (1967, p.39) reported that he was unable to observe the contact on Tupper Creek, but that he did measure 4.8 m (16 feet) of shale with scattered pebbles at the base of the Muskiki Formation. I was unable to locate these sections, presumably because of slumping or vegetation growth.

Stott (1961, 1967) proposed that the Baytree Member was part of the Cardium Formation, recognising that the shales observed above the conglomerate on Tupper Creek belonged to the basal portions of the Muskiki Formation. He also measured 11 m (37 feet) of conglomerate at the type locality and stated (Stott 1967, p.36) that "the conglomerate apparently grades westward into coarse-grained sandstone with disseminated pebbles". Stott (1967) believed the Baytree Conglomerate to be a coarse-grained equivalent of the generally fine-grained sediments of the non-marine Moosehound Member. Jones (1966) also included the Baytree Member within the Cardium Formation, and noted that for this to be true, the Cardium must shale out rapidly to the east of Bay Tree. This, he noted, was in agreement with the isopach data of Burk (1963).

1.3 Age and Correlation

There have been few studies on the biostratigraphy of the Cardium Formation, at least in the present study area.

In the present author's experience this is probably because the formation is largely unfossiliferous here. Stott (1967) noted that the Cardium in the north is best dated by its relative position between dated beds of the underlying Kaskapau and overlying Muskiki formations. These contain fauna representative of the middle Turonian *Prionocyclus woollgari* Zone, and of the Lower Coniacian *Scaphites preventricosus* Zone respectively. This suggests the Cardium is of Middle to Late Turonian age. Stott (1967, p. 37) reported that an ammonite (*Scaphites carlislensis*) diagnostic of the Middle Turonian *Prionocyclus hyatti* Zone was collected from "a unit of splintery mudstone in the type Smoky section". He correlated this unit with the Cardium, and it will be shown in Chapter 5 that this unit, shown in Stott's Figure 8, corresponds to the Raven River Allomember of Plint *et al.* (1986).

Further south, the upper part of the formation appears to be more fossiliferous. Stott (1963) reported that the uppermost of his members, the Sturrock, lies within the Lower Coniacian *Scaphites preventricosus* Zone of Cobban and Reeside (1952). *S. preventricosus* was also found by Stott (1963) on Sheep River, southwest of Calgary in a unit which appears close to the base of the Dismal Rat Allomember (Plint and Hart *in prep.*). Specimens of *P. wyomingensis* have only recently been identified by Cobban from strata immediately overlying the E5 surface, and other Late

Turonian forms have been collected from just above the E5 surface at Sebee and elsewhere (Russell Hall, written communication). Fossils of the *S. preventricosus* Zone have been collected in the lower part of the Muskiki Formation in the northern Foothills (Stott 1967). In this case, it would appear that the very base of the Dismal Rat Allomember represents a condensed section (three or possibly four of the Late Turonian zones), and that the rest of the upper portion of the Cardium was deposited in a very short period of time (1 faunal zone). No temporally significant hiatus is present at the E7 surface.

The period of time represented by each of the allomembers below the E5 surface can be *estimated* by first dividing the length of the Turonian Stage (about 3 m.y., e.g. Haq *et al.* 1987) by the number of faunal zones (8, according to Merewether and Cobban 1986). This suggests that each zone lasted about 375,000 years. The E1 to E5 interval appears to belong entirely to the *P. hyatti* Zone (Plint and Hart *in prep.*), and represents 4 progradational episodes. Thus, each regressive/transgressive cycle (assuming that they represent equal periods of time) formed over a period of about 93,000 years. Equivalent calculations yield comparable durations for each of the "upper" (above E5) allomembers of the Cardium Formation, and cycles in the overlying Muskiki and Marshybank formations (Plint 1990; Plint and Hart *in prep.*).

The recognition that the Raven River Allomember belongs to the *Prionocyclus hyatti* Zone allows for more detailed interregional correlation than has previously been possible. In particular, it can be shown that this member can be correlated with the Ferron and Semilla Sandstone members of the Mancos Shale (Utah and New Mexico respectively), the Tres Hermanos Formation (New Mexico), the Codell Sandstone Member of the Carlile Shale (Colorado), the Ferdig Shale (Montana), and part of the Frontier Formation (Wyoming) (Merewether *et al.* 1983, Cobban *et al.* 1976, Merewether and Cobban 1986). The faunal evidence from the southern Foothills (Stott 1963) suggests that the upper part of the Cardium (i.e. above E5) is probably equivalent to units such as the Gallup Sandstone (New Mexico) and the Turner Sandy Member (Wyoming) (Merewether *et al.* 1983; Merewether and Cobban 1986). A chart showing these suggested correlations is presented in Figure 1.3.

1.4 Tectonic Setting

The Cardium Formation forms part of the "third clastic wedge" of Stott (1984). These units consist of detritus shed from the rising Cordillera into the subsiding foreland basin. At this time, a continuous seaway, the Western Interior Seaway, occupied the foreland basin and extended from the Arctic Ocean to the Gulf of Mexico (Fig. 1.4). Stockmal and Beaumont (1987) related foreland basin development to overthrust loading and resulting lithospheric

Figure 1.3. Tentative correlation chart for deposits of selected portions of the Western Interior Seaway during deposition of the Cardium Formation. Based on Cobban *et al.* (1976), Merewether *et al.* (1983) and Merewether and Cobban (1986).

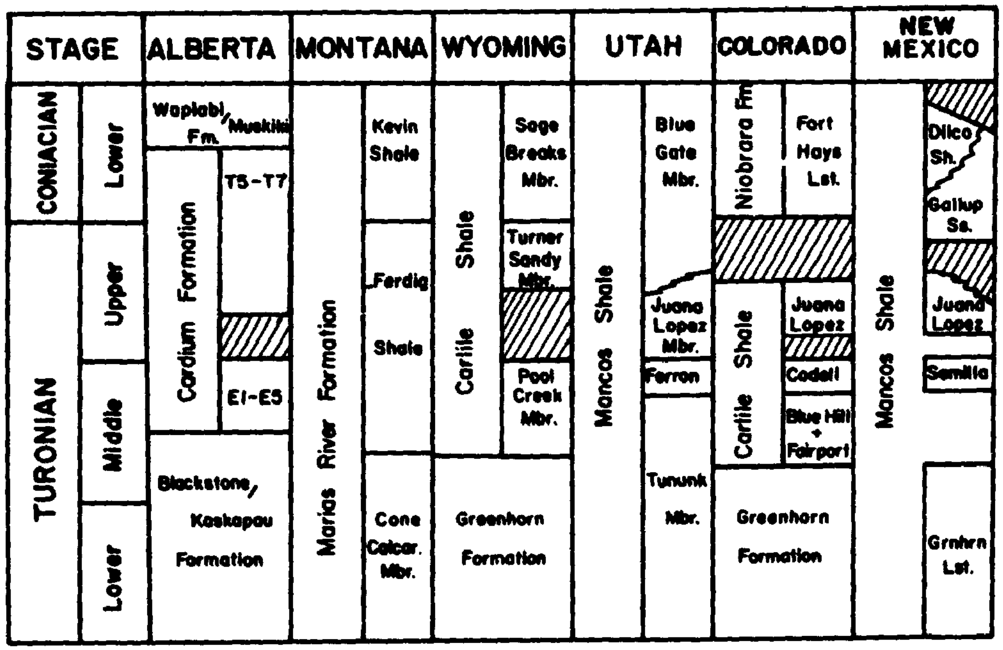
STAGE
ALBERTA
MONTANA
WYOMING
UTAH
COLORADO
NEW MEXICO
CONIACIAN
TURONIAN
Lower
Upper
Middle
Lower
Wapiabi/Muskiki Fm.
Cardium Formation
T5-T7
E1-E5
Blackstone/Kaskapau Formation
Marias River Formation
Kevin Shale
Ferdig Shale
Cone Calcar. Mbr.
Carlile Shale
Sage Breaks Mbr.
Turner Sandy Mbr.
Pool Creek Mbr.
Greenhorn Formation
Mancos Shale
Blue Gate Mbr.
Juana Lopez Mbr.
Ferron
Tununk Mbr.
Niobrara Fm
Fort Hays Lst.
Carlile Shale
Juana Lopez
Codell
Blue Hill + Fairport
Greenhorn Formation
Mancos Shale
Dilco Sh.
Gallup Ss.
Juana Lopez
Semilla
Grnhrn Lst.

Figure 1.4. North American paleogeography during the Turonian. Based on Williams and Stelck (1975).

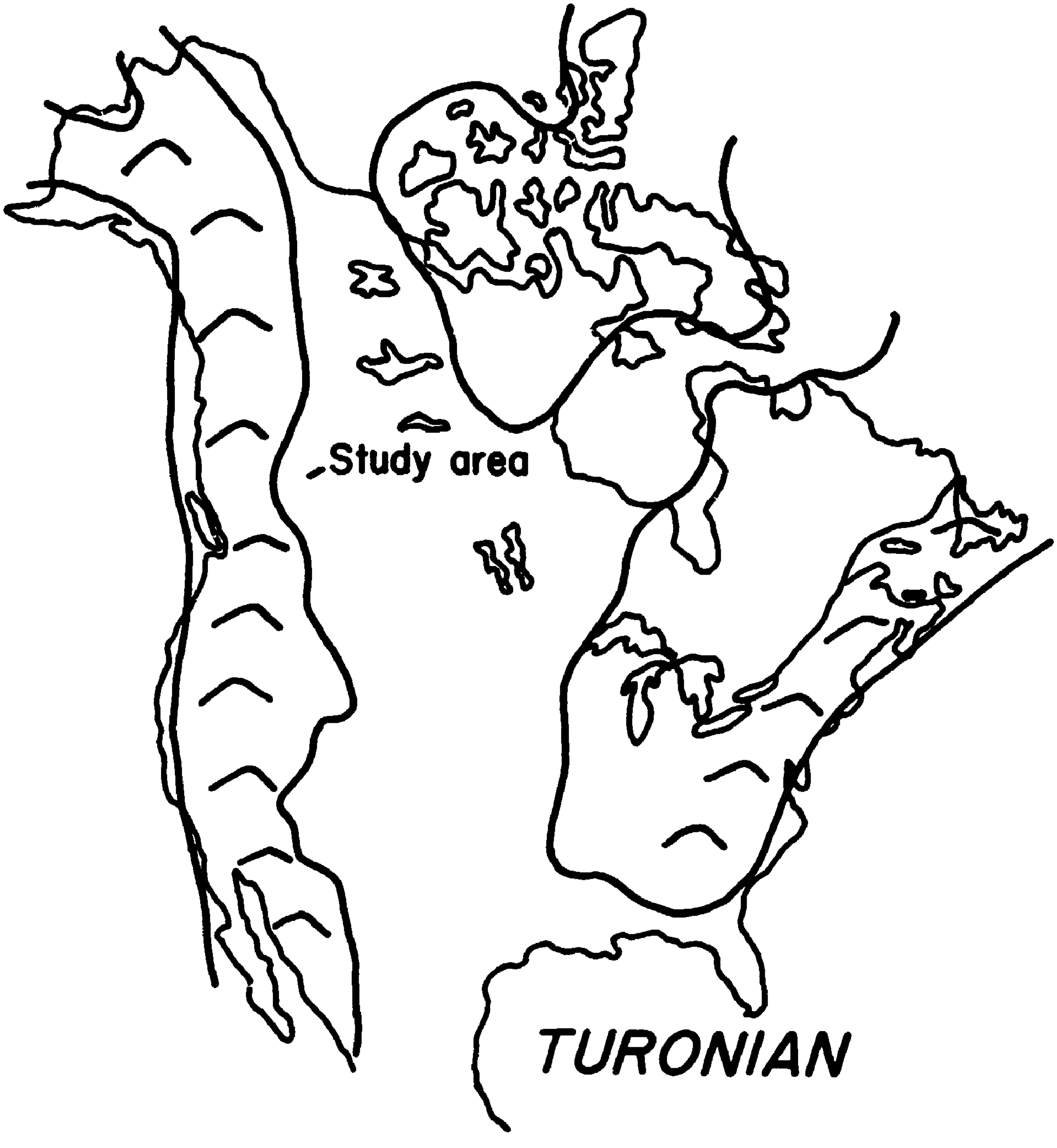
Study area
TURONIAN

flexure. These authors presented a concise summary of the development of the southern part of the Western Canada Basin in response to accretionary events along the Pacific margin of Canada during the Mesozoic and Tertiary. Superimposed on the clastic input were various transgressive/regressive episodes of various magnitudes (e.g. Stott 1963, 1984). A conceptual model of sequence development in a foreland basin will be presented in Chapter 2.

The northern part of the study area is underlain by the Peace River Arch. Cant (1988) has proposed that this structural element initially developed as part of a failed rift system in the Palaeozoic. He outlined the evidence for both positive (upward) and negative (downward) movement on the arch up to the Lower Cretaceous when it appears to have been subsiding. Burk (1962, 1963) presented isopach maps which suggested that the arch, presently a positive feature, began upward motion during deposition of the upper part of the Smoky (Colorado) Group.

1.5 Purpose of the Study

The present study has two main objectives:

1) To reconstruct the depositional history of the Cardium Formation in an area bounded to the south by Township 65, in the east by Range 18 W 5, and in the north and west by the outcrop limit of the formation (in the Foothills). This area (Fig. 1.5) was expected to serve as a testing ground for the stratigraphic subdivisions of Plint

Figure 1.5. Data base for present study. Area of main interest from Township 65 north to limit of preservation of the Cardium Formation (approximately Twp 78 in outcrop), and west of Range 18 west of the Fifth Meridian to the Rocky Mountain Foothills.

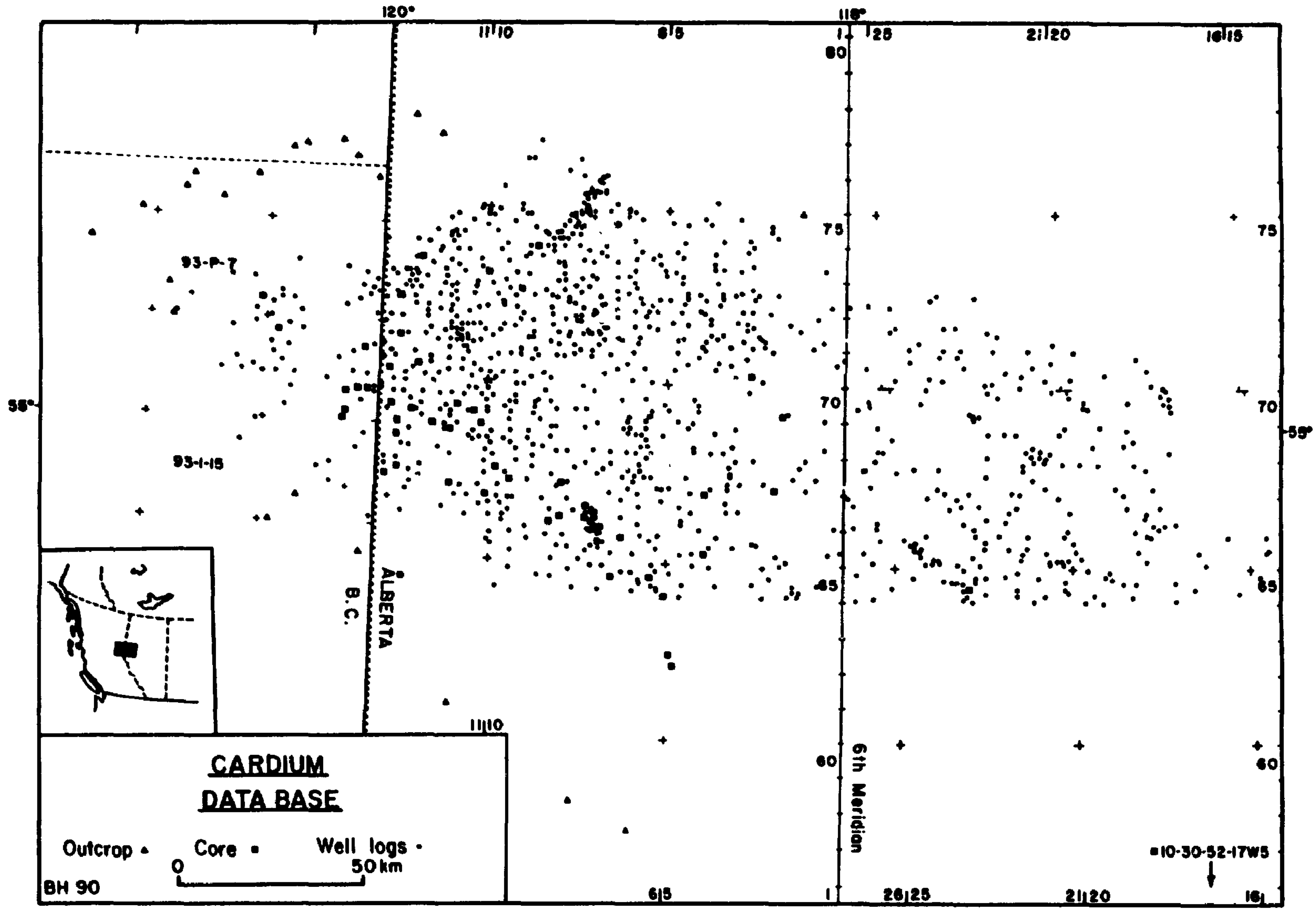

120°
118°
11|10
6|5
1
26|25
21|20
16|15
80
75
70
65
60
55°
93-P-7
93-I-15
B.C.
ALBERTA
6th Meridian
■10-30-52-17W5
CARDIUM
DATA BASE
Outcrop ▲
Core ■
Well logs •
0
50 km
BH 90

et al. (1986, 1987, 1988).

2) To examine the origin and distribution of conglomerate in the Cardium in the study area. As early reconnaissance work on the formation in the Dawson Creek area suggested that conglomerates of the Baytree Member may represent shoreface conglomerates, it was decided that an in depth study of the origin and characteristics of such conglomerates was appropriate. Of particular interest was the identification of diagnostic criteria for the recognition of similar deposits in the subsurface.

1.6 Data Base

This study is based on both outcrop and subsurface data (Figure 1.5). In particular, 57 cores (1101 m of section) and 51 sections from 21 outcrop localities (963 m of section) were measured in the summers of 1987, 1988 and 1989. These data are supplemented by over 1100 well logs, collected at Home Oil Co. in Calgary. Further details will be given in subsequent chapters.

1.7 Previous Publications

Some of the material presented in this thesis has already been published in various forms (Hart 1990; Hart and Plint 1989, *in press*; Hart, Vantfoort and Plint 1990; Plint and Hart 1988, *in prep.*). For simplicity, and to avoid the possibility of incestuous arguments, these papers will generally not be cited. Exceptions to this rule will be made to reference subject matter not directly issuing from the author's Cardium study.

CHAPTER 2

SEQUENCE DEVELOPMENT IN A FORELAND BASIN

2.1 Introduction

In this chapter, I will examine the variables which control sequence[1] development in a foreland basin. As most sequence stratigraphic models presented to date have been developed for passive margins, this chapter will be of importance to the understanding of the processes responsible for the deposition of units such as the Cardium Formation. The main factors which need to be considered here are the tectonic forces which create foreland basins, the factors which induce sea level change (on various time scales), and sequence stratigraphic principles and terminology.

2.2 Origin of Foreland Basins

Foreland basins are asymmetric, wedge-shaped depressions which develop in response to lithospheric loading of a former continental margin during overthrusting (Beaumont 1981). In the case of the Western Interior Basin, overthrusting resulted from the collision of the western margin of the North American plate with various oceanic terranes from Middle Jurassic to Early Cretaceous times

---

[1] Although the term *sequence* is becoming increasingly identified with the EXXON usage of the term (e.g. Van Wagoner *et al.* 1988), its usage in sedimentology and stratigraphy as a synonym of *succession* has a long history (see Bergman and Walker 1988). I will employ the original term *depositional sequence* when referring to the stratigraphic units described by users of the EXXON paradigm.

(Porter, Price and McCrossan 1982; Cant and Stockmal 1989). During collision, part of the former passive margin sedimentary cover was detached and pushed cratonward, forming a series of imbricate thrust slices.

Several attempts have been made to numerically model the development of foreland basins (e.g. Beaumont, Keen and Boutilier 1982; Schedl and Wiltschko 1984; Stockmal and Beaumont 1987). To a large degree, the behaviour of the models depends on whether the lithosphere is considered to be elastic (i.e. it will bend, but not deform plastically) or viscoelastic (behaves elastically on short time scales, but is ductile over longer periods).

For an elastic lithosphere, thrust loading results in the development of an asymmetric depression, with the greatest subsidence immediately below the load. Elastic models predict the development of a forebulge ("outer regional high", Schedl and Wiltschko 1984; "peripheral bulge", Beaumont *et al.* 1982), an elevated area on the cratonward side of the basin. The distance between the thrust load and the forebulge is determined by the flexural rigidity of the lithosphere - largely a function of age, and thickness. In most elastic models, as thrust sheets advance cratonward, the forebulge migrates in the same direction, maintaining a constant distance from the thrust load.

In viscoelastic models, the initial response to thrust loading is the same as that for an elastic lithosphere.

With time however, viscous relaxation occurs, and the basin deepens and narrows (as the forebulge migrates toward the thrust belt). Here, in addition to the flexural rigidity, another parameter, the relaxation time, becomes important. As the value of this variable approaches infinity, the viscoelastic lithosphere model behaviour becomes increasingly similar to the elastic lithosphere example.

Both types of models seem to provide reasonable approximations of the gross characteristics of foreland basin fills, provided that "correct" values are chosen for the input variables (making the reasoning somewhat circular; c.f. Schedl and Wiltschko 1984). It is also possible that, for an elastic lithosphere, certain values of input factors, such as rates of thrust loading, sediment transport rates, and source rock lithology can produce results which mimic the response of a viscoelastic lithosphere (Flemings and Jordan 1989).

A shortcoming of the numerical models is that they portray the loaded lithosphere as an uniform, homogeneous slab. In many cases however, such as the Western Canada Basin, it can be demonstrated that the basement consists of a number of separate tectonic blocks (Ross and Stephenson 1989). Just south of Alberta, Tonnsen (1986) demonstrated how the existence of Precambrian terranes has influenced Phanerozoic sedimentation in the north-central Rocky Mountain region of the United States. He showed how these blocks have been remobilised up to the Tertiary, and how they have influenced stratigraphic and facies development there. Cant (1988) suggested that the origin of the Peace River Arch lies in the existence of a failed rift arm, and that repeated remobilization of this feature throughout the Phanerozoic has had significant effects on sedimentation in that part of Alberta. Thus, basement tectonic elements, where they can be shown to exist, must be considered as possible candidates for the origin of some stratigraphic characteristics in a foreland basin.

It also appears that the sedimentary response of foreland basins to thrusting has been misinterpreted by many. Although it has often been assumed that the introduction of coarse-grained sediments into a foreland basin represents renewed tectonic activity (i.e. thrusting) and development of relief in the hinterland, there seems to be a growing consensus that the opposite is true (Blair and Bilodeau 1988; Burbank *et al.*, 1988; Heller *et al.* 1988; Heller and Paola 1989). These authors contend that the initial response of thrusting is increased subsidence, and that consequentially, coarse clastic detritus is trapped adjacent to the thrust belt. It is only during times of tectonic quiescence that flexural rebound in the proximal part of the basin allows coarser sediment to prograde into the basin. Thus, in marine basins, thrusting is indicated by shale-dominated stratigraphic assemblages (except immediately adjacent to the thrust belt), whereas the progradation of coarse-grained units implies a cessation of thrust activity. These relationships are presented on the assumption that eustatic sea level remains constant.

Paola (1988) presented a semi-quantitative model of gravel transport in a foreland basin dominated by alluvial sedimentation. He suggested that slow, uniform subsidence favours the development of thin gravel sheets, whereas rapid, asymmetric subsidence produces thick, areally restricted gravel units. Flemings and Jordan (1990) added the effects of erosion (principally in the thrust belt) and deposition (in the foreland basin) to a numerical model of foreland basin behaviour (assuming an elastic lithosphere). Their results again suggest that the effects of loading in the thrust belt will generally overwhelm the sediment supply rate, and coarse sediment will be trapped close to the basin margin (Fig. 2.1). During post-thrust quiescent periods, sedimentary facies will prograde in the direction of thrust movement, causing the forebulge to migrate in the same direction. The onset of renewed thrusting will be recorded by an abrupt shift in facies toward the thrust belt, and erosion in the center of the basin as the forebulge moves back toward the thrust belt. These mathematical analyses support the contention that evidence of progradation should be used to infer periods of tectonic quiescence, rather than periods of thrusting and development of relief.

Figure 2.1. Chronostratigraphic diagram representing foreland basin sedimentation according to Flemings and Jordan (1990). The initiation of thrusting is recorded by a rapid shift of sedimentary facies toward the thrust belt, accompanied by erosion of strata deposited on the forebulge. During quiescent periods, sedimentary facies prograde basinward.

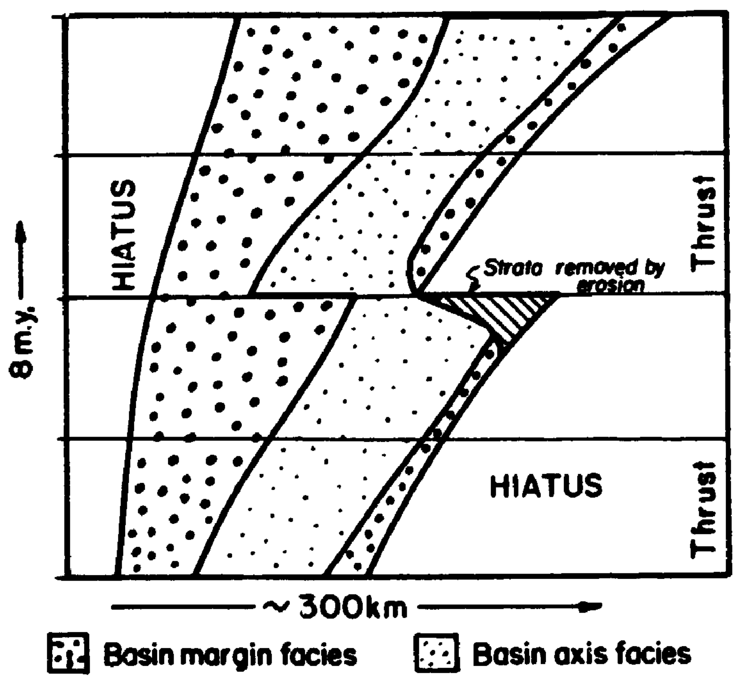
HIATUS
Strata removed by erosion
Thrust
HIATUS
Thrust
8 m.y.
~300km
Basin margin facies
Basin axis facies

Other relationships between tectonic activity and sedimentation have been suggested. Swift *et al.* (1987) suggested that subsidence patterns in a foreland basin were likely to be strongly asymmetrical, with the highest rates closest to the thrust belt. As noted above, this is likely to be the case during periods of thrust loading. In these cases the extent of shoreline movement will be a function of sediment supply, with significant progradation probably only possible in regions of abundant sediment supply.

Cant and Stockmal (1989) suggested that periods of terrane accretion in the Canadian Cordillera correlate with periods of thrusting and coarse-grained sedimentation in the Alberta Basin, and that tectonically quiet periods were represented by shales. This interpretation is contrary to that presented above, and the differences might be explainable in terms of: a) differing scales of investigation (clastic wedges *versus* formations); b) whether the basin is overfilled or underfilled with sediment (c.f. Burbank *et al.* 1988); and c) problems in constraining the exact timing of terrane accretion.

2.3 Sea level changes

The subject of global (eustatic) sea level changes has received considerable attention in recent years. The two themes receiving the most attention are: 1) understanding the controls on cyclically deposited sediments of various scales; and 2) understanding the economic and environmental consequences of present globally rising sea levels. The present review will examine the mechanisms responsible for eustatic sea level changes, and the signature of such changes in the stratigraphic record. As there is evidence for several different temporal scales of cyclicity, each will be examined separately.

2.3.1 Eustasy

Most geologists define eustasy as global changes in the elevation of the sea surface, as measured with respect to a fixed point such as the earth's center (e.g. Burton, Kendall and Lerche 1987; Posamentier, Jervey and Vail 1988). It is generally understood that eustatic sea level changes are due to either of two effects. These are changes in the volume of the ocean basins, or changes in the volume of sea water (Donovan and Jones 1979).

Tectonoeustasy is the term employed to refer to changes in the volume of the ocean basins. As its name implies, these changes are tectonic in origin. The principal mechanism for changing the volume of sea water in the oceans is the growth and decay of continental ice masses, known as glacioeustasy. Changes in water volume could also be produced thermally, but these are generally considered to be of minor importance (Donovan and Jones 1979).

It is important to distinguish between eustatic and relative sea level changes. The latter are of local to regional extent and are a function of two factors, eustasy and local or regional vertical crustal movements (subsidence or uplift). Relative sea level is measured with respect to a datum at or near the sea floor (Posamentier *et al.* 1988). It can be shown that relative sea level can rise during periods of eustatic fall, provided the local subsidence rate is greater than the rate of eustatic fall. Thus, evidence of falling sea level at any one point does not necessarily indicate a eustatic fall. Hancock and Kauffman (1979) noted that eustatic sea level changes are indicated when 2 criteria are satisfied. These are: 1) when major transgressive and regressive episodes can be shown to be synchronous for many different places; and 2) approximately equal sea level changes are indicated for these regions.

In Figure 2.2, one can see an example of how the effects of eustatic sea level change and subsidence might combine to produce a relative sea level curve (based on Goodwin and Anderson 1985). Note that the eustatic curve consists of two superimposed oscillation frequencies. Depending on the rate of subsidence in the area, eustatic sea level falls will be felt as relative sea level falls, stillstands, or periods of decreased relative sea level rise. Many other combinations are possible.

2.3.2 Phanerozoic sea level changes: cycles on cycles

The most widely accepted eustatic sea level curves are those published by Haq, Hardenbol and Vail (1987, 1988). These curves were originally based on seismic stratigraphic

Figure 2.2. An example of how eustatic sea level fluctuations (here caused by climate fluctuations) can combine with differing subsidence rates to produce different styles of relative sea level fluctuation. Modified from Goodwin and Anderson (1985).

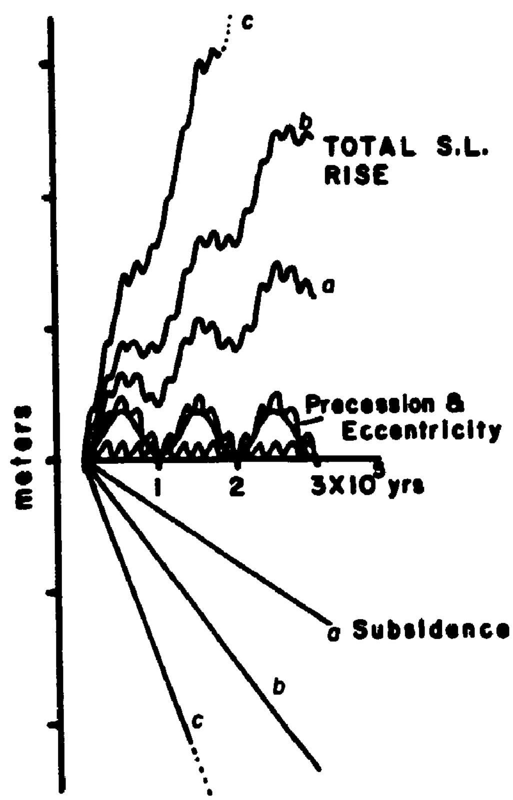
c
b
TOTAL S.L.
RISE
a
Precession &
Eccentricity
meters
1
2
3X10⁵ yrs
a Subsidence
b
c

analysis (Section 2.4). A full discussion of the methodology involved in the derivation of these curves is given in Vail *et al.*(1977), Haq *et al.*(1987,1988), Cross and Lessenger (1988), and Van Wagoner *et al.* (1988).

Haq *et al.* (1987, 1988) presented two superimposed sea level curves for eustatic fluctuations since the Triassic. The first is a "long-term" curve in which geohistory analysis has been used to compensate for variations in subsidence rates between basins. The second comprises a "short-term" curve in which the magnitude of sea level excursions is "a best estimate from seismic and sequence stratigraphic data" (Haq *et al.* 1988, p.93). They conceded that the short-term curve may need to be modified as new information becomes available.

Many other authors have proposed eustatic sea level curves for various parts of the Phanerozoic. Burton *et al.* (1987) presented a critique of the various methods employed to determine the magnitude of eustatic sea level changes. They concluded that no method can accurately determine the absolute magnitude of past eustatic changes. This is because the geometry of a sedimentary basin fill (the "evidence" used to reconstruct sea level changes) is determined by the interaction of 3 independent variables: 1) crustal movements; 2) sediment supply and compaction; and 3) eustasy. All schemes which attempt to isolate the eustatic component are forced to make assumptions about the other two variables (e.g. Posamentier *et al.* 1988). Even geohistory analyses are based upon assumptions which cannot be proved (Burton *et al.* 1987).

Despite these limitations, most authors concede that the evidence for *many* globally synchronous sea level changes is convincing (e.g. Miall 1986; Burton *et al.* 1987), although contrary, or cautionary views have been expressed (e.g. Jeletzky 1978; Hubbard 1988). Jeletzky and Hubbard suggested that the effects of regional to local tectonic movements can dominate over eustatic sea level changes in producing depositional sequences. Such discrepancies may reflect the different study areas of the authors (tectonically active zones or "passive" margins) and different bio- and chronostratigraphic interpretations.

Three main scales of eustatic cycle were defined by Vail *et al.* (1977), and a fourth added by Ryer (1983). In this system, the higher order cycles represent higher frequency (i.e. shorter time scale) eustatic movements. At times, the division between different orders of cyclicity is somewhat arbitrary. It should also be noted that the use of the word "cycle" may be misleading, as no periodicity is necessarily implied.

2.3.2.1 First Order Cycles

This order of cyclicity is represented by the two main periods of maximum flooding in the Phanerozoic, and represent cycles on the scale of 200 to 400 million years.

Worsley, Nance and Moody (1984) showed how this order of cyclicity is controlled by the formation and break up of supercontinents (i.e. the Wilson Cycle). They modelled eustasy as a function of three variables: 1) sea floor elevation; 2) continental area; and 3) continental elevation. The Worsley *et al.* (1984) results compare quite favourably with the first order sea level curve of Vail *et al.* (1977), leading one to accept the basic tenets of their model.

2.3.2.2 Second Order Cycles

These were termed "supercycles" by Vail *et al.* (1977) and were grouped into "supercycle sets" by Haq *et al.* (1987). They correspond in part to the "sequences" of Sloss (c.f. Sloss (1988)). These cycles range from about 10 to 100 million years in length, and their origin is attributable to changes in the volume of oceanic spreading ridges (Miall 1986). Pitman (1978) showed how changes in the spreading rate at mid-ocean ridges could be translated into changes in their volume, the elevation of the oceanic crust being a function of its age. As the volume of the spreading ridges increases, the volume of the ocean basin is diminished, and eustatic sea level rises. Kauffman (1985) showed how an increase in spreading rate (lasting about 20 million years) during the Mid- to Late Cretaceous can be correlated with a period of general transgression in the Western Interior Bas· ı of the United States.

2.3.2.3 Third Order Cycles

Third order cycles are of 1 to 10 million years duration. A portion of the Haq *et al.* (1987) curve which covers the Cretaceous Period is presented in Figure 2.3. The origin of this scale of cyclicity is the most problematic. Although Vail *et al.* (1977) and Haq *et al.* (1987, 1988) concluded that they represent the growth and decay of continental ice masses, there are several problems with this hypothesis. First, although such a mechanism can be postulated for certain parts of the Phanerozoic, there are long periods for which evidence of large continental ice masses is absent, but which still exhibit third order cyclicity. Second, it can be shown that ice sheet growth and decay is a process which operates on a time scale of tens to hundreds of thousands of years (Hays, Imbrie and Shackleton 1976; Boyd, Suter and Penland 1988). Further discussion of the controls and effects of ice ages will be given in the section on fourth order cycles.

Harrison (1985) calculated that variations in ocean ridge spreading rates could account for the timing of third order cycles, but that the magnitude of these changes (tens of meters) is an order of magnitude less than that calculated from the stratigraphic record. Worsley *et al.* (1984) suggested that collision-induced changes in continental area could explain some third order cycles. Kauffman (1985) suggested that third order cycles in the

Figure 2.3. A portion of the eustatic sea level curve proposed by Haq *et al.* (1987, 1988), representing eustatic fluctuations during the Cretaceous period.

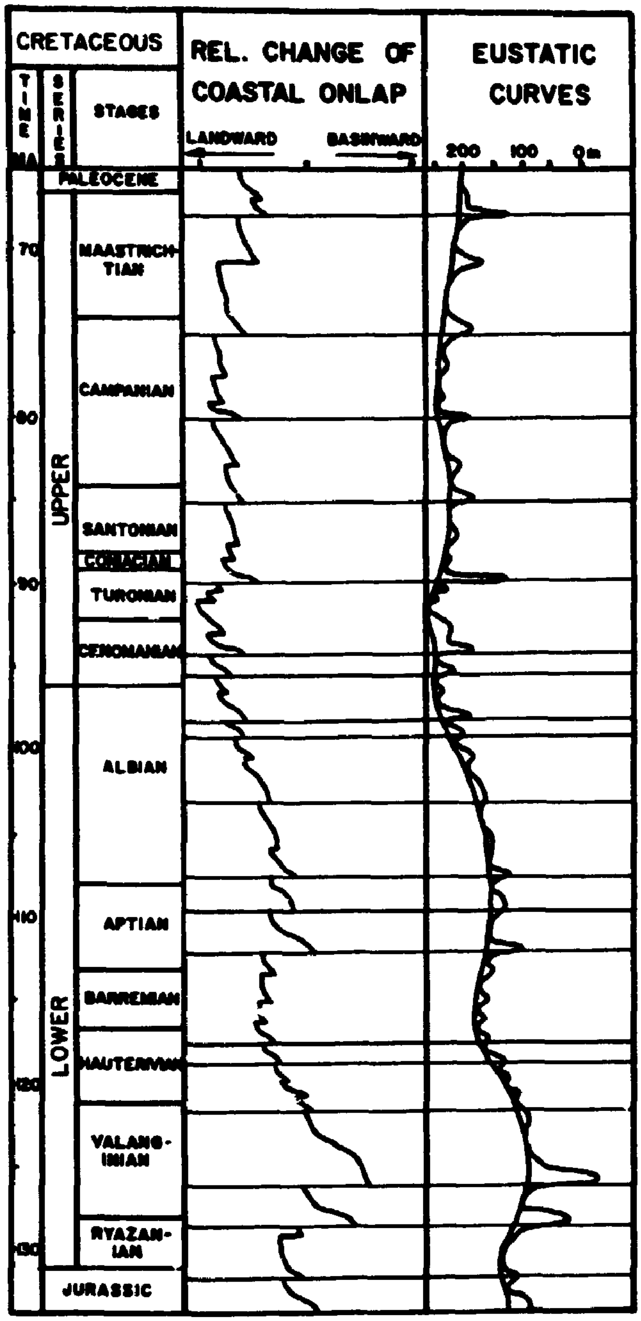

(HAQ et al., 1987)

western interior of the United States were related to seafloor spreading rates and volcanic activity. Tectonically active intervals were associated with eustatic rises, whereas eustatic falls were associated with lower spreading rates and less volcanism. This suggests that higher spreading rates at oceanic ridges are accompanied by increased rates of convergence at destructive plate margins, leading to thrusting and subsidence in foreland basins (Section 2.2).

It has also been suggested that the inundation and desiccation of isolated basins may produce eustatic excursions. Burke and Sengör (1988), for example, suggested that an Aptian sea level event recognised by Haq *et al.* (1987) may have been produced by the flooding of an isolated portion of the early South Atlantic Ocean. Although such events may occur episodically, they are probably unlikely to be responsible for the majority of observed third order cycles.

2.4.2.4 Fourth and higher order cycles

Ryer (1983) proposed that the term "fourth order" be applied to cycles superimposed on third order cycles (Fig. 2.4). They appear to have durations of a few hundred thousand years (the fourth order cycles of Kauffman (1985) have durations of 1-3 million years and so belong to the third order cycles of the EXXON group). The global correlation of this scale of cyclicity is probably beyond

Figure 2.4. An example of fourth order cycles (inset) superimposed on a third order cycle (above), from the Mid-Turonian Ferron Sandstone. Sandstones are stippled, and represent shoreline progradation to the northeast. Based on Ryer (1981, 1983).

CENOMANIAN-SANTONIAN (UTAH)

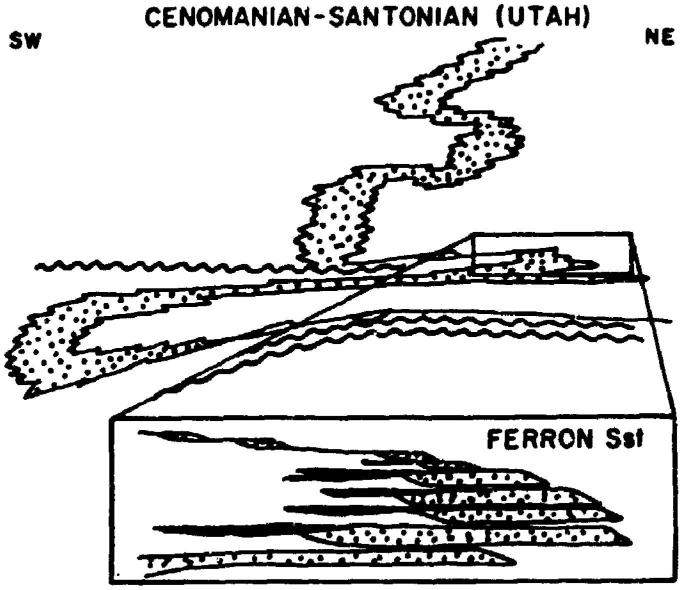

(Ryer, 1981)

the resolution of biostratigraphic methods (Boyd *et al.* 1988; Kauffman 1988).

Cycles with time scales of less than a few hundred thousand years were considered by Kauffman (1985) to be of climatic origin. Other workers have suggested that fluctuations in sediment supply (Cant 1984; Fig. 2.5), short-term tectonic movements (Plint *et al.* 1986) or autocyclic phenomena such as delta lobe switching (Ryer 1981) may be responsible for this order of cyclicity.

Even smaller-scale (<100,000 years) cycles have been noted elsewhere, such as in the Cretaceous system of Alberta. Cant (1984) stated that the 8 members (fourth order cycles) of the Spirit River Formation were deposited in 3 million years, suggesting a time interval of about 375,000 years per member. The Wilrich B member itself contains 8 minor (fifth order?) cycles, each apparently representing about 47,000 years. Cant (1984) suggested that sediment supply fluctuations controlled the development of the minor cycles. Cycles of a similar scale were observed in the Raven River Allomember of the Cardium Formation (Eyles and Walker 1988; Walker and Eyles 1988). They suggested the member could represent from 167,000 to 333,000 years (but see Section 1.3); the seven sandier upward cycles which comprise the member at Willesden Green could then represent periods of 24,000 to 47,000 years. Eyles and Walker (1988) maintained that these cycles were controlled

Figure 2.5. Fourth order cycles from the Albian Spirit River Formation. A - non-marine facies; B - Shoreface and beach deposits; C - marine sandstones; D - marine shales. Based on Cant (1984).

SPIRIT RIVER FORMATION

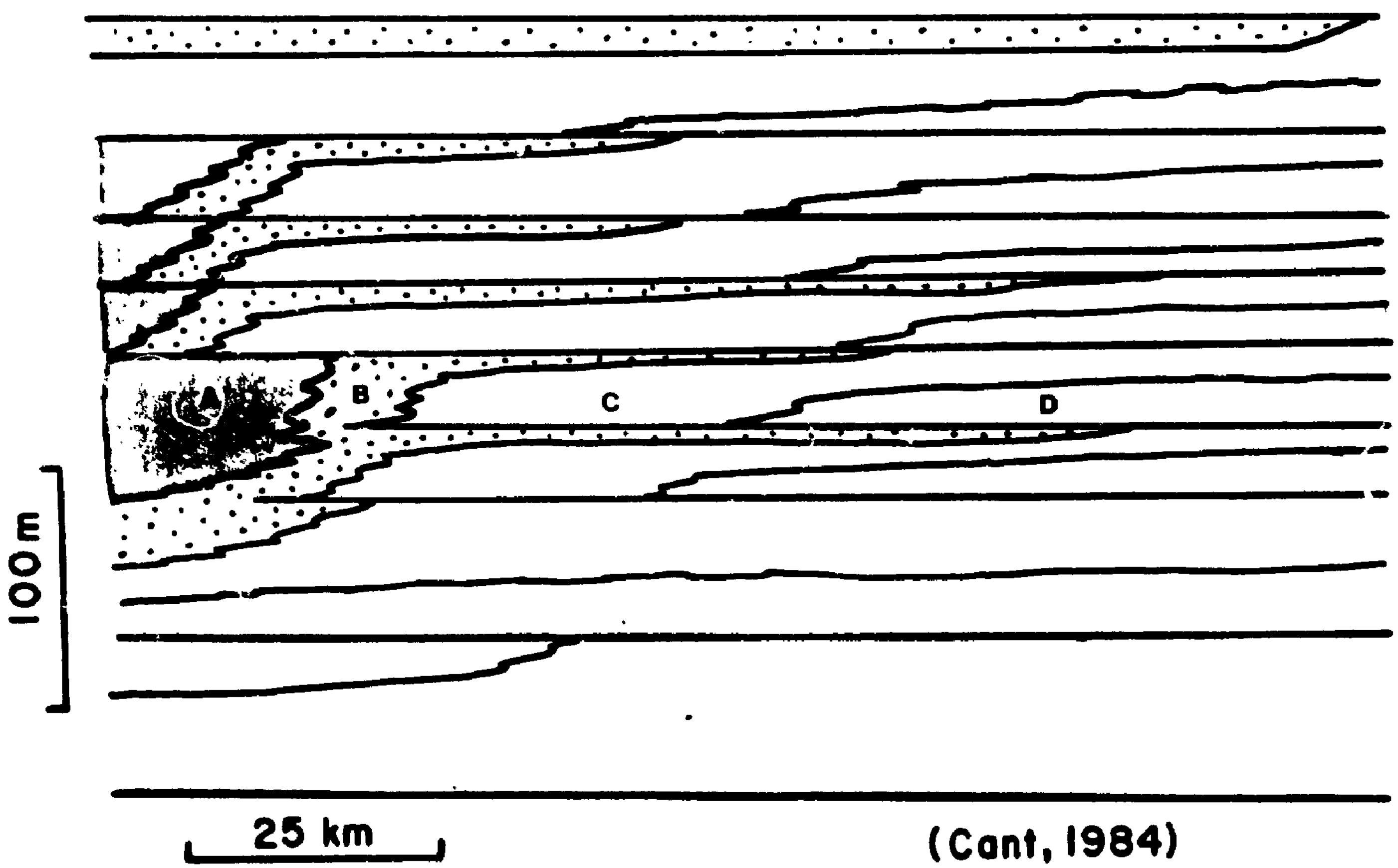

by rapid tectonic movements, although this interpretation will be discounted later (Chapter 7).

Proponents of the climate response mechanism suggest that gradual, periodic changes in the earth's orbital parameters have an effect on terrestrial climate. This is known as Milankovitch theory. The three main parameters are: 1) the precession cycle, due to the precession of the equinoxes, with a periodicity of about 21,000 years; 2) the axial obliquity cycle, or the rotation of the earth's orbital axis through about 3°, with a periodicity of about 41,000 years; and 3) the eccentricity cycle, related to changes in the eccentricity of the earth's orbit, with a main periodicity of 100,000 years superimposed on a larger cycle of about 400,000 years. The climatic influence of these variables has been discussed by Berger (1978), Hays *et al.* (1976), Kutzbach (1981) and many others. Hays *et al.* (1976) demonstrated conclusively that the succession of Quaternary ice ages was controlled by variations in the earth's orbital geometry, particularly the 100,000 year eccentricity cycle.

The effect of Milankovitch climate cycles on ancient sedimentary assemblages has been best described for carbonate sequences (e.g. Fischer, Herbert and Premoli-Silva 1985). Kauffman (1988) illustrated how the eccentricity cycle could be correlated in an onshore direction (using bentonites) from basinal carbonates to shoaling upward clastic sequences in deposits of the Western Interior Seaway of the central United States. He suggested that during wet, possibly cooler intervals, erosion and thus sediment supply increased, causing the progradation of nearshore clastic systems and the delivery of argillaceous sediment to distal, carbonate-dominated regions. During dry, possibly warmer intervals, sediment supply would be reduced, transgression would ensue, and "distal" shales would replace sandstones or siltstones at the top of the shoaling upward sequence. Offshore, clean carbonates would be deposited as the amount of clastic detritus fell.

Barron *et al.* (1985) provided strong evidence for climate-mediated bedding successions from Cenomanian to Turonian strata of the Western Interior Seaway in the southwestern United States. Wright *et al.* (1989) described evidence for several orders of cyclicity in shallow marine successions of Late Cretaceous age in the San Juan Basin. They concluded that transgressive/regressive cycles about 5 m thick were probably developed in response to climatic forcing mechanisms.

It should be noted that although climate cycles can lead to fluctuations in sediment supply, it appears that the only means by which climate can directly influence eustatic sea level is through the development and melting of glaciers. This poses a problem when one attempts to explain the origin of fourth order sea level changes in ice-free periods.

2.3.2.5 "Geoidal Eustasy"

No discussion of eustatic sea level changes would be complete without reference to the work of Mörner (e.g. 1976, 1981). As Mörner has continued to point out, the present sea surface, as measured by satellite, is *not* spherical, but rather highly irregular with a relief of up to 180 m. In part, the observed topography can be related to variations in the geoid, the equipotential surface of the attraction and rotation potentials of the earth (Mörner 1976). The geoidal anomalies can, in turn, be related to the irregular distribution of mass in the Earth's interior. Mörner (1976) contended that any process which affects eustatic sea level will also affect the configuration of the geoid (on a comparable time scale). Hence, the timing and magnitude (and possibly even the sign) of eustatic changes will vary interregionally, and so there can never be a unique global eustatic curve.

The significance of Mörner's work is difficult to evaluate. Although the existence of geoidal topography is not open to debate, most authors (e.g. Haq *et al.* 1987) ignore past geoidal fluctuations. This is probably either because the magnitude of the geoidal fluctuations relative to the eustatic change is considered negligible, or because their effects are unpredictable, and so simply ignored. Neither of these two approaches refutes Mörner's claims, and so it would appear that geoidal perturbations should be considered when searching for causative mechanisms to explain past sea level changes. This would especially be true when sequence boundaries can be shown to be diachronous.

2.4 Sequence Stratigraphy

A major objective of stratigraphic studies of clastic deposits is the reconstruction of depositional history with as much precision as possible. In this regard, the limits of traditional lithostratigraphy have been demonstrated in recent years. Lithostratigraphy involves the correlation of units based on similarity of lithology and stratigraphic position (North American Commision on Stratigraphic Nomenclature (NACSN) 1983). Such correlations have commonly been supported by biostratigraphic considerations based on faunal content of the units involved.

The limitations of this approach become apparent when one considers that lithostratigraphic units are usually time transgressive. Such units were produced by the vertical and/or lateral movement of sedimentary environments (facies) through time. As a consequence, "time lines" cross lithologic boundaries. Other stratigraphic systems have been developed (e.g magnetostratigraphy), but the temporal resolution of such systems is variable and generally decreases with increasing age. Kauffman (1988) and Haq *et al.* (1988) provided discussions of the limitations of each approach.

In an attempt to obtain improved temporal resolution, some geologists have employed the identification and correlation of various types of distinct physical, biological and chemical "event" horizons. By correlating these horizons, an *event stratigraphy* may be constructed whereby the relative temporal resolution is considerably greater than that obtained through traditional stratigraphic techniques. Unfortunately, the high precision in relative dating available through this method may be beyond the resolution of absolute dating techniques. A complete review will not be presented here (see Kauffman 1988), but these horizons might include bentonite layers, extinction events, anoxic events, etc. Of particular interest here is the use of the physical characteristics of clastic units in the construction of event stratigraphies.

A common depositional theme in clastic units is the vertical stacking of lithologic packages, each of which is composed of a similar succession of members. Wanless and Weller (1932) termed such units "cyclothems" and suggested that if they are of regional rather than local extent, they could be used as units of correlation. In a similar vein, Goodwin and Anderson (1985) proposed that small-scale (1-5m) shallowing-upward cycles (termed Punctuated Aggradational Cycles, or "PAC"s) could be used as basin-wide time-stratigraphic units.

The use of unconformities to distinguish major depositional episodes was advocated by Sloss (c.f 1988). He identified six major transgressive/regressive episodes on the North American Craton during the Phanerozoic, each of which was bounded by inter-regional unconformities. Sloss proposed that the term *sequence* be used to identify such units, and was later able to correlate the North American sequences with coeval units on other continents.

The advent of modern sequence stratigraphy was heralded in 1977. In that year, the term *depositional sequence* was defined by Vail *et al.* (1977) as "a stratigraphic unit composed of a relatively conformable succession of genetically related strata and bounded at its top and base by unconformities or their correlative conformities". These sequences could be much smaller than those identified by Sloss. Unconformities were defined as "a surface of erosion or non-deposition that separates younger strata from older rocks and represents a significant hiatus" Vail *et al.* (1977). Subsequently, this definition has been modified (Van Wagoner *et al.* 1988) such that evidence of subaerial erosion must also be present, thus restricting application of the term sequence. It is to be noted that this definition of an unconformity is not universally accepted (e.g. Bates and Jackson 1987).

The chronostratigraphic significance of unconformities is that they separate older strata (below) from younger strata (above). Seismic sequence analysis begins with the recognition of discontinuities (unconformities or correlative conformities) to delineate "packages" of strata. Within these packages (depositional sequences), the characteristics of the reflectors (reflection configuration, continuity, amplitude, etc.) are studied to interpret the stratigraphy in terms of lithology, environment of deposition, subsidence patterns and changes in relative sea level (see Vail *et al.* 1977 for further details). Of particular importance here is the identification of relative sea level changes (Section 2.3).

One of the trademarks of sequence stratigraphic analysis is the interpretation of depositional history as a function of sea level change. A full discussion of this type of analysis will not be presented here, and the reader is referred to works by Posamentier and Vail (1988), Posamentier *et al.* (1988) and Van Wagoner *et al.* (1988). These workers suggested that individual segments of the sea level curve will be represented by distinctive associations of depositional facies and stratal "geometries". In this type of analysis, the controlling variables are generally considered to be: 1) eustatic (i.e. global - see next section) sea level changes; 2) subsidence rates and patterns; and 3) sediment type, rate of supply and dispersal (e.g. Curray 1964; Jervey 1988).

The main depositional sequences commonly consist of stacked *parasequences*, the latter represent a relatively conformable succession of strata bounded by marine flooding surfaces (developed during transgression), and are indicated by a sudden increase in depositional water depth above the flooding surface (Van Wagoner *et al.* 1988). These cycles develop in response to higher frequency relative sea level changes. In cases where subaerial exposure is suggested but no supporting evidence is preserved (because of erosion during transgression), distinction between depositional sequences or parasequences becomes problematic for fourth order cycles under the EXXON system (e.g. Van Wagoner *et al.* 1988; see below).

Although originally the emphasis was placed on the identification of depositional sequences from seismic sections ("seismic stratigraphy"), Vail *et al.* (1977) noted that closely spaced well logs may be employed to identify sequences much smaller than those identified on seismic sections. This is because geophysical logs can resolve units with thicknesses of sometimes less than a meter, whereas the vertical resolution of seismic sections is commonly several tens of meters. As a consequence, the relative temporal resolution of well log correlations can be much greater than that attainable through seismic stratigraphy.

There are a number of criticisms which have been levelled at the EXXON sequence stratigraphy paradigm (e.g. Miall 1986). Perhaps the most obvious objection (for the present purposes) concerns the use of preserved subaerial exposure surfaces to define the sequence bounding unconformities. In many cases, these surfaces may not be preserved due to transgressive erosion (Swift 1975; Demarest and Kraft 1987). Here, the preserved succession is likely to be a parasequence-like unit, with a shoaling-upward sequence capped by a ravinement surface. In these instances, it may be impossible to distinguish parasequence-style relative sea level changes (stillstand/rise/stillstand/rise) from events involving a distinct sea level drop.

Even where non-marine strata are preserved, the sequence boundary developed during lowstand tends to be less prominent on a formational scale than the ravinement surface developed during transgressive erosion, and can be mistaken for it (e.g. Demarest and Kraft 1987). Galloway (1989) recognised these shortcomings, and proposed the use of *genetic stratigraphic sequences* (as opposed to the *depositional sequences* of EXXON workers). These units are bounded by the marine flooding surfaces. As noted in Chapter 1, it can be demonstrated that the allomembers of the Cardium Formation more closely resemble the genetic stratigraphic sequences of Galloway (1989) than the depositional sequences of EXXON workers, in that evidence of subaerial exposure (where it developed) is generally not preserved at the top of individual units.

2.5 Summary

It is unlikely that a single model can be developed which will allow unambiguous evaluation of the factors controlling sequence development in all foreland basins. This is because many of the factors are interrelated, and the number of "unknowns" is likely to be too great to weigh the effects of most variables individually. For example, fourth order cycles could develop in response to fluctuations in sediment supply (difficult to quantify), tectonic activity (which may itself influence sediment supply), or eustatic sea level change (probably not provable). Identification of any one of these as the prime cause of such cyclicity is likely to be exceptionally difficult. Similarly, there may be a link between eustatic sea level (tectonoeustasy) and subsidence in foreland basins, since increased spreading rates at mid-ocean ridges should lead to increased convergence at destructive margins and, ultimately, thrusting and subsidence in foreland basins. How does one isolate the effects of eustatic sea level rise from loading-induced subsidence in these cases?

Despite these problems, a general picture describing the interaction between tectonic activity and sedimentation *is* developing for the Western Interior Basin during Cretaceous times. Based on the material presented above, it appears that periods of thrust activity are most likely to be represented by shales throughout most of the basin (Fig. 2.6a), and that evidence of substantial shoreline progradation probably indicates periods of relative quiescence (Fig. 2.6b). Thick clastic wedges with evidence of strongly asymmetric subsidence (greatest closest to the thrust belt) are probably indicative of high rates of sediment supply (with respect to relative sea level change), and are most likely to develop close to the thrust belt. Given the coupling between rates of mid-ocean ridge spreading and convergence at destructive margins (Section 2.2), there may also be a general link between (tectono)eustasy and subsidence in foreland basins.

Variations on the proposed model must be expected, given that rates of sediment supply, lithospheric thickness, thrust load thickness, basin configuration (overfilled or underfilled), and many other factors can be variable between and even within foreland basins. Eustatic sea level fluctuations may or may not make themselves felt at any given point, depending upon local rates of subsidence. Given that the factors controlling thrusting (such as terrane accretion) are localised both in time and space, synchroneity of transgressive/regressive cycles along the entire length of a basin such as the Western Interior Basin may not always be evident.

Figure 2.6. Generalised model of sedimentation in a foreland basin. 2.3a) Periods of thrust loading are represented by eustatic highstands and strongly asymmetrical subsidence, hence coarse sediments are trapped close to the thrust belt, and shales are delivered to the more axial portions of the basin. 2.3b) Following thrust episodes, relative sea level drops, thrust asymmetry decreases and coarse clastic units can prograde basinward. Based on models of Blair and Bilodeau (1988); Burbank *et al.* (1988); Heller *et al.* (1988); Flemings and Jordan (1990).

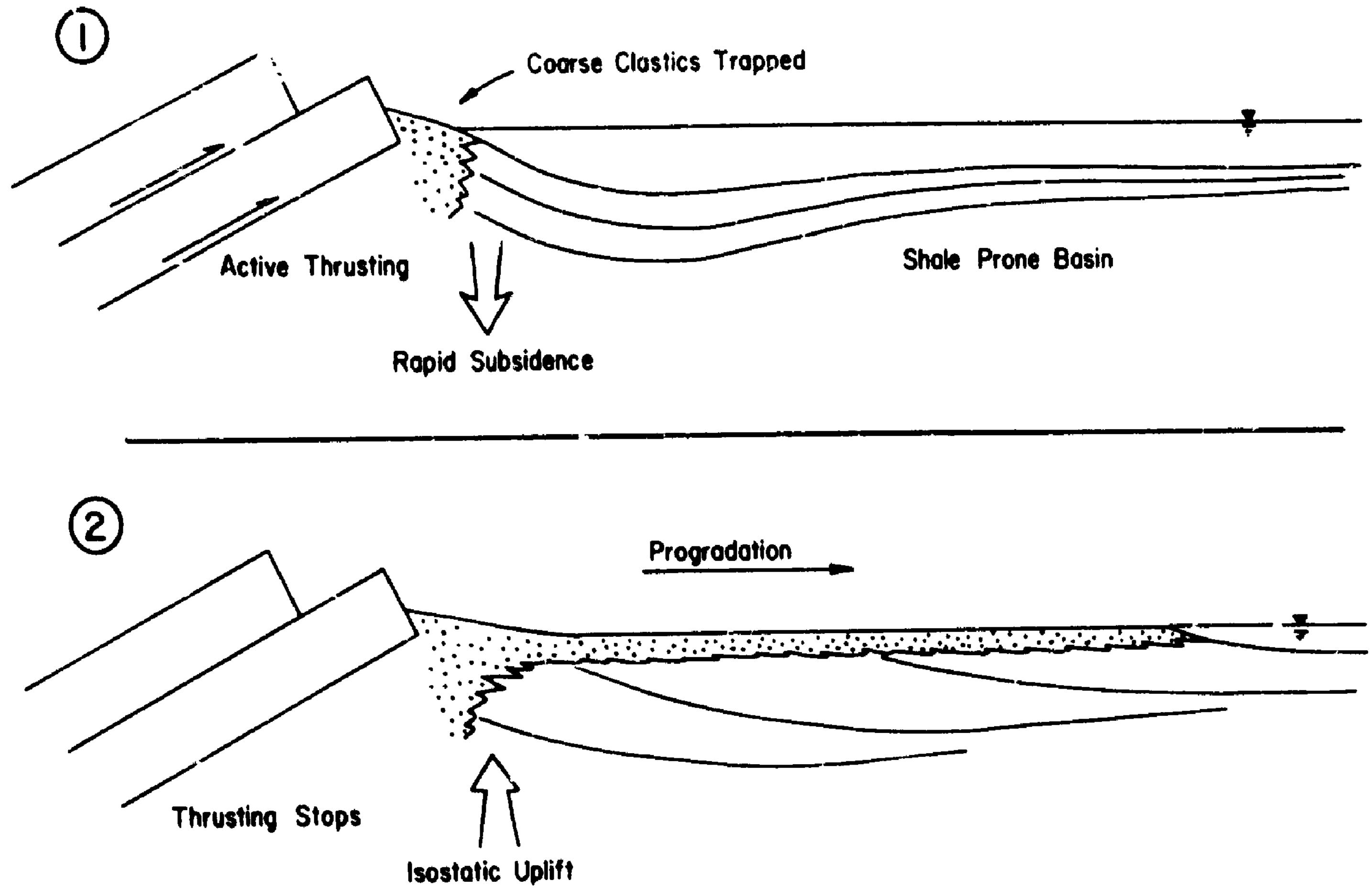
1
Coarse Clastics Trapped
Active Thrusting
Shale Prone Basin
Rapid Subsidence
2
Progradation
Thrusting Stops
Isostatic Uplift

CHAPTER 3

SEDIMENTARY FACIES OF THE CARDIUM FORMATION

3.1 General

The physical properties of sedimentary rocks provide the evidence by which the basin analyst may reconstruct the depositional history of the units. These properties range from the primary physical and biogenic structures contained in the rocks (as observed in outcrop or core), to their large-scale stratal "geometry" (commonly derived through subsurface studies involving geophysical logs or seismic profiles). Given that many of these properties are controlled by the depositional evironment of any given lithologic unit, the investigator must determine which properties to measure, and how much importance to assign to each.

As outlined by Anderton (1985; see also Walker 1984), the first objective of the sedimentolcgist studying ancient strata is to describe the lithologies present in as much detail as is warranted. This done, he/she must then establish a number of descriptive sedimentary facies, based on the physical attributes (lithology, sedimentary structures, etc.) of the rocks. The number of categories (i.e. descriptive facies) will depend upon the objectives of the study. Ultimately, these descriptive categories will be assigned genetic interpretations, from which the interpretive sedimentary facies will be defined. This last step in the analysis is absolutely critical to the further interpretation of the depositional history of the strata, and is based on the geologist's ability to recognize the units as products of specific modes of deposition, active in a given depositional environment. Inaccurate interpretations at this point will confuse facies relationships (both horizontal and vertical) and can only lead to erroneous reconstructions of depositional history.

3.2 Present Data Base

The present study is based on examination of the Cardium Formation in outcrop and in core. This duality presents certain problems, in that the structures observed in any given lithology may not be directly comparable from one "source" to the other. For example, exposures of fine-grained units (shales, siltstones) in outcrop are generally recessive, whereas "cleaner" and more complete vertical sections through them can sometimes be measured in core. With regard to trace fossils, core through interbedded sandstones and shales generally allows better examination of exichnia and endichnia, whereas epichnial and hypichnial traces are best viewed in outcrop. Outcrop has the advantage of allowing for greater two or three dimensional exposure of the rocks, a decided advantage for the recognition of large structures. Paleocurrent measurements are generally only obtainable from outcrop exposures. From a logistic perspective, outcrop is not always easily accessible and generally only a very limited portion of the formation being studied is exposed. The rest (in the subsurface) can only be examined directly as core.

For the present study, I have decided to retain the facies scheme constructed for the Cardium by Walker (1983) and Plint and Walker (1987). This way, the present study will be directly comparable with those works, and with others from the McMaster Cardium Group which have employed that system. This said, I will point out that the data base employed by those authors differs somewhat from that presented here. In particular, facies representing more "basinward" units of the Cardium (e.g. Bickerdike, Hornbeck, Raven River, Dismal Rat and Karr Members) tend to be much less "available" for examination in the present study area than in the earlier studies. In addition, thick conglomerates from the Waskahigan, Burnstick, and Carrot Creek members were not observed in core or outcrop in the present study area. Since the stratigraphic sections measured for this study are neither always complete or representative of the Cardium as a whole, I have not included statistical parameters of the frequency of occurence, average thickness, etc.

Eight facies were described by Walker (1983) in the Caroline-Garrington area. Plint and Walker (1987) subsequently added another eight facies, and Bergman (1984, 1987) subdivided the conglomerates. The six facies described by Walker (1985) at Ricinus have not been described elsewhere in the formation and will not be discussed here.

For this chapter, I have constructed discrete facies associations based on the observed inter-relationships of the facies in both core and outcrop. The name of each facies association is based on the interpretation of the depositional environment of the constituent units, and will provide a convenient reference in later discussions. In the following discussion, individual facies will be presented in the context of the facies association to which they belong, rather than in strictly numerical order. The facies descriptions will be based upon the characteristics of the rocks observed in the present study area only.

3.3 Offshore facies association

This facies association comprises those mudstones, interbedded mudstones and sandstones, and muddy sandstones interpreted to have been deposited in inner to outer shelf environment (i.e. below fairweather wave base). These facies occur in the Kaskapau and Muskiki formations, and in the Nosehill, Bickerdike, Hornbeck, Raven River, Dismal Rat, and Karr allomembers of the Cardium. In the present study area, they are much less commonly cored than the sandstones of the Kakwa Member. In outcrop, the offshore facies association was observed generally only in the Nosehill Allomember and the Kaskapau and Muskiki formations.

3.3.1 Facies 1. Massive Dark Mudstones (Walker 1983)

Description

This facies consists of very dark grey to black mudstones which may be faintly bioturbated, although the lack of silt prevents identification of distinct burrow traces. Pyrite and siderite are locally present. This facies was seen in outcrop only at the Smoky River section (Fig. 3.1a), where sulphurous blebs, probably representing weathered pyrite, and fragments of inoceramid bivalves can be observed.

In core, complete thicknesses for this facies could not be measured, but up to 2 m of Facies 1 was observed in basal units of the Muskiki Formation (overlying the Cardium), and in basal portions of the Dismal Rat Allomember. Thin (less than .5 m thick) black shales, probably assignable to Facies 1, may be observed in some cores near the middle of the Kakwa Member.

Interpretation

Based on the foraminiferal content of this facies, Walker (1983) suggested that they could represent an "inner shallow marine" or "coastal subaqueous" environment, with water depths probably greater than 50 m. The lack of coarser sediment (silt, sand, gravel) indicates that prevailing sediment transport mechanisms did not supply such material. This is suggestive of deep (below storm wave base) water condition relatively far offshore.

Figure 3.1. Offshore facies association. A) Facies 1: Smoky River Section. Note sulpherous "bleb" (arrow, lower left), probably produced by weathering of pyrite. B) Facies 2: core from 4-10-72-13W6 C) Facies 3: core from 4-10-72-13W6 D) Facies 4: note *Arenicolites* (solid arrow), *Asterosoma* (open arrow) and *Planolites* in lower portion of core. Core from 2B-11-67-8W6 E) Facies 5: large burrow in center is *Rosselia*, dark traces in lower left (arrow) are *Helminthopsis*. Core from 11-22-65-6W6. Width of all cores shown is about 7 cm.

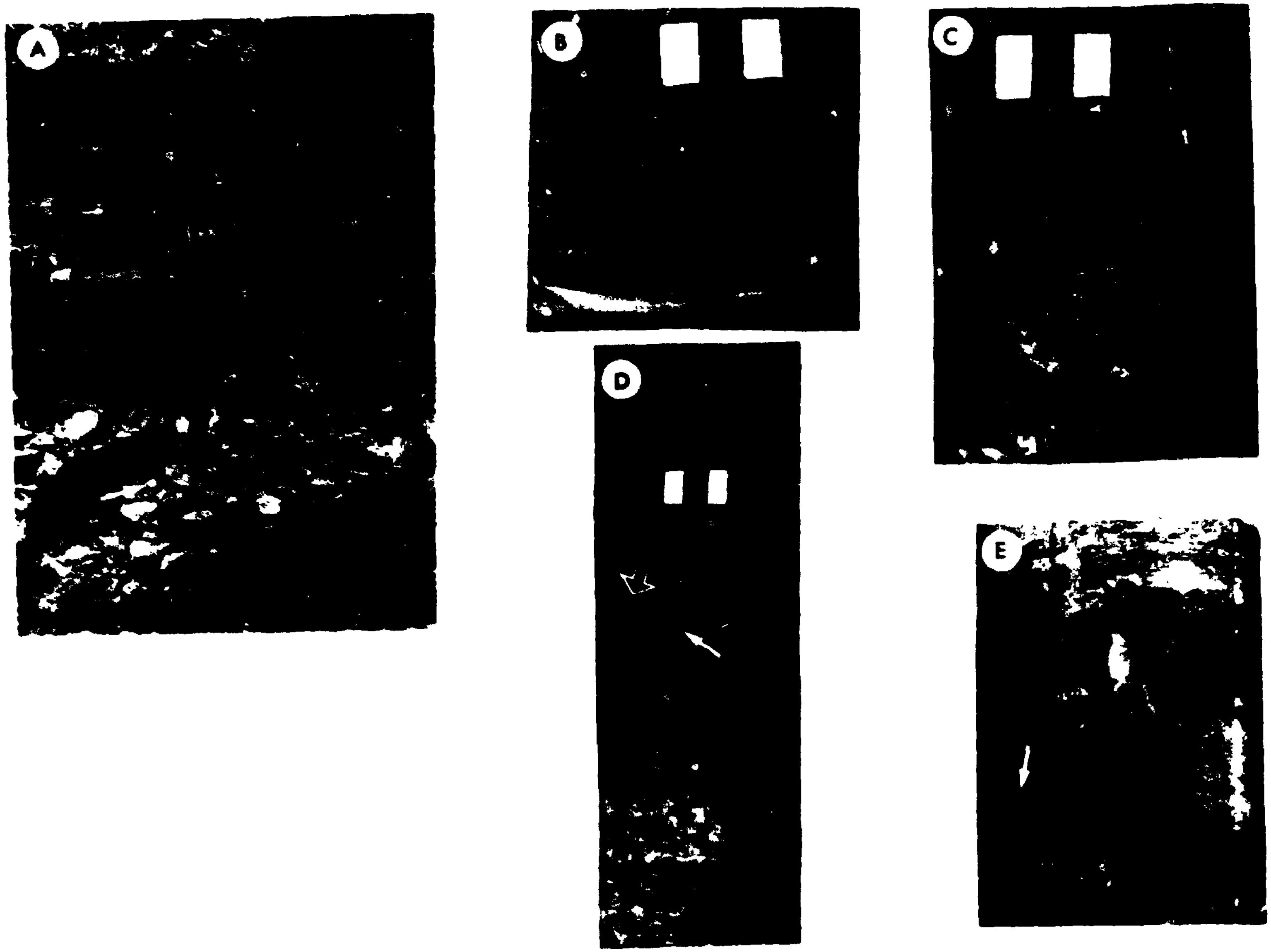
A
B
C
D
E

Figure 3.1 (cont.) F) Facies 7: hummocky cross-stratified sandstone bed, with symmetrical wave ripples preserved on upper bedding surface Nosehill Allomember, Mistanusk Creek section. G) Facies 7: bioturbated (post-depositional) base of a sandstone bed, Opabin Member, Kaskapau Formation, Calliou Creek section. Most traces can be assigned to *Skolithos, Chondrites,* or *Planolites*. H) Facies 15: probable *Chondrites* burrows in upper left. Width of core shown is about 7 cm. I) Large gutter casts from strata of facies 7/15, Muskeg River Railroad cut. J) Few meter thick sandier upwards cycles (arrowed) from Opabin Member of Kaskapau Formation, Murray River section.

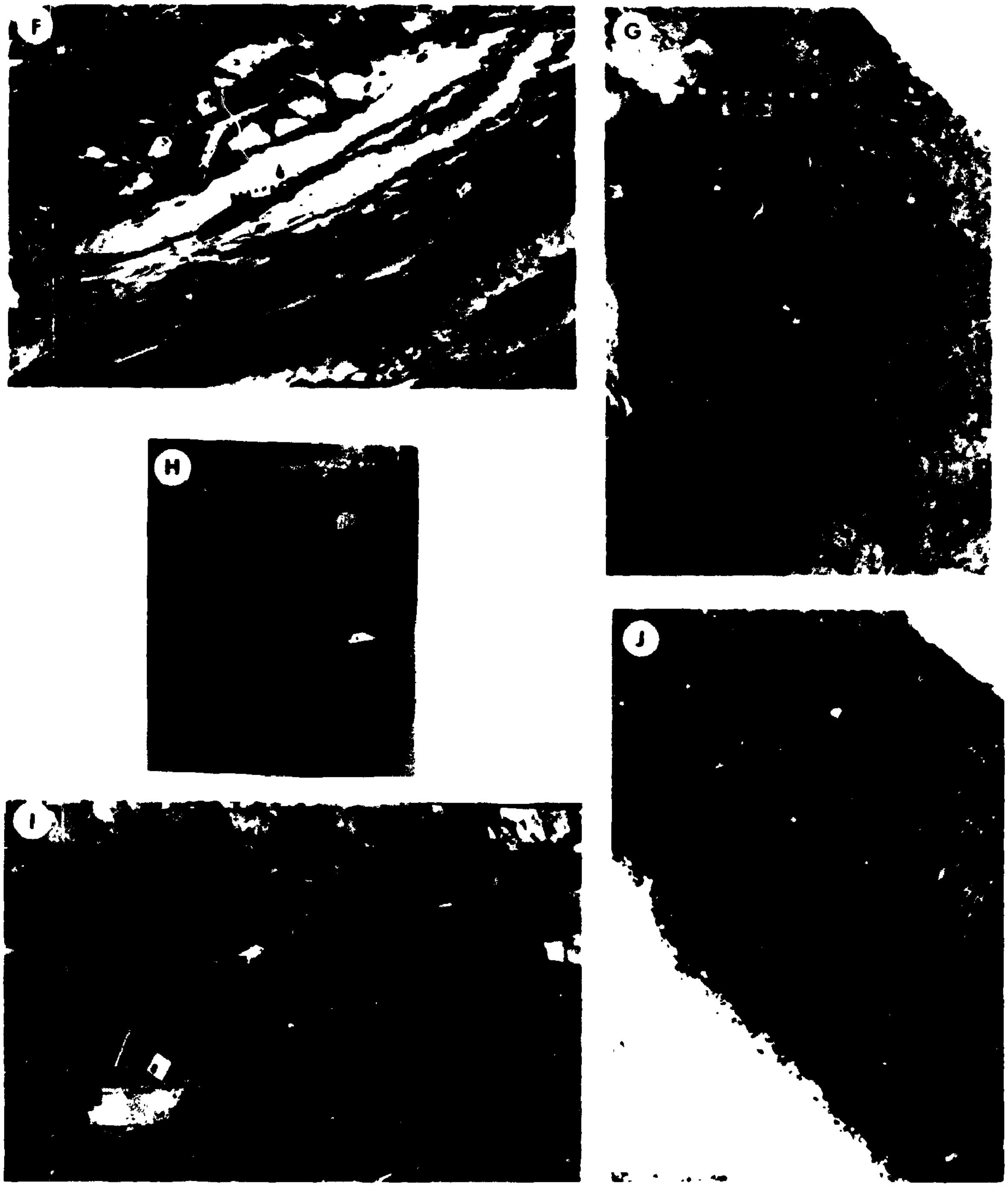
F
G
H
I
J

3.3.2 Facies 2. Laminated Dark Mudstones (Walker 1983)

Description

This facies resembles the mudstones of facies 1 but contains discrete silty laminations 1 to 4 mm in thickness (Fig. 3.1b). Small horizontal burrow systems, and some pyrite and siderite may be observed. I also observed fragments of inoceramid bivalves.

This facies generally occurs as 2 or 3 m thick intervals at the base of sandier upward successions (e.g. Facies 2-3-4-5), although such units tend to be infrequently and incompletely cored in the present study area. Gradational relationships may be noted with the bioturbated muddy siltstones of Facies 3, and the interbedded sandstones and black mudstones of Facies 15.

Interpretation

Walker (1983) again indicated a "coastal subaqueous" or "inner shallow marine" environment of deposition, probably in greater than 50 m water depth based on micropaleontological evidence. The occurrence of silty laminae indicates that material of this size grade could be transported into these environments; they could represent the deposits of geostrophic flows in a distal shelf setting (e.g. Kachel and Smith 1986). The preservation of the laminae suggests that bioturbation was largely inhibited, either by oxygen depleted bottom waters or rapid sedimentation rates (Howard 1975; Nittrouer *et al.* 1986).

3.3.3 Facies 3. Dark Bioturbated Muddy Siltstones (Walker 1983)

Description

Walker (1983) reported that mudstones of this facies are gradational with the mudstones of facies 1 and the muddy sandstones of facies 4. Discrete silty or very fine sand laminae can be observed, but these tend not to be laterally continuous for more than a few centimeters. This is due to the pervasiveness of the bioturbation which provides a "stirred" appearance to the deposit (Fig. 3.1c). *Chondrites* was the only trace fossil observed, and small inoceramid bivalve fragments were observed once.

This facies, like facies 2, tends to have been both infrequently and incompletely cored in the present study area. I am including strata of similar appearance but slightly coarser grain size (fine sand). Furthermore, it is also generally found close to the base of coarsening-upward successions, and in places just above horizons interpreted to be transgressive surfaces ("E" surfaces).

Interpretation

The bioturbated texture of this facies suggests that prevailing environmental conditions permitted the establishment of an abundant, if not diverse, infauna. The stirred aspect of the rock probably represents early post-depositional activity of organisms in non-cohesive substrates, with *Chondrites* indicating the later activity of deep burrowers occupying firmer, more compacted sediment (*cf.* Bromley and Eckdale 1986). Sediment transport mechanisms were probably similar to those active during the deposition of facies 2, although sedimentation rates may have been somewhat slower (Nittrouer *et al.* 1986).

3.3.4 Facies 4. Pervasively Bioturbated Muddy Sandstones

Description

This facies is sandier than facies 3, with relict bedding of 1 to 4 cm thick very fine- to fine-grained sandstone beds, and recognizeable trace fossils (Fig. 3.1d). In the present study area, *Thalassinoides, Rosselia, Asterosoma, Arenicolites, Zoophycus, Chondrites, Skolithos, Terebellina, Rhizocorallium, Planolites, Teichichnus, Helminthopsis,* and indistinct bioturbate fabrics can be observed in units assigned to this facies in core. Sideritic horizons are locally observed.

In core, facies 4 generally occurs as 2 to 4 m thick intervals as part of coarsening- or sandier upward successions (e.g. facies 2-3-4-5, 3-4, 4-5). In outcrop, bioturbated muddy sandstones (to sandy mudstones) 1 - 2 m thick immediately overlying sandier upward successions in the Kaskapau Formation and Nosehill Allomember were assigned to facies 4.

Interpretation

The coarser-grained and more thickly bedded aspect of facies 4 with respect to facies 2 or 3 suggests a position closer to sandy sediment sources (i.e. closer to shore). The abundant and diverse trace fossil assemblage is similar to comparable assemblages assigned to the *Cruziana* ichnofacies by Pemberton and Frey (1984) from the Cardium Formation at Seebe. A similar assemblage was described by Frey and Howard (1985) from the Star Point Formation (Campanian age) of Utah. The latter authors suggested deposition occured in an "intermediate" environment between nearshore and offshore zones.

3.3.5 Facies 5. Bioturbated Sandstones (Walker 1983)

Description

Relative to facies 4, this facies contains a higher proportion of very fine to fine sand, and better preservation of sandstone beds (Fig. 3.1e). The sandstones are sharp-based, generally on the order of a few centimeters thick, and are parallel- to gently undulating with low-angle truncation surfaces. Symmetrical wave ripples can be noted on the upper surface of some sandstones in outcrop. Trace fossils recognized in this facies from the present study include *Chondrites, Teichichnus, Planolites, Rhizocorallium, Arenicolites, Skolithos, Rosselia, Thalassinoides, Terebellina, Asterosoma, Cylindrichnus,* and *Helminthopsis*. Some fragments of inoceramid bivalves are also present.

This facies is gradational with facies 4, 7, and 15, with which it tends to form part of sandier upward successions. The interval occupied by facies 5 is generally

2 to 3 m thick. The greater preservation of bedding results in better outcrop exposure of this facies than facies 4.

Interpretation

Walker (1983) suggested that the trace fossil assemblage of this facies (similar to facies 4) was indicative of a mid-shelf environment, below fairweather wave base. The presence of wave ripple forms in outcrop indicates deposition above storm wave base.

3.3.6 Facies 6. Speckled Gritty Mudstone (Walker 1983)

Description

This facies resembles facies 4 but contains scattered coarse to very coarse sand (chert and quartz grains) and rarely grains up to pebble grade. Bioturbation appears to have eliminated original bedding. Siderite is a common authigenic mineral in this facies This facies was not common in the cores examined (4 occurrences) and was not observed in outcrop.

Interpretation

Although Walker (1983) originally suggested gravel transport by turbidity currents, this mechanism is no longer supported (e.g. Bergman and Walker 1987). Further interpretation is not possible given the very limited data available in the present study area.

3.3.7 Facies 7. Nonbioturbated Sandstones (Walker 1983)

Description

This facies comprises very fine- to fine-grained sandstones (up to several tens of centimeters thick) with thin bioturbated mudstone partings. Sandstones are sharp-based, and contain gently dipping (to undulose) sub-parallel laminations, ripple cross-lamination, and in outcrop, good hummocky cross-stratification (Fig. 3.1f). In outcrop, the bases of the sandstones (where exposed) are commonly bioturbated (Fig. 3.1g), and the upper surfaces preserve wave ripples (either straight crested or interference). Sandstone beds of this facies may be either laterally continuous or discontinuous, with one type tending to dominate at a given outcrop.

In the present case, use of the term "nonbioturbated" is somewhat misleading; trace fossils observed in this facies include *Thalassinoides* and *Planolites* (both fairly common), *Chondrites*, and *Diplocraterion*. This facies is distinguishable from the bioturbated sandstones of facies 5 by the dominance of physical, rather than biogenic sedimentary structures.

Facies 7 is gradational with facies 5, 15, and 16, and may form a substantial portion (up to 7 meters thick) of sandier upward successions.

Interpretation

The dominance of physical sedimentary structures suggests higher sedimentation rates than facies 4 or 5 (Howard 1975). The ichnofossils which are present belong to the *Cruziana* ichnofacies and generally represent the activities of deposit feeders selectively mining the substrate (Pemberton and Frey 1984).

Although the origin of hummocky cross-stratification remains an issue of considerable debate, it would appear that strong oscillatory wave motion (with or without a superimposed unidirectional flow) is generally considered the principal formative agent (e.g. Allen 1985; Arnott and Southard 1990; Nottvedt and Kreisa 1987). Leckie and Krystinik (1989) recently summarised the paleocurrent evidence from several hummocky cross-stratified sandstones inferred to have been deposited in an inner shelf setting. They concluded that the sand was emplaced by shore-normal flows directed offshore, rather than by shore-parallel geostrophic flows as suggested by some authors (but see Duke 1990). In the present case, the bases of the hummocky cross-stratified sandstones (where visible) tended to be bioturbated, and thus no paleocurrent information was available from these beds.

3.3.8 Facies 15. Interbedded sandstones and black mudstones (Plint and Walker 1987)

This facies consists of interbedded very fine- to fine-grained sandstones (up to a few centimeters thick) and black mudstones (Fig. 3.1h). Eyles and Walker (1988) labelled such units "facies 7A". The sandstones are sharp-based and preserve ripple cross-lamination, ripple form sets, and undulose to horizontal lamination. Small shale intraclasts can be noted in the sandstones. Bioturbation is generally low, although ichnofossils observed in units assigned to facies 15 include *Teichichnus, Terebellina, Planolites, Thalassinoides* and *Chondrites*. Fugichnia can be observed in places, but are not abundant.

This facies tends to form part (a few meters thick) of the sandier upward successions which are common in the offshore facies association. Facies 15 may be gradational with facies 2 (change of grain size and lamina thickness) and facies 7; an interbedding of facies 7 and 15 is commonly observed. Large gutter casts (several decimeters thick and a few meters wide) are observed locally in outcrop in strata consisting of this facies interbedded with facies 7 (Fig. 3.1i).

Interpretation

Plint and Walker (1987) proposed that the interbedding of facies 15 with facies 7 indicated that the thinner sandstones of this facies were generated by smaller (or waning) storms than the thicker sandstones of facies 7. In some instances, it is probable that facies 15 also represents sedimentation further offshore than facies 7. Again, the dominance of physical sedimentary structures is interpreted as an indication of high sedimentation rates. Based on paleocurrent evidence from the Opabin and Haven members of the Kaskapau Formation, Hart *et al.* (1990)

suggested that it is the thinly bedded sandstones of units comparable to this facies which probably represent the product of geostrophic flows, rather than the thicker-bedded sandstones of facies 7.

3.3.9 Sandier upward successions

Good outcrop exposures of the offshore facies association typically consist of stacked sandier upward cycles, each a few to several meters thick (Fig. 3.1j). These can be described in terms of successions composed of facies 2 to 15, 15 to 7, 4 to 5, 2 to 4 to 5, etc. Below the Kakwa sandstones, these smaller cycles are generally grouped to form larger sandier upward successions tens of meters thick, presenting the appearance of a compound cyclicity. Where good exposure is available, both orders of cycle can be seen to have high lateral continuity.

Similar successions from the Raven River Allomember have been described by Walker and Eyles (1988) at Willesden Green. As noted in Chapter 2, those authors interpreted each few meter thick sandier upward unit in terms of rapid tectonic movements. An alternative explanation (preferred here) is that the cycles represent the sedimentary response to Milankovitch-type climatic forcing. The cycles observed here are quite similar to those observed by Barron *et al.* (1985), Kauffman (1988) and Wright (1989) in deposits of Upper Cretaceous age from the southwest United States. These studies suggested that climate, and in particular precipitation (and hence runoff and sediment supply), was sensitive to variations in orbital parameters during the Cretaceous, much as it is at the present. Milankovitch theory has been discussed previously (Chapter 2), and the interested reader is referred to the references cited for further information.

3.3.10 Siderite

The occurence of concretionary siderite horizons in units of the offshore facies assemblage deserves special mention, although I will not erect a new facies to cover this lithotype. The following discussion will be based upon observations made mostly from siderites of the Kaskapau Formation and Nosehill Allomember in outcrop. Eight thin sections were examined from samples of these rocks. Bartlett (1987) has also studied sideritic horizons from offshore units of the Raven River through Karr allomembers in core.

Description

Sideritic horizons, generally a few to over 10 cm thick, commonly cap the sandier upward successions of the offshore units occuring below the Kakwa sandstones in outcrop. These horizons can generally be traced laterally by eye over the entire extent of any given outcrop. It will be shown in Chapter 6 that where close correlation with well logs is possible, these horizons can be correlated with resistivity markers which can be traced on a regional scale (e.g. Plint

1990).

There are two main modes of occurence. The first of these (Fig. 3.2a) consists of concretionary layers, in places composed of discrete nodules or, alternatively, of a layer of relatively uniform thickness. Siderite here occurs as crypto- to microcrystalline pore-filling cement, typically comprising about 70 - 80% of the sample by volume (visual estimates). The rest of the rock is generally composed of silt-sized quartz and clay minerals (and micas?), with minor chert and glauconite. Pyrite is a very minor authigenic constituent, and was recognized only by backscatter electron microscopy and microprobe analysis (see Chapter 5). These horizons may be burrowed (Fig. 3.2b), and may have several cross-cutting burrow phases or burrows with meniscate backfills. These burrows are generally circular in cross-section, and thus appear not to have been deformed by compaction.

The second mode of occurence consists of the "gritty" or granular siderites (Fig. 3.2c,d,e). These may contain pebble to cobble sized intraclasts of sideritic siltstone or silty siderite, and have silt to pebble size grains of quartz, chert, rock fragments, organic debris (fish scales, teeth, etc.) and phosphatic (fecal?) pellets. Generally, these detrital constituents are set in a matrix of sideritic siltstone or silty siderite. Both types of siderite may be found at different places on the same correlative horizon

Figure 3.2. Siderite. A) Massive concretionary siderite, with (?) dolomite-filled septarian fissures. B) Photomicrograph of different burrowing phases in silty siderite, E1 surface, Mistanusk Creek section. C) Granular siderite, with large sideritic intraclasts, in silty siderite matrix. E1 surface, core 6-15-65-13W6. Note truncation of laminae in underlying sandstone bed (arrow). D) Photomicrograph of granular siderite showing siltstone intraclast (S), chert (C) and phosphate (P) grains in silty, sideritic matrix. Opabin Member, Kaskapau Formation, Calliou Creek section. E) Photomicrograph of granular siderite showing inoceramid fragment (top) and chert grains (C) in silty, sideritic matrix. E7 surface, Smoky River section. Note similarity to 3.2D.

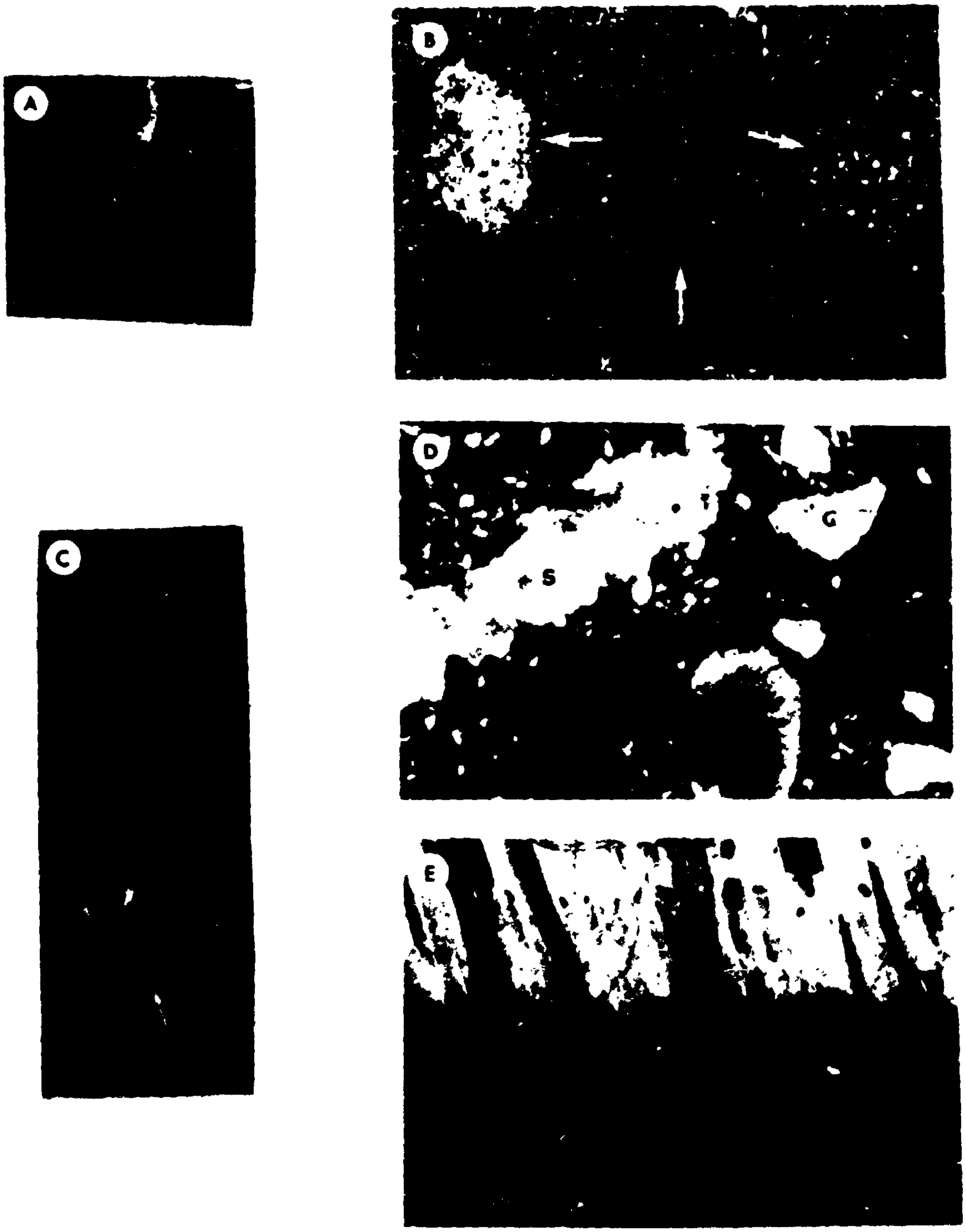
A
B
C
D
S
G
E

(Fig. 3.2b, 3.2c; Chapter 5).

Interpretation

The high percentage of siderite in the concretionary layers, combined with the crystal size and burrowing relationships all imply very early diagenetic siderite precipitation close to the sediment/water interface in marine to brackish conditions (Gautier 1982). The sideritic intraclasts appear to represent concretionary layers which have been eroded after minimal burial in the sediment column. Erosion could have been effected by tidal, thermohaline, or storm-induced flows.

The occurence at the top of sandier upward successions and the regional extent of these beds suggests that they formed during transgressions. At such times, the quantity of detrital material supplied from the shoreline would be expected to diminish significantly. During such intervals, clastic material which *is* supplied offshore would tend to be supplied by "unusual" modes of transport (e.g. biologically - *cf.* Jolliffe and Wallace 1973; Leithold 1989) and the relative importance of chemical sedimentation would be augmented (e.g. Baum and Vail 1988).

A problem with this scenario is that siderite is generally not expected to precipitate from marine porewaters (e.g. Berner 1981). It is generally held that a bacterially-mediated chemical zonation develops in the sediment column, and that siderite can not be precipitated until the sediment has passed below the oxic and sulphate reducing layers (Irwin, Curtis and Coleman 1977). At this point, siderite precipitation will occur in the methanogenic zone. Early siderite precipitation could occur in environments of very low sulphate concentrations (the "post-oxic" enviroments of Berner 1981), but the dissolved sulphate concentrations of seawater would normally prevent the development of such a zone.

A solution to this problem may have been supplied recently by Pye *et al.* (1990). These authors documented rapid siderite precipitation in a modern intertidal area, where the porewaters consist of seawater and sulphate is not limited. They suggested that siderite could precipitate wherever the rate of iron reduction exceeds the rate of sulphate reduction. In such cases, insufficient sulphate would be available to precipitate all the reduced iron as pyrite (or iron monosulphides) and siderite could form. This mechanism provides a possible explanation for early siderites in rocks from the Cretaceous Western Interior Seaway, although details of its application are beyond the scope of the current project.

3.4 Shoreface sandstone facies association

The sandstones of this facies association overlie the mudstones and sandstones of the offshore facies association. In almost all cases, they can be assigned to the Kakwa Member of the Cardium. In outcrop, they tend to be highly resistant, and tend to form prominent ridges or escarpments; they are generally well-exposed. In the subsurface, they tend to be the most frequently cored portion of the Cardium in the study area.

3.4.1 Facies 16, Thick-Bedded, Non-Bioturbated Sandstones (Plint and Walker 1987)

Description

This facies typically consists of a gradually coarsening upward assemblage of very fine- to fine-grained sandstones. The dominant sedimentary structure in outcrop consists of swaley cross-stratification (Fig. 3.3a). Comparison of outcrop exposures with equivalent units in core (Figs. 3.3b,c) demonstrates that the low angle truncation surfaces seen in core represent sections through swaley cross-stratified sandstones. They can be distinguished from medium-scale cross-bedding on the basis of dip angle and the nature of the contacts between cross-sets (e.g. Hart 1990). Ripple cross-lamination is only observed locally.

Occasional higher-angle scours can be seen in core, and in outcrop. Generally though, the swales are wide and shallow. Scours locally contain pebbles (pebble size and thickness of the pebble layers generally increasing upward; Chapter 4), or siderite "clasts". Bioturbation is rare, with *Skolithos* (generally sideritized) being the most common form. *Teredo* borings were noted from the interior of a single siderite "clast" and *Phycodes* was also observed once.

Figure 3.3. Shoreface sandstone facies association. A) Facies 16: swaley cross-stratification, Kakwa Member, Gundy Station section. B) Facies 16: low-angle intersections in core through swaley cross-stratified sandtones. Kakwa Member C) Facies 16: low-angle intersections in core through swaley cross-stratified sandstones. Kakwa Member D) Facies 17: medium-scale cross-bedding, Kakwa Member, Noetai Hill section. Pocket knife (arrow) for scale. E) Facies 17: sigmoidal solitary cross-bed set, interpreted as being produced by onshore migration of a ridge during fairweather periods. Kakwa Member, Bay Tree section. F) Facies 17: planar-laminated sandstone, Kakwa Member, core 10-31-67-4W6. G) Facies 17: root traces from top of planar (beach) laminated sandstones, Kakwa Member, Mistanusk Creek section. H) Facies 17: *Macaronichnus*, Kakwa Member, Mistanusk Creek section. Width of all core shown is about 7 cm.

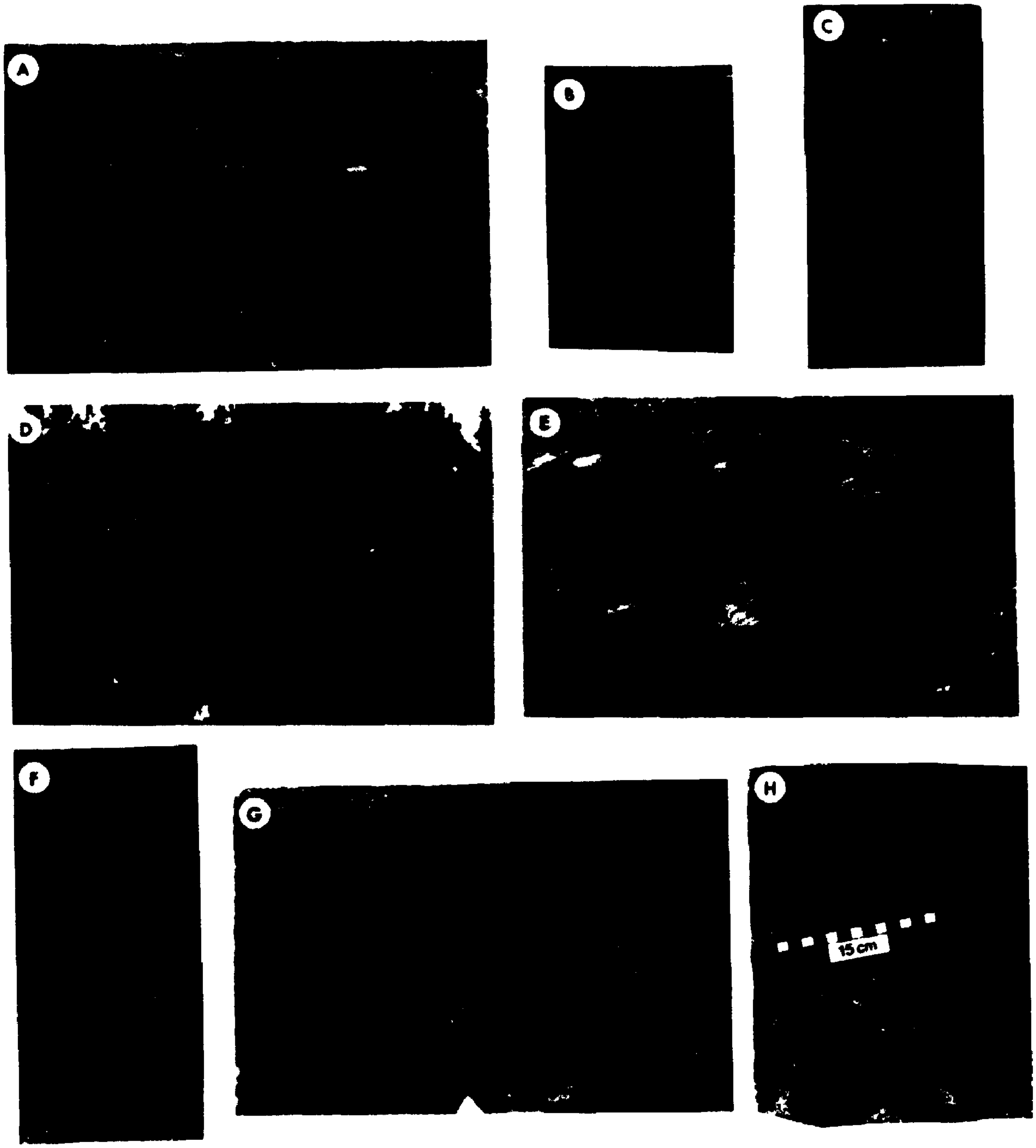
A
B
C
D
E
F
G
H
15 cm

Small fragments of inoceramid bivalves are not uncommon and once, an accumulation of sideritized bivalves formerly attributed to the genus *Cardium* was observed once along the base of a shallow scour fill. Thin laminae of highly carbonaceous material can be observed locally.

The thickness of units comprised of facies 16 is highly variable, from over 20 m (in some outcrops), to less than 2 m (in core) with an average thickness of about 7 - 8 m. In general, this facies occupies a position above facies 7 or 15 of the offshore facies association. In places, it can be seen to be gradationally overlain by planar laminated sandstones of facies 17. As noted previously, pebble stringers (single grain thickness) to beds (up to a couple decimeters thick) of facies 8 can locally be observed in the upper portions of this facies.

Interpretation

The dominant sedimentary structure of facies 16 is swaley cross-stratification. This structure was originally interpreted to represent deposition *above* fairweather wave base (Leckie and Walker 1982) and the present data from the Cardium Formation is in agreement with such an interpretation. The occurence of facies 16 gradationally above facies 7, and locally gradationally below planar-laminated sandstones of facies 17 interpreted as beach laminations (see below) is strongly suggestive of a shoreface setting. The sparse trace fauna, dominated by

Skolithos, indicates a high-energy environment.

Like hummocky cross-stratification, the origin of swaley cross-stratification remains a subject of some controversy (e.g. Allen and Underhill 1989, 1990; Hart 1990; Sun 1990). It is probable though, that the "hummocky cross-stratification" described by Greenwood and Sherman (1986) from the surf zone would be described as *swaley* cross-stratification by those familiar with the geometry of the latter in outcrop. Oscillatory and/or combined flows above fairweather wave base are thus probably responsible for the formation of swaley cross-stratification.

The association of siderite with shell lags, *Skolithos* burrows, and wood suggests that this mineral formed early in the diagenetic history of the sandstones. I suggest that decaying organic matter might have created local reducing environments. Any H_2S generated could have escaped through the porous sandstone (*cf*. Pye *et al*. 1990) leaving reduced iron to react with dissolved bicarbonate.

3.4.2. Facies 17. Cross-bedded and Parallel-laminated sandstones (Plint and Walker 1987)

Description

This facies consists of the cross-bedded to parallel-laminated sandstones which tend to form the upper portion of the Kakwa Member. A repetitive sequence of sedimentary structures can generally be measured, with medium-scale cross-bedding near the base of the facies (Fig. 3.3d). A special type of cross-bedding deserves special mention. This is represented by solitary sets of sigmoidal cross-beds with preserved topsets and tangential to planar toesets (Fig. 3.3e). Where observable, paleocurrent evidence suggests these features were generated by bedforms migrating onshore. They tend to be found towards the top of shoreface successions. These structures are closely comparable to those produced by ridges (of ridge and runnel systems) migrating onshore under the influence of shoaling fairweather waves (Davis *et al.* 1972), and are interpreted here as such.

The cross-bedded sandstones generally pass upwards into parallel-laminated sandstones towards the top (Fig. 3.3f). Grain size decreases upward, typically from medium-grained sandstones at the base, to fine-grained sandstones near the top. Set thickness of the cross-bedded units is variable, ranging from a few centimeters to over 1 meter. The toesets of the cross-beds are locally pebbly, especially in the lower portions of this facies. Carbonaceous laminae, intraclasts and irregular scour and fill structures may be noted in some sections near the base of this facies. Parting lineations can be observed in some outcrop exposures of the parallel-laminated sandstones. A rooted to bioturbated (pedoturbated?) and locally shaley horizon up to 30 cm thick generally occurs at the top of the facies (Fig. 3.3g).

Trace fossils are not commonly observed in facies 17 sandstones. An exception to this is *Macaronichnus* (Fig. 3.3h), which tends to be present near the transition zone from cross-bedded to parallel-laminated sandstones. *Skolithos, Bergaueria, Paleophycus,* and *Arenicolites* can also be observed. Molds of oyster shells were observed once in parallel-laminated sandstones from Cutpick Hill (Chapter 5).

The thickness of this facies is variable, but is generally between 5 and 10 meters. It can locally be found interbedded with conglomerates of facies 8; generally, but not always (see Chapter 4), the conglomerates comprise only a minor portion of the section in these cases. Wave-rippled granule to pebble conglomerates may be present near the base of facies 17. Parallel-laminated sandstones assigned to this facies gradationally overlie the swaley cross-stratified sandstones of facies 16 in some instances. The sandstones of this facies are most commonly gradationally overlain by coals or mudstones of the non-marine facies association.

In core, the portion of the Kakwa Member generally occupied by facies 17 may be replaced by rocks of the non-marine facies association. In these cases, cross-bedded or planar laminated sandstones can be attributed to either facies 17 *or* facies 21 and distinction between the two is impossible. These sandstones will be designated by the symbol 17/21 in subsequent chapters to avoid attributing facies names (normally objectively defined) on the basis of the inferred depositional environment.

Interpretation

Like facies 16, the dominance of physical sedimentary structures over bioturbation suggests a high-energy environment. *Macaronichnus* is considered as diagnostic of high-energy intertidal to shallow subtidal environments (Clifton and Thompson 1978). The observed association of cross-bedded and laminated sandstones probably indicates deposition in a shoreface setting. The cross-beds could have been generated by longshore, rip, or possibly even tidal currents (see Chapters 4 and 5); in outcrop, paleocurrent evidence could sometimes be employed to distinguish between these possibilities. Parallel-lamination has been reported from both the surf and swash zones (e.g. Davidson-Arnott and Greenwood 1976; Hunter, Clifton and Phillips 1979). Where found towards the top of facies 16 or 17, parallel-laminated sandstones probably represent beach laminations from the swash zone as suggested by Plint and Walker (1987), although similar structures have been observed from intertidal flats of estuarine environments (Hart and Long 1990a).

Plint and Walker (1987) suggested that the abrupt upward transition from facies 16 to facies 17 represented the transition from the lower to upper shoreface environment.

A similar interpretation was presented by Rahmani and Smith (1988) for the Cadotte Formation. These interpretations are based on the work of Hunter *et al.* (1979) who reported that a grain-size break could be developed by the lateral migration of rip channels in a barred nearshore system. Although I do not wish to completely rule out the existence of such successions, I will argue later (Chapters 5 and 6) that *in the present case*, this explanation is unsatisfactory.

3.4.3 Facies 8 Conglomerates (Walker 1983)

Conglomerates interpreted to have been deposited in a shoreface setting were observed locally (generally in outcrop). A full description of the nature and origin of these units will be deferred to the next chapter, which specifically examines these units. It will be noted here that three conglomerate types were originally proposed by Walker (1983): clast-supported, mud-supported and thin gravel layers. Later additions and modifications have been proposed by Bergman (1987), Bergman and Walker (1987), Plint and Walker (1987) and Walker and Eyles (1988). In the present study, three main types of conglomerate were observed: clast-supported, sand-supported, and thin gravel layers. Mud-supported conglomerates (the most abundant type in Walker's 1983 study) were not observed.

3.5 Non-marine facies association

These rocks lie conformably above the Kakwa sandstones and belong to the Musreau Member of the Cardium Formation. Occasionally, non-marine sandstones appear to have channeled into the Kakwa Member and replaced the interval normally occupied by facies 17. In both outcrop and in core, the Musreau Member is dominated by fine-grained facies; outcrops of these units tend to be rubbly and are generally covered. In outcrop, this facies association is generally several tens of meters thick. In the subsurface its thickness can be seen to decrease to the northeast, pinching out to 0 meters thick close to the progradational edge of the underlying Kakwa Member sandstones (*cf.* Plint *et al.* 1988).

3.5.1 Facies 18. Coal (Plint and Walker 1987)

Description

Beds of vitreous coal up to 40 cm in thickness can locally be present. They are generally found directly above the shoreface sandstones of the Kakwa Member, but can occur higher up in the section as well. Coals of this facies can contain authigenic pyrite, and variable amounts of shale. A gradation between shaley coals and coaly shales (assigned to facies 19) may be observed.

Interpretation

Coals are formed when rising base level buries thick organic deposits before oxidisation can occur. Thick accumulations of organic material might be expected in lagoons, bogs, marshes etc., although it has been argued that some lagoonal marshes do not contain enough organic matter to be converted into coals upon burial (Jones and Cameron 1988).

3.5.2 Facies 19. Black, nonmarine mudstones (Plint and Walker 1987)

Description

This facies consists of the dark mudstones which tend to immediately overlie the Kakwa sandstones. A gradation can be noted between this facies and facies 18, 20 and 22. Oyster shells (generally fragmented) are sometimes present in this facies. Units assigned to this facies range in thickness from .25 to about 2 meters thick, with an average of about a meter.

Interpretation

Plint and Walker (1987) suggested deposition of facies 19 in a lagoonal setting and the present observations agree with that interpretation. The lack of coarser (silt or sand sized) sediment suggests a quiet water environment. The gradational relationship observed with facies 18 could represent variations in vegetation accumulation rates, due to differences in water depth or sediment influx.

3.5.3 Facies 20. Carbonaceous black mudstones and sandstones (Plint and Walker 1987)

Description

This facies consists of dark mudstones, similar to facies 19, with variable amounts of siltstone or sandstone. The siltstones can be planar-laminated, undulose-laminated or ripple cross-laminated (Fig. 3.4a), and commonly have been disturbed by syn-sedimentary deformation (Fig. 3.4b). Sandstones tend to be convoluted. Body fossils are not commonly observed, but include gastropods and bivalves. Bioturbation is not common, but some sandy intervals (a few 10's of centimeters thick) contain densely-packed exichnial burrows (Fig. 3.4c) generally close to 1 centimeter in diameter (probably assignable to *Planolites* or *Thalassinoides*). Other inderterminate bioturbate textures, and posssibly *Terebellina*, can be observed but are not common. In an outcrop of the Musreau Member on Tepee Creek, 3.2 m of dark mudstones assigned to this facies contains sand-filled gutter casts (Fig. 3.4d), which become progressively more numerous and larger towards the top of the unit. Some sideritic horizons are present in this facies.

In core, facies 20 is gradational with facies 19, 21, and 22. Coarsening and fining-upward successions are both present in this facies, and in composite units with facies 20 and any of facies 19, 21, and 22. These units are generally 4 to 6 meters in thickness, but can be over 13 meters thick. In outcrop, intervals presumably occupied by this facies tend to be rubbly and poorly exposed;

Figure 3.4. Non-marine facies association. A) Facies 20: ripple cross-laminated silty sandstones, core 6-36-66-8W6. B) Facies 20: convoluted mudstones, core 10-1-67-8W6. C) Facies 20: intensively burrowed sandy mudstones, core 10-26-69-11W6. D) Facies 20: sandstone-filled gutter cast in black non-marine mudstones, Tepee Creek section. E) Facies 21: cross-bedded and planar-laminated sandstones, Tepee Creek section. F) Facies 21: cast *Teredolites*-like borings from branch mold, Cutpick Hill section. G) Facies 21: angular mudstone intraclasts in fluvial sandstone incised into upper portion of Kakwa Member (see Chapter 5), core 15-16-68-13W6. H) Facies 22: Rooted mudstone. Pedogenic slickensides, core 6-8-71-13W6.

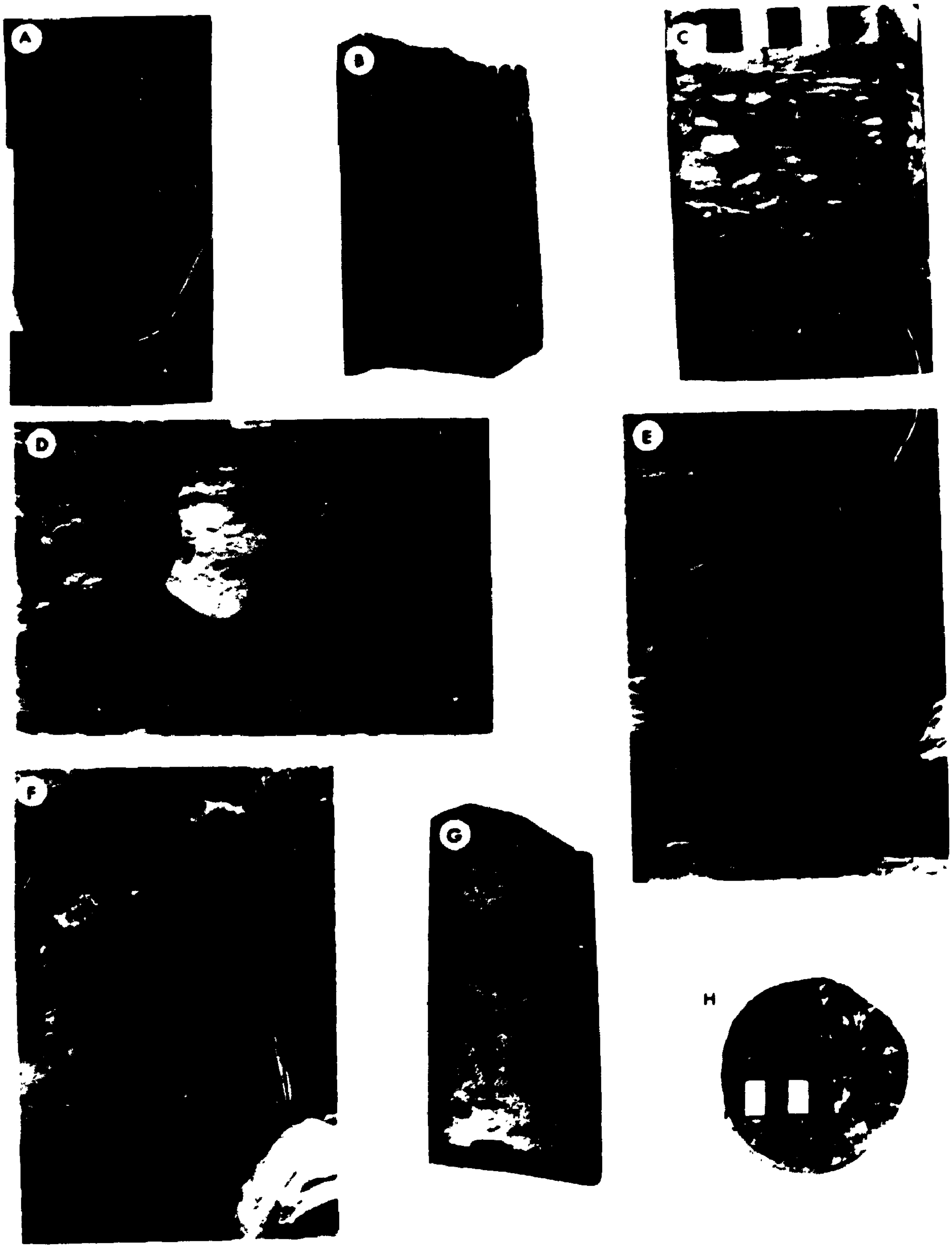
A
B
C
D
E
F
G
H

distinction between this facies and facies 22 becomes difficult.

Interpretation

Plint and Walker (1987) interpreted this facies as deposits of a brackish lagoon or coastal lake. Here, I suggest that this facies is more likely the product of a variety of processes, operative on a low-gradient floodplain.

Laminated to ripple cross-laminated, very fine-grained sandstones and siltstones interbedded with mudstones closely resemble the millimeter to centimeter-scale sandy and silty rhythmites described by Farrell (1987) from core through levée and splay deposits of the Mississippi River. She interpreted each silt/sand layer as the product of a single sheet flood spreading from the flood-stage river into adjacent lakes and backswamps. Coarsening-upward successions in these deposits, similar to those observed here, were interpreted by her as representing incipient crevassing and progradation of a splay into a lake/backswamp, whereas fining-upward successions represented splay abandonment. Intensely burrowed intervals ("wormy fabrics" of simple horizontal to sub-vertical burrows .8 to 3 centimeters in diameter) were locally present. Farrell also reported intergradational relationships with rooted, concretionary, slickensided to massive mudstones similar to facies 22 of the Cardium

Formation (see below).

Gutter casts have been reported from lacustrine deposits (T. Martel, unpublished manuscript) and shallow lagoonal deposits (Plint 1983). Plint and Walker (1987) suggested that earthquake-triggered degassing or dewatering might be responsible for much of the convolution noticed in this facies. Some of the observed deformation textures might have been created by large vertebrates; Smith (1983), for example, noted that the movement of ungulates (moose) through shallow lakes in proximity to the Saskatchewan River could completly disrupt original bedding.

3.5.5 Facies 21. Cross-bedded sandstone (Plint and Walker 1987)

Description

This facies consists of medium-scale cross-bedded sandstone, and some ripple cross-laminated sandstones. In outcrop, trough- , planar-tabular and planar-tangential cross-bedding can be observed (Fig. 3.4e). I am expanding this facies to include parallel-laminated sandstones which can be either interbedded with the other sandstones or isolated. Coaly plant debris or branch molds (which may be bored; Fig. 3.4f) and angular to rounded intraclasts of mudstone (which may be sideritic) up to several centimeters thick (Fig. 3.4g), can be noted in this facies both in outcrop and in core. Extraformational pebbles (principally of chert) are only observed in units which appear to have cut into the Kakwa Member, occupying the place of facies 17 (see Chapters 5 and 6).

Facies 21 can be gradational with facies 20 (ripple cross-laminated sandstones), and where facies 21 replaces facies 17, distinction between the two can be problematic at times. Sharp-based facies 21 sandstones commonly become finer-grained upward into facies 20, but coarsening-upward successions (20 to 21) are also observed. The thickness of this facies is highly variable, from less than a meter to about 7 meters. The thinner units tend to be dominated by ripple cross-lamination, whereas the thicker sandstones are dominated by medium-scale cross-bedding. In outcrop, the thinner (meter scale) sandstones can be seen to be lenticular, pinching out over a few to several tens of meters, within fine-grained units of facies 20 or 22. In nearly all cases, sandstones facies 21 are clearly subordinate volumetrically to the fine-grained units.

Interpretation

The stratigraphic context (interbedded with facies 20 and 22), combined with the lenticular nature, lack of shallow marine trace fauna and paleocurrent evidence (see Chapter 5) all suggest that the sandstones of this facies were probably deposited by rivers. These sandstones appear closely comparable to fluvial sandstones described by Rust, Gibling and Legun (1984) from Pennsylvanian strata in Nova Scotia. The size and morphology of the rivers appear to have been highly variable. Smaller, more lenticular sandstones might have formed as meandering distributary channels feeding into lakes or lagoons, whereas thicker sandstones with abundant planar-tabular cross-bedding and planar lamination probably represent the main extrabasinal (Galloway 1981) fluvial channels. The origin of the channeling into the Kakwa sandstones will be discussed in Chapter 6.

3.5.6 Facies 22. Rooted mudstone (Plint and Walker 1987)

Description

Generally massive (to rubbly) grey, grey-green and brown mudstones, in places with *in situ* root traces, "waxy" appearance, and pedogenic slickensides (Fig. 3.4h), are assigned to this facies. Disseminated carbonaceous debris, discrete plant debris (e.g. leaf imprints, coaly plant fragments) and some amber are also present in rocks assigned to facies 22. Spherulitic siderites, and siderite concretions may also be present.

This facies can be observed to be gradational with facies 19 and, more commonly, facies 20. It is commonly 1 to 2 meters thick. As noted previously, fine-grained facies such as this tend to be poorly exposed in outcrop, and complete thicknesses can be hard to measure.

Interpretation

The characteristics of facies 22 are considered diagnostic of paleosols. Preservation of root traces, lack of stratification, and grey colouration are suggestive of reducing conditions developed in waterlogged soil (gley soils; Wright 1989). Siderite concretions are common in the lower portions of gley soils (Wright 1989). Although spherulitic siderites are poorly documented from modern soils, their occurrence in paleosols is attributed to formation in the lower portions of the soil profile (Tucker 1981). Pedogenic slickensides are characteristic features of vertisols, soils which develop in response to seasonal wetting and drying, and are well-documented from modern and ancient soils (Gray and Nickelsen 1989). Gradational relationships with facies 19 and 20 suggest soil development took place during intervals of locally reduced sedimentation rates. The vertisols may have developed on topographically higher areas such as levées, while gley soils developed in low-lying areas.

3.5.7 Fluvial architecture in the Cardium Formation

With the exception of the very basal part of the Musreau (dominated by facies 18 and 19), most of the member consists of fine-grained deposits interpreted as lacustrine, overbank and splay deposits, any of which may be altered by soil-forming processes. Observed paleosols suggest wet (either permanently or seasonally) conditions. The sandstones tend to be lenticular in cross-section, suggesting a ribbon-like geometry in plan. Lateral accumulation surfaces and fining-upward channel sequences, typical of meandering fluvial systems (e.g. Walker and Cant 1984), are not well developed. These characteristics are suggestive of an anastomosing fluvial system (Smith 1983, Rust *et al.* 1984).

Anastomosing rivers are typically developed in areas undergoing rapid base-level rise (due to subsidence *or* sea level rise), with abundant (fine) sediment supply, and a wet enough climate to maintain stable channels (Smith 1983). Rapid subsidence is interpreted to have led to the formation of ribbon-like sandstones, greater avulsion, and a dominance of fine-grained lithologies in the Glenns Ferry Formation of the U.S. western interior (Krause and Middleton 1987).

3.6 Petrography of the Cardium Sandstones

In this section, I will present the results of a petrographic study of Cardium sandstones. Sixty-one thin sections of sandstones from the Kakwa and Musreau members (facies 16, 17, 21; outcrop and core) were examined petrographically to determine their detrital mineralogy and textural relationships, and to assess whether early diagenetic minerals might provide evidence of depositional events. Detailed paragenetic sequences for these samples were not constructed. Percentages of detrital constituents were estimated visually, and sandstone types were named using the classification of Folk (1980; Fig. 3.5).

3.6.1 Thin section descriptions

Twenty-six samples were examined from the fine- to very fine-grained swaley cross-stratified sandstones of facies

Figure 3.5. Classification of sandstones from the Kakwa and Musreau members of the Cardium Formation, using system of Folk (1980). Q - quartz; F - feldspar; RF - rock fragments.

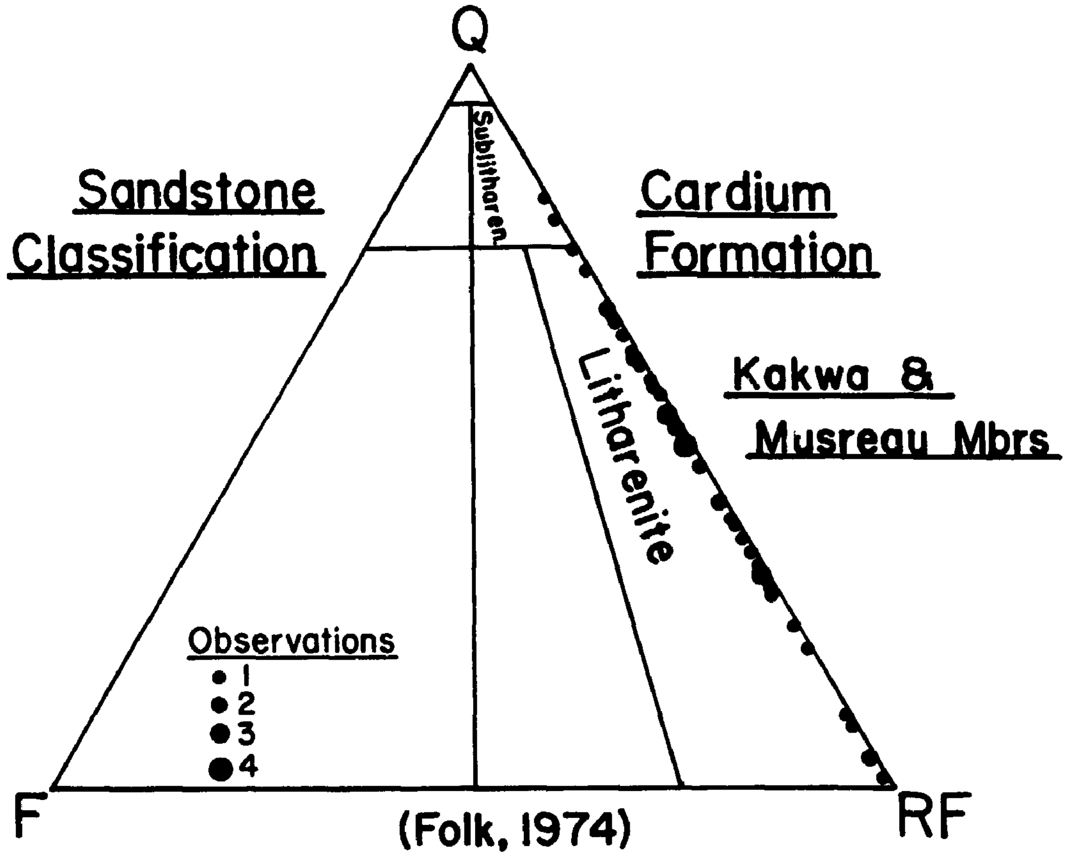
Q
Sandstone Classification
Cardium Formation
Sublitharen.
Litharenite
Kakwa & Musreau Mbrs
Observations
1
2
3
4
F
RF
(Folk, 1974)

16 (Fig. 3.6a,b). These samples are all arenites (i.e. no detrital matrix), generally litharenites (2 sublitharenites). The two principal detrital constituents are quartz and sedimentary rock fragments. Quartz content varies between 28% and 82%, with an average of 52%, and is generally monocrystalline. Rock fragments comprise between 17% and 66%, with an average of 42%, and consist of chert, "dirty" chert, silicified shales, and low-grade argillites. Feldspar is not common, generally present as an accessory mineral (less than 1%). Calcite is present as generally fine sand-sized shell fragments (often apparently inoceramid bivalve fragments) and can comprise up to 8% of the sample. Micas (muscovite, chlorite, biotite) are common accessories, and tourmaline, zircon, and glauconite were noted occasionaly.

Syntaxial quartz overgrowths are present in nearly all samples, and are best developed where there are local concentrations of quartz grains. Siderite cement, from silt-sized rhombs to cryptocrystalline masses and eogenic nodules (*cf.* Scholle 1979, p. 163), is a common diagenetic phase. The siderite predates the formation of the quartz overgrowths, as siderite rhombs can locally be seen "enclosed" in the overgrowths. Textural evidence presented in Section 3.4.1 also suggested that siderite is an early diagenetic phase. Other diagenetic events noted were compaction (pressure solution, deformation of labile grains)

Figure 3.6. Photomicrographs of sandstones from the Cardium Formation. A) Facies 16 sandstones showing good sorting, and development of quartz overgrowths (solid arrows) and early diagenetic silt-sized siderite (open arrow). Core 10-21-65-7W6, 2.5X magnification, plane-polarised light. B) Facies 16 sandstones, showing early diagenetic siderite rhombs (e.g. open arrow) enclosed by syntaxial quartz overgrowths (compromise boundary indicated by solid arrow). Note detrital carbonate (dolomite) grain (d). Mistanusk Creek section, 25X magnification, crossed nicols. C) Facies 17 sandstones, showing poorer sorting, lack of quartz overgrowths, siderite or other carbonates, and effects of compaction (pressure solution, white arrow; brittle deformation of mica flake, black arrow). Core 10-7-70-11W6, 2.5X magnification, plane-polarised light. D) Facies 17 sandstones, with abundant chert, and evidence of compaction (line and concave-convex contacts, arrows). Mistanusk Creek section, 10X magnification, crossed nicols. E) Facies 21 sandstones, showing abundant detrital carbonate grains, including calcite (c), ferroan calcite (f) and dolomite (d). Core 6-16-69-13W6, 2.5X magnification, plane-polarised light.

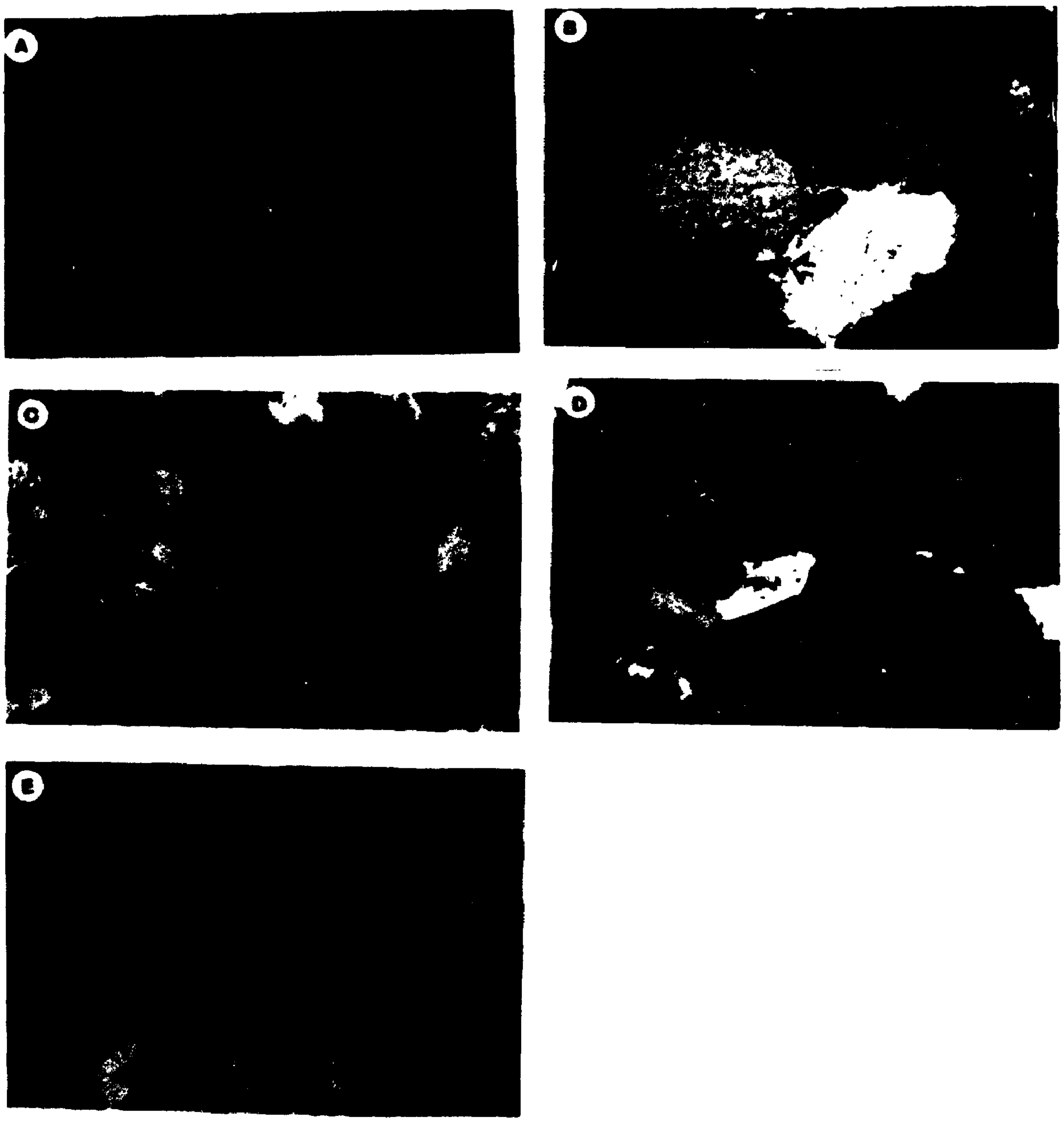
A
B
C
D
E

and minor authigenic clay formation.

Facies 17 consists of the cross-bedded and laminated fine to coarse shoreface sandstones (Section 3.4.2), and twenty seven thin sections from this facies were examined (Fig. 3.6c,d). All samples are litharenites according to the classification of Folk (1980). The quartz content of this facies ranges from 2% to 67% with an average of 40%. Rock fragments comprise on average 58%, and range from 32% to 98%. The composition of the rock fragments is essentially the same as in facies 16, however some of the larger grains consist of metaquartzites, or tightly cemented quartz-rich siltstones and very fine-grained sandstones. Feldspar is again present only in trace amounts (never more than 2%), and micas again are a common accessory mineral. Tourmaline, glauconite, carbonate, and phosphate grains are minor accessories.

Siderite is *not* an abundant diagenetic phase, and is noted only in those samples which directly overlie the basal contact with facies 16. Quartz overgrowths are not common either. The dominant diagenetic event appears to have been compaction-induced pressure solution and deformation of labile grains. Minor authigenic clays and probable Fe-oxide rims were also noted.

Eight samples were collected from sandstones assigned to facies 21 (Fig. 3.6e). These are fine- to medium-grained litharenites with quartz comprising between 10% and 72% of the rock, and rock fragments comprising between 28% and 90%. The rock fragments observed in facies 16 and 17 are also present here, as are detrital limestone and dolomite grains which together can comprise up to 46% of the rock, but are also absent in some cases. Of the two samples from fluvial units which have cut into the Kakwa shoreface (replacing facies 17), one contains carbonate rock fragments (32%) and the other does not. Feldspars and micas are minor constituents (less than 1% each).

Sandstones from this facies appear to have had more varied diagenetic histories. Poorly-developed quartz overgrowths, hematite (weathered siderite?), and poikilotopic calcite cements may be noted, as can some compaction-related features (pressure solution, deformation of labile grains).

3.6.2 Interpretation

The the composition of the sandstones described here closely resembles previous petrographic reports of Kakwa and Musreau member sandstones (Staley 1988; Stott 1963, his Ram and Moosehound members). The near absence of feldspar is typical of "recycled orogen" provenances (Schwab 1986) where sediments are derived from tectonically elevated supracrustal sedimentary and metasedimentary rocks. The lack of igneous rock fragments can be ascribed to topographic "shielding" of the foreland basin from westward sources by the uplifted area (*cf.* Schwab 1986). In the present case, low-grade argillites could have been supplied by erosion of the Proterozoic Windemere Group, quartz arenites from the Cambrian Gog Group, and chert, shales, and carbonates from elsewhere in the Lower Paleozoic succession to the west (see references in Ricketts 1989).

The lack of matrix in samples of facies 16 and 17 is characteristic of a high-energy coastal environment. The lack of limestone and dolomite grains in these facies, but their presence (at least locally) in fluvial sandstones, suggests that abrasion in the nearshore zone was the dominant mechanism for their destruction. It is probable that some sandstones from the Musreau Member have enough matrix to be classified as lithic wackes (*cf.* Staley 1988), but these rocks were not collected in the present study. The higher average proportion of rock fragments in facies 17 probably reflects a grain-size effect; coarser-grained sandstones tend to have a higher percentage of chert and less quartz, suggesting that the supply of "larger" (coarser than medium sand size) was restricted.

The petrographic evidence suggests that siderite was the earliest diagenetic phase in facies 16, and a possible mechanism for its formation (localised reducing environments produced by decaying organic material) was suggested in Section 3.4.1. The absence of siderite in most of facies 17 (except at the very base) indicates that pore water chemistries were different (either oxidising or acidic waters) during deposition of this unit.

The occurence of quartz overgrowths appears to a first approximation to be a function of the quartz content of the rock; samples with little detrital quartz have few or no overgrowths, whereas quartz-rich samples have well-developed overgrowths. It also appears that sandstones from facies 16 have better developed overgrowths than samples from facies 17 which have approximately the same mineralogy. This could indicate that precipitation of authigenic quartz began early after the deposition of the facies 16 sandstones, but before the deposition of the facies 17 units.

Evidence of compaction is most apparent in those samples (typically in facies 17) with no or poorly-developed quartz overgrowths, suggesting overgrowth formation before deep burial. Thus, porosity reduction in facies 16 was accomplished primarily through the precipitation of cements (quartz and siderite), whereas compaction was the principal agent leading to the destruction of porosity in facies 17. Similar relationships between sandstone composition, quartz overgrowth development, and compaction were noted by Winn *et al.* (1984) from the Lower Frontier Sandstones of Wyoming.

CHAPTER 4

COARSE-GRAINED SHOREFACE DEPOSITS: PERSPECTIVES FROM THE CARDIUM FORMATION

4.1 Review of previous work

Gravelly shorefaces, and their preserved conglomeratic counterparts, represent a type of environment which has received very little attention from sedimentologists. Although modern gravel beaches have received considerable attention (Bluck 1967; Carr 1969; Dobkins and Folk 1970; Carter and Orford 1984; Forbes and Taylor 1987), there have been very few studies of the movement of pebble-sized material on the shoreface (Neate 1967; Mathews 1980; Gillie 1983), largely due to the technical difficulties involved in working in these environments. Examples of studies which have recognized ancient conglomeratic shoreface deposits have been published both from outcrop (Clifton 1973, 1981; Leckie and Walker 1982; Bourgeois and Leithold 1984; DeCelles 1987; Leckie 1988; Massari and Parea 1988) and the subsurface (Cant 1984; Bergman and Walker 1987). In general, the Baytree conglomerates (at the type section) contain less interbedded sandstone than those from the other outcrop studies, and the conglomerates recognized in the subsurface as shoreface deposits were identified as such largely on stratigraphic and not sedimentologic evidence.

There are three "end member" settings where one might expect to find gravelly shorefaces. The first of these involves areas of active erosion of coastal bedrock outcrops (e.g. Zenkovitch 1967; Ogren and Waag 1986). The preservation potential of these deposits must be considered to be minimal. The second setting is in high latitude areas which were subjected to Pleistocene glaciation (e.g. Forbes and Taylor 1987). In these cases, gravel can be derived from tills, outwash deposits, or other coarse-grained sub- to pro-glacial deposits. Finally, gravelly coastlines develop in proximity to tectonically active areas. Where the shoreline is adjacent to uplifted areas, fan-deltas may form (e.g. Ethridge and Wescott 1984), whereas the maximum distance from the tectonic belt should be a function of stream gradient and discharge, sediment type, and the time available for basinward transport (e.g. Paola 1988). In the case of the Cardium Formation, gravel was supplied from the rising cordillera to the west and southwest (Stott 1984).

4.2 Sediment movement on the shoreface

In this section, I will review the major processes which transport sediment on the shoreface and adjacent beachface. This discussion will be of importance in understanding the mechanisms responsible for deposition of conglomerates in the Cardium. The principal sources for the material to be presented are Zenkovitch (1967), Komar (1976), Davis (1985) and Niedoroda, Swift and Hopkins (1985). In a general way, there are 3 main forces responsible for sediment transport on the shoreface. These are: 1) wave motions; 2) currents induced by shoaling waves; and 3) other currents.

4.2.1 Wave-induced sediment motion

Surface gravity waves are generated by the transfer of energy from wind (blowing across the water surface) to the water. The principal factors which control wave character are the *wind speed*, the *duration* of time the wind acts on the water, the *fetch* over which the wind blows, and the *water depth*, which limits the size waves may attain (Komar 1976).

In deep water, wave form approximates a simple sinusoid. However, as waves enter water shallower than about one half the deep water wavelength they start to "feel" the bottom and begin to distort. In this case, the wavelength decreases, the wave height increases, troughs become flatter and crests become steeper until eventually the wave oversteepens and breaks.

The deformation of the wave form leads to deformation of the wave oscillatory motion at the bottom. Under a simple sinusoid, water motion at the sea floor (in water depths less than $^1/_2L$) consists of a simple back-and-forth motion; the forward motion under the wave crest equalled by the backward motion under the trough. As a wave starts to deform in shallow water, the forward motion under the wave crest becomes shorter but faster, with the backward motion under the trough being longer and slower.

This time-velocity asymmetry (*not* a combined flow) has important consequences for sediment movement. As described by Zenkovitch (1967) and Bruun (1988), the shoreface profile (i.e. submarine slope) is a function of sediment grain size and wave type (height, wavelength, period, form). For any particle resting on the shoreface and subject to oscillatory wave motion, there are forces acting to move the particle upslope (forward motion under the crest) and downslope (backward motion under the trough; gravity). Given a certain grain size, slope and wave conditions, there will exist a point at which the two are balanced, and forward motion will equal the backward motion. Seaward of this point, sediment will migrate offshore, whereas landward sediment will migrate onshore - provided that the available wave energy is sufficient to initiate sediment movement at these depths (Bruun 1988). This effect is grain size dependant; for the same wave conditions and bottom slope, fine-grained sediments may move offshore whereas coarse-grained sediments are moved onshore (Zenkovitch 1967). When a mix of grain sizes is available on the sea floor, a graded profile can be developed with large particles moving upslope (i.e. onshore) and smaller particles downslope (offshore; Zenkovitch 1967, p. 115). It is also this process which drives sand and gravel landward during transgressions over shallow slopes.

Davis (1985) and Bruun (1988) explained how non-storm waves, characterised by low steepness and wave height, move sediment landward creating "constructive", "summer or "fairweather" profiles. Storm waves, characterised by greater steepness and longer period, result in considerable offshore movement and create "destructive", "winter" or "storm" profiles. This type of process has been reported from a modern gravelly shoreface by Hart and Plint (1989). These authors suggested offshore movement of gravel took place during peak storm conditions, followed by subsequent onshore movement during constructive wave conditions. How much gravel is retained on the shoreface, and how much "escapes" seaward depends on the bottom slope and the relative frequency of constructive and destructive events. Gillie (1983) described both onshore and offshore movement of gravel on the inner shelf in response to differing wave conditions. Kidson and Carr (1959) used radioactively "tagged" pebbles and found that at some critical (but undefined) distance offshore, pebble movement was very limited (even during storms) and exchange of gravel between the shore and shelf did not occur. Intuitively, this "critical" distance must be related to the offshore slope and wave climate. Gravels in these shelf settings can be moulded into coarse-grained wave ripples by long-period waves (see review by Leckie 1988).

4.2.2 Wave-induced currents and sediment transport

Longshore currents are generated in the breaker zone by the dissipation of shore-parallel wave energy. The velocity of longshore currents is proportional to both the breaker height and the angle of wave approach (Komar 1976). In the following paragraphs I will develop a model for sediment transport due to longshore currents. This model is of interest, in that only the wave height and breaker angle need be specified. Typically, wave period is also employed to calculate longshore current velocity (see review by Sherman 1988).

As given by Allen (1982), the near breaker celerity can be given by:

$$c = [\, g\,(h + H)\,]^{0.5} \tag{1}$$

where g is the gravitational constant, h is water depth, and H is wave height. For any given wave height, the critical water depth for the onset of wave breaking can be approximated by:

$$H = 0.78 * h \tag{2}$$

as given by Clifton (1986). Thus, by specifying either the breaker height or water depth, one can arrive at a near breaker celerity (equation 1).

The near-bottom orbital velocity under near-breakers can be estimated by:

$$U_m = (\, H * c\,) \,/\, (\, 3 * h\,) \tag{3}$$

(Allen 1982). From this, the longshore current velocity (U_l) can be derived by specifying the breaker angle (θb):

$$U_l = 2.7 * U_m * \sin\theta b * \cos\theta b \qquad (4)$$

(Komar 1976).

Comparison of longshore current velocities predicted by this model and three others (Sherman 1988) indicates that it gives results which are comparable to, or better than the other models, albeit for a limited data base (Fig. 4.1).

The bottom stress exerted by a longshore current (T_b) can be estimated by:

$$T_b = f * p * U_m * U_l \qquad (5)$$

(Longuet-Higgins 1970), where f is a friction factor, and p is the water density. Hammond, Heathershaw and Langhorne (1984) found that for gravels in a marine setting, the critical shear stress for the onset of movement (T_t) can be approximated by:

$$T_t = 5.5 * D_i^{0.42} \qquad (6)$$

where D_i is the median particle diameter in centimeters (the constant being converted here to give the same units - Pascals - as in equation 5). Madsen and Grant (1975) suggested that the shear stress under waves (T_w) could be given by:

$$T_w = .5 * f * p * Um^2 \qquad (7)$$

For any given grain size and water depth, it can be shown that during rising storm conditions (i.e. increasing breaker height) the shear stress generated by wave oscillatory

Figure 4.1. Comparison of longshore current models. Data from Sherman (1988).

LONGSHORE CURRENT MODELS

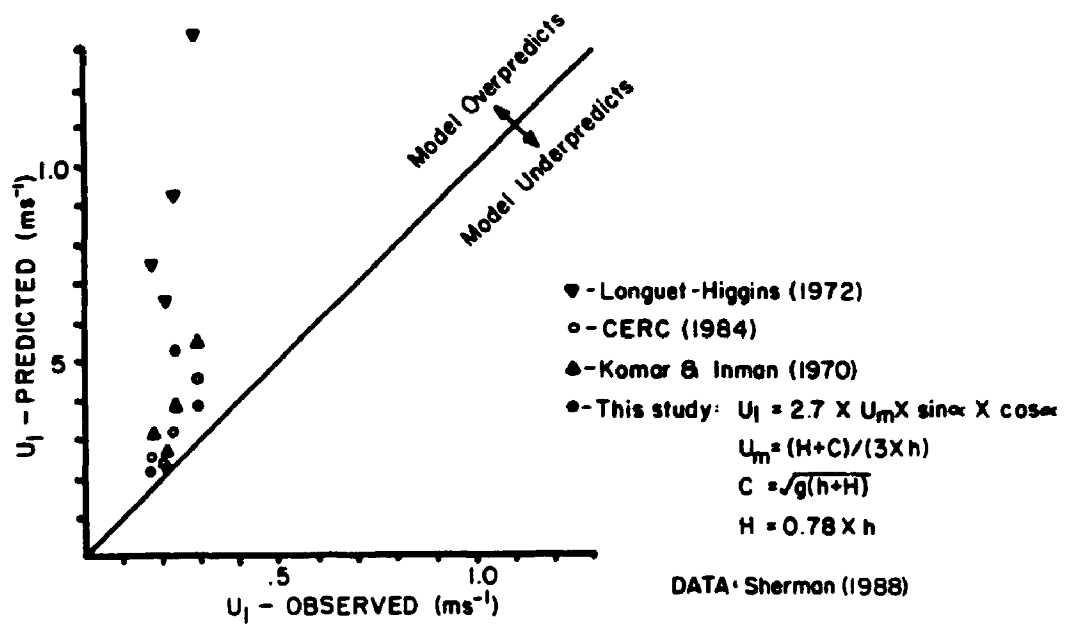

motion alone will initiate sediment movement *before* longshore currents become active in that zone. That is to say that as wave height grows, the region affected by the oscillatory motion "grows" seaward, in advance of the surf zone (the zone of longshore currents *sensu stricto*). Thus, wave motion will set a grain in motion and the grain is then "available" for transport by unidirectional currents.

Rip currents are another type of current induced by breaking waves. As waves deform in shallow water, eventually breaking, a landward mass transfer occurs. Water piles up against the shore, eventually being released seaward in the form of rip currents. Davis (1985) described the factors which control rip current development, including wave conditions and shoreline configuration. Channels can be excavated during these seaward flows (e.g. Davidson-Arnott and Greenwood 1976) and pebbles can be transported offshore (Zenkovitch 1967). This coarser material accumulates as lags in the base of the channels (Davidson-Arnott and Greenwood 1976; Hunter, Clifton and Phillips (1979).

Finally, tidal currents and wind-induced currents can also be important on the shoreface. In wave-dominated settings, perhaps the most important role of tides is to change water depth, and hence the processes active, at any one particular point (e.g. Ross and Long 1989). Currents generated by coastal set-up (with onshore winds) flow offshore along the seafloor in the shoreface zone, and thus enhance offshore sediment transport during storms (Neidoroda *et al.* 1985).

4.3 The Baytree conglomerate

As noted in Chapter 1, the term "Baytree conglomerate" was first coined by Stelck (in Gleddie 1949). Stott (1967) considered the Baytree conglomerate to be a coarse-grained facies of the non-marine Moosehound (i.e. Musreau - see Ch. 1) Member. Here, it will be demonstrated that the conglomerates at the Baytree locality were deposited in a shoreface setting.

In this section, conglomerate facies will be identified by letters (A-G). Conglomerate facies from Mount Niles (Section 4.4) and Horseshoe Mountain (Section 4.5) will also be identified by letters (H-K, and L-N respectively). Some of the descriptive lithofacies overlap between sections (e.g. clast-supported conglomerates), but they have been given separate facies codes so as not to imply genetic equivalence. Some of these facies can be associated with conglomerate facies observed by Bergman (1984, 1987) in the Cardium Formation from the Carrot Creek area in core, although it should be emphasised that the lettering scheme employed here is completely different.

4.3.1 Lithology

Description

The Baytree type locality consists of a cliff exposure over 250 m in length and typically about 10 m in height. For the present study, seven sections were measured along the cliff face (Fig. 4.2), generally with a spacing of about 20 m between sections, or wherever access up the cliff face was possible.

The base of the section, where exposed (sections BT1, BT2, BT3, BT5) consists of swaley cross-stratified fine-grained sandstones (facies 16) with abundant pebble stringers. Up to 3 m of this facies was measured, although the base of this unit is never exposed. The pebbly layers line upwardly concave surfaces, and are never more than a few grain diameters in thickness; typically they are a single grain diameter thick. Facies 16 is sharply overlain by pebbly medium-grained sandstones (facies 17), generally less than a meter thick. These facies 17 sandstones can be either cross-bedded, or comprise low-angle cross-beds (?scour fill structures). This interval is in turn overlain by up to 12 m of conglomerate (facies 8) with minor (less than 20%) interbedded sandstones. It is the thick conglomerates (and interbedded sandstones) which will form the basis of the present discussion.

The most abundant distinct conglomerate type (18.7% of total conglomerate thickness) consists of massive, clast-supported pebbly units up to 1.6 m thick (Facies A; Fig. 4.3a). Clasts in these units are typically 2 to 3 cm in

Figure 4.2. Measured sections from Bay Tree locality. Letters and numbers to left of each section refer to facies described in text. Codes with arrows point to position of pebble fabric measurements (see Fig. 4.8).

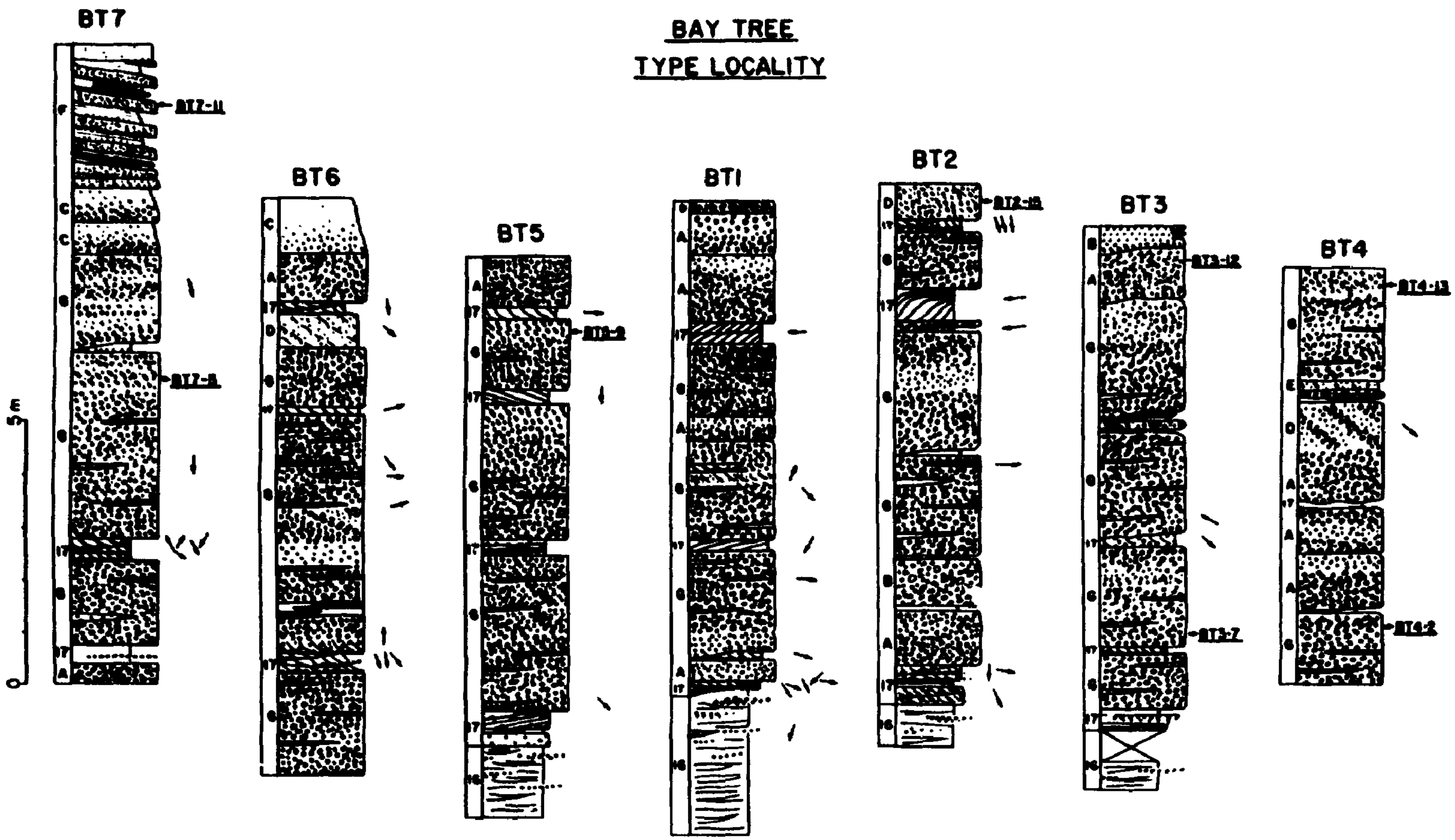
BAY TREE
TYPE LOCALITY
BT7
BT6
BT5
BT1
BT2
BT3
BT4
BT7-11
BT7-8
BT5-9
BT2-10
BT3-12
BT3-7
BT4-13
BT4-2
5 m
0

Figure 4.3. Conglomerate facies from Bay Tree locality. A) Clast-supported pebble conglomerate, open framework in upper portions, closed framework below. B) Imbricated clast-supported pebble conglomerate. C) Conglomerate cross-bed set 40 cm thick. Inferred bedform migration direction is to the southeast.


A

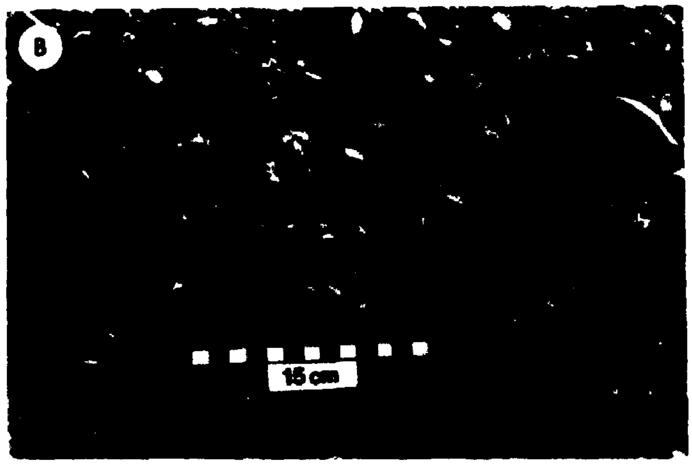
B
15 cm


C

Figure 4.3 (cont.) D) Interstratified conglomerates and laminated sandstones interpreted as beach deposits. E) Amalgamated conglomerates with minor interbedded sandstones. Note the lateral impersistence of the sandstones, and the pronounced horizontal stratification. F) Close-up of amalgamated conglomerate bed. Except for the horizontal stratification, the conglomerate appears structureless. G) Solitary planar-tabular conglomerate cross-bed interpreted to have formed by the offshore (NE) migration of a plunge step.

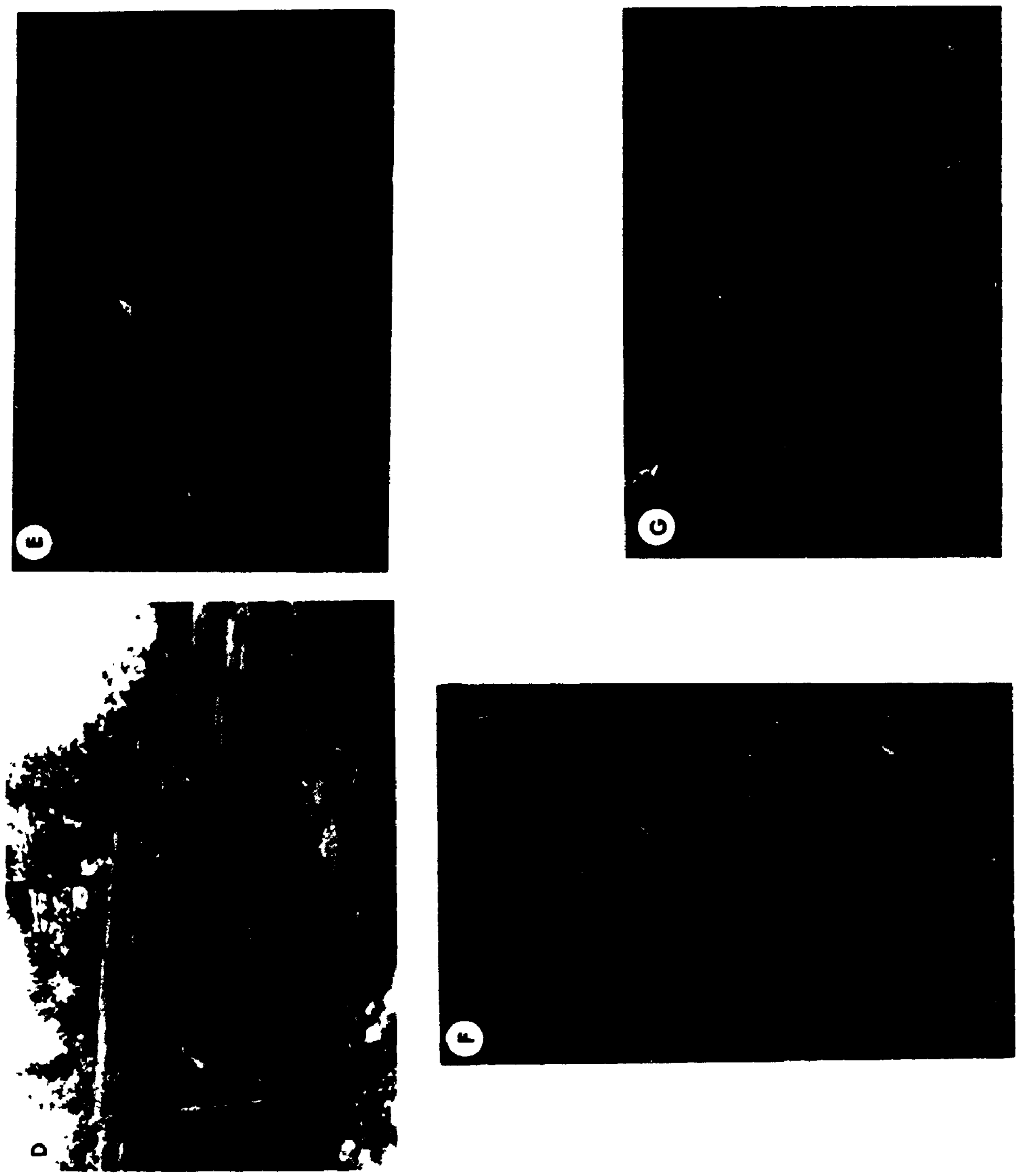
E
G
D
F

diameter, although coarser- (with clasts up to 16 cm) and finer-grained (e.g. granule conglomerates) are also present. Other discrete, identifiable units include: a) imbricated, clast-supported conglomerates (Facies B; Fig. 4.3b) comprising 8.1% of the total thickness; b) graded (normal and coarse-tail) conglomerates (Facies C; 5.5%); c) cross-bedded conglomerates several decimeters thick (Facies D; Fig. 4.3c), with cross-bedding defined by size or textural variations (3.8%); d) matrix-supported conglomerate (Facies E; 2.3%); and e) gently dipping, interbedded pebbly conglomerate and laminated sandstone (Facies F; Fig. 4.3d) from one section only (3.8%). Bed thicknesses of these latter units (facies B-F) range from several centimeters to a few decimeters.

The bulk of the conglomerate (58%) consists of crudely-bedded, amalgamated units (generally from 1 to 3 meters thick) in which individual units of the individual conglomerate sub-facies and minor sandstones are identifiable (again as centimeter to decimeter thick units), but are not laterally continuous over distances greater than a few meters (Facies G; Fig. 4.3e). Shallow scours, depositional thinning and lateral facies changes all appear to contribute to the lateral discontinuity of individual units. In some places, it appears that these units could be oblique sections through decimeter-scale cross-beds. Despite the internal scouring, the overall appearance of the conglomerate, especially brought out by the sandstones, suggests a pronounced horizontal stratification pattern. Large-scale "clinostratification" such as that observed by Massari and Parea (1988) could not be observed (if it exists) with the available outcrop exposure.

A solitary planar-tabular cross-bedded conglomerate set up to 40 cm thick is found at the top of sections BT1 and BT2. Discoidal pebbles appear to rest on the foresets, dipping in the direction of cross-bed migration (Fig. 4.3f).

Sandstones interbedded with the conglomerate range from fine- to coarse-grained, and are commonly pebbly. They may be cross-bedded, or undulose to parallel laminated. As noted earlier, they comprise only a minor proportion (less than 20%) of the total section but their presence helps define the horizontally-stratified nature of the outcrop.

Clast-supported conglomerates dominate the section volumetrically. These units tend to have bimodal grain size distributions (i.e. clasts and matrix), with a fine to coarse sand matrix. Openwork conglomerates (unimodal size distributions) tend to be well-sorted granule to fine (average diameter 5 to 10 mm) pebble conglomerate. Poorly-sorted polymodal conglomerates are not common.

Evidence of bioturbation is virtually absent, although rare pebble-filled vertical burrows (about 1.5 cm in diameter) in sandstones beds can be found.

The average diameter of the ten largest clasts in a given bed (D_{10}) is commonly employed to characterize the grain size distributions of conglomerates, especially where they are highly indurated and cannot be disaggregated for sieve analysis; its value is commonly interpreted as a measure of flow competence (e.g. Graham 1988). Maejima (1982) noted that "very similar trends" are shown by the distributions of D_{10} and mean grain size on a gravelly beach in Japan, and suggested that measurement of D_{10} could provide a more convenient way of characterizing grain size distributions than the mean grain size, which can sometimes be difficult to evaluate. In the present case, D_{10} values were measured for discrete conglomerate beds and, in the case of the amalgamated units, values were measured at the base, top, and sometimes the middle of the unit (depending on the thickness of the unit).

The results are presented in Figure 4.4. Linear regression has been performed on the data to determine whether coarsening- or fining-upward trends are present. To do this, I have "normalised" the distance above the base of the conglomerate, setting the base equal to 0 and the top of the section equal to 10. This distance is plotted along the x-axis, and D_{10} is plotted as a function of the distance from the base of the section. In this way, regression lines from coarsening-upward successions will have positive slopes, although the absolute value of the slope is

Figure 4.4. Correlation between height above base of section and D_{10} for Bay Tree sections. Correlation coefficient (r) and slope of regression line (m) indicated for each section. See text for further discussion.

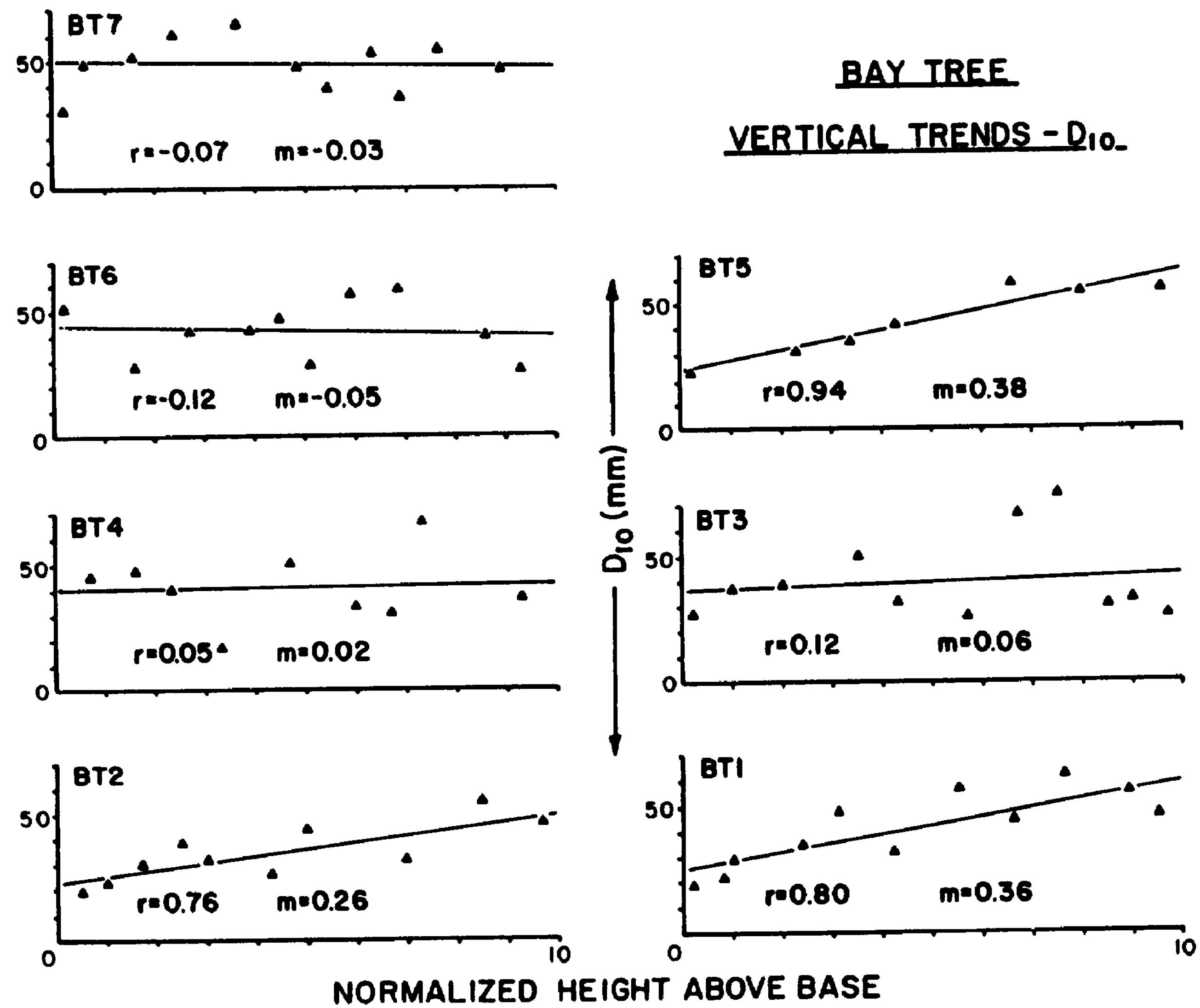
BAY TREE
VERTICAL TRENDS - D_{10}
BT7
r=-0.07 m=-0.03
BT6
r=-0.12 m=-0.05
BT4
r=0.05 m=0.02
BT2
r=0.76 m=0.26
BT5
r=0.94 m=0.38
BT3
r=0.12 m=0.06
BT1
r=0.80 m=0.36
D_{10} (mm)
0
50
0
10
NORMALIZED HEIGHT ABOVE BASE

meaningless.

Regression lines from three of the sections have positive slopes and high correlation coefficients. These three sections (BT1, BT2, BT5) are adjacent to one another near the middle of the outcrop (Fig. 4.2). The other four sections show no overall correlation between height from the base and D_{10}. Visual inspection of BT3 and BT7 suggests that at least the lower part of both sections could display an upward coarsening trend.

As a test for lateral variations, histograms for each section of the number of occurrences of D_{10} within a 5 mm class interval, plus the mean value of D_{10} of each section are presented in Figure 4.5. A general southward fining is present from section BT7 to BT2, but sections BT3 and BT4 (at the southern end) are slightly coarser.

Interpretation

Numerous attempts have been made to establish diagnostic criteria to differentiate shallow-marine (or beach) from fluvial conglomerates (see Reddering and Illenberger (1988) for the most recent summary). To date, no single criterion has been proposed which can unequivocally distinguish between the two. A possible exception could be the presence of a shallow-marine trace fauna in interbedded sandstones (Clifton 1973).

Although the textural parameters of conglomerates (e.g. bed segregation, sorting, abundance of matrix) may help

Figure 4.5. Histograms showing distributions of D_{10} along the face of the Bay Tree outcrop. Triangles indicate mean D_{10} of each section. See text for further discussion.

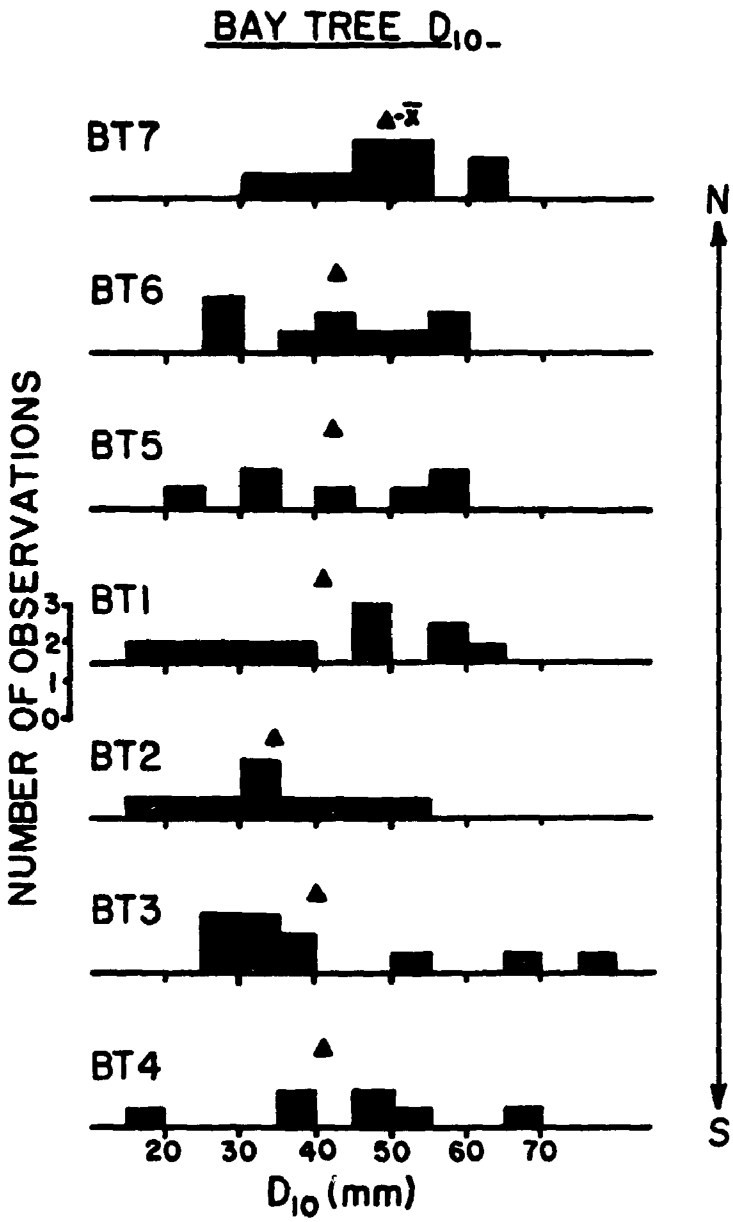
BAY TREE D_{10}
$\blacktriangle$-$\bar{x}$
BT7
BT6
BT5
BT1
BT2
BT3
BT4
NUMBER OF OBSERVATIONS
3
2
1
0
N
S
20
30
40
50
60
70
D_{10} (mm)

distinguish between fluvial and marine conglomerates, comparisons of the deposits of these two settings have indicated that texture alone is insufficient (Nemec and Steel 1984). Perhaps one of the better criteria is bed lenticularity, which reflects the persistence and regularity of the depositing agent (Clifton 1973). Clifton pointed out that flows in fluvial systems tend to be channelized, whereas the influence of waves is spread out over larger areas. Beds in fluvial conglomerates should then be more lenticular than those from systems where wave energy was high.

At the Baytree type locality, there tends to be good segregation of sand- and gravel-sized constituents. Matrix-supported conglomerates and highly pebbly sandstones are not present in abundance. These characteristics, along with the pronounced horizontal stratification at the type locality (especially as highlighted by the sandstones, or toward the top of the section), suggest strong wave action in a shallow-marine environment (Clifton 1973).

Interstratified sandstones and conglomerates from the top of the section at BT7 (Fig. 4.3d) are clearly recognisable as beach deposits (e.g. Nemec and Steel 1984; Forbes and Taylor 1987; Massari and Parea 1988), showing excellent clast segregation and bed continuity (albeit with internal very low angle truncation surfaces). The presence of this unit at the top of the section suggests simple progradation of beach deposits over shoreface deposits during regression (as can be seen elsewhere in stratigraphically equivalent sections of the Cardium Formation - see next chapter).

The 60 cm thick cross-bedded conglomerates at the top of sections BT1 and BT2 (Fig. 4.3f) probably record the progradation of a gravel plunge step at the toe of the beach (low tide level) - a feature common on coarse-grained beaches (e.g. Forbes and Taylor 1987; Hart and Plint 1989). Based on my own (unpublished) observations at Chesil Beach, progradation of the plunge step seems most likely to occur following either high tide or after a storm surge. At these times, the water table in a beach would still be high. After waves swash up the beachface, the water -instead of percolating into the beach as typically occurs on gravelly beaches (e.g. Bluck 1967)- returns as backwash, dislodging and transporting pebbles seaward. These clasts then avalanche over the plunge step and make the form migrate seaward.

Lower in the section, the sedimentary structures are more difficult to interpret. The cm to dm-scale conglomerates are interpreted as the products of gravel bedload sheets (e.g. Hein and Walker 1977; Whiting *et al.* 1988). The lateral dimensions of these "bedforms" were probably in the order of several meters, explaining the lateral impersistence of the resulting deposit. The possible existence of this type of sediment transport has been suggested by Mathews (1980), who found that tracers on a modern gravelly foreshore moved alongshore as discrete "slugs" of sediment (representing volumes of 1 to 10 m^3), rather than as a uniform gravel sheet. These slugs formed during periods of high wave energy, moved alongshore 10 to 50 m per day, and were reworked during fairweather conditions.

The large-scale cross-bedding (Fig. 4.3c) was produced by the migration of dune-like forms at least 60 cm high. Paleocurrent evidence to be introduced later (Section 4.3.4.) will show that these bedforms migrated in a shore-parallel direction. Such bedforms have not been documented from modern gravelly shorefaces. Possibly, during strong longshore flows, the bedload sheets may have grown in height and developed slipfaces, a process observed in modern gravelly streams (Whiting *et al.* 1988). As noted previously, some of the "amalgamated" units may in fact have been oblique sections through cross-bedded units, suggesting these structures are probably more abundant than they appear.

The sandy matrix in the conglomerates may have been transported with the bedload sheets; examination of a graph relating clast size to sand grade in suspension presented in Harms, Southard and Walker (1982) suggests this possibility is not unreasonable. Alternatively, at least some of the sand may have been introduced into the framework after the deposition of the gravels through the action of "wave pumping" (Vincent 1986). This mechanism pumps water and fine sediments into the pore spaces of a coarser deposit due to the differential pressure gradients developed under waves. Possible supporting evidence for this mechanism is that sand matrix is generally absent from well-sorted granule-size units, but is present in adjacent coarser-grained units. This could suggest that the pore openings between granules were not big enough to allow infiltration of the sands.

The cross-bedded sandstones could have been the product of lower-intensity flows either following larger (gravel-moving) storms, or during less-intense storm activity.

Grain-size trends, as reflected by D_{10}, show overall coarsening-upward trends in at least three of the sections (BT5, BT1, BT2), all from near the middle of the outcrop. If these sections were originally located far enough away from the immediate source of the gravel (i.e. far enough from a distributary mouth so that the effects of short-term fluctuations in calibre of the sediment supplied are minimal), then D_{10} should be controlled by marine transport and reworking. In this light, the upward-coarsening could reflect size sorting on the shoreface by waves (Section 4.2.1). Those sections which do not show a consistent grain size trend could be close enough to a distributary mouth so that the short-term fluctuations in sediment calibre cannot be ignored. Whether or not such differences should be observable here, given the scale of the outcrop at Bay Tree (about 0.25 km long), cannot be determined without studies of textural parameters from modern systems.

The lateral variations between sections do in fact suggest that sections BT5, BT1, BT2 may indeed have been located on the down-drift side of a gravel source: a general fining is apparent from BT7 to BT2 is seen in Figure 4.5. The reappearance of coarser clasts in sections BT3 and BT4 could be interpreted as indicating the presence (at least temporarily) of another gravel source. In this way a conceptual model can be constructed, where those sections originally closest to fluvial sources are the coarsest-grained and show no up-section grain-size trend. Down-drift from sediment sources, the grain-size decreases, and an overall upward coarsening is developed.

4.3.2 Clast form

Description

It has often been suggested that clast shape in gravelly/conglomeratic units can be used to distinguish beach (marine) deposits from fluvial ones (e.g. Cailleux 1945; Dobkins and Folk 1970). To test this hypothesis, I have measured pebble shape parameters (length of long, intermediate and short axes) for 25 pebbles judged visually to represent the modal clast size of the conglomerate units of sections BT2 and BT7 (a total of 1200 measurements), and used these measurements to calculate subsequent shape parameters as suggested by the various authors (see below).

Zingg (1935) classified pebble shapes into 4 categories (blades, disks, equant, and rollers) based on plots of the ratio of the short to intermediate axes versus the intermediate to long axis length (Fig. 4.6a). It is often assumed that beach (marine) conglomerates have a greater proportion of disks. In Figure 4.6b, the vertical variation in the relative numbers of each shape type from two sections are plotted. In general, there appears to be an increase in the number of disk-shaped pebbles in the upper few meters of both sections.

It has been suggested that "critical" values of certain shape indices can be used to distinguish fluvial from marine conglomerates. For example, Dobkins and Folk (1970) suggested using both a sphericity coefficient:

$$\text{sphericity} = (C^2 / A * B)^{1/3} \qquad (8)$$

where values greater than 0.65 indicate fluvial environments, and an Oblate-Prolate Index (OPI):

$$OPI = (10 * ((A - B)/(A - C)) - .5)/ (C/A) \qquad (9)$$

the value of which determines whether the intermediate axis is closer in length to the long or short axis. Values of OPI less than -1.5 are supposed to represent beach pebbles, whereas values greater than -1.5 characterize pebbles from fluvial environments. Stratten (1974) suggested that a

Figure 4.6. A) Diagram to illustrate the shape categories of Zingg (1935). B) Distribution of pebble shape types for sections BT2 and BT7.

A

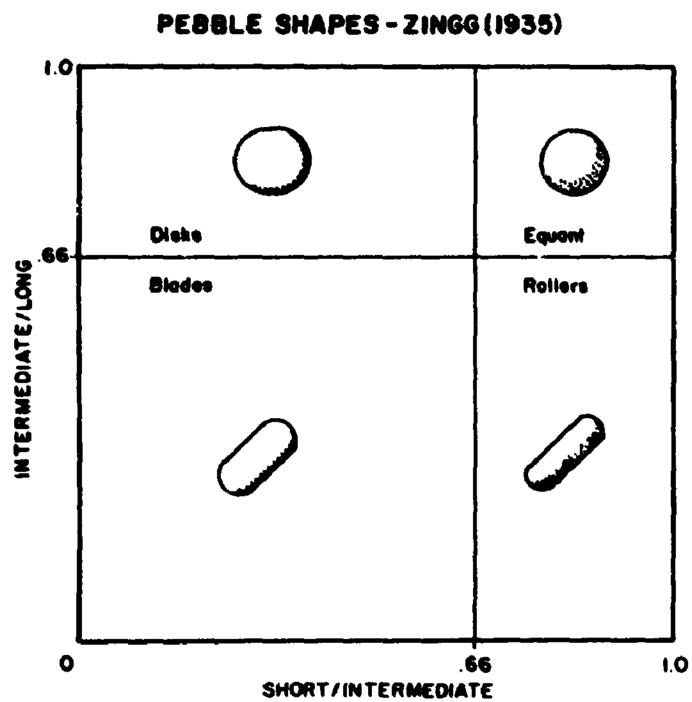

PEBBLE SHAPES - ZINGG (1935)
Disks
Equant
Blades
Rollers
INTERMEDIATE/LONG
SHORT/INTERMEDIATE
1.0
.66
0
.66
1.0

B

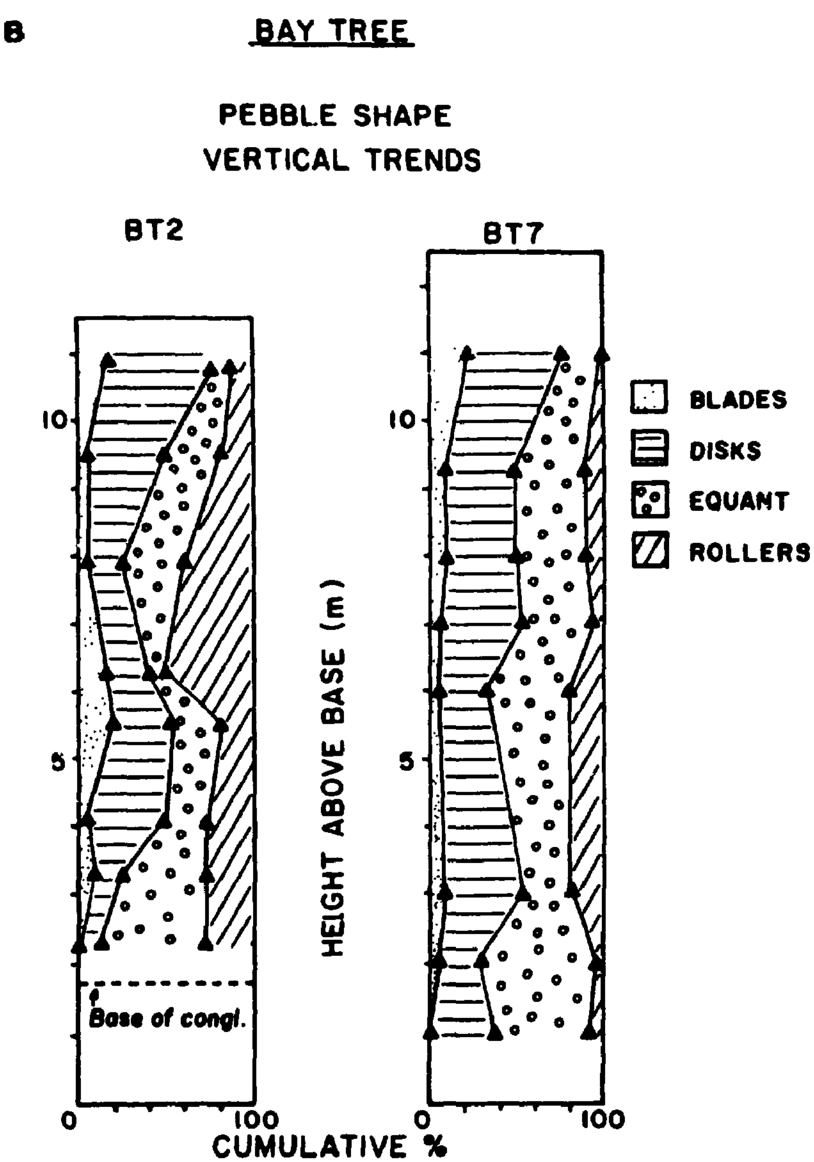

BAY TREE
PEBBLE SHAPE
VERTICAL TRENDS
BT2
BT7
BLADES
DISKS
EQUANT
ROLLERS
Base of congl.
HEIGHT ABOVE BASE (m)
CUMULATIVE %
10
5
0
100

coefficient of flatness:

$$\text{flatness} = (100 * C) / A \qquad (10)$$

could also be used, with fluvial pebbles having coefficients of flatness greater than 45.

In Figure 4.7 I have plotted the vertical trends in average values of these three values for sections BT2 and BT7. It can be seen that the majority of the values for the shape parameters fall within the *fluvial* domain.

Roundness values, as estimated visually, indicate that clasts are almost always rounded to well rounded. Clasts are composed primarily of chert, with quartzite being the other main constituent.

Interpretation

There are two possibilities which could explain the existence of "fluvial" pebbles in the Baytree conglomerate. These are: a) the conglomerate is a fluvial unit; or b) the proposed shape parameters are not valid. For reasons presented in this chapter (Sections 4.3.2, 4.3.4) I believe that the Baytree conglomerate *was* deposited in a shoreface setting, and hence conclude that the proposed shape criteria cannot be employed to unambiguously differentiate between shoreface and fluvial conglomerates.

It must first be established that the sample size employed here (25 pebbles) adequately characterizes the average form of the parent population. To test this, I have employed two data sets, each comprised of shape data from

Figure 4.7. Comparison of observed average shape parameters and "critical values" separating fluvial (f) from marine (m' pebble shapes for sections BT2 (A) and BT7 (B). Graphs are for oblate-prolate index (O), sphericity (S) and flatness (f). Shoreface conglomerates of Bay Tree locality generally plot in "fluvial" realm. See text for further discussion.

Ⓐ BAY TREE - PEBBLE SHAPE PARAMETERS : BT2

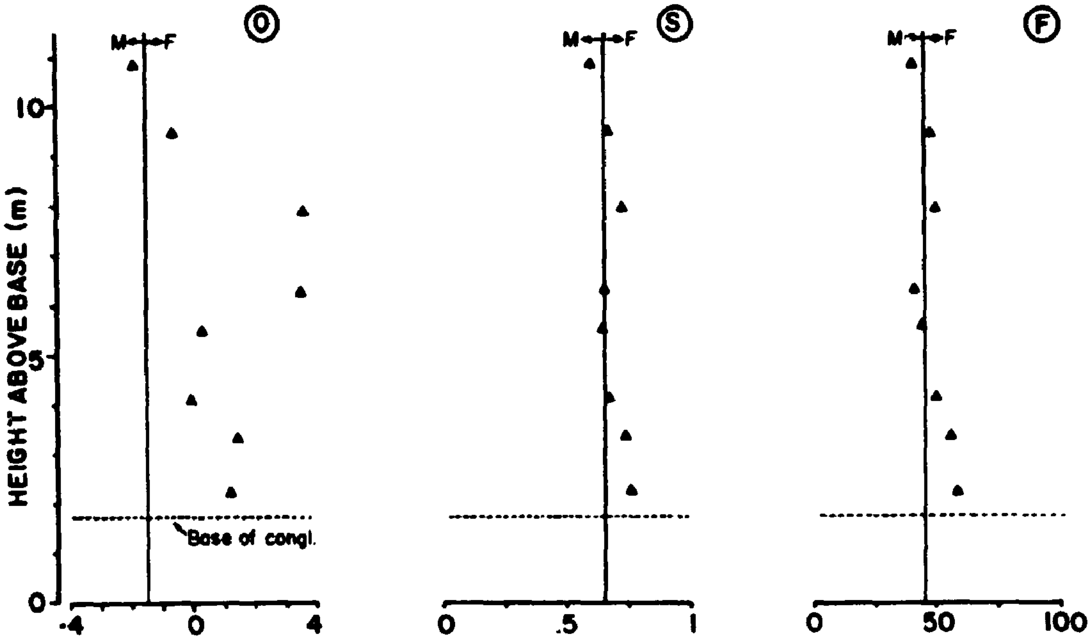

Ⓑ BAY TREE - PEBBLE SHAPE PARAMETERS : BT7

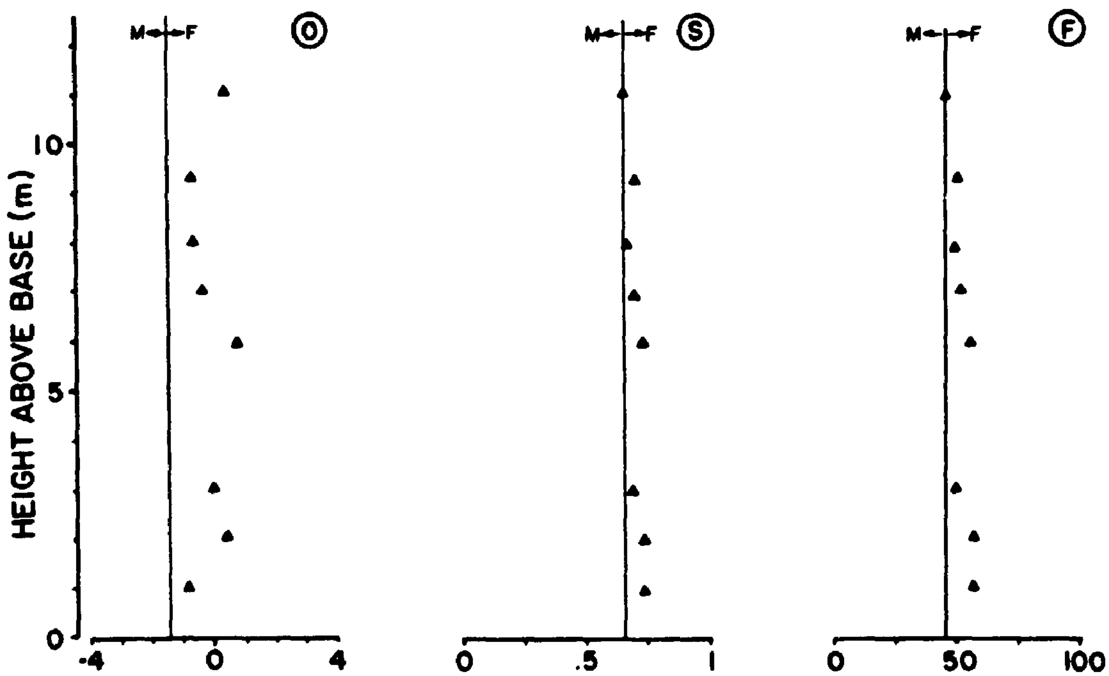

100 pebbles collected (with Jeremy Bartlett and Guy Plint) from the shoreface at Chesil Beach in the Spring of 1989 (Table 4.1). Sample CHES8902 was collected from the breaker zone, whereas CHES8903 was collected about 7 m offshore from the crest of a large wave ripple (*cf.* Hart and Plint 1989).

A GWBASIC program was written by the author which performed the following calculations on the two data files individually. A subset of 25 pebbles was selected at random from the parent population. The mean values of shape parameters were then calculated for the subset, and these values were compared against the mean values of the parent population using the t-test as outlined in Davis (1986). If the mean values for the two groups were significantly different, no point was awarded, whereas a point was awarded if the two values were *not* significantly different. By repeating the procedure 100 times (randomly selecting 25 "new" pebbles each time) and keeping score, the percentage of time that the shape values of the subsample did not significantly differ from those of the parent population could be determined. The results of the test indicate that the shape parameters of the subsets were not significantly different from the shape parameters of the parent population over 90% of the time. This is interpreted to indicate that 25 pebbles will generally be adequate to determine the shape characteristics of the parent pebble population.

TABLE 4.1
PEBBLE SHAPE PARAMETERS
CHESIL BEACH SAMPLES[1]

SAMPLE	SETTING	N	AXIS LENGTH (mm) A	B	C	C/B	B/A	OPI[2]	SPHER.[3]	FLAT.[4]
CHES8901	FORESHORE	50	17	12	7	0.60	0.74	-0.9	0.63	44
CHES8902	BREAKER ZONE	100	14	11	8	0.73	0.77	0.34	0.74	56
CHES8903	RIPPLE CREST	100	16	12	8	0.70	0.76	0.29	0.71	52

[1] Samples are not from a single beach/shoreface profile, but all come from the West Bexington area

[2] Oblate/Prolate index of Dobkins and Folk (1970)

[3] Sphericity index of Dobkins and Folk (1970)

[4] Flatness index of Stratten (1974)

As a separate test, 25 pebbles from a given interval at Bay Tree were selected and measured twice, by different operators. The two data sets were then compared using the Mann-Whitney test as presented in Davis (1986). The results suggest that no significant difference exists between the means of two data sets. Hence, it is concluded that the shape data presented here *are* representative of the pebbles at Bay Tree, and that these generally have "fluvial" forms.

It is possible that pebbles with shapes derived during fluvial transport could retain their shape if they were deposited and buried quickly enough. Although this possibility can not be discounted, it must be noted that samples CHES8902 and CHES8903 (noted above) both have average shape values which fall in the "fluvial" realm (OPI > -1.5, Sphericity > .67, Flatness > 45; Table 4.1). There is little new material added to Chesil Bank (Carr 1969) and therefore the "rapid deposition" model is not applicable there. Thus, it must be concluded that the shape criteria proposed above will not always differentiate between fluvial and marine pebbles (see also Reddering and Illenberger 1988).

In spite of the present observations, there exists sufficient documentation from modern beaches to suggest that shape zonation is present in such environments (e.g. Bluck 1967; Dobkins and Folk 1970; Orford 1975). Sample CHES8901 (Table 4.1) was selected from the beachface at Chesil Bank and *does* have average shape indices which do fall in the "marine" realm. Perhaps the most satisfactory explanation is that shape criteria developed for beach pebbles (i.e. inter- to supratidal) are not appropriate for shoreface gravels. This could be either because the processes active on the beachface produce disk-like forms *in situ* (e.g. Dobkins and Folk 1970), or because shape sorting is an efficient process in the shoreface/beachface system. In such environments, disks, with their higher suspension properties in turbulence (Orford 1975) might tend to be selectively winnowed from subaqueous settings and accumulate intertidally (Reddering and Illenberger 1988). According to this model (preferred here), shape criteria derived from the readily accessible beachface should not be employed to identify subtidal deposits because of the effects of shape sorting. It is possible that the upward increase in proportion of disks noted in the two Baytree sections could be characteristic of gravelly shorefaces.

Two final points deserve mention. First, some authors (e.g. Orford 1975; Williams and Caldwell 1988) have noted that shape sorting on the beachface is less efficient during high-energy conditions (storms), and that the best shape zonation is developed during periods of swell. Shape sorting might not be expected then from high-energy gravelly shorefaces, provided the stratigraphic record is represented by the infrequent high-energy events (storms) rather than intervening periods of swell. Finally, a grain size effect could be present. Massari and Parea (1988) presented data which suggest that the effects of shape sorting increase with grain size. Thus, perhaps measurement of the larger clasts at Bay Tree might have yielded "marine" shapes.

4.3.3 Paleocurrents

Description

Two principal types of paleocurrent data were obtained from the outcrop at Bay Tree. The first includes cross-bed orientations from the sandstones and, to a lesser extent from the conglomerates themselves. The second type of paleocurrent information is derived from measurements of the strike and dip of A-B planes of clasts in the conglomerates. Unfortunately, extraction of pebbles for measurement of the orientation of the principal axes was not possible because of the highly-indurated nature of the conglomerate.

A rose diagram of total cross-bedding is presented in Figure 4.8a. It can be seen that the principal sediment transport direction was to the southeast. In the case of the cross-bedded conglomerates, it was often impossible to measure accurately the foreset dip direction, but dips to the southeast were commonly observed.

Rose diagrams of the orientation of A-B planes are presented in Figure 4.8b-i. Pebble fabrics from units BT7-11 (Fig. 4.8b) and BT2-15 (Fig. 4.8c) are from the top of the section. A pebble fabric from a single conglomerate bed

Figure 4.8. Rose diagrams of paleocurrent indicators from Bay Tree locality. A) Total cross-bedding. Note dominant trend to southeast. B) to I) are pebble fabrics for: B - BT7-11, C - BT2-15, D - BT4-2, E - BT7-5, F - BT3-7, G - BT3-12, H - BT5-9, I - BT4-13. Locations shown in Fig. 4.2.

BAY TREE

PALEOCURRENT DATA

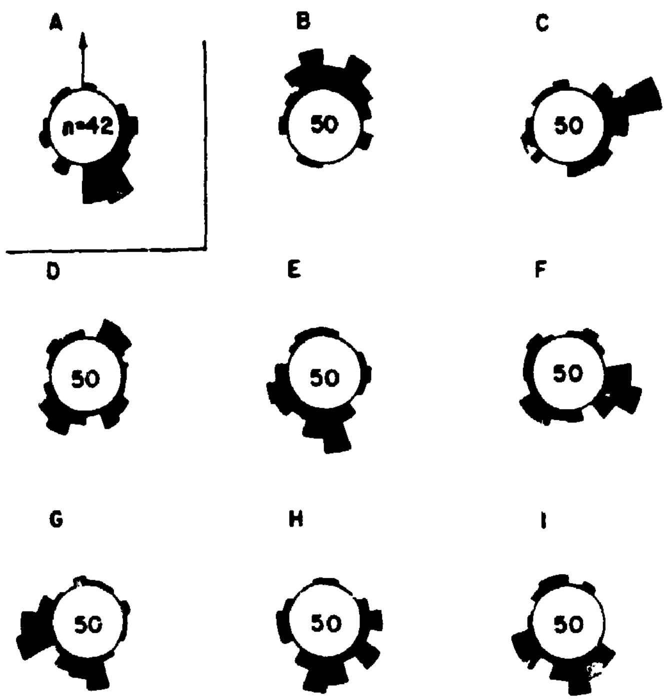

in the beachface deposits (BT7-11; see section 4.3.2) shows a bimodal distribution, with a mode to the northwest and another to the northeast. These gently inclined, interstratified conglomerates and sandstones dip at about 4° to the northeast. A strong mode to the northeast is evident in BT2-15; this is the cross-bedded conglomerate interpreted as produced by the offshore migration of a plunge step (cross-bed orientation to the northeast) in Section 4.3.2.

It can be seen that most of the other pebble fabrics are polymodal (Figs. 4.8d-i). For units BT3-7, BT4-13, BT5-9 and BT7-5 the principal mode is towards the south or southeast, and a prominent mode in this direction is evident in unit BT3-12. Other modes are observed at about 90° and 180° to the principal mode in nearly all cases. Unit BT4-2 also shows a polymodal fabric (Fig. 4.8c), with the two principal modes oriented to the northeast and southwest and smaller modes to the northwest and southeast. All of these samples represent crudely stratified to cross-bedded clast-supported pebble conglomerates generally from the middle to lower portions of the section.

Interpretation

It will be seen later (Chapter 5) that indicators of Cardium shoreline trend in outcrop show a consistent northwest-southeast trend. The dip direction of the beachface deposits at the Bay Tree locality is also indicative of a northwest-southeast striking beach. Pebbles in this unit are imbricated to the NE, indicating that this was the offshore direction (e.g. Bluck 1967; Maejima 1982). The bimodality of the pebble fabric in this unit could reflect both the influence waves approaching at right angles to the shoreline, and waves approaching at an oblique (more northerly) angle (e g. Ogren and Waag 1986). That the offshore direction was to the northeast (indicating a NW-SE beach strike) is also suggested by the orientation of the cross-bedded plunge step gravels. Discoidal pebbles from the plunge step dip in the direction of form migration.

Lower in the section, the dominant southeast cross-bed orientation (both conglomerates and sandstones) is suggestive of shore-parallel transport by longshore currents. The thickness of the cross-bedded conglomerates indicates that gravel bedforms at least 60 cm high migrated parallel to shore. The existence of bedforms of this type and scale has not been reported from modern gravelly shorefaces.

The pebble fabric from the base of section BT4 (BT4-2) shows two dominant modes to the northeast and southwest. These represent offshore and onshore directions respectively. This fabric probably indicates the presence of shore-parallel symmetrical wave ripples (*cf.* Leckie and Walker 1982) although ripple form sets are not observed.

Pebble fabrics from the bulk of the conglomerate display dominant dip modes to the southeast. This is approximately the same direction as the dominant cross-bed orientation in the sandstones. Here, I suggest that this represents a downstream dip of clasts lying on the lee side of gravel bedforms transitional between bedload sheets and dunes. Thus, the pebble fabric strengthens the interpretation of strong longshore flows to the southeast.

Paleocurrent relationships between pebble fabric and cross-bed direction similar to those observed here were noted by Carmichael (1988) in the Gates Formation. There, both the dominant sandstone cross-bed orientation and pebble "imbrication" are to the southeast. He interpreted this relationship to indicate onshore (SE) transport of sand and offshore (NW) transport of gravel. Alternatively, using the Bay Tree example as a guide, the pebbles could dip in the transport direction, indicating pebble transport in the same direction as the sand.

These interpretations highlight the problems associated with the use of the term "imbrication". This term is generally employed to describe a grain fabric wherein flattish pebbles dip in the same sense, generally assumed to be the upstream direction (see Middleton and Southard (1984) for a discussion of the forces on a flat pebble). It is often emphasized that this type of fabric must be distinguished from the preferred orientation of clasts in cross-bedded gravels indicating downstream dips. This distinction may not always be evident, especially in core, and hence I suggest using the term "imbrication" in a purely descriptive sense.

Pebbles dipping in the direction of mass transport have been noted from ancient (this study) and modern (Hart and Plint 1989) gravelly shorefaces, and there is an underlying reason for this. Figure 4.9 shows a conceptual model of a discoidal pebble in a nearshore zone subjected to shore-normal oscillatory wave motion and shore-parallel longshore flow. Should the pebble imbricate itself with respect to the unidirectional flow, its orientation will be unstable with respect to the oscillatory component. A pebble which is imbricated with respect to either the onshore or offshore component of the oscillatory flow will be toppled by the reversing flow. Under these conditions, the most stable position for the pebble might be for it to lie as flat as possible on the sea floor, or on the lee face of gravel bedforms - if present. In the event of an oscillatory motion producing symmetrical coarse-grained ripples, the pebble would orient itself in either sense (e.g. Leckie and Walker 1982), but if the bedform migrates, discoidal pebbles should lie on the lee face (Hart and Plint 1989). Upcurrent imbrications would therefore not be expected in most shallow marine settings.

Figure 4.9. Cartoon showing a discoidal pebble under the influence of a longshore current and wave-induced oscillatory currents at nearly right angles. A pebble dipping into the current will be unstable with respect to the oscillatory flows.

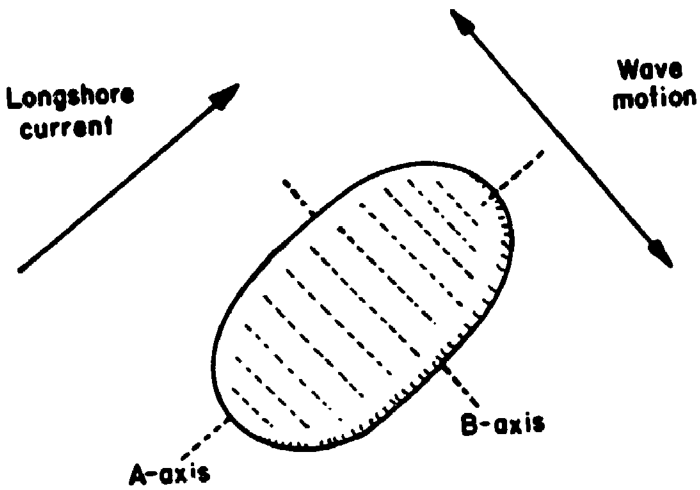
Longshore current
Wave motion
A-axis
B-axis

4.3.4 Summary - Bay Tree

The section at Bay Tree appears to represent a simple, upward-shallowing, progradational package, with shoreface conglomerates conformably overlain by beach conglomerates. Paleocurrent evidence suggests a NW-SE trending shoreline, with sediment transport to the SE produced by longshore currents. A schematic reconstruction of the principal morphological components at this locality is presented in Fig. 4.10.

The large-scale form of the conglomerate body at this site cannot be determined. However, given the evidence for strong longshore pebble dispersal, I would suggest that the conglomerate body is probably elongate in a shore-parallel direction. In Section 4.7, evidence will be presented which suggests that conglomerate units with this orientation can be found in the subsurface.

4.4 Mount Niles - Elephant Ridge

This locality has not previously been described. In 1987, this outcrop was visited for reconnaissance purposes to investigate what appeared to be the most westerly exposure of the Cardium Formation (based on Stott's (1967) fig.2). As a result of that visit, a longer stay was spent on the outcrop in the summer of 1988.

The thickest part of the conglomerate is situated in a trough-shaped lens on the western face of Mt. Niles which

Figure 4.10. Reconstruction of depositional conditions at the Bay Tree locality.

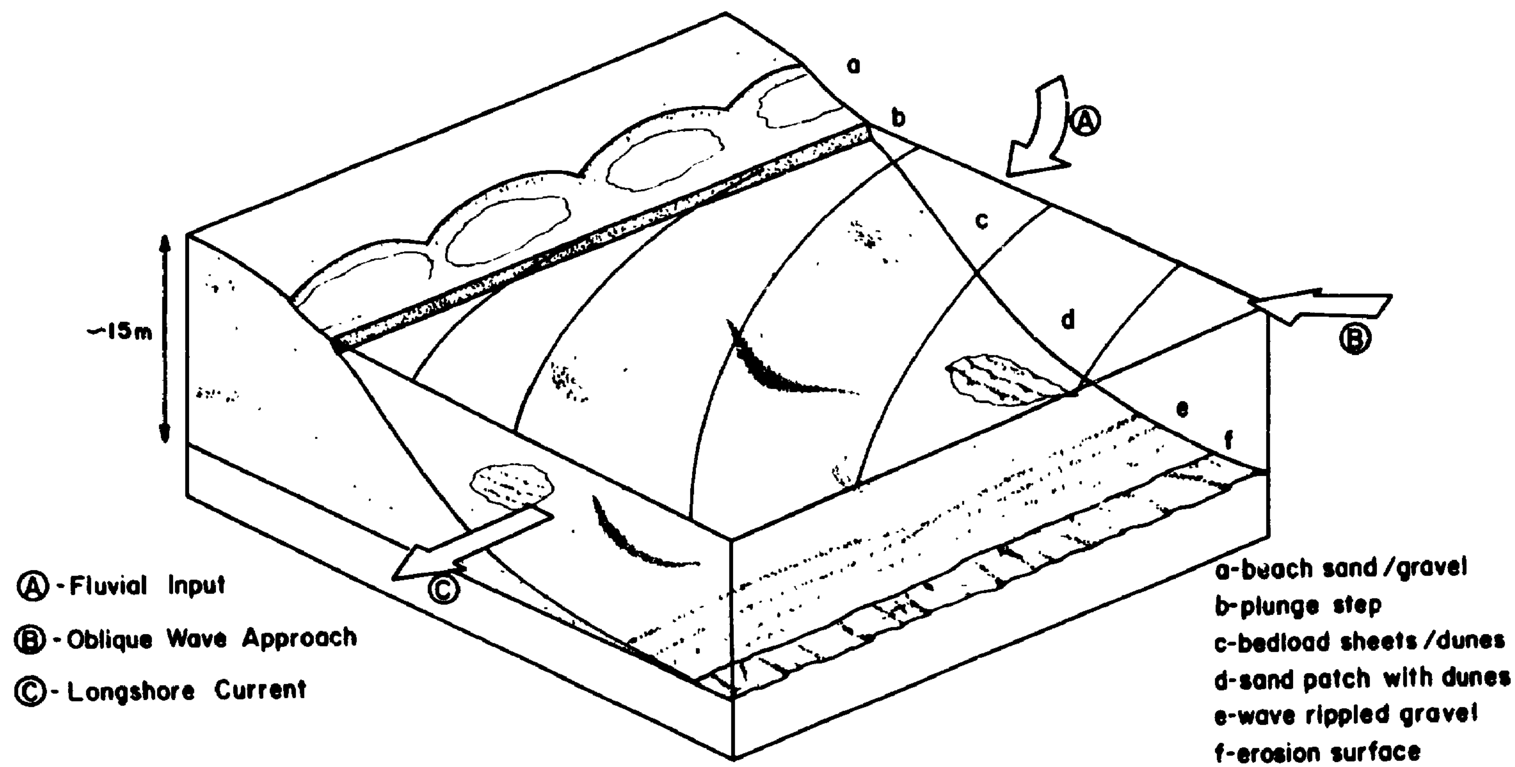
a
b
c
d
e
f
Ⓐ
Ⓑ
Ⓒ
~15m
Ⓐ - Fluvial Input
Ⓑ - Oblique Wave Approach
Ⓒ - Longshore Current
a-beach sand/gravel
b-plunge step
c-bedload sheets/dunes
d-sand patch with dunes
e-wave rippled gravel
f-erosion surface

appears to have incised several meters into a swaley cross-stratified shoreface package (Fig. 4.11a). I was unable to locate the conglomerate (a "resistant" unit) during a reconnaissance study of the eastern face of the mountain, suggesting it may die out in that direction. Where exposed, the upper surface of the conglomerate is covered in coarse-grained wave ripples (Fig. 4.11a,b). Several hundred meters to the south, the wave-rippled surface is overlain by a few meters of swaley cross-stratified sandstone. The exact stratigraphic position of this outcrop is uncertain, but here the wave-rippled surface is tentatively correlated with the transgression of the E1 surface (Chapter 6).

4.4.1 Lithology

Description

A cross-section from the trough-shaped unit is presented in Figure 4.12. The cross-section is hung (wherever possible) on the wave-rippled gravel surface. At least four meters of incision are apparent at the base of the conglomerates. I will restrict the following discussion to the facies overlying the basal erosion surface, and hence facies 16 sandstones with pebble stringers will not be discussed (see section 4.6).

The dominant facies (Facies H) from the main conglomerate unit consists of matrix-supported pebbly granule conglomerate (32% of total thickness). The matrix generally consists of medium- to coarse-grained sand. Bed

Figure 4.11. Mount Niles locality. A) View to north of main conglomerate body, showing how base cuts down (arrows) while top surface remains nearly horizontal. B) Symmetrical coarse-grained wave ripples. Where found *in situ*, a NW-SE orientation is generally apparent. C) Coarse-grained interference wave ripples. D) Cross-bedded matrix-supported conglomerate indicating flows to southeast. Pocket knife for scale (arrow). E) Very poorly sorted pebbly sandstone.

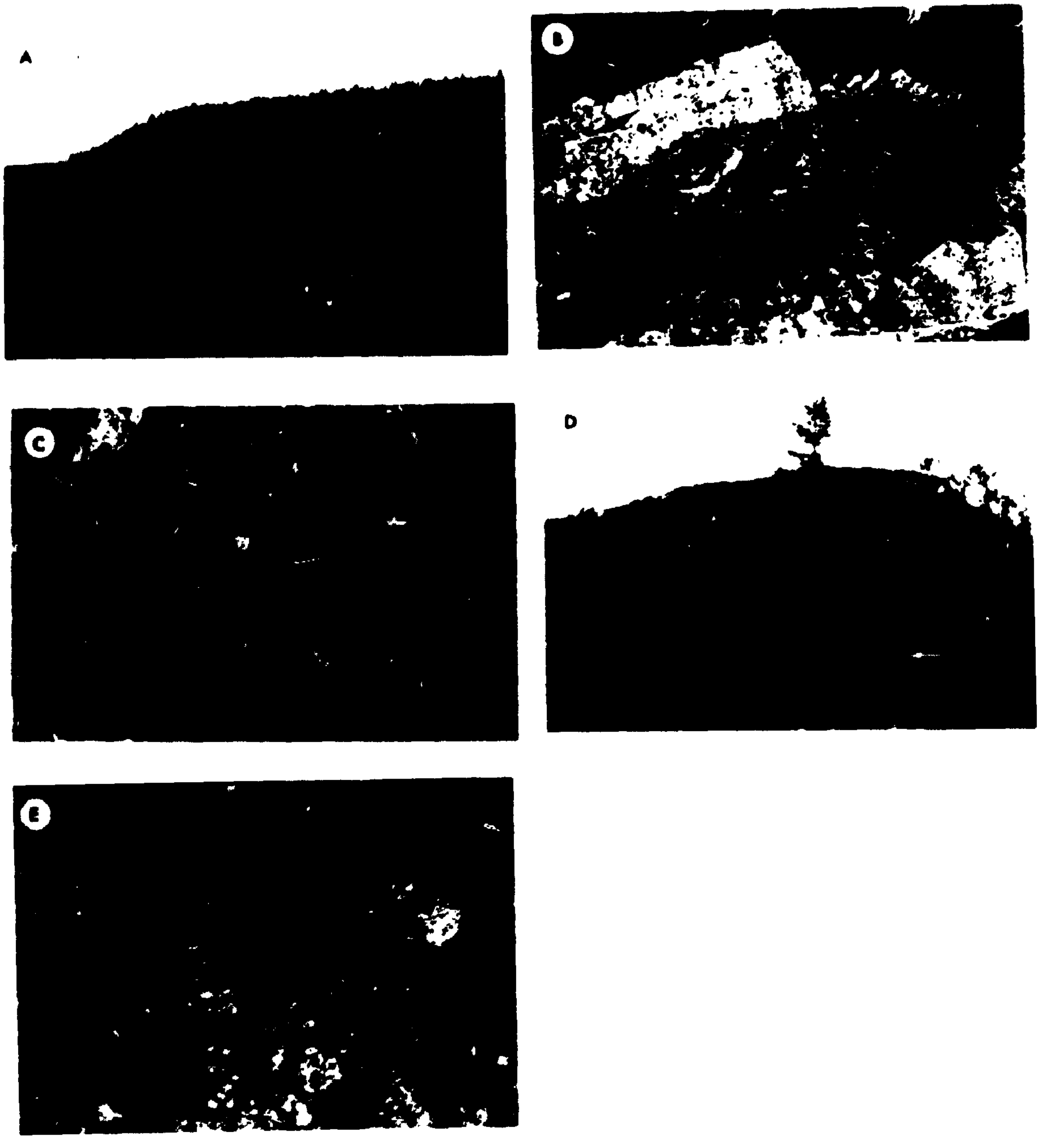
A
B
C
D
E

Figure 4.12. Measured sections from Mount Niles locality. Letters and numbers to left of each section refer to facies described in text.

MT. NILES

CHANNEL MOUTH ASSEMBLAGE

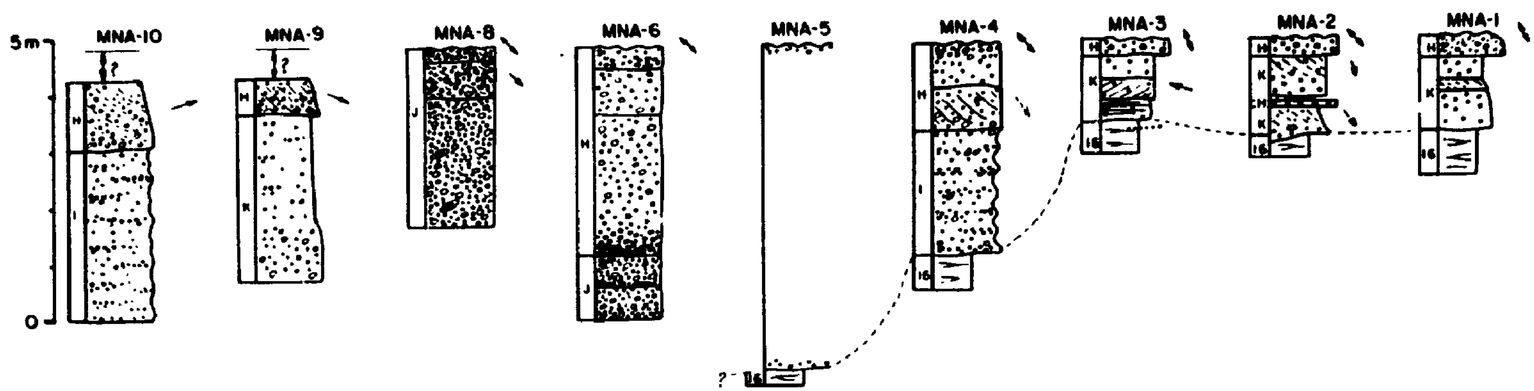

thickness ranges from .25 to 2.5 m, and beds can be either massive or cross-bedded, with sets up to 1.2 m thick (Fig. 4.11d). The wave-rippled surface at the top of the section may be formed on the upper surface of beds of this facies.

Units consisting of interbedded matrix-supported pebbly conglomerate and pebbly medium- to coarse-grained sandstone (Facies I) comprise 25 % of the measured section. These units range from 2 to 3 m thick and are crudely stratified, in places with conglomerate lining shallow scours.

Clast-supported pebbly conglomerates and pebbly granule conglomerates (Facies J) form 23% of the measured section. They range from .25 to 2.3 m thick, and may be cross-bedded. This facies can underlie the wave-rippled upper surface.

Poorly-sorted pebbly sandstones are the last facies (Facies K; Fig. 4.11e), comprising 20% of the measured section. The sandstone ranges from fine- to coarse-grained. Unit thickness varies from .1 to .9 m, and they can be either massive or cross-bedded. Graded units may be noted locally.

Because of the relative thinness of the conglomerate body, there are generally not enough measurements of D_{10} from individual sections to look for meaningful vertical trends. Section MNA-6 has the most measurements of D_{10} at 6, and no vertical trend is apparent. An overall fining trend, from North to South, is apparent when the lateral variations are examined (Fig. 4.13).

Figure 4.13. Lateral trends in D_{10} at Mount Niles locality. See text for discussion.

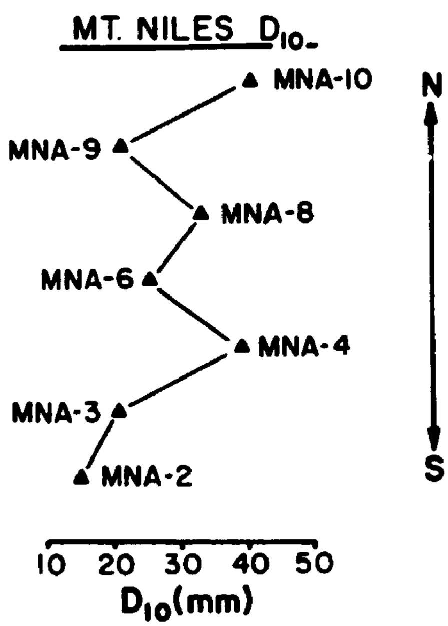

MT. NILES D_{10}
MNA-10
MNA-9
MNA-8
MNA-6
MNA-4
MNA-3
MNA-2
N
S
10 20 30 40 50
D_{10}(mm)

Interpretation

The two-dimensional "geometry" of the conglomeratic body, with its incised base and horizontal upper surface, suggests a channel fill. It should be noted however that the "channel" appears to terminate to the east (somewhere under the crest of the mountain). Clast segregation is noticeably more poorly developed than at the Bay Tree section; there are proportionately more matrix-supported conglomerates and pebbly sandstones at Mount Niles. Lenticular units are present in places, especially in the interbedded conglomerate and pebbly sandstone facies. All these characteristics suggest fluvial activity. The southward-fining trend could indicate longshore transport (by analogy with the Bay Tree locality), or could be indicative of decreased flow competence toward the channel margin.

The cross-bedded conglomerates and pebbly sandstones could have formed in either a fluvial or marine setting. The wave-rippled upper surface suggests marine conditions, and is tentatively identified with a short-lived(?) transgression surface (Chapter 6) based on analogies with Recent sediment-starved coarse-grained sea floors (see review by Leckie 1988).

4.4.2 Paleocurrents

Description

The compiled paleocurrent data are presented in Figure 4.14a. Wave-ripple crestlines are relatively tightly grouped, trending generally NW-SE. The mean cross-bed orientation from the conglomerates and pebbly sandstones is to the southeast. Many more cross-beds with a general orientation to the southeast can be noted on slumped blocks for which precise paleocurrent data is not determinable. Other cross-beds are oriented toward the northeast.

A pebble fabric from a coarse-grained wave-ripple form is shown in Figure 4.14b. It can be seen that the dominant dip direction is to the west, with the ripple crestline trending NW-SE.

Interpretation

The crestline orientations of coarse-grained wave-ripples tend to give a good approximation of local shoreline trend (Leckie 1988). In the present case, this indicates a NW-SE trending shoreline. Like the Baytree type locality, the southeast orientation of cross-bedded conglomerates and pebbly sandstones indicates longshore transport in that direction. Average D_{10} values also decrease to the southeast, strengthening the longshore interpretation. Some seaward transport of gravel is suggested by the northeast paleocurrent orientations. This transport may have been driven by strong fluvial discharge events. The pebble fabric from the coarse-grained ripple suggests onshore migration of the ripple form (Section 4.3.3).

Figure 4.14. Paleocurrent indicators from Mount Niles locality. A) Spoke diagram showing coarse-grained wave ripple crestline orientation and conglomerate and pebbly sandstone cross-bed orientation. Mean crestline orientation probably approximates shoreline orientation. B) Pebble fabric from a coarse-grained wave ripple, suggesting onshore pebble migration as described in text.

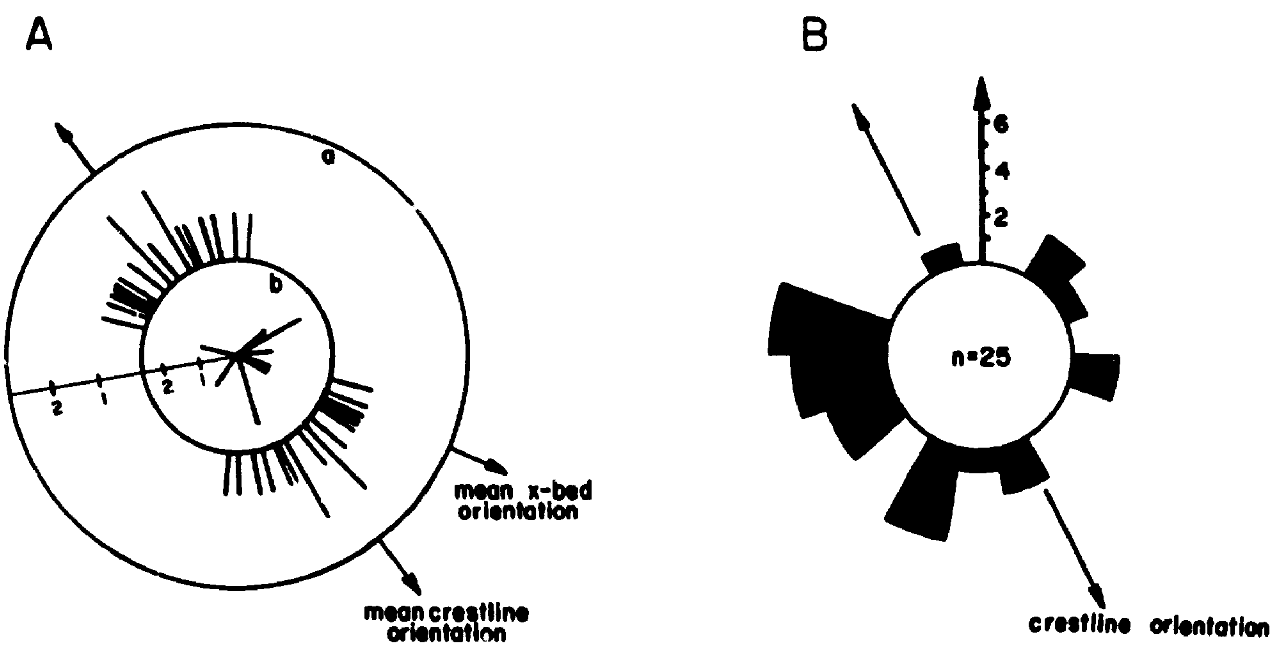

a - coarse-grained wave ripple crestlines
b - cross-bedded conglomerate

4.4.3 Summary - Mount Niles

The conglomeratic unit at this locality appears to represent an environment in which both fluvial and shoreface processes were operative. In this context, the unit appears rather analogous to the "channel mouth assemblages" described by Kleinspehn *et al.* (1984), although the evidence of bioturbation noted by them was not apparent at Mount Niles.

4.5 Horseshoe Mountain

This locality has not previously been described. The name Horseshoe Mountain is here employed for an unnamed mountain to the southwest of Squaw Mountain on NTS 1:50,000 map sheet 93-I-16. Three sections were measured along the north side and end of a U-shaped embayment which opens to the northeast. Paleocurrent measurements were also obtained from exposures between measured sections. In general, the sections here are comprised of several meters of flaggy-weathering sandstones of facies 16 overlain by cross-bedded pebbly sandstones and conglomerates (Fig. 4.15).

Stratigraphically, the lower swaley cross-stratified unit can be correlated with the lower part of the Kakwa Member (Chapter 6). The pebbly sandstones and conglomerates appear to represent a fluvial unit (see below) which has replaced the upper, coarser-grained portion of the Kakwa Member (Chapter 3). It is the pebbly sandstones and conglomerates which form the basis of the present section.

Figure 4.15. Measured sections from Horseshoe Mountain locality. Letters and numbers to left of each section refer to facies described in text.

HORSESHOE MT.

FLUVIAL ASSEMBLAGE

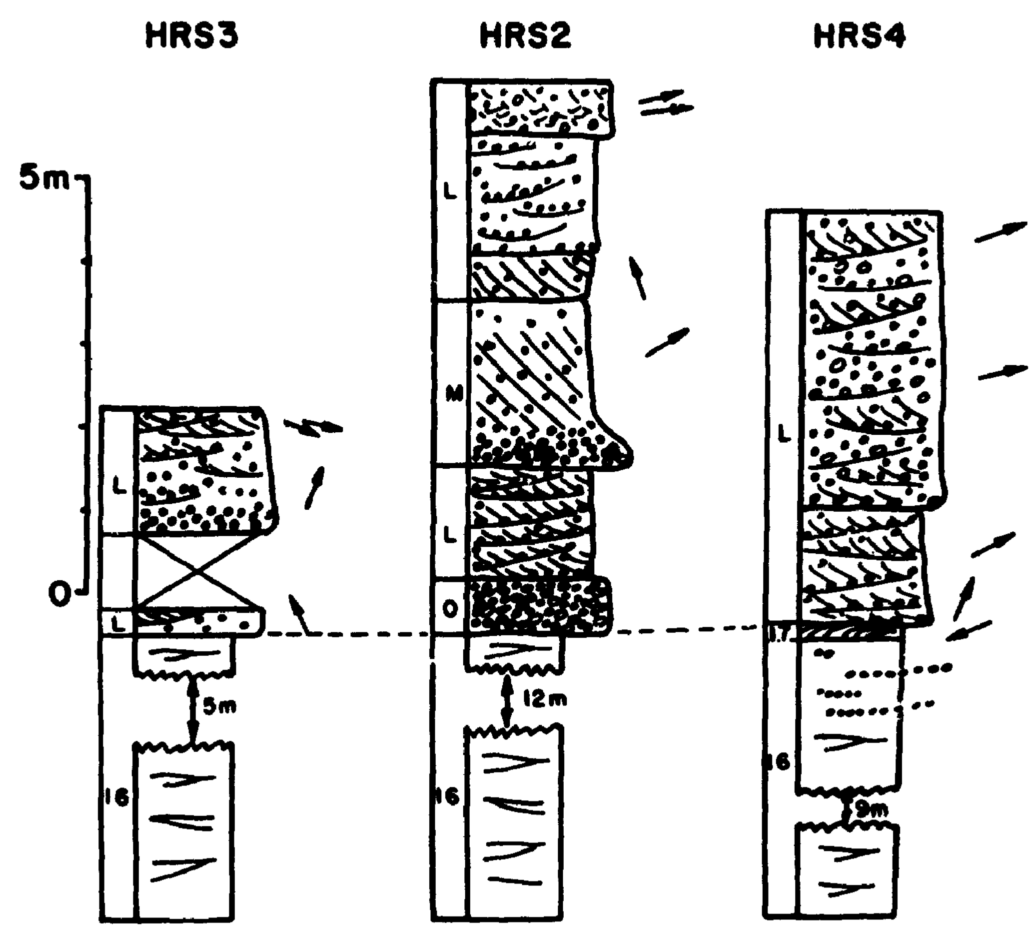

4.5.1 Litholcgy

Description

Over 95% of the measured section consists of cross-bedded pebbly sandstones and conglomerates which can be divided into two main sub-types. Facies L consists of units up to 3.4 m thick comprising dm-scale cross-bedded pebbly sandstones and matrix-supported conglomerates (Fig. 4.16a,b). Continuous gradation was noted between the matrix-supported conglomerates and the pebbly sandstones both within and between units. Conglomerates can be found along the toesets of cross-beds. These units comprise 69% of the total section. Graded (conglomerate to pebbly sandstone) units typically between 1 and 2 m thick consisting of single trough cross-beds (Facies M) comprise 26% of the measured section. Clast-supported pebble conglomerates (Facies N) account for less than 5% of the measured section.

The cross-bedded units are highly lenticular, this is especially true of the larger, 1 to 2 m thick sets. In some cases, the pebble-lined concave-up scours appear to represent the toesets of festoon cross-beds.

Paleocurrent information from the cross-bedded units is presented in Figure 4.17. There, it can be seen that the dominant sediment transport direction was to the northeast.

Interpretation

Figure 4.16. Lenticular, cross-bedded pebbly sandstones and matrix-supported conglomerates from the Horseshoe Mountain locality. Pocket knife for scale (arrow) in (B).


A

Figure 4.17. Cross-bed orientations, Horseshoe Mountain locality. Dominant trend is to the NE, roughly perpendicular to Cardium shoreline trend indicators.

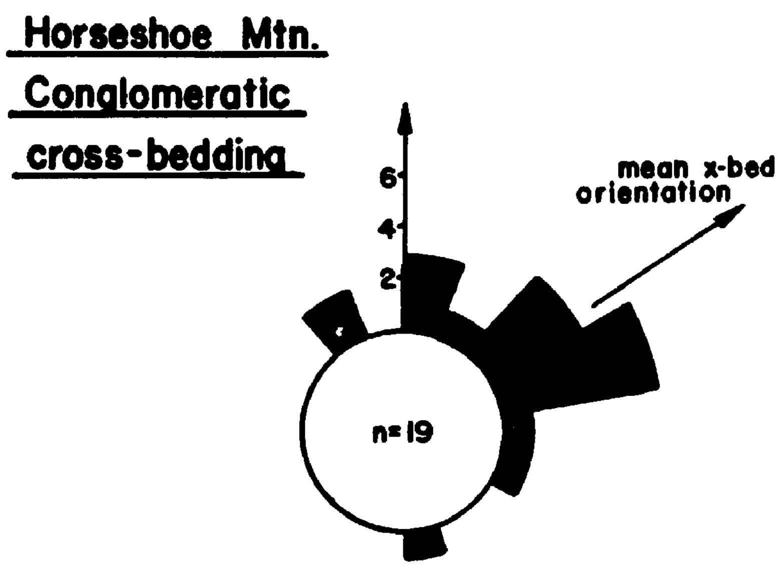
Horseshoe Mtn.
Conglomeratic
cross-bedding
mean x-bed
orientation
6
4
2
n=19

The poor clast segregation (high abundance of matrix-supported conglomerates and pebbly sandstones), and pronounced lenticularity are both suggestive of fluvial deposition (Clifton 1973). The meter-scale cross-bedded units could have been produced by the downstream migration of slip-face bounded lobate bars (Ashmore 1982), with the lenticular base representing the base of the scour pools into which the bars migrated. The upward-fining grain size trend noted in these units is that which would be expected to develop on the slip-face (Ashmore 1982). The fluvial interpretation is strengthened by the paleocurrent evidence, which suggests a principal transport axis at nearly a right angle to contemporaneous shoreline trends in the Cardium Formation (next chapter).

4.5.2 Summary - Horseshoe Mountain

The poorly-sorted matrix-supported conglomerates and pebbly sandstones from this locality were probably deposited by a braided fluvial system carrying a mixed load of sand and gravel. The principal transport direction was to the northeast, perpendicular to the Cardium shoreline trend. There is no evidence of reworking of these deposits by shallow marine processes.

4.6 Other shoreface and beachface conglomerates in outcrop

In this section, I will briefly document some other occurrences of littoral conglomerates from the Cardium Formation in outcrop in the present study area.

A relatively common type of shoreface conglomerate can be found locally in the swaley cross-stratified (facies 16) sandstones of the Kakwa Member (e.g. Bay Tree, Mt. Niles, Horseshoe Mt.). This consists of pebbly units of variable thickness lining broad shallow scours in the swaley cross-stratified sandstones which are typically pebble-free. High-angle scour walls are never observed. In well-exposed sections (e.g. Cutbank Lake), the character of the pebbly units increases upward from stringers a single or a few grains thick near the middle of facies 16, to clast-supported pebble conglomerates up to 30 cm thick near the top of that unit (Figs. 4.18a-d).

I interpret the pebbly units in facies 16 sandstones to have been transported and deposited by rip currents. The up-section thickening is that which would be expected from a prograding shoreline, given that the velocity (and hence sediment transport capabilities) of rip currents decreases seaward (Section 4.2.2). A pebble fabric from a 30 cm thick unit at Cutbank Lake is presented in Figure 4.19. It can be seen that the dominant dip direction is offshore to the Northeast. Visual inspection of this unit suggests an alignment of pebble long axes in a shore-parallel NW-SE orientation. This fabric appears similar to the a (transverse) b (imbricate) type of imbrication described by Harms *et al.* (1982). In this case however, the conglomerate would have had to have been deposited by clasts rolling

Figure 4.18. Shoreface/beach conglomerates in outcrop. A)-D) Upsection increase in conglomerate thickness from Cutbank Lake section. Conglomerates are interbedded with facies 16 sandstones and are interpreted primarily as rip current deposits. Pocket knife for scale (arrowed in C and D). E) Conglomeratic scour-fill in planar-laminated sandstones, interpreted as the product of a small stream crossing a beach. Note high angle walls to left. F) Gently inclined, thinly-bedded conglomerates at Cutpick Hill section interpreted as beach conglomerates.

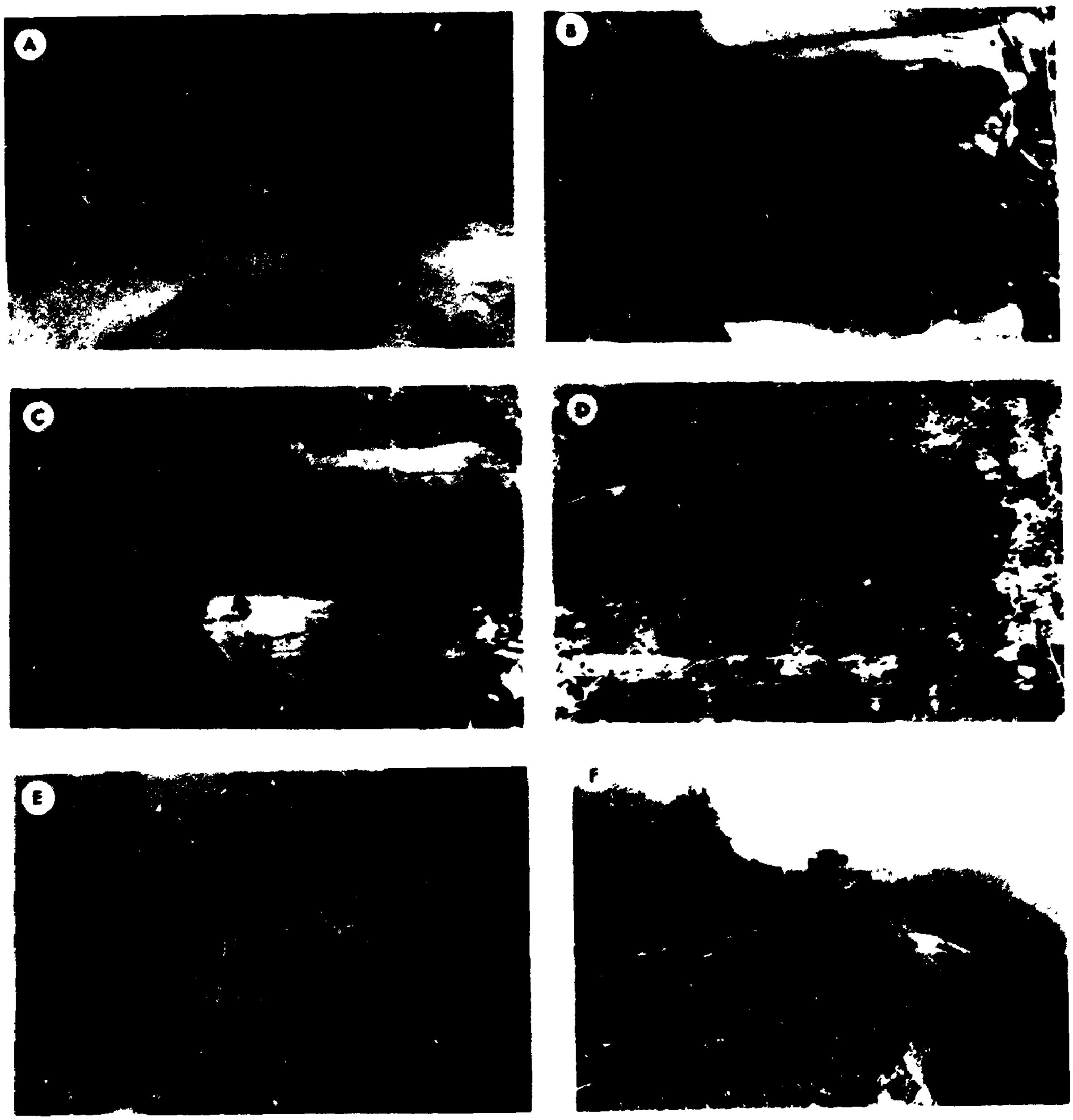
A
B
C
D
E
F

Figure 4.19. Pebble fabric from a 30 cm thick conglomerate bed, Cutbank Lake locality. See text for explanation.

Pebble fabric

Cutbank Lake

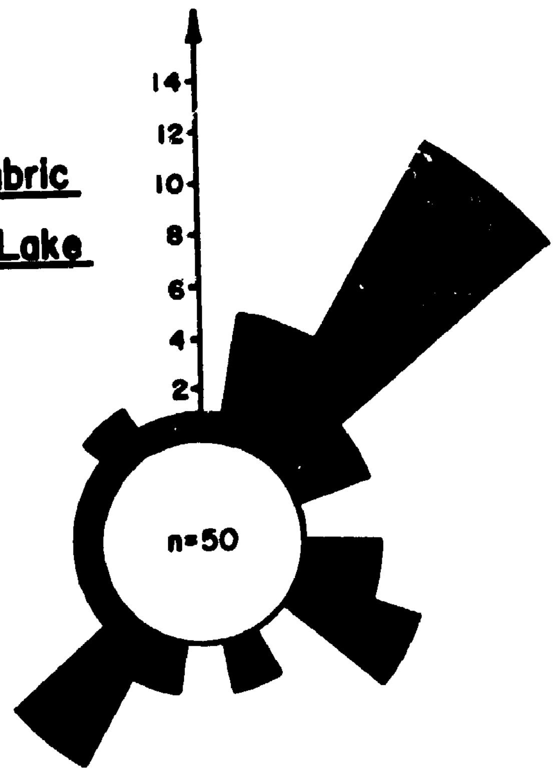

onshore under the influence of strong, localized unidirectional currents (considered unlikely). An alternative (preferred here) is that the fabric developed by grains rolling along the bed in an offshore direction, and coming to rest on the lee side of migrating gravel bedload sheet, or a offshore migrating gravel wave-ripple.

An uncommon type of beach conglomerate was present at the Murray River section. Here, pebbly granule conglomerates and pebbly sandstones fill steep-walled scour fills up to 40 cm thick cut into planar laminated fine sandstones interpreted as beach deposits (Fig. 4.18e). Pebbly units can be cross-bedded, and multiple episodes of fill can be indicated. Scour walls are oriented in a NE-SW direction. The conglomerates were probably deposited in small streams cutting across the beach (e.g. Clifton, Phillips and Hunter 1973; Clifton 1981). My own (unpublished) observations of modern beaches suggest that high-angle walls (such as those observed here) can be maintained subaerially, apparently because of the cohesive properties imparted by capillary waters.

In addition to the Bay Tree locality, thick beach conglomerates were observed at two other sections. These were located at Cutpick Hill (Fig. 4.18f) and Mount Puggins. In both cases, the conglomerates comprise well-sorted and thinly-bedded units at the top of the Kakwa Member, gently dipping to the Northeast. Normal and inverse grading are noted in individual "beds" (few cm thick) at the Cutpick Hill location.

It should be noted that the interpretations presented here appear to be essentially opposite to those presented by Bourgeois and Leithold (1984). These authors interpreted high-angle asymmetric pebble-filled scours (similar to those observed at the Murray River section; their figure 11) as being the product of some type of unknown subaqueous flow from the upper shoreface. Shallow, disk-lined scours (their figure 7c) were interpreted by them as the products of streams crossing a beach. Given the sedimentologic and stratigraphic constraints, I believe the present interpretations to be correct, at least in the present case. The problem of maintaining subaqueous, high-angle walls in cohesionless sand (*especially* in the presence of strong wave action) must surely be considered as overwhelming evidence against the Bourgeois and Leithold (1984) explanation.

The lenticular nature of the rip current conglomerate deposits (lining upwardly-concave surfaces) warrants special mention. This characteristic might lead an observer, following Clifton (1973), to lean towards a fluvial interpretation. I will point out however, that this criterion is strictly applicable only for *wave-reworked* conglomerates. Pebbles lining the base of a rip channel appear to be buried before significant reworking by waves can occur.

4.7 Other conglomerates in subsurface

Given that one of the principal aims of this study was to attempt to propose diagnostic criteria for the identification of shoreface conglomerates in the subsurface (Chapter 1), it is unfortunate that thick conglomerate units were not observed in cores from the present study area. That said, here I present the subsurface data I was able to gather.

A conglomeratic shoreface to beach succession was measured in core 10-18-63-5W6, from just south of the study area. In this core, it is possible to identify a variety of conglomerate types, including: a) lenticular conglomerates in facies 16 sandstones interpreted as rip-current deposits (Fig. 4.20a); b) low-angle cross-bedded clast-supported pebble conglomerates, with flattish pebbles lying on foresets (Fig. 4.20b); and c) planar-laminated, interstratified granule conglomerates and sandstones interpreted as beach deposits (Fig. 4.20c). The well-segregated nature of the conglomerates and sandstones, combined with the well-rounded mineralogically mature clasts (chert and quartz), lack of shales, high degree of sorting of the conglomerates and the stratigraphic context (conformably underlying beach conglomerates, and laterally equivalent to known shoreface-to-beach successions in sandstones; *cf.* Chapter 5), help identify these conglomerates as shoreface deposits.

Figure 4.20. Shoreface/beach conglomerates in core 10-18-63-5W6. A) Thin conglomerates interbedded with facies 16 sandstones, interpreted as rip current deposits. B) Low-angle cross-bedding with flatish pebbles lying on foresets. C) Very well sorted, horizontally-stratified pebble and granule conglomerates, and (very) coarse-grained sandstones, interpreted as beach deposits. Arrow points up section in all photographs.

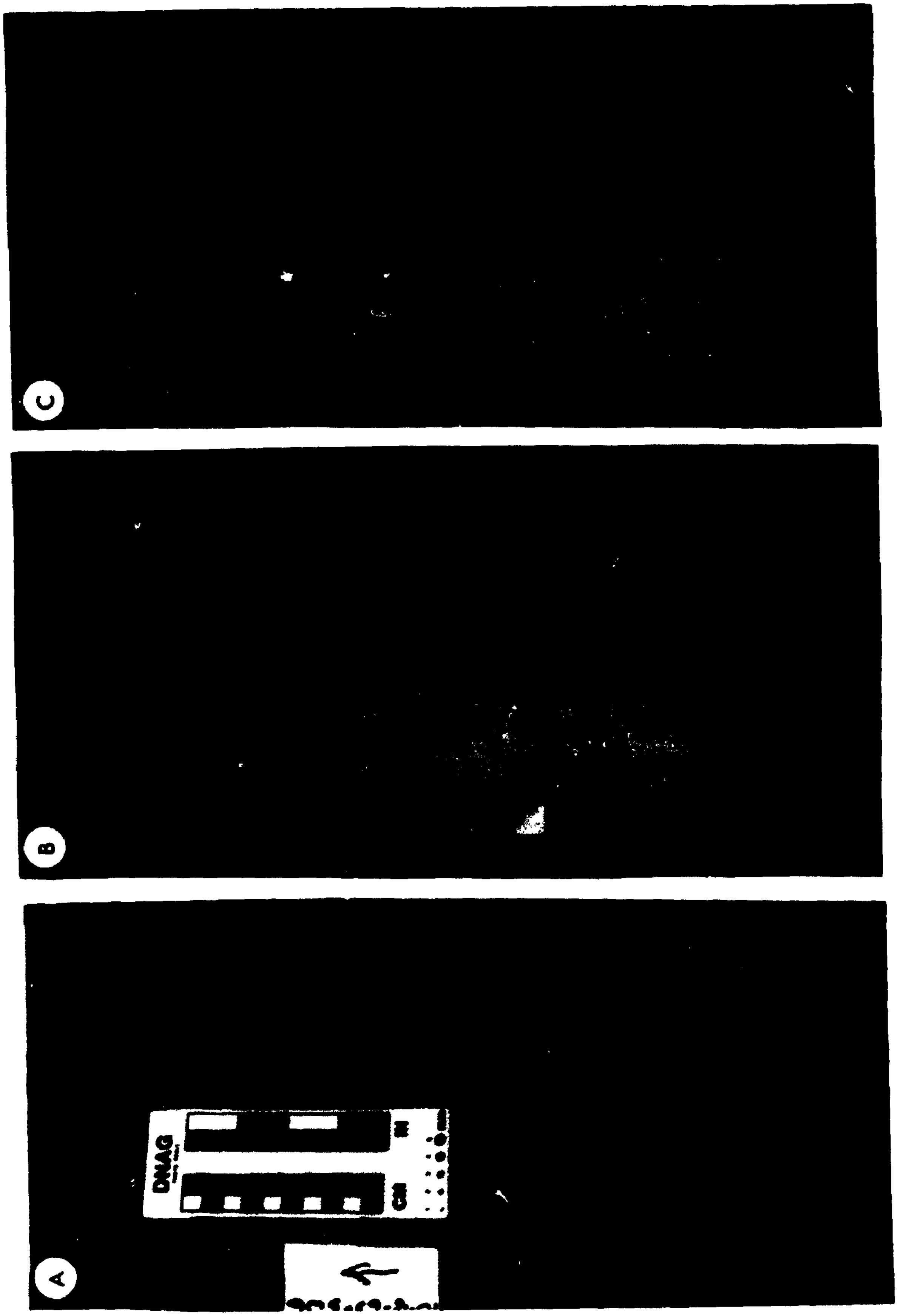
C
B
A
DNAG

Pebbly units inferred to have been deposited in a fluvial setting are present in 15-16-68-13W6. Here, pebbly sandstones and thin (up to 20 cm) matrix-supported conglomerates are interbedded with horizontally-laminated and cross-bedded sandstones, shaley and carbonaceous units, and sandstones containing angular mudstone intraclasts (Fig. 3.4). The latter would not have survived in a high energy shoreface environment.

The orientation of a conglomerate body in the subsurface may help in its identification; shoreface conglomerates should be aligned parallel to other regional shoreline trends. An example of this type of conglomerate appears present in the cross-section of Figure 4.21. Although the wells are not cored, conglomerates in this area can be identified in the wells on the basis of their high resistivities, suggesting either that they are hydrocarbon-bearing, or that invasion of porosity by drilling fluid occurred (J. Nurkowski, written communication, 1989). In plan, the conglomerates are not inconsistent with a NW-SE trending body which would be parallel to other regional shoreline indicators (see Chapter 5).

Elsewhere in the Cardium Formation in subsurface, conglomerates interpreted as shoreface deposits on the basis of their stratigraphic position can be found in the Carrot Creek area (Bergman and Walker 1987). At the Carrot Creek "K" Pool, the sand content of the conglomerate decreases

Figure 4.21. Probable linear shoreface conglomerate in subsurface. See text for explanation.

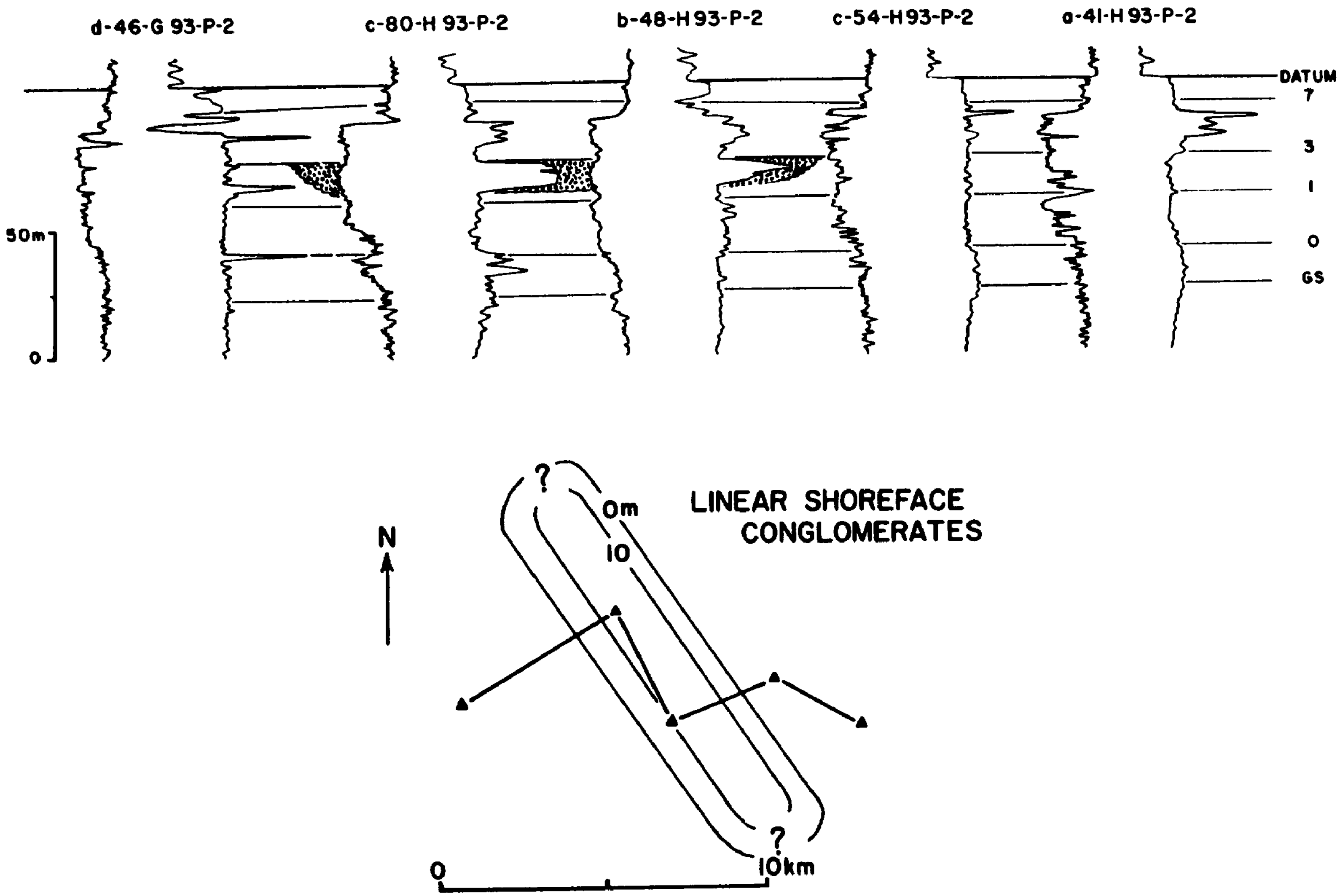
d-46-G 93-P-2
c-80-H 93-P-2
b-48-H 93-P-2
c-54-H 93-P-2
a-41-H 93-P-2
DATUM
7
3
1
0
GS
50m
0
LINEAR SHOREFACE
CONGLOMERATES
N
?
0m
10
?
0
10km

basinward away from inferred fluvial point sources, and clast size diminishes alongshore in the downdrift direction; porosity and permeability data can be employed to help identify these trends (Arnott *in press*). Sinha (1970), working in the Edson area, indicated that clast size decreased towards the southeast in units identifiable as shoreface conglomerates from the Burnstick Allomember (cf. Pattison 1988; Plint 1988); this again is the downdrift direction.

4.8 Summary of shoreface conglomerates

Outside of the presence of an *in situ* shallow marine trace fauna, there appears to be no single criterion which can be employed to distinguish between fluvial and shoreface conglomerates. The distinction must continue to be made on the basis of combinations of observed suggestive features. This is, in principal, no different from the procedure employed in the identification of shoreface sandstones.

In outcrop, the available criteria appear to be adequate for the identification of shoreface conglomerates. Based on observations from Bay Tree, it can be seen that paleocurrent evidence can be extremely useful in deciphering the depositional environment of conglomerates. The stratigraphic evidence at that site (the conglomerates sit conformably under units identifiable as beach deposits) also helps in their interpretation. An upward coarsening, and upward increase in the proportion of clasts having "beach" form indices might also be developed in shoreface conglomerates, but these criteria need to be more rigorously tested, preferably from modern environments. Average values of form indices developed from *beach* gravels cannot be used to identify shoreface conglomerates.

The bed lenticularity criterion suggested by Clifton (1973) does appear to be applicable to the Bay Tree outcrop. A well-defined horizontal stratification is developed there. Elsewhere though, lenticular shoreface conglomerates do occur. These represent channel mouth deposits (Section 4.4) or rip current deposits (Section 4.6). In both cases, the conglomerates were probably deposited by strong offshore flows, then buried below the influence of wave reworking. Sherman, Short and Takeda (1990) have demonstrated that the depth of reworking in rip channels is generally greater than the depth of reworking by wave activity alone.

In the subsurface, many of the criteria used in outcrop studies cannot be observed. This places a greater emphasis on establishing the stratigraphic position of the conglomerates, the orientation of the conglomerate body, and regional trends in grain size and sorting.

THE STRATIGRAPHY AND SEDIMENTOLOGY OF THE UPPER CRETACEOUS CARDIUM FORMATION IN NORTHWESTERN ALBERTA AND ADJACENT BRITISH COLUMBIA

VOLUME II

by

Bruce S. Hart

Department of Geology

Submitted in partial fulfilment
of the requirements for the degree of
Doctor of Philosophy

Faculty of Graduate Studies
The University of Western Ontario
London, Ontario
August 1990

TABLE OF CONTENTS

LIST OF FIGURES

LIST OF TABLES

Page

LIST OF APPENDICES

CHAPTER 5

DETAILED DISCUSSION OF SELECTED VERTICAL SECTIONS THROUGH THE CARDIUM FORMATION

5.1 Introduction

Measured stratigraphic sections are the building blocks of the basin analyst. They provide both the raw materials for the definition of sedimentary facies (Chapter 3) and the stratigraphic framework within which these facies are interpreted. Subsequently, by correlating between sections, depositional systems tracts (Brown and Fisher 1977) are delimited and an event ("sequence") stratigraphy may be constructed.

In this chapter, I wish to present selected measured sections through the Cardium Formation both from outcrop and core. As these sections will form the basis of the event stratigraphy to be presented in the next chapter, and as it is in the subsurface that the event stratigraphy has been constructed, correlations between the measured core and outcrop sections and geophysical logs will be established.

Two points should be borne in mind. First, while in some cases identification of well markers as specific "E" or "E/T" surfaces of the Plint *et al.* (1986, 1987, 1988) Cardium allostratigraphy is straightforward, in other cases the identity of specific horizons is only clear once the subsurface correlations have been established. Although the event stratigraphy of the Cardium Formation in the present study area is the object of the next chapter, my choice of picks on the well logs accompanying the measured sections are presented in this chapter for future reference. Second, although the correlation between measured core sections and the corresponding well logs is usually clear, correlation between measured outcrop sections and well logs tends to be more subjective, especially when the distance between the two is large.

5.2 Measured outcrop sections

Twenty-one outcrop localities of the Cardium Formation were visited in the summers of 1987 and 1988. All but one of these sites are located either in (or at the edge of) the Rocky Mountain Foothills, or along the "Cardium Escarpment" which runs approximately E-W south of Dawson Creek, British Columbia (see Appendix 1). These sections provide various degrees of exposure of the Kaskapau Formation, Cardium Formation (Nosehill, Kakwa, Musreau and Amundson (allo)members), and Muskiki Formation. At the final locality, near river level close to the junction of the Smoky and Bad Heart Rivers, part of the Raven River Allomember and the overlying strata up to the Puskwaskau Formation are exposed.

In this section, I will begin by presenting my measured sections from the southern part of the Foothills area, then proceed northwest through the Foothills, and finally east along the escarpment. Only those sections which are either particularly well exposed, or which have other features which makes their presentation important will be presented. A correlation diagram of these and other sections will be presented in the next chapter. Figure 5.1 presents a location map of the outcrop sections described here and the correlation lines of Chapter 6. Selected outcrop photographs from the foothills sections are presented in Figure 5.2, whereas photographs from the Cardium escarpment outcrops are presented in Figure 5.7.

5.2.1 Cutpick Hill

The Cutpick Hill locality (Fig. 5.2a) has been described previously by Stott (1967; his section 58-3), Duke (1985) and Plint *et al.* (1988; based on measured sections of Duke and the present author). As such it provides a convenient reference point for a tie-in with those works. Two sections were measured here by the present author (Fig. 5.3), neither of which were apparently those measured by Stott or Duke. All three of the facies associations described in Chapter 3 are present here.

The base of Section 1 (Fig. 5.3) was selected at the base of the first "obvious" sandier upward succession in the Kaskapau Formation 35 m below the shoreface units. The heterolithic strata of the offshore facies association tend to comprise sandier upward successions, generally 2 or 3 m thick, superimposed on a much larger sandier upward trend (Fig. 5.2b). In Chapter 3 it was suggested that the smaller

Figure 5.1. Location map of outcrops presented in this chapter and correlation lines presented in Chapter 6. Clockwise from bottom: CH - Cutpick Hill, HM - Hat Mountain, MC - Mistanusk Creek, CC - Calliou Creek, HR - Horseshoe Mountain, MR - Murray River, TC - Tepee Creek, MN - Mount Niles (Elephant Ridge), NH - Noetai Hill, FH - Fellers Heights, BM - Bear Mountain, PC - Pouce Coupé, GS - Gundy Station, BT - Bay Tree, CL - Cutbank Lake, SR - Smoky River.

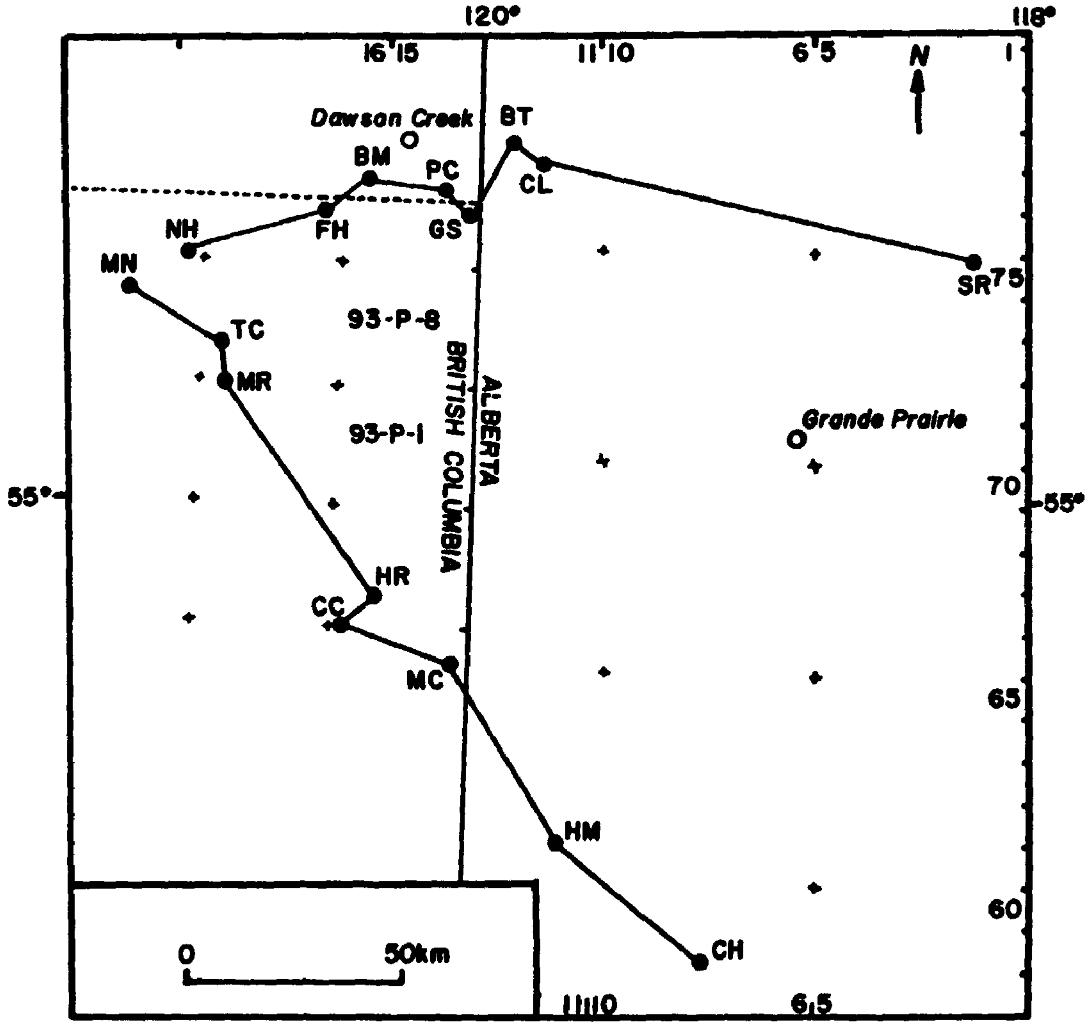
120°
118°
16 15
11 10
6 5
1
N
Dawson Creek
BT
BM
PC
CL
NH
FH
GS
MN
SR
75
TC
93-P-8
MR
BRITISH COLUMBIA
ALBERTA
Grande Prairie
93-P-1
55°
70
55°
HR
CC
MC
65
HM
60
0
50km
CH
11 10
6 5

Figure 5.2. Outcrop photographs from Foothills outcrops of the Cardium Formation. A) Aerial view of the Cutpick Hill locality. Lowest arrow, E1 surface; middle arrow, E3 surface; top arrow, E7 surface. B) Outcrop exposure of offshore facies association at Cutpick Hill. Kakwa Member sandstones and conglomerates in upper right. C) Cardium Formation at Mistanusk Creek. Note near-planar break between "lower" and "upper" parts of the Kakwa Member (the E3 surface; arrow, explained in text). D) Detail of the erosion surface (straight arrows) separating the lower (facies 16) and upper (facies 17) portions of the Kakwa Member (the E3 surface). A thin sandstone, grading upward into carbonaceous mudstone (curved arrow) drapes the underlying topography. E) Plan view of the erosion surface (E3) developed on top of the lower (facies 16) portion of the Kakwa Member. Note smooth, "sculpted" appearance and locally overhanging walls (arrows). Field of view is about 4-5 m wide.

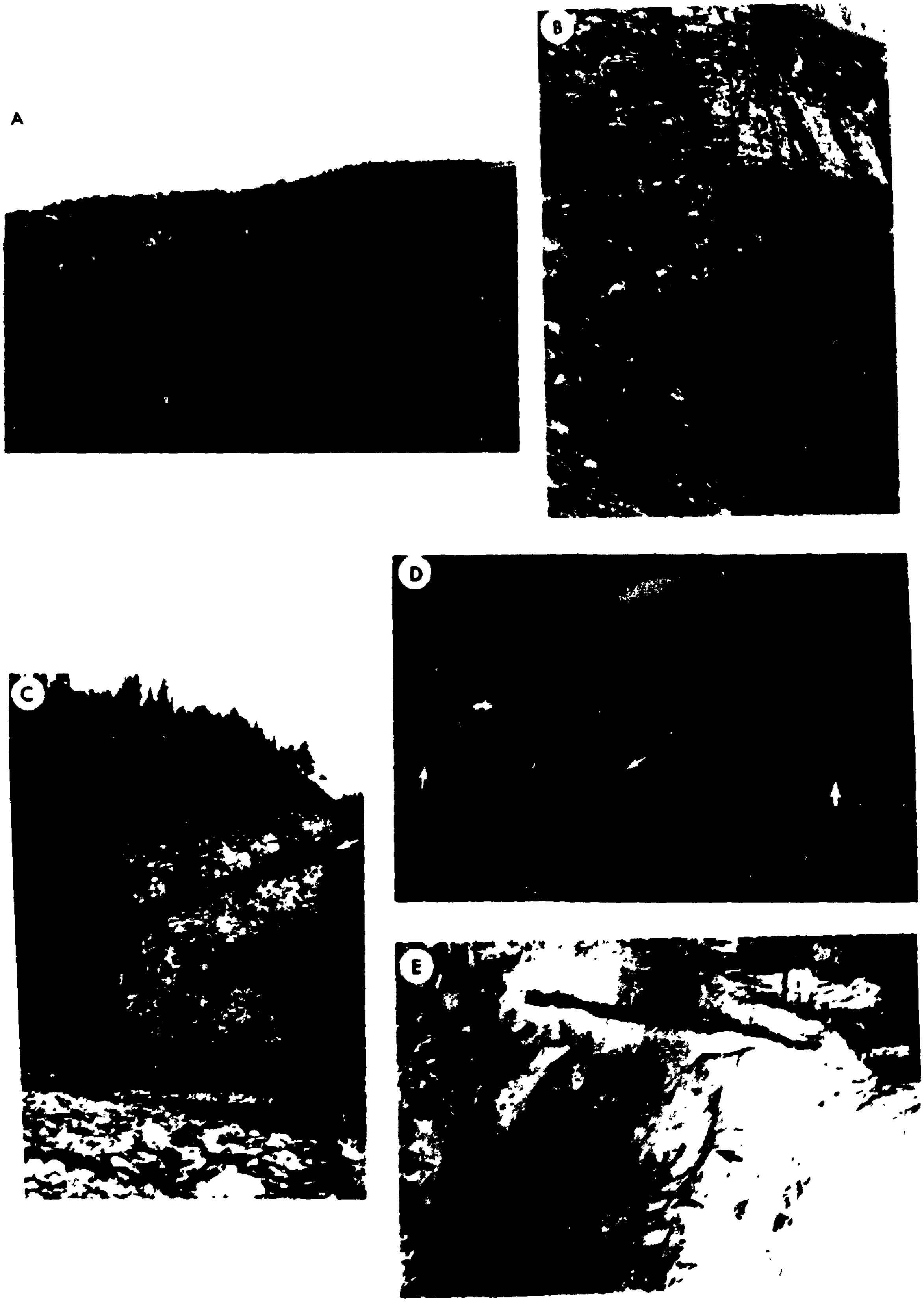

Figure 5.2 (cont.) F) Pebble/cobble layer (E7 surface) separating non-marine strata of the Musreau Member (below) from offshore units of the Muskiki Formation (above) at Mistanusk Creek. Locally, the thickness of the pebble layer increases to a conglomerate a few 10's of cm thick. G) Plan view of pebble/cobble layer (E7 surface) separating non-marine strata of the Musreau Member from the offshore units of the Muskiki Formation at the Calliou Creek section. Note *Thalassinoides* burrows (arrows). H) Aerial view of the Murray River section. Lowest arrow indicates base of facies 16 sandstones; middle arrow indicates approximate position of break between "lower" and "upper" portions of the Kakwa Member (E3 surface); upper arrow indicates position of top of Kakwa Member.

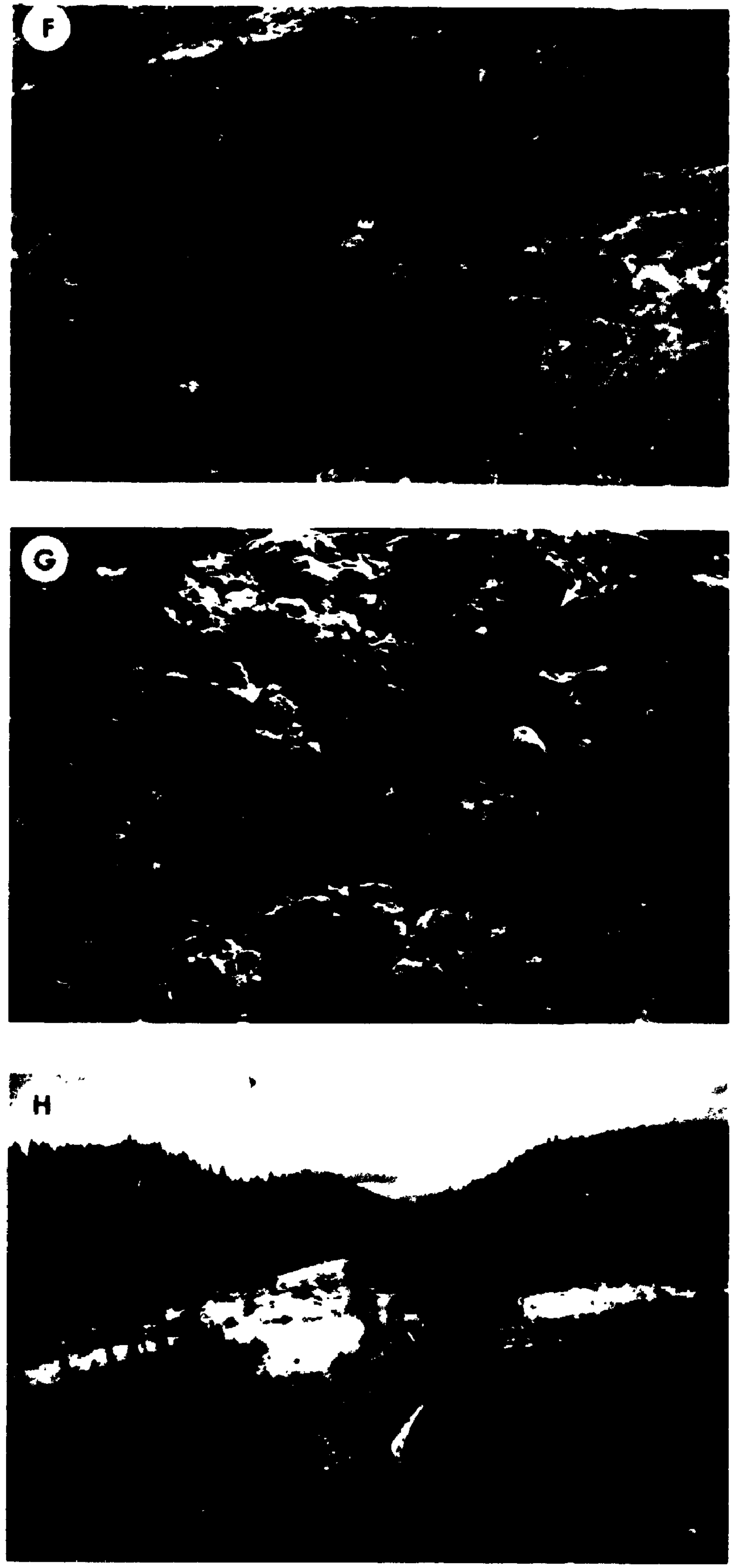
F
G
H

Figure 5.3. Measured Cutpick Hill sections, and suggested correlation to nearby well log (gamma ray to left, resistivity to right). Labelled markers refer to horizons defined in Chapter 6. Numbers to left of sections refer to sedimentary facies defined in Chapter 3. Legend of paleocurrent indicators for this and subsequent sections listed below.

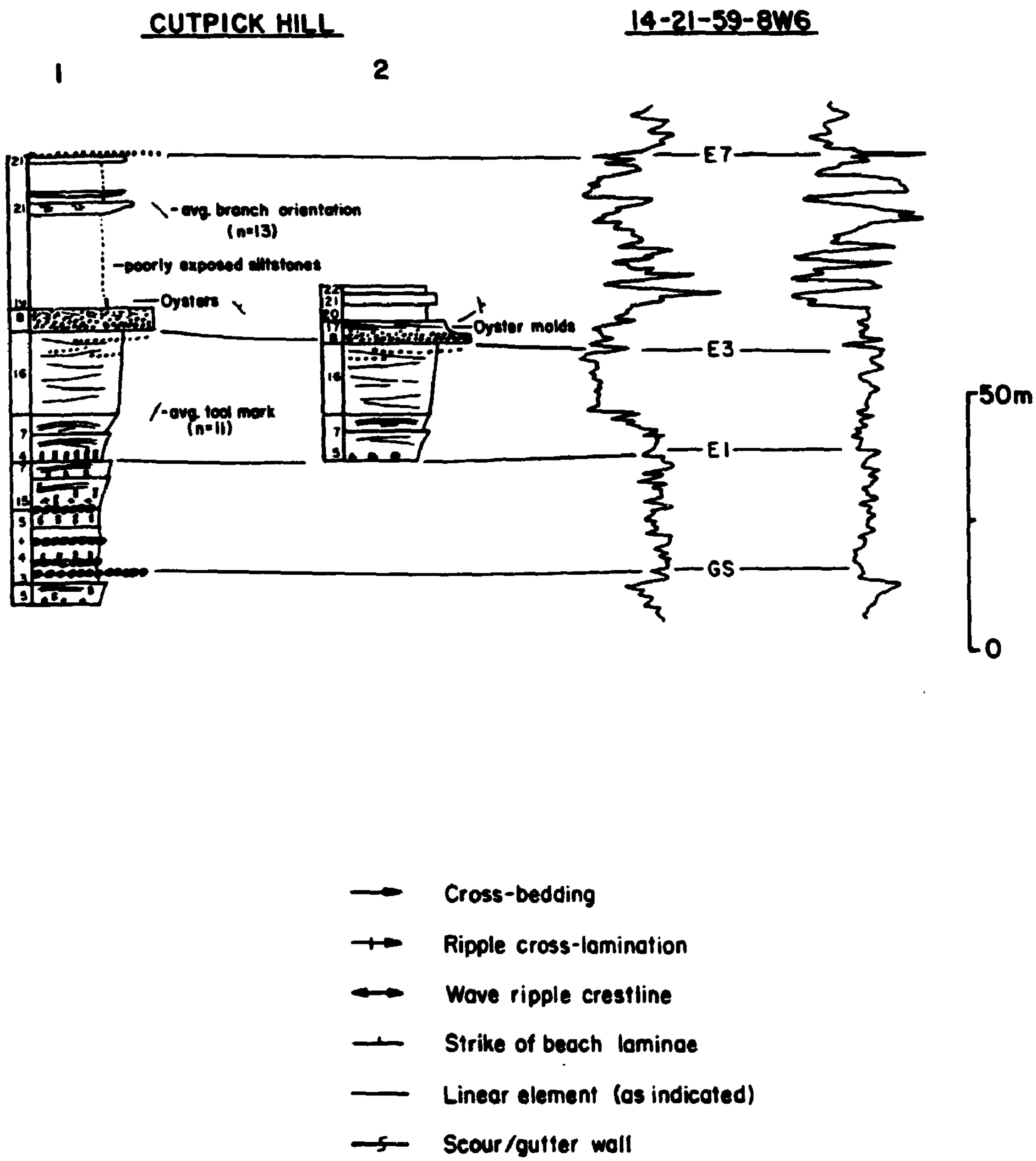

CUTPICK HILL
14-21-59-8W6
1
2
avg. branch orientation (n=13)
poorly exposed siltstones
Oysters
Oyster molds
avg. tool mark (n=11)
E7
E3
E1
GS
50m
0
Cross-bedding
Ripple cross-lamination
Wave ripple crestline
Strike of beach laminae
Linear element (as indicated)
Scour/gutter wall

packages were the product of Milankovitch-scale climate forcing. As indicated in Plint *et al.* (1988), it is possible to correlate the top of one of these small cycles (underlying 1.7 m of heavily bioturbated sandy mudstones) with the E1 surface at the base of the Cardium Formation. According to this correlation, the base of the formation lies then at about 9 m below the base of the shoreface package (Kakwa Member).

The Kakwa Member here consists of about 15 m of swaley cross-stratified sandstones which are sharply overlain by about 4 m of conglomeratic strata. The lower, swaley cross-stratified sandstone shows an upward coarsening trend, consisting of very fine-grained sandstones at the base, and comprising fine-grained sandstone with pebble stringers at the top. As indicated in Chapter 4, these pebbly layers probably represent rip current deposits. At Section 2, this lower unit is overlain by 2.2 m of conglomerate, which is itself overlain by 2.2 m of planar (beach) laminated fine-grained sandstone. At Section 1, the entire interval is conglomeratic, with well-developed conglomerate foreshore deposits exposed at the top (Fig. 4.18f). When corrected for tectonic tilt, the beach deposits indicate a NW-SE trending shoreline. Tool marks exposed at the base of the swaley cross-stratified unit at Section 1 are perpendicular to the shoreline trend presumably the result of offshore-directed flows (see Leckie and Krystinik (1989) and Duke

(1990) for conflicting views on the nature of offshore flows during storms).

Overlying the beach deposits are strata of the non-marine facies association (Musreau Member). Black muddy sandstones with fragmented oyster shells occur at the base of the Musreau Member at Section 1. Above, this facies association is poorly exposed, consisting primarily of rubbly-weathering mudstones and siltstones. Casts of tree branches (with *Teredolites*-like impressions) are found at the base of a convolute-laminated sandstone in the upper part of the member (Fig. 3.4f). Long axes of the branches tend to be oriented in a NW-SE sense.

The top of the Cardium Formation is not particularly well-exposed here, but is visible locally as a layer of scattered pebbles and intraclasts lying on top of a thin fine-grained sandstone, and below the offshore deposits of the Muskiki Formation.

In summary, the Cardium Formation at Cutpick Hill *appears* to represent the product of a single progradational episode. The offshore units are overlain by a shoreface package capped by beach deposits. These in turn are conformably overlain by non-marine strata.

5.2.2 Mistanusk Creek

This section was measured by Stott (1967; his section 58-12) and has not been described since. The Cardium Formation here is similar in its stratigraphic characteristics to its occurrence at Cutpick Hill, although the outcrop is found within a narrow valley (Fig. 5.2c).

The base of the section (Fig. 5.4) was selected arbitrarily 21 m below the base of the swaley cross-stratified sandstones of the Kakwa Member. The E1 surface (the base of the Cardium Formation) appears to be represented by a burrowed nodular siderite layer (Fig. 3.2b) separating a 4 m sandier upward succession (below) from 1.5 m of heavily bioturbated muddy sandstone (above) 11 m below the base of the shoreface sandstones.

The lower portion of the Kakwa Member consists of 17 m of swaley cross-stratified sandstones (facies 16) with occasional sideritic layers apparently associated with accumulations of organic matter (Chapter 3). A coarsening-upward trend is again present, with very fine-grained sandstones at the base grading into fine-grained sandstones with thin (<20 cm) lens-shaped conglomerates in the upper portion.

A "bedding" surface with a topography of several centimeters is present at the top of the facies 16 unit (Figs. 5.2c,d,e). This surface appears to represent a scoured (?partially) lithified substrate. Lithification prior to erosion is suggested by the local presence of overhanging and near-vertical walls, and the "sculpted" appearance in plan view. In places, sandstones directly overlie the surface, whereas over a horizontal distance of

Figure 5.4. Correlation of Mistanusk Creek section with nearby well log. See Figure 5.3 for explanation of symbols.

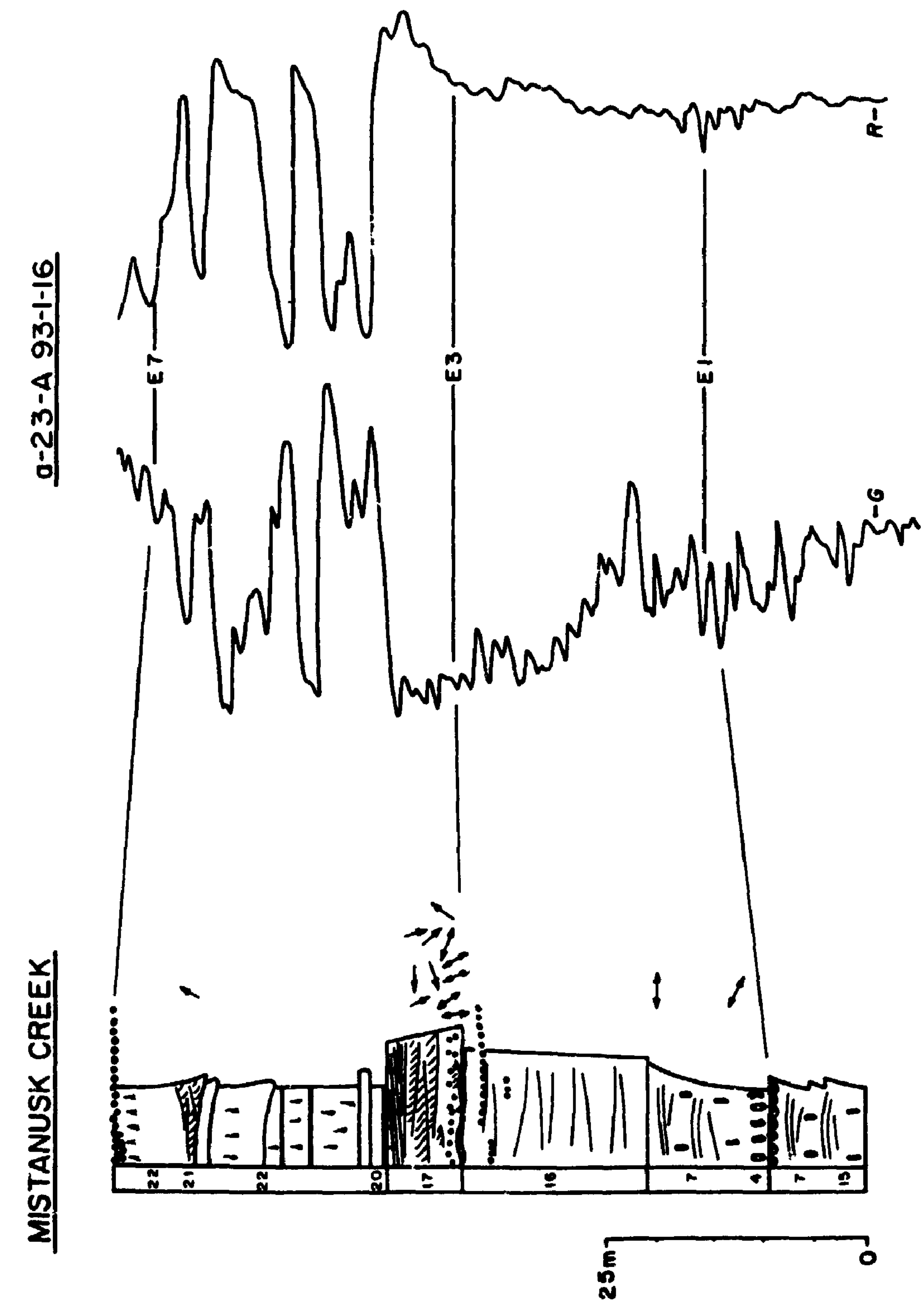
MISTANUSK CREEK
a-23-A 93-I-16
E7
E3
E1
G
R
25m
0
22
21
22
20
17
16
7
4
7
15

a few tens of meters, a thin (about 10 cm) graded unit (sandstone to carbonaceous black mudstone) appears to drape the underlying topography. The origin of this surface (shown as the E3 surface in Fig. 5.4) will be discussed later (Chapter 6).

The upper 7 m of the Kakwa Member here consists of an upward-fining package. The lowest part (about 1 m) contains pebbly sandstones and minor conglomerate with coarse-grained wave ripples and irregular scour-and-fill structures (locally with sandstone intraclasts). This portion is transitional upward into a medium-scale cross-bedded interval which is in turn overlain by 2.6 m of planar (beach) laminated fine-grained sandstones with a well-developed rooted horizon at the top (Fig. 3.3g). A horizon with well-developed *Macaronichnus* is present near the transition from cross-bedding to planar lamination (Fig. 3.3h). Coarse-grained ripple crestlines have on average a NW-SE trend, suggesting a similarly-oriented shoreline (*cf.* Leckie 1988). Paleocurrents derived from the medium-scale cross-bedded interval indicate diverse flow directions, probably in the surf zone.

The non-marine facies association (Musreau Member) is represented here by 26 m of strata. Root traces and sideritic horizons are abundant, while sandstones with paleocurrent indicators are not. Most of the units appear assignable to facies 22, and represent pedogenicallymodified fine-grained floodplain deposits (overbank, marsh, etc.). Thin coals are present in the lower part of this interval.

A pebble to cobble layer (Amundson Member) at the top of the Cardium Formation marks the E7 surface, and separates the non-marine strata below from the offshore units (Muskiki Formation) above (Fig. 5.2f). Its thickness varies from a single clast thick to a few decimeters over a horizontal distance of a few tens of meters. A similar surface (with *Thalassinoides* burrows) is well exposed at the Calliou Creek section (Fig. 5.2g) to the northwest.

Although the measured section here resembles the measured section at Cutpick Hill, the presence in the shoreface unit of a surface indicative of early lithification suggests at least a partial pause in sedimentation followed by erosion. This interpretation is supported by evidence from early diagenetic siderite at this locality; this will be presented in Section 5.4.

5.2.3 Murray River - Tepee Creek

The section at Murray River (Fig. 5.2h) does not appear to have been visited by Stott (1967, figure 1). At this locality, the upper part of the Cardium has been truncated by Pleistocene erosion, and so a previously undescribed section through the Musreau Member on Tepee Creek (where the Kakwa Member and lower units are inaccessible) will also be presented here. When combined, these two sections suggest that the Cardium Formation here is similar in nature to the sections at Cutpick Hill and Mistanusk Creek further south (Fig. 5.5).

At the Murray River section, 38 m of heterolithic strata of the offshore facies association were measured below the base of the main shoreface sandstone. As noted at Cutpick Hill, these units tend to compose 2 or 3 m thick sandier upward successions (Fig. 3.1j). A bioturbated, "gritty" sideritic bed with quartz and chert granules can be correlated to a prominent well marker (here labelled the G.S. horizon) which is traceable throughout most of the study area (e.g. Cutpick Hill, Fig. 5.3). Six meters below the main shoreface sandstone, a 2.6 m thick package of facies 16 can be correlated to another regionally-traceable well marker, here labelled the E0 surface. The regional correlation of these surfaces will be elaborated upon in the following chapter.

The swaley cross-stratified sandstone portion of the Kakwa Member (facies 16) is thicker here (23 m) than at either Mistanusk Creek (17 m) or Cutpick Hill (16 m). Like its equivalents at those two localities, it displays an upward-coarsening trend, and has pebble stringers in its upper portions. It is conformably overlain by about 2 m of planar (beach) laminated fine-grained sandstones with conglomeratic scour fills interpreted as the product of small streams cutting across the foreshore (Fig. 4.18e).

Figure 5.5. Correlation of Murray River and Tepee Creek sections with nearby well log. "Fluvial sandstone" in well appears to overlie top of shoreface sandstone as predicted from other local wells (see text). See Figure 5.3 for explanation of symbols.

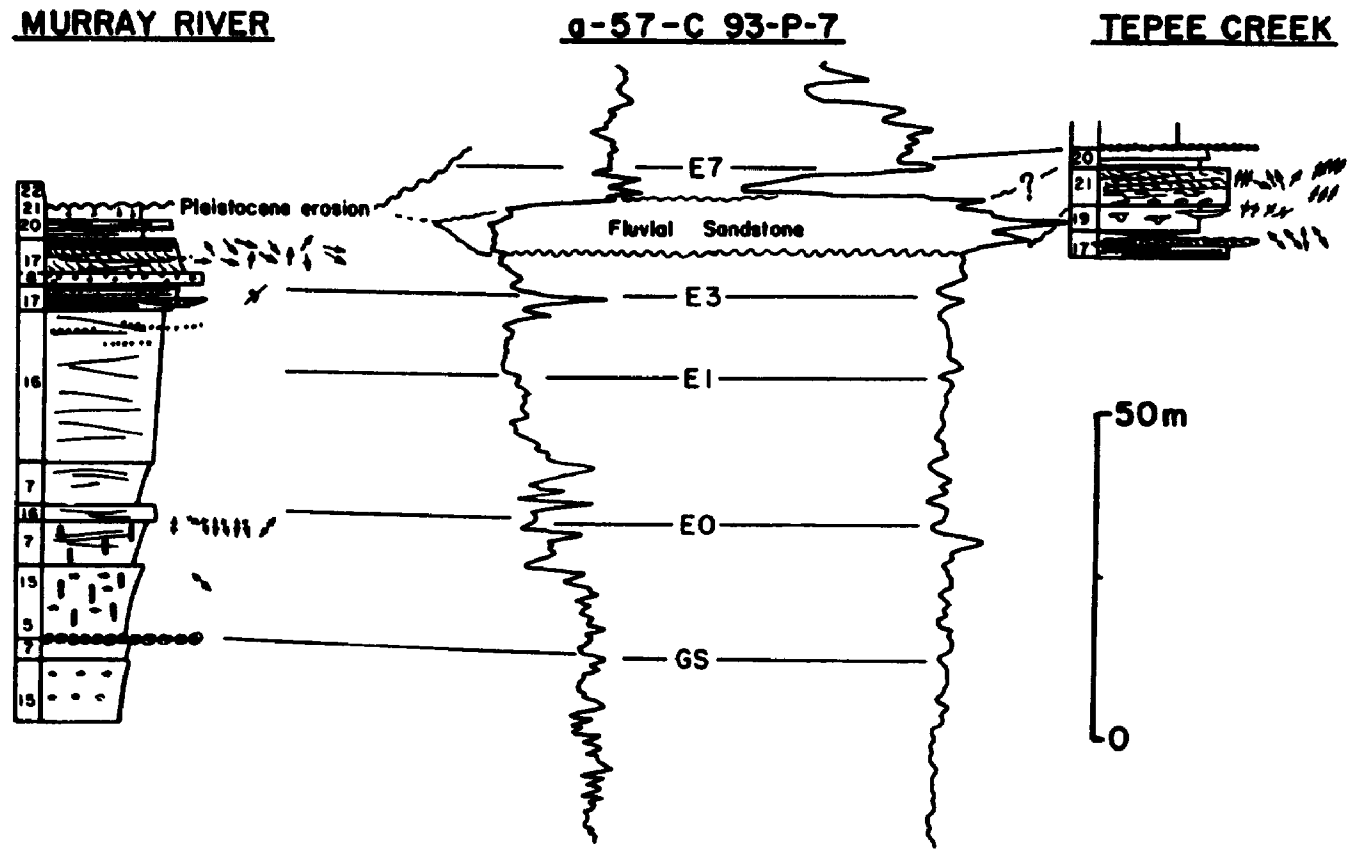

MURRAY RIVER
a-57-C 93-P-7
TEPEE CREEK
Pleistocene erosion
Fluvial Sandstone
E7
E3
E1
E0
GS
50m
0

A thin (10 cm) shale with sideritic sandstone intraclasts (here labelled the E3 surface) overlies the beach laminated unit.

The upper portion of the Kakwa Member (7 m) comprises an upward-fining package, with 2 m of conglomerate (inaccessible) overlain by medium-scale cross-bedded sandstones which are overlain by massive to planar (beach) laminated fine sandstones. Like the Mistanusk Creek section, a *Macaronichnus* horizon is present near the transition from medium-scale cross-bedding to planar lamination.

Overlying the beach laminated sandstones at the Murray River section are 5 m of non-marine strata (facies 20, 21, 22) representing a lagoonal environment. A 1.5 m thick parallel-laminated sandstone in this package resembles a beach laminated package, but parallel-laminated sands have also been noted from estuarine sand flats (e.g. Hart and Long 1990a). The relatively high detrital carbonate content of this unit (5%, with poikilotopic calcite cement) is not typical of beach and shoreface sandstones from the Kakwa Member, but compares more closely with sandstones in the Musreau Member (Chapter 3).

At Tepee Creek (Fig. 5.5), only the top 2 m of the Kakwa Member were measurable. Here, the planar (beach) laminated sandstones are directly overlain by 0.6 m of interbedded fine-grained sandstones and pebbly granule conglomerate.

The conglomerate preserves coarse-grained ripple forms with NW-SE trending crestlines. Above this, are 5 m of dark siltstones with sandy gutter casts (Fig. 3.4d); flute marks on the bases of the sandstones suggest flows to the NNE. This package, containing the coarse-grained ripples and the gutter casts resembles deposits of the offshore facies association. A marine trace fauna is absent however. The stratigraphic context (see Chapter 6) suggests that this is probably a lacustrine deposit.

The lacustrine package is sharply overlain by 6.2 m of facies 21 sandstones (Fig. 3.4e). Paleocurrent indicators from this unit indicate predominant flows to the NE. This in turn is overlain by 1.4 m of coal, which is overlain by 1.3 m of siltstones, and the E7 surface is marked by 0.3 m of conglomerate (Amundson Member).

The correlation of these two sections with a well log (a-57-C 93-P-7) located approximately mid-way between outcrops is shown in Figure 5.5. Although it appears that the top of the shoreface sandstones has been mis-correlated, reference to other wells in the area indicates that the top of the shoreface should be at the level indicated, suggesting that the "extra" thickness of sandstone in well a-57-C 93-P-7 is probably a fluvial unit (possibly contiguous with the thick fluvial sandstone at Tepee Creek?) situated directly on the Kakwa Member.

In summary, the Cardium Formation along the Murray River is generally similar to its occurrences further south at Cutpick Hill and Mistanusk Creek. The thickness of the facies 16 portion of the Kakwa Member is greater along the Murray River, while the thickness of the Musreau Member is diminished. North of Tepee Creek, and along the "Cardium Escarpment", the Musreau Member is not exposed, probably because of Pleistocene erosion of these poorly-lithified strata. It should also be pointed out that the lacustrine interval at Tepee Creek strongly resembles strata of the offshore facies association. It is conceivable that, based on outcrop work alone, this could be misinterpreted to indicate a transgressive "tongue" followed by a non-marine "tongue". Subsurface correlations (next chapter) indicate that this is not the case. Finally, the thickness of strata forming the shoreface facies association is considered to be too thick to represent the product of a single progradational episode (assuming the base of the facies 16 sandstones approximates fairweather wave base and the beach laminated sandstones at the very top of the shoreface package represents sea level). The presence of *two* beach laminated horizons at the Murray River section suggests that at least 2 shoreface sandstone packages have been superimposed.

5.2.4 Noetai Hill

This outcrop has not been previously described. Its interest lies not in the great thickness of strata exposed here, but rather in the paleocurrent information which can be gleaned from it.

Only about 6 m of strata from the shoreface facies association are exposed here. The lower half of the section consists of flaggy-weathering swaley cross-stratified fine-grained sandstones with thin pebble stringers in the upper portions. These sandstones are abruptly overlain by 3 m of medium-scale cross-bedded slightly pebbly medium-grained sandstones (Fig. 3.3d). This upper unit is continuously exposed for several tens of meters along strike, and abundant paleocurrent data are available (much more is present on slumped blocks, but this was not measured). A rose diagram is presented in Figure 5.6 from which it can be seen that the dominant sediment transport direction was to the southeast (vector mean = 143°, vector magnitude = 82.5). This direction is approximately parallel to most shoreline indicators in the Cardium Formation (strike of beach laminated sandstones/conglomerates, coarse-grained wave ripple crestlines, etc.) and so I interpret the southeast flow directions to represent longshore flows (*sensu stricto*).

Figure 5.6. Rose diagram of cross-bed orientations from facies 17 portion of Noetai Hill section. Average trend to SE interpreted to approximate shoreline orientation.

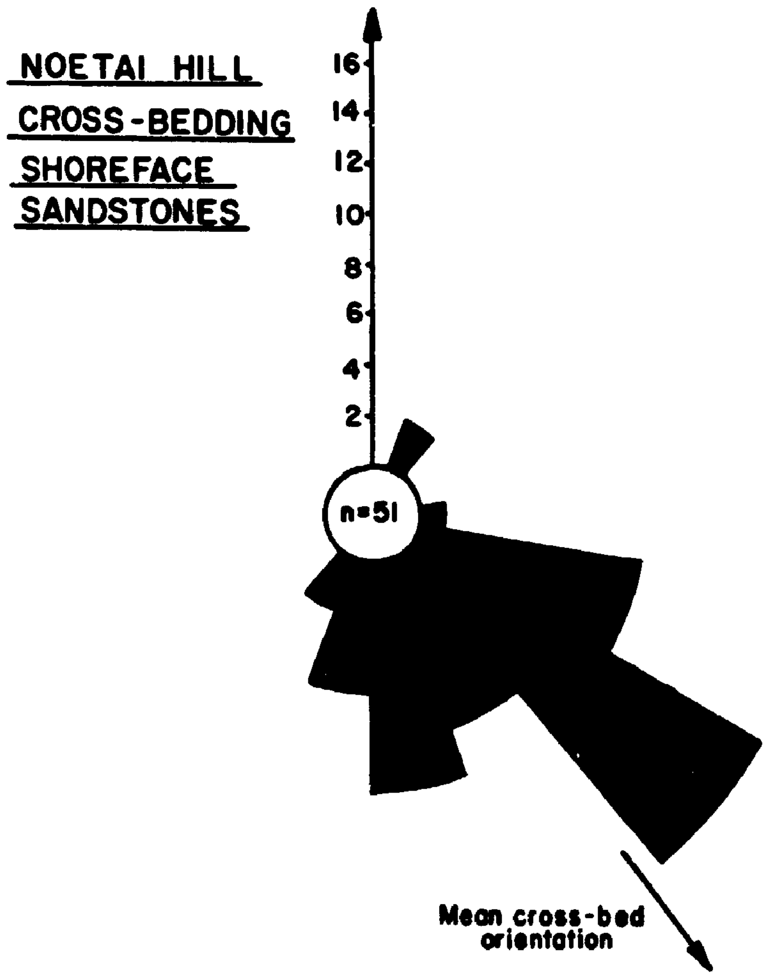
NOETAI HILL
CROSS-BEDDING
SHOREFACE
SANDSTONES
16
14
12
10
8
6
4
2
n=51
Mean cross-bed orientation

In summary, the Kakwa Member here can again be divided into two portions, a lower portion dominated by facies 16, and an upper portion consisting of facies 17 sandstones. Paleocurrent information suggests a NW-SE trending shoreline.

5.2.5 Dawson Creek area: Fellers Heights, Bear Mountain, Gundy Station, Bay Tree, Cutbank Lake

These sections (and several others) are located along the "Cardium Escarpment" which runs south of Dawson Creek. Generally, only the Kakwa Member of the Cardium Formation is exposed here, although locally a few meters of strata from the offshore facies association is exposed below the shoreface sandstones. Non-marine units of the Musreau Member are not exposed. I will suggest that the conglomerates and coarse-grained sandstones of the "Baytree Member" of Stott (1967) are in fact part of the Kakwa Member, and that the term "Baytree Member" be abandoned. Some of these sections were visited by Stott (1961, 1967) whereas others were apparently not.

Almost 18 m of strata are exposed at Fellers Heights. Here, 10 m of facies 16 sandstones (underlain by hummocky cross-stratified sandstones and shales) pass conformably upward into beach laminated sandstones which are capped by a rooted horizon at the top of the section (Fig. 5.7a). The overlying strata having been removed by Pleistocene erosion. The significance of this section is that it demonstrates that the swaley cross-stratified portion of the Kakwa Member did, at least locally, shoal upward and become subaerially exposed. As noted previously, beach laminated sandstones conformably overlie facies 16 sandstones at the Murray River section (Section 5.2.3) but no rooted horizon was present.

Four sections measured sections from the Bear Mountain locality are presented in Figure 5.8. They provide exposures of sandstones and conglomerates assigned to the Kakwa Member. The maximum measured thickness (28 m) was at site BM2.

I would like to distinguish three components to this section. First, up to 9 m of facies 16 sandstones are exposed here (the basal contact with the offshore facies association is not exposed). As in previous sections, a coarsening-upward trend occurs within the swaley cross-stratified interval. The second part of the section (2.5 to 6 m thick) overlies facies 16. This heterolithic package consists of a mix of wave rippled granular sandstones, (locally) pebbly undulose laminated sandstones with abundant carbonaceous "coffee grounds" material (Fig. 5.7b), and medium-scale cross-bedded sandstones (facies 17; Fig. 5.7c). Opposing cross-bed orientations are noted between adjacent sets in places. Locally, this unit becomes silty in its upper portions (few cm), but generally this part is not preserved. Finally, the third portion of the section begins with conglomerates (facies 8) which abruptly overlie the

Figure 5.7. Selected outcrop photographs of Cardium Formation in Dawson Creek (B.C.) area. A) Rooted horizon developed at top of facies 16 portion of Kakwa Member. B) Undulose-laminated fine-grained sandstones with carbonaceous "coffee grounds" laminae. C) Overview of a portion of section BM4 showing facies 17 sandstones overlain by amalgamated shoreface conglomerates (facies 8). D) Probable tidal inlet sequence from top of section BM2. Figure points to convex-up surface separating centimeter-scale planar tabular cross-beds (flood-tidal delta) below, from internally-scoured, trough cross-bedded sandstones (tidal inlet) above. E) Beach-laminated sandstones which conformably overlie facies 16 sandstones at Gundy Station section. F) Irregular contact (E3 surface) which overlies beach-laminated sandstones, separating "lower" from "upper" portion of the Kakwa Member.

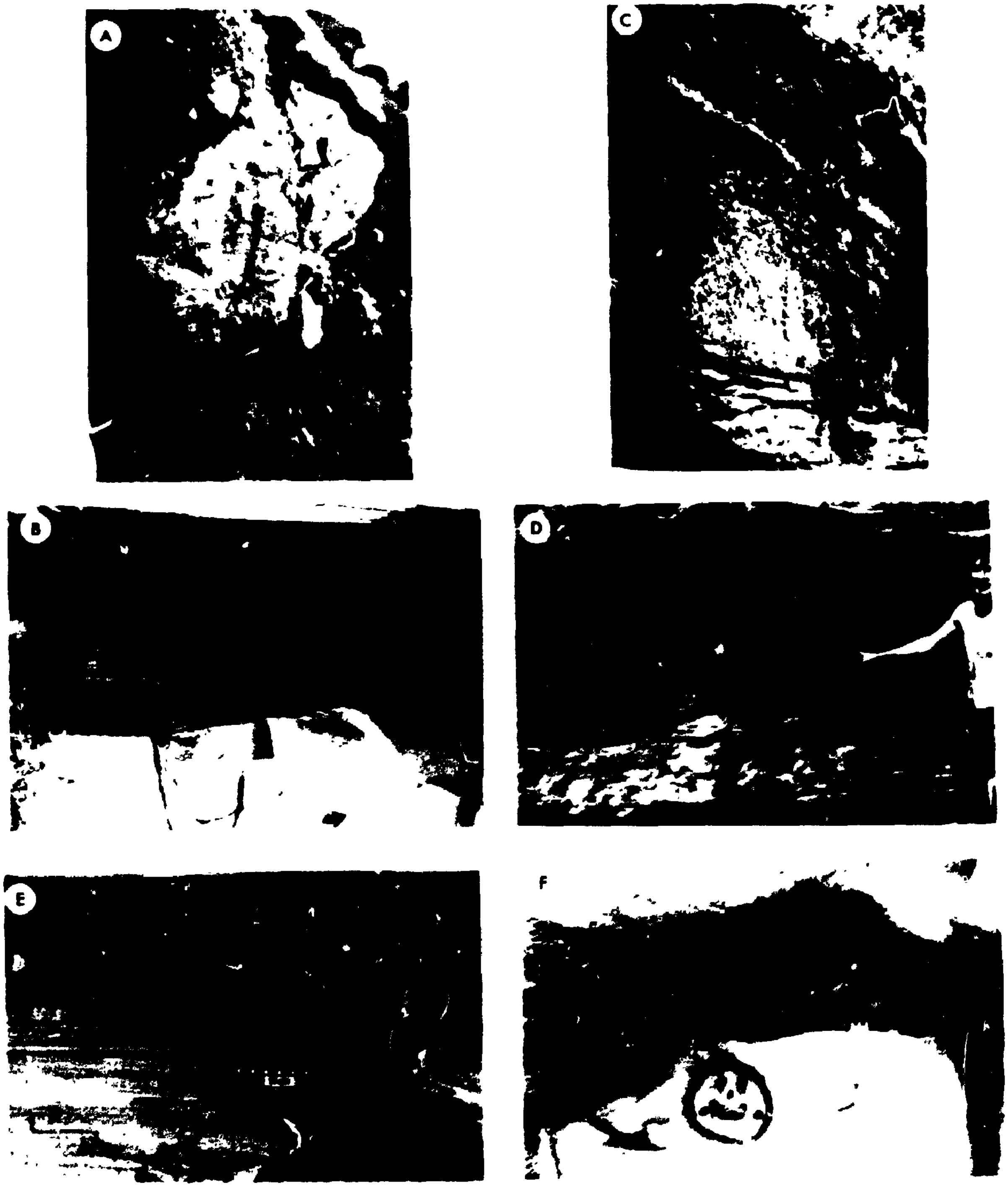
A
C
B
D
E
F

Figure 5.8. Measured sections from Bear Mountain locality. See Figure 5.3 for explanation of symbols.

BEAR MOUNTAIN

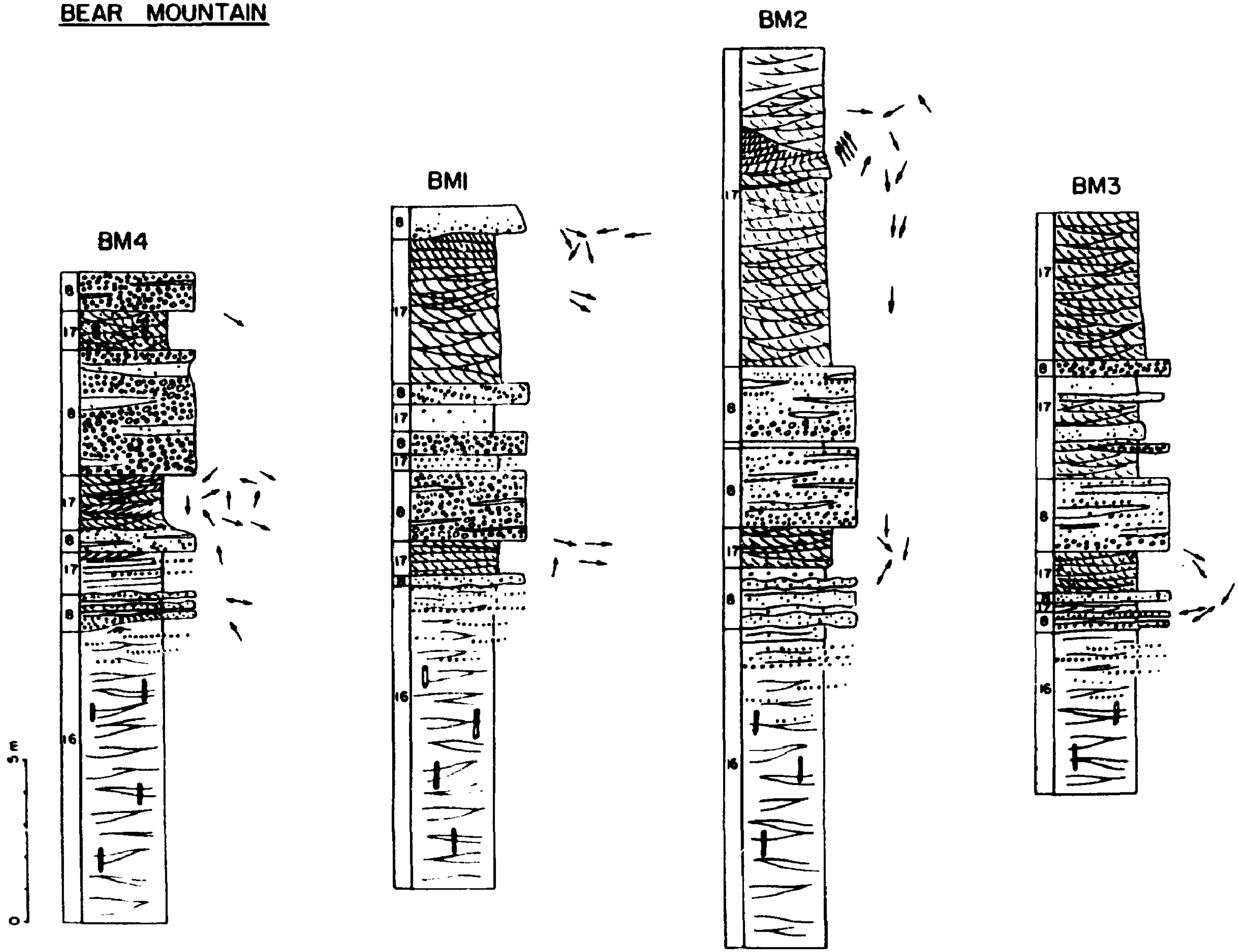

lower units (Fig. 5.7c). These conglomerates resemble the conglomerates at Bay Tree (Chapter 4) although they are less well developed here. They become finer grained, and more matrix rich as one moves south from section BM4 to section BM3. Because of the nature of the outcrop here (a sheer cliff face) it is difficult to observe sedimentary structures in the conglomerate.

The upper part of sections BM1, BM2 and BM3 consists of up to 10 m of medium-scale cross-bedded sandstone which grades from medium sandstone at the base to fine sandstone at the top. The upper part the of section at BM2 may represent a flood tidal delta/tidal inlet environment (Fig. 5.7d). Here, at the 24 m level (Fig. 5.8), one finds a scoured surface overlain by a "lag" deposit of medium-grained sandstone, molds of branches, and siltstone intraclasts. This is in turn overlain by about 1.5 m of fine-grained planar-tabular cross-bedded sandstones, with set thicknesses of only several centimeters, and a paleocurrent orientation to the NW which varies by only a few degrees between sets. This unit is erosionally truncated by a medium-scale trough cross-bedded sandstone with abundant evidence of internal scouring. I suggest that the scoured base at the 24 m level represents the base of a tidal channel, that the small planar-tabular sets represent the deposits of low-amplitude straight-crested dunes ("sandwaves") migrating up onto a flood tidal delta (e.g. Boothroyd 1985), and that the overlying sandstones represent later modification/erosion of the delta by tidal channels. Hubbard, Oertel and Nummedal (1979) have shown that flood tidal deltas can be well-developed in micro-tidal environments.

The paleocurrent data from this locality do not give any clear indication of the local contemporaneous shoreline trend. Although coarse-grained wave ripple crestlines suggest a NW-SE orientation, paleocurrent directions from cross-bedded sandstones do not reveal a clear dominance of onshore, offshore or alongshore flows. This probably indicates that a variety of flow types (longshore, rip currents, tidal currents) were active at various times here.

The Bear Mountain locality is significant for two reasons. First, the thickness of the section (at least 28 m of shallow marine strata) appears too great to be the product of shoreline progradation into a standing body of water. This suggests that the section either records progradation into a subsiding basin, or that more than one shoreface package is preserved here. Similar arguments have been advanced for the Murray River section. Second, the presence of a tidal inlet/tidal delta sequence at the top of the section suggests that one should not always expect the preserved shoreface package to grade up into beach deposits. The development of tidal inlets might be expected locally, especially if shoreline progradation was punctuated by minor transgressive episodes and subsequent development of barrier systems.

About 25.5 m of strata were measured at the Gundy Station section (Fig. 5.9). Here, 8.5 m of heterolithic strata belonging to the offshore facies association are exposed. Wave ripple crestlines from the upper surfaces of hummocky cross-stratified sandstones have a dominant NW-SE orientation, probably reflecting local shoreline orientation (*cf.* Leckie and Krystinik 1989).

Thirteen meters of swaley cross-stratified sandstones overlie strata of the offshore facies association (Fig. 3.3a). As noted in the other sections, the sandstones become coarser-grained (with pebble stringers near the top) upsection. Overlying the facies 16 sandstones are 1.6 m of low-angle to planar-laminated sandstones representing a beach (Fig. 5.7e). The strike and dip of these deposits indicates a NW-SE trending shoreline, in agreement with the wave ripple crestlines from the offshore facies association. Like the Murray River and Fellers Heights sections, the lower part of the Kakwa Member here indicates that it built up to sea level and became subaerially exposed.

Directly overlying and cutting into the beach strata is an irregular surface showing at least 60 cm of relief (Fig. 5.7f). Sideritic intraclasts and minor shales are found along this surface, which lies at the base of 3 m of cross-bedded medium-grained sandstones.

Figure 5.9. Correlation of measured section at Gundy Station with gamma ray log from a nearby well. Figure shows suggested correlation of section measured by Gleddie (1949) from nearby on Tupper Creek. See Figure 5.3 for explanation of symbols.

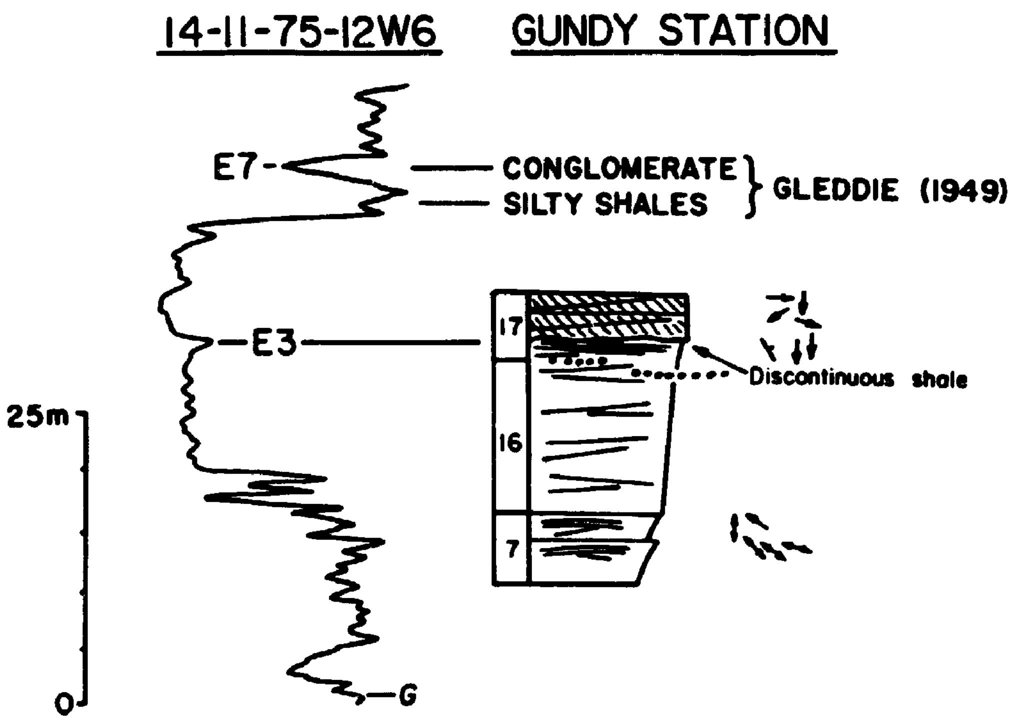

14-11-75-12W6
GUNDY STATION
E7
CONGLOMERATE
SILTY SHALES
GLEDDIE (1949)
E3
17
16
7
Discontinuous shale
25m
0
G

In Figure 5.9, the Gundy Station section is correlated with a nearby well log (14-11-75-12W6). The sideritic and shaley break above the beach laminated sandstones is clearly correlative with a distinct break in the gamma ray log (labelled the E3 surface). In that figure is shown how the section measured by Gleddie (1949) on Tupper Creek (the Gundy Station section is also located on Tupper Creek) would probably fit in. Gleddie measured .3 m (1 foot) of conglomerate separated from the "main conglomerate" (Kakwa Member?) by 3 m of silty shales (Musreau Member?). As noted in Chapter 1, neither I nor Stott (1967) were able to locate Gleddie's section.

A "composite" section from Bay Tree and a section from Cutbank Lake are correlated with a nearby well (more or less along strike with the outcrop sections) in Figure 5.10. The nature of the conglomerates from these two sections has been discussed in Chapter 4. Note the NW-SE orientation of the shoreline at Bay Tree, and that the type section of the "Baytree Member" correlates with the Kakwa Member of the Cardium Formation of Plint *et al.* (1986, 1988). Note also that the Bay Tree outcrop consists of three "components" (the lower two of which are exposed at Cutbank Lake), facies 16 sandstones at the base overlain by up to 1 m of cross-bedded pebbly sandstones, with up to 12 m of conglomerate above.

Figure 5.10. Correlation of "composite" Bay Tree and Cutbank Lake sections with nearby well. See Figure 5.3 for explanation of symbols.

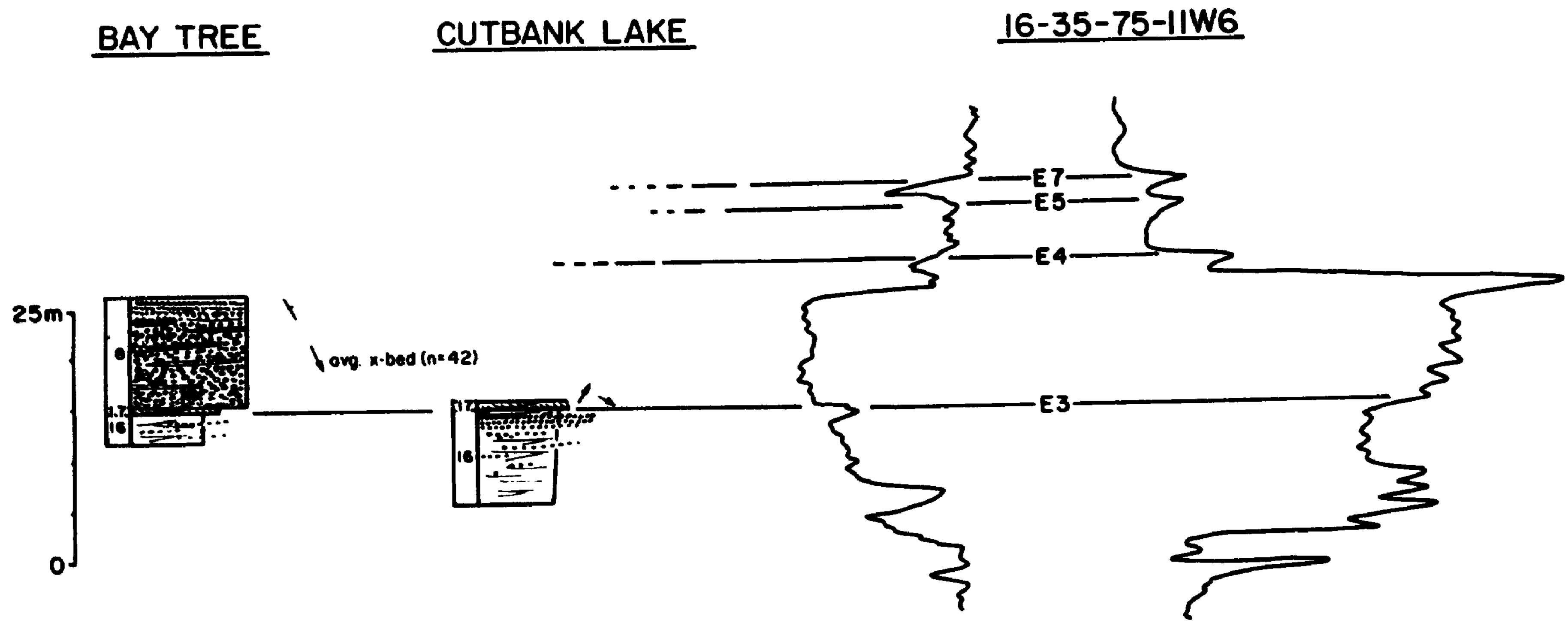
BAY TREE
CUTBANK LAKE
16-35-75-11W6
25m
0
avg. x-bed (n=42)
E7
E5
E4
E3
16
17
16

5.2.6. Smoky River

The Smoky River section is located about 100 km to the east of the Cutbank Lake and Bay Tree sections, and the strata exposed there are different from those exposed anywhere else in the present study area (Fig. 5.11). The author's present measured section through the Cardium Formation has previously been incorporated into a figure showing the correlation between the Cardium, Muskiki and Bad Heart formations with a nearby well log by Plint *et al.* (1990).

At the base of the section are .5 m of black silty shales with thin (less than 1 cm thick) lenticular very fine-grained sandstone beds (facies 15). This unit is capped by a layer of very large (up to 60 cm diameter) slightly discoidal siderite concretions. Above this is a 4.8 m thick sandier upward succession (facies 1 to 2 to 15), capped by a concretionary siderite layer which can clearly be correlated with the E5 surface in the well log. These lower units are the "splintery shales" from which Stott (1967) collected a specimen of *Scaphites carlilensis*, considered to be diagnostic of the mid-Turonian *Prionocyclus hyatti* Zone (Chapter 1).

Above the E5 surface are 20 m of blocky-weathering massive black shales (facies 1; Fig. 3.1a), with scattered sulphurous blebs (weathered pyrite) and large inoceramid

Figure 5.11. Correlation of measured section from Smoky River with nearby well log. Arrow points to fossil locality of Stott (1967). See Figure 5.3 for explanation of symbols.

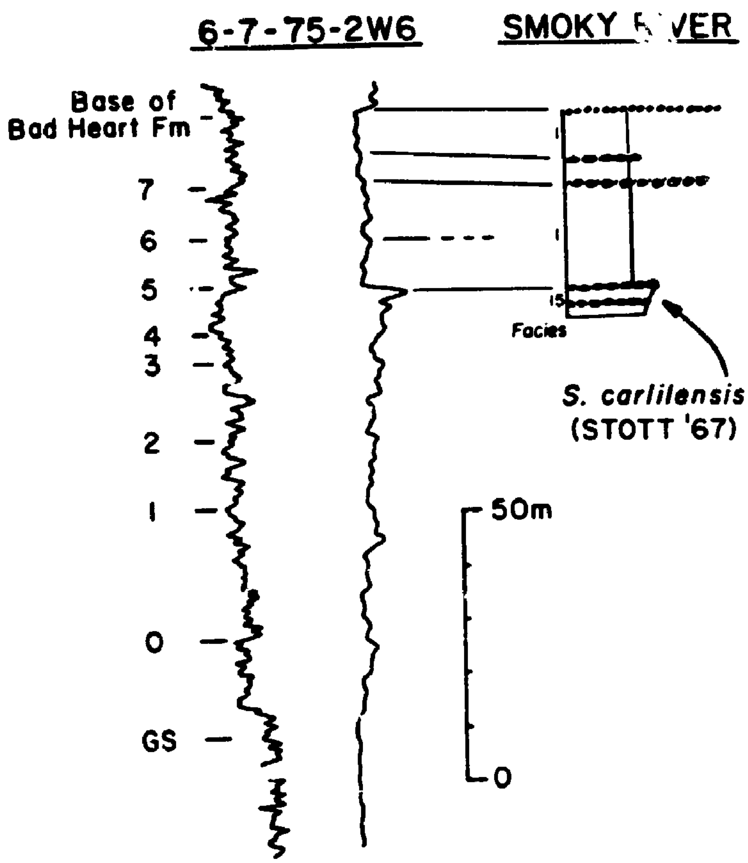
6-7-75-2W6
SMOKY RIVER
Base of
Bad Heart Fm
7
6
5
4
3
2
1
0
GS
15
Facies
S. carlilensis
(STOTT '67)
50m
0

fragments. If the E6 surface has an outcrop expression in this area, it was not observed. The E7 surface consists of a 20 cm thick gritty siderite layer. In both thin section and outcrop expression, this layer is similar to other gritty siderite horizons from lower down in the Smoky Group (upper Kaskapau Formation or base of the Cardium Formation; see Section 3.3.9, and Figs. 3.2d,e), suggesting that they too may be correlative with prominent erosion surfaces developed further landward (see Chapter 6).

The Smoky River section is important in that it provides the only outcrop exposure of the "distal" (i.e. basinward) portions of the Cardium Formation. Correlation between this section and the adjacent well log allowed the inter-regional correlations presented in Chapter 1. Finally, the identification of the E7 surface as a gritty siderite horizon suggests that at least some of the gritty siderite horizons observed in the upper Kaskapau Formation could be the basinward expression of important erosion surfaces.

5.2.7 Summary - The Cardium Formation in outcrop

Outcrop exposures of the Cardium Formation in the Rocky Mountain Foothills and along the "Cardium Escarpment" are remarkably consistent. Generally, swaley cross-stratified sandstones (facies 16) overlie strata of the offshore facies association, although the lower unit is not always exposed (especially in the north). Facies 16 sandstones are locally conformably overlain by beachface sandstones (facies 17) and, once, a rooted horizon. This lower sandstone unit (facies 16 and 17) is generally sharply overlain by coarser-grained (locally conglomeratic) shoreface deposits which most often preserve an upward shoaling succession to beach laminated sandstones or conglomerates. The contact between the two can have a relief of several centimeters, and locally suggests prelithification of the underlying strata. A unit consisting of a mix of cross-bedded pebbly sandstones and/or carbonaceous sandstones and/or coarse-grained wave ripples is found between the two shoreface "packages" in places. Together, these shoreface units are assignable to the Kakwa Member. Paleocurrent indicators from this part of the formation suggest a NW-SE trending shoreline.

Where exposed (only in the Foothills), strata of the non-marine facies association (the Musreau Member) conformably overlie the Kakwa Member of the Cardium Formation. Beds containing oyster shells are locally exposed near the base of the member, whereas upsection, rooted horizons become more abundant. This might indicate a transition from lagoonal to more "terrestrial" (e.g. floodplain) conditions higher up in the section. As noted in Chapter 3, many of the characteristics of this part of the section are suggestive of an anastomosed fluvial system.

At the top of the section, a pebble "veneer" (the Amundson Allomember) ranging in thickness from a few scattered pebbles to a few decimeters thick separates the

Cardium Formation from the overlying Muskiki Formation. There is no evidence in outcrop of any of the other allomembers which overlie the Musreau Member in the subsurface (e.g. Raven River, Dismal Rat). This is in agreement with Stott (1967) who found only two of his six original members of the formation, the Ram (equivalent to the Kakwa Member), and the Moosehound (equivalent to the Musreau Member). The "Baytree Member" has been shown here to be a coarse-grained portion of the Kakwa Member.

An outcrop on the Smoky River provides the only opportunity to examine any of the more "basinward" parts of the Cardium Formation at the surface. Without subsurface control, correlation between this outcrop and the remainder of the sections is not immediately apparent.

5.3 Measured core sections

I will now present selected measured core sections. These sections, like their outcrop counterparts, have been selected because they illustrate relationships which are essential to the reconstruction of the depositional history of the formation. The core sections will be grouped together "thematically", rather than presented as individual sections.

5.3.1 Offshore facies association - sub-Kakwa Member

In general, this part of the Cardium Formation (or upper Kaskapau Formation) is either not cored, or only a couple of meters of strata are sampled below the Kakwa Member (see examples below). An exception to this rule is present in core 6-15-65-13W6 (1188.7 - 1215 m; Fig. 5.12). In this core, 20 m of rocks assignable to facies 4, 7 and 15 are present. They compose two main sandier-(and thickening-) upward successions, each about 9 m thick. The lower of the two is capped by a gritty siderite bed (with sideritic intraclasts) 15 cm thick (Fig. 3.2c), overlain by 1.4 m of pervasively bioturbated sandy mudstones (facies 4). Correlation of this section with the Mistanusk Creek outcrop (exposed less than 15 km away) suggests that the gritty siderite here is equivalent to the bioturbated concretionary siderite horizon (E1) found about 11 m below the base of the main shoreface sandstones at that section. Six meters of facies 16 sandstones from the Kakwa Member are found at the top of the core.

5.3.2 The Kakwa Member in the subsurface

As noted in Chapter 3, this is the most extensively cored part of the Cardium Formation in the study area. Essentially the same three-fold division of the Kakwa Member seen in outcrop can be observed in core. Eight measured core sections through the member, and their corresponding well logs, are presented in Figure 5.13.

In all cases, the base of the measured section through the Kakwa Member is composed of facies 16 sandstones. Where well-developed, this unit displays the same upward-coarsening as observed in outcrop (very fine-grained to

Figure 5.12. Measured core section from well 6-15-65-13W6.

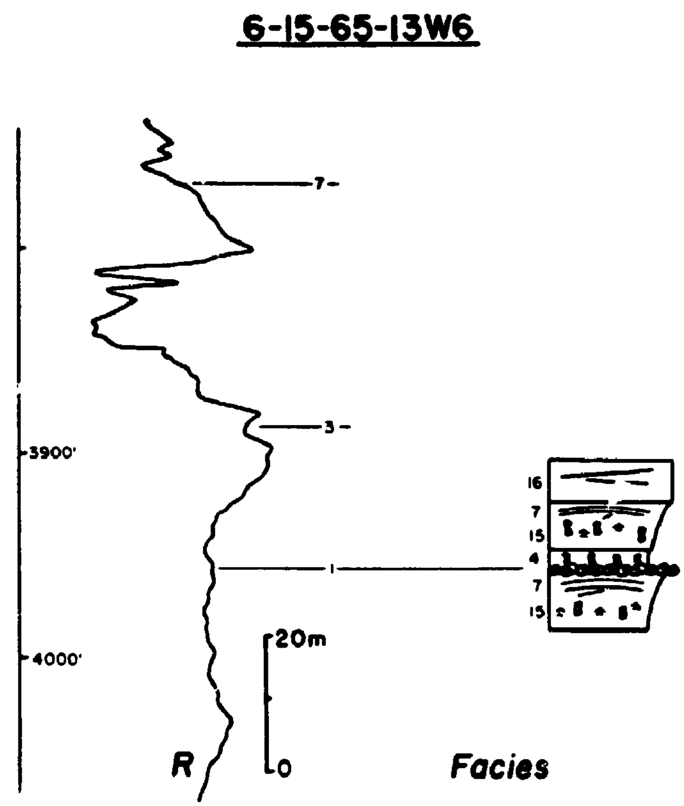
6-15-65-13W6
7
3
1
3900'
4000'
20m
0
R
Facies
16
7
15
4
7
15

Figure 5.13. Selected measured core sections through the Kakwa Member. In all cases, the break between lower (dominated by facies 16) and upper (dominated by facies 17) portion of the member can be associated with a gamma ray or resistivity signature.

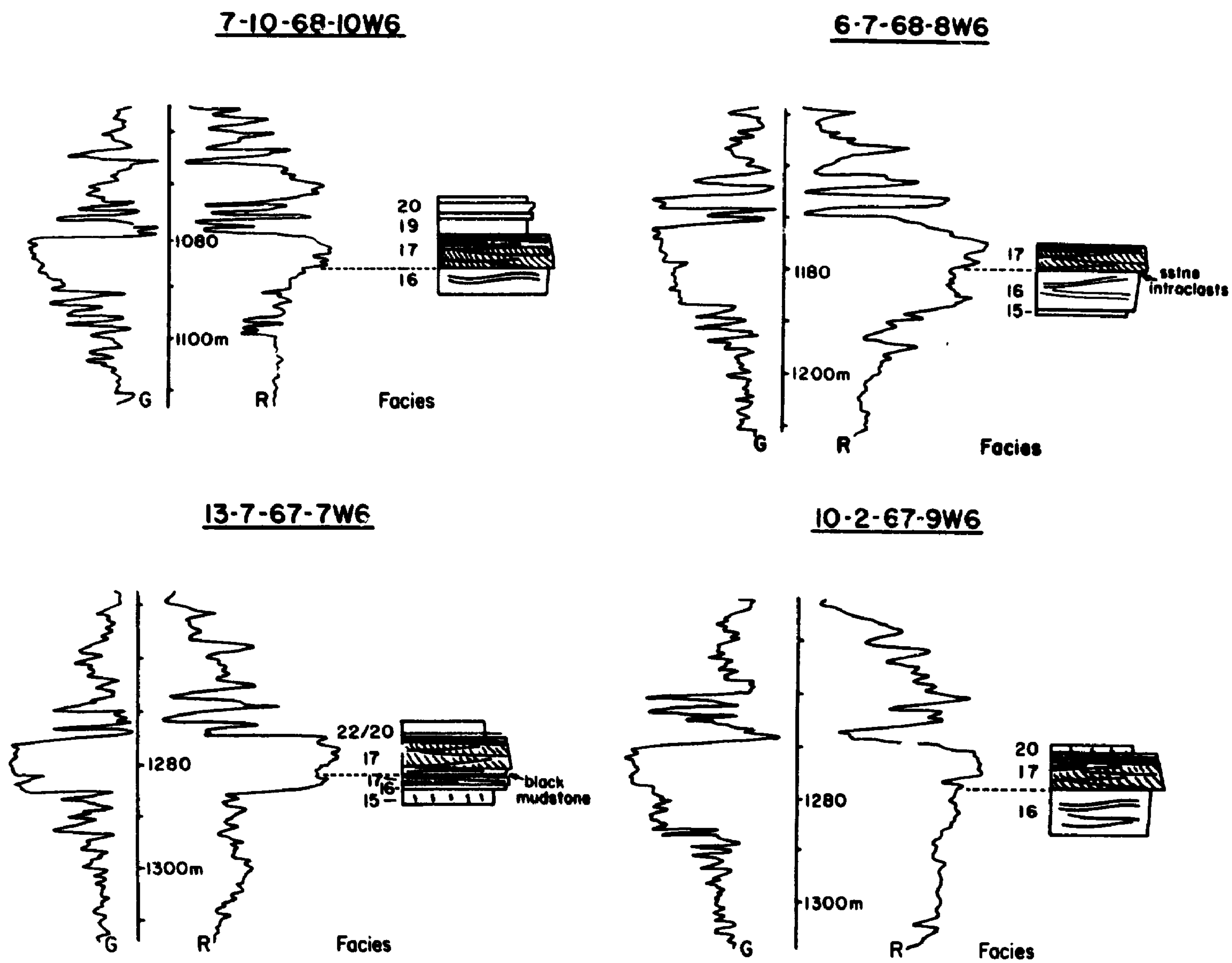
7-10-68-10W6
1080
1100m
G
R
20
19
17
16
Facies
6-7-68-8W6
1180
1200m
G
R
17
16
15-
ss(?)tne
intraclasts
Facies
13-7-67-7W6
1280
1300m
G
R
22/20
17
17
16
15
black
mudstone
Facies
10-2-67-9W6
1280
1300m
G
R
20
17
16
Facies

Figure 5.13 (cont.) Selected measured core sections through the Kakwa Member. In all cases, the break between lower (dominated by facies 16) and upper (dominated by facies 17) portion of the member (E3 surface) can be associated with a gamma ray or resistivity signature.

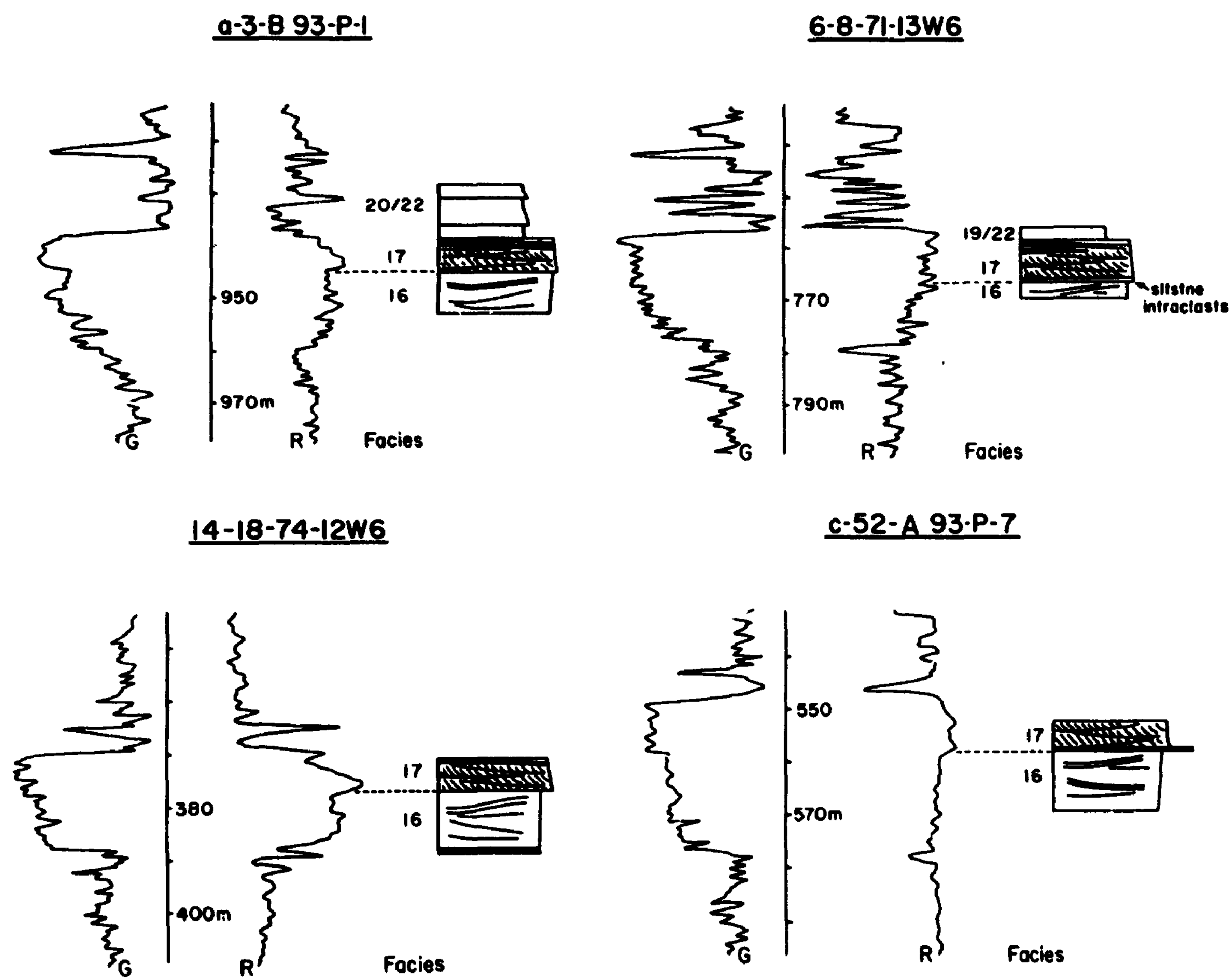
a-3-B 93-P-1
20/22
17
16
950
970m
G
R
Facies
6-8-71-13W6
19/22
17
16
siltstne intraclasts
770
790m
G
R
Facies
14-18-74-12W6
17
16
380
400m
G
R
Facies
c-52-A 93-P-7
17
16
550
570m
G
R
Facies

fine-grained sandstones), although pebble stringers are generally not present in the upper portions. The base of this part of the Kakwa Member is not always cored, but it is possible to use the corresponding gamma ray logs to estimate the thickness of this unit. In the examples presented, the well logs suggest that the thickness of facies 16 sandstones can range from over 20 m (c-52-A 93-P-7) to less than 2 m (13-7-67-7W6).

The sandstones of facies 16 are overlain by sandstones assignable to facies 17. The latter again typically display a succession of sedimentary structures similar to that observed in outcrop: cross-bedding near the base overlain by a *Macaronichnus* horizon, and capped by a parallel-laminated horizon with root traces. The contact between the two is generally sharp, in places with high-angle (to overhanging) walls (Figs. 5.14a,c,d,f,g), and locally marked by a thin (up to a few clasts thick) pebble bed of extraformational (chert; Fig. 5.14e) or intraformational (sandstone, siltstone, shale; e.g. 6-7-68-8W6, 6-8-71-13W6, Fig. 5.13) clasts. A black carbonaceous mudstone up to a few centimeters thick occurs in some cores overlying the lower surface (e.g. 13-7-67-7W6, Fig. 5.13; Fig. 5.14b). Undulose-laminated carbonaceous sandstones may also found directly above the upper contact of the facies 16 sandstones (Fig. 5.14i); they appear to represent strata similar to those seen at an equivalent stratigraphic level in outcrop

Figure 5.14. Selected examples of features associated with contact between lower and upper portions of Kakwa Member (E3 surface) in core. A) Sharp contact with distinct grain-size break, erosional truncation of underlying laminae and steep-sided walls (arrows). Core from 10-7-70-11W6. B) Heavily sideritised sandstone (base) overlain by black shale (under scale bar), sharply overlain by facies 17 sandstones. Core from 6-8-70-13W6. C) Sharp contact with overhanging wall (arrow), suggesting prelithification of underlying sandstone. Core from 16-25-67-11W6. D) Sharp contact (arrows) with erosional truncation of underlying laminae and abrupt grain-size break. Core from 7-14-68-7W6. E) Sharp contact (arrows) with slight grain size break and concentration of chert pebbles. Core from 3-26-66-7W6. F) Sharp contact with overhanging wall (arrow) suggesting prelithification of underlying sandstone. Core from 7-10-68-10W6. G) Sharp contact (arrows) with distinct grain-size break. Core from 11-7-66-4W6. H) Rooted horizon developed on top of facies 16 sandstones (i.e. below contact). Core from 14-5-63-5W6. I) Carbonaceous "coffee grounds" laminae from sandstones immediately overlying contact. Core from 6-24-69-12W6.

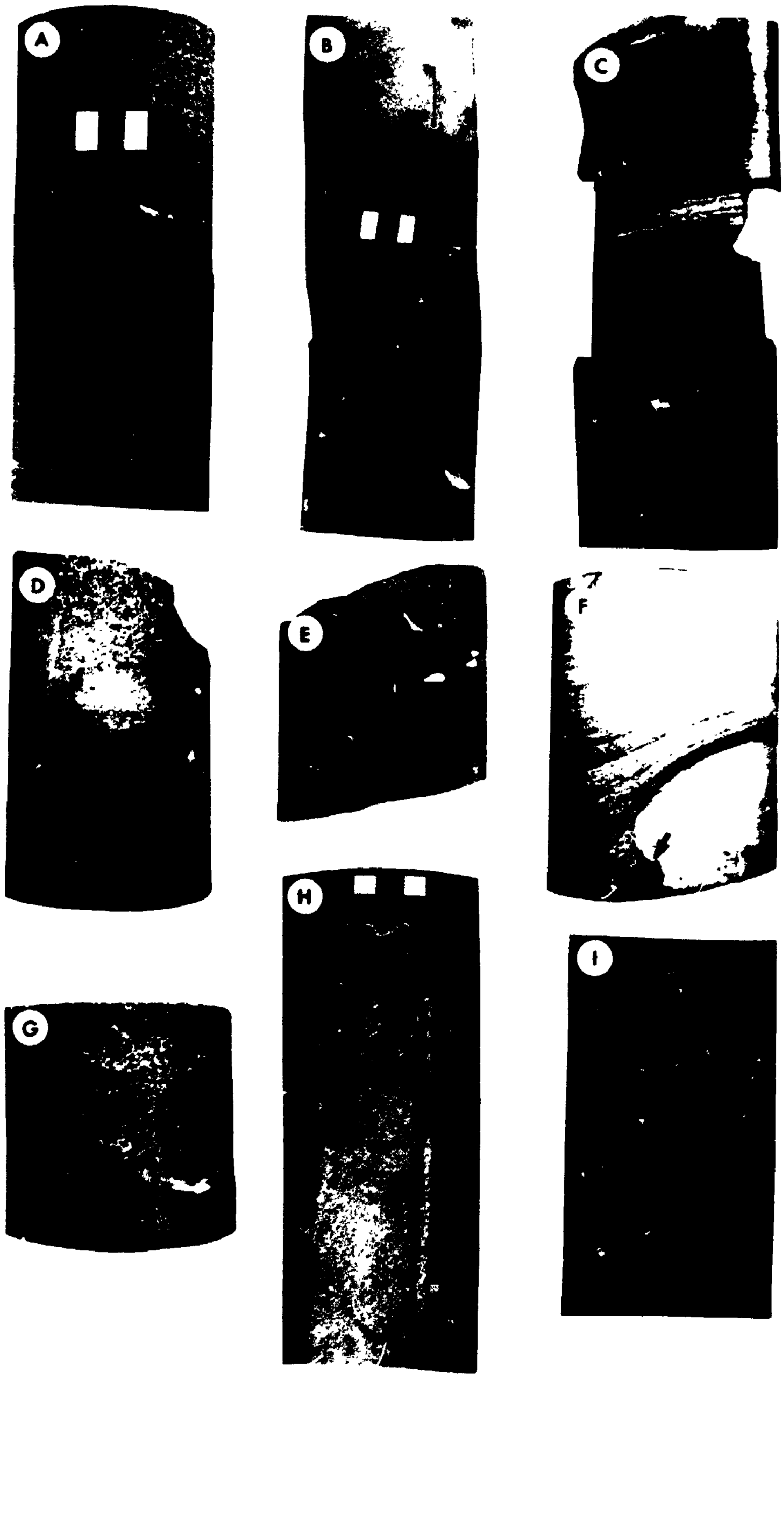
A
B
C
D
E
F
G
H
I

(e.g. Bear Mountain, Fig. 5.7b). A rooted horizon was noted at the top of the facies 16 sandstones in a core from slightly south of the present study area (14-5-63-5W6; Fig. 5.14h). The thickness of the "upper" part of the Kakwa, consisting of facies 17 sandstones, tends to be much less variable (usually 7 - 8 m) than that of the facies 16 part.

It is possible to identify a similar succession in wells where no core is available by recognising the distinctive well log signature of the contact between the two parts of the Kakwa Member. Two examples of this are shown in Figure 5.15. In both cases, the well logs clearly indicate the position of the contact between the facies 16 and facies 17 dominated portions of the member. This is the case in most wells penetrating the Kakwa.

Locally (e.g. Fig. 5.16), the typical succession of shoreface to beachface sandstones has been replaced by strata consisting of parallel- to undulose laminated sandstones, ripple cross-laminated and trough cross-bedded sandstones, and thin siltstones, shales, and conglomerates. Angular to contorted mudstone intraclasts are common in these units (e.g. Fig. 3.4g). Herringbone cross-bedding, mud drapes, or other features suggestive of a tidal influence (which might suggest an estuarine depositional environment) are not observed. This association of sedimentary structures and lithologies is best interpreted as representing fluvial deposits. The recognition of the

Figure 5.15. Examples of how well logs alone can be used to identify contact (E3) between lower (dominated by facies 16) and upper (dominated by facies 17) portions of the Kakwa Member. Well logs are spontaneous potential (SP), gamma ray (GR), sonic (S) and resistivity (R).

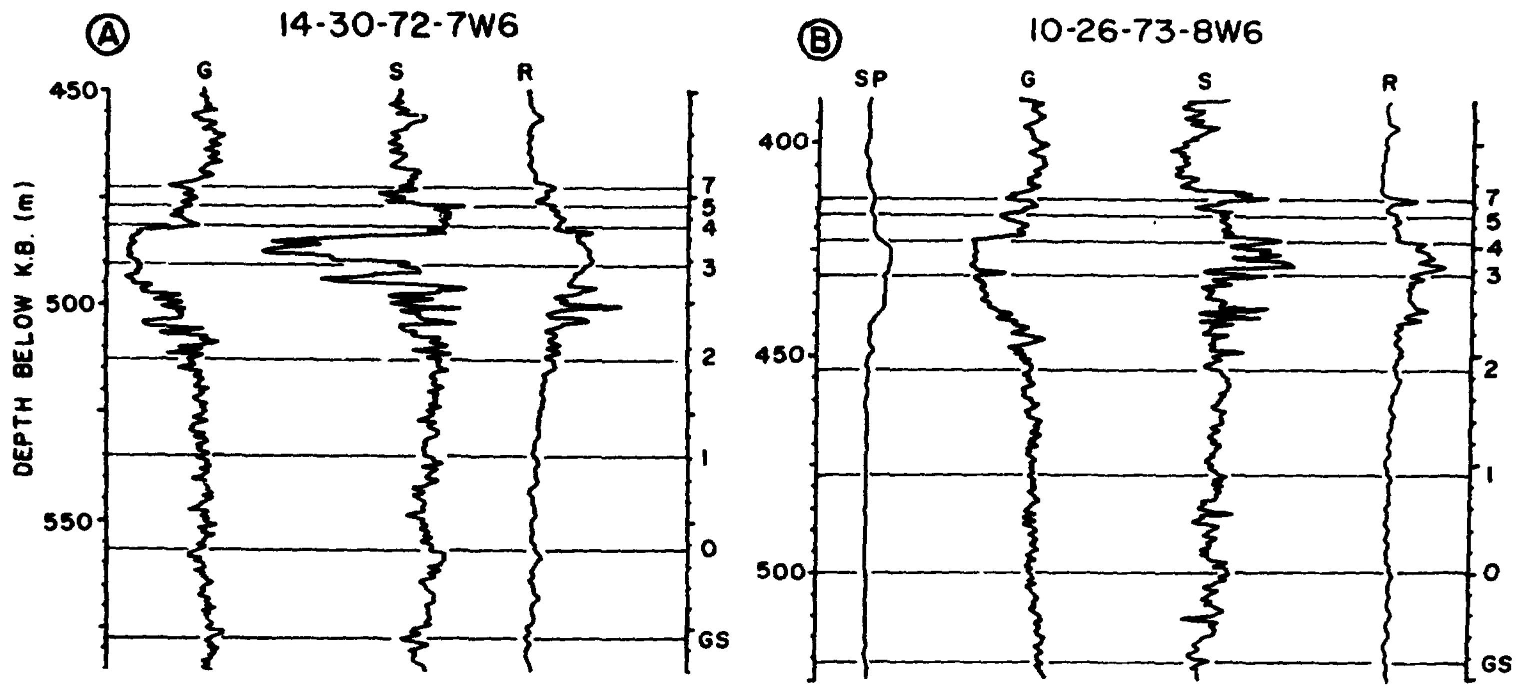
A
14-30-72-7W6
B
10-26-73-8W6
DEPTH BELOW K.B. (m)
G
S
R
SP
450
500
550
400
7
5
4
3
2
1
0
GS

Figure 5.16. Examples of replacement of "upper" portion of Kakwa Member by fluvial units. Note apparent "fining-upward" trend of gamma ray log (arrows) and "serrated" rather than "blocky" appearance. Wherever cored, this log response corresponds to similar fluvial units.

6-28-69-13W6

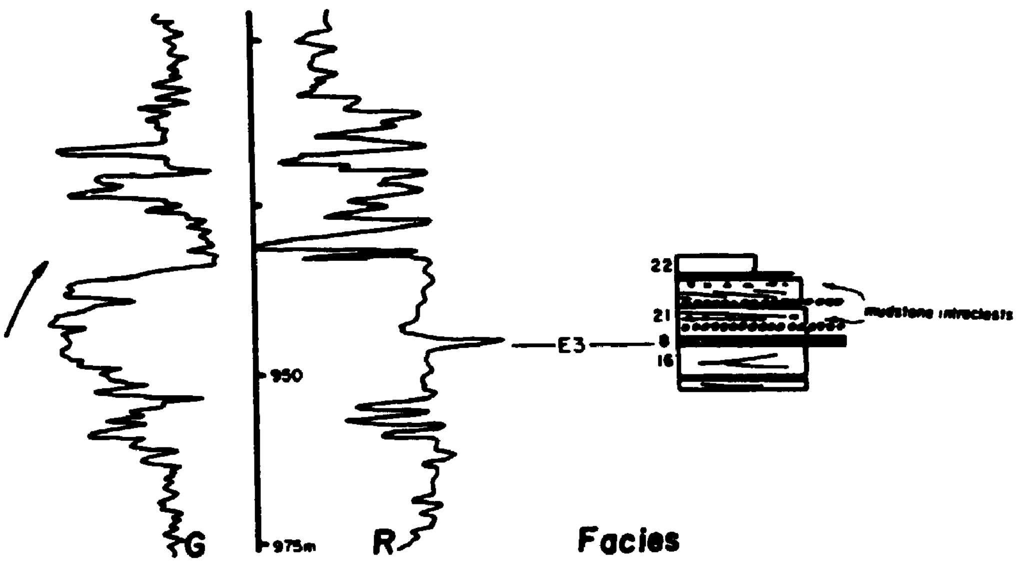

15-16-68-13W6

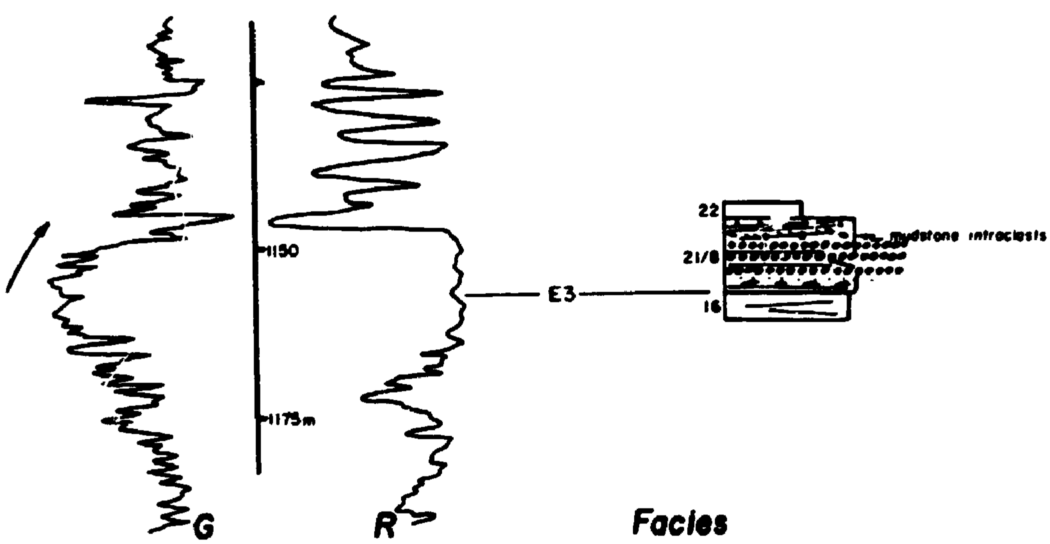

distinctive gamma ray log signature developed in these cases (compare Figs. 5.13 and 5.16) allows similar successions to be identified where core is not available.

5.3.3 The Musreau Member in the subsurface

Rocks of the non-marine facies association are less frequently cored than those of the shoreface facies association (Section 5.3.2). Typically, either only the basal few meters of these units are cored along with the Kakwa Member (examples in Fig. 5.13), or the upper few meters of the Musreau Member are cored along with the overlying strata (see below). Only infrequently (e.g. 6-28-69-12W6, not illustrated) do sandstones of this member appear to have been the drilling target.

The thickness of this unit is greatest in the southwest and decreases to the northeast (e.g. Plint *et al.* 1988). I measured a complete section through the Musreau (from the top of the Kakwa Member to the overlying transgression surface) only in one core from the western part of the study area. In the core from well c-16-I 93-P-1, 9 m of fine-grained strata (facies 20 with some coaly shales) at the base of the Musreau Member are sharply overlain by two cross-bedded sandstone units (facies 21) separated by 20 cm of black sandy mudstone, each of the sandstone units is about 4.5 m thick. A pebble veneer (E5) caps the upper sandstone.

In the vicinity of TWP67 R7W6, several cores penetrate the entire thickness of the Musreau Member (e.g. 6-36-66-8W6, see below). Here, carbonaceous black mudstones (facies 19) or thin coals (facies 18) commonly directly overlie the Kakwa Member. Thick sandstones such as those seen in c-16-I 93-P-1 are not observed, and the section is dominated by fine-grained lithologies (facies 20 and 22). In well 11-7-66-4W6 (Fig. 5.17), the Musreau Member is only 1.5 m thick. Here, .7 m of black carbonaceous mudstones (facies 19) are overlain by .75 m of pervasively burrowed (monospecific) muddy sandstones (assigned to facies 20; *cf*. Fig. 3.4c) which are in turn capped by a thin (< 1 cm) layer of very-coarse sand and granules (the E4 surface). Finally, to the northeast in well 8-32-74-9W6, a pebble layer overlain by strata of the offshore facies association rests directly upon the Kakwa Member, and the Musreau Member is non-existent.

5.3.4 "Upper" allomembers of the Cardium Formation

Cores which allow examination of the units which overlie the Kakwa or Musreau members are most abundant in an area running from TWP68 R7W8 to TWP65 R6W6. Three measured core sections from this area are illustrated in Figure 5.18. In this area, allomembers are typically bounded above and below by pebble beds (e.g. Figs. 5.19a-d). The strata belong for the most part to the offshore facies association, and may compose sandier upward successions. The vertical succession

Figure 5.17. Measured core section from 11-7-66-4W6.

The Musreau Member is only 1.5m thick.

11-7-66-4W6

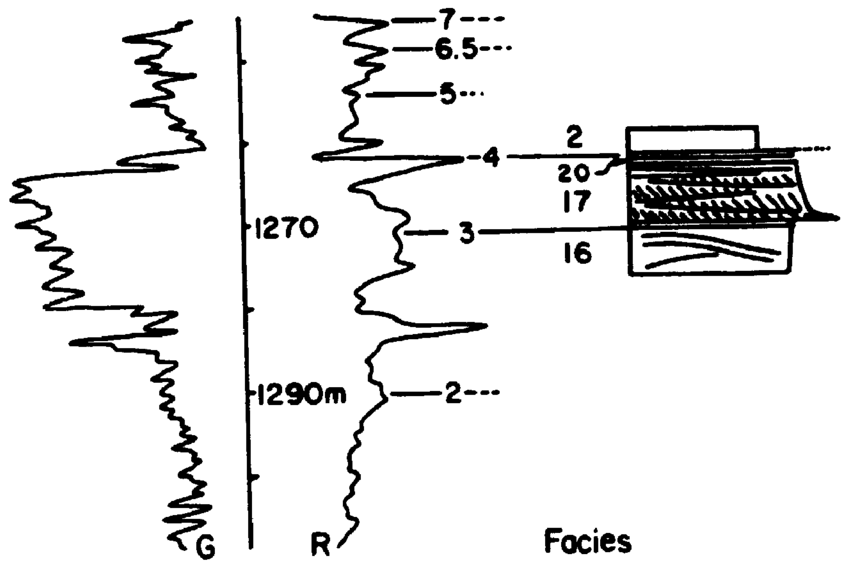

Figure 5.18. Measured core sections through "upper" allomembers of Cardium Formation, as described in text.

6-36-66-8W6

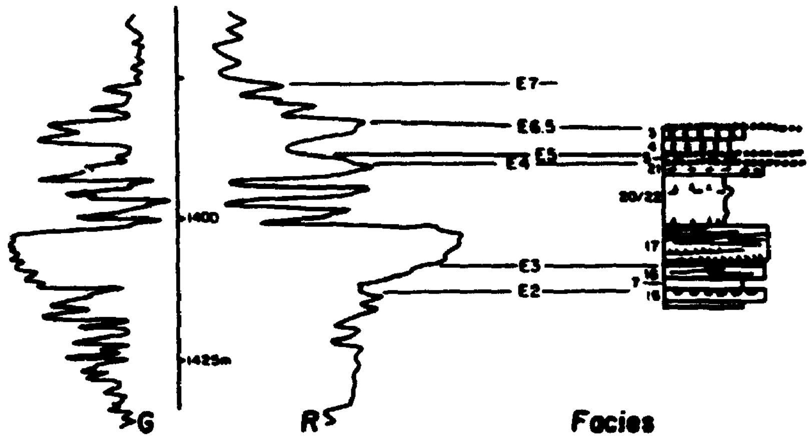

6-19-66-7W6

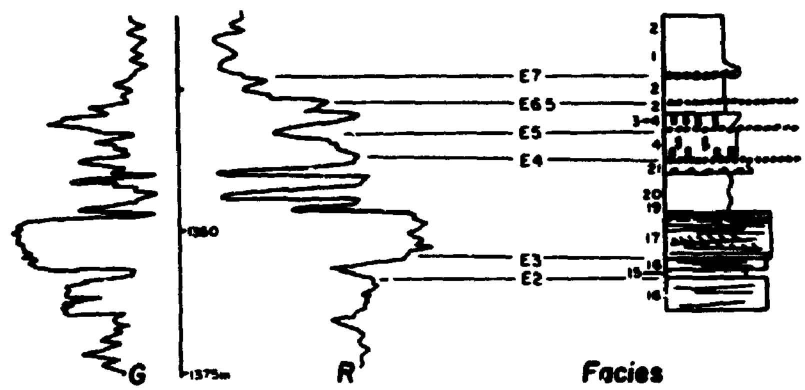

11-22-65-6W6

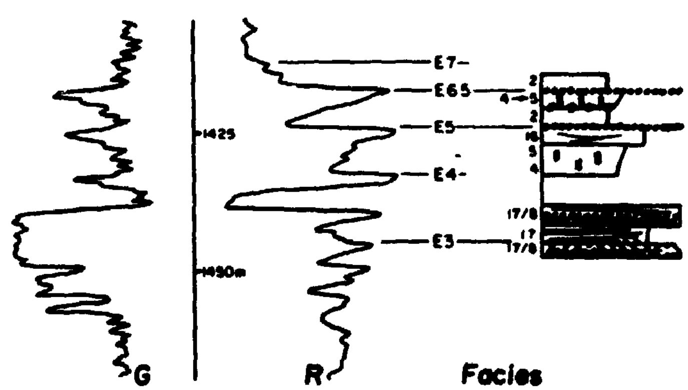

Figure 5.19. Core photographs of E surfaces. A) Pebble layer at E5 surface, 11-22-65-6W6. B) Pebble layer at E5 surface, 2B-11-67-8W6. C) Pebble layer at E4, 8-32-74-9W6. D) E4 (at finger level). Surface has no pebble veneer, and is only distinguishable by colour change and differences in bioturbation.

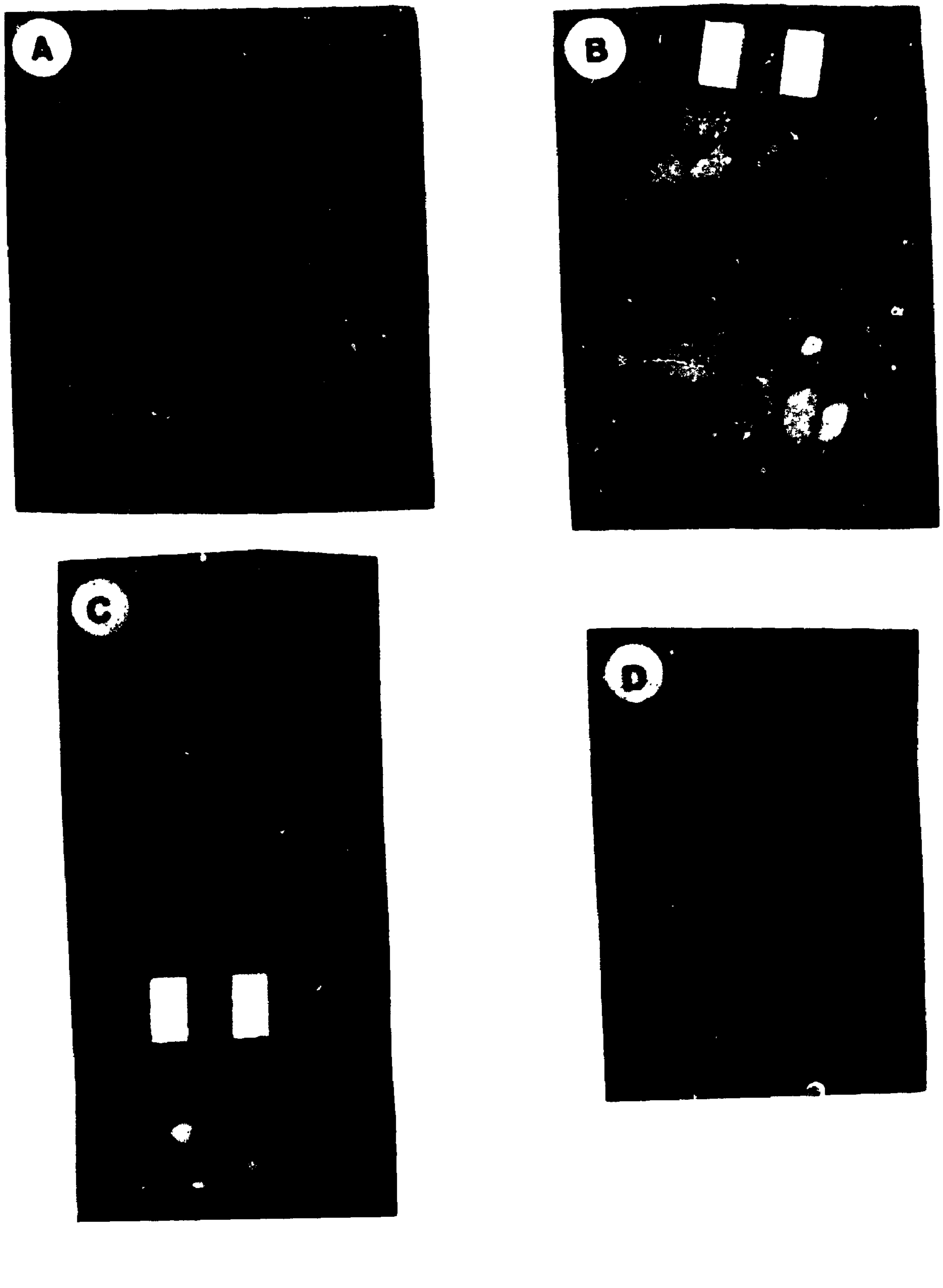
A
B
C
D

of facies within any given allomember is not necessarily identical from one location to the next. At least in part, these differences can be ascribed to thickness variations, probably reflecting subsequent erosional truncation. For example, the E4 to E5 interval (the Raven River Allomember) consists of a well-developed sandier upward succession (facies 4-5-16) about 9 m thick (of which the upper 2.65 m consists of swaley cross-stratified sandstones) in core 11-22 ˊ5-6W6. In core 6-19-66-7W6 the same interval consists of 5 m of strata assigned to facies 4, whereas in core 6-36-66-8W6 the thickness has decreased to 1.15 m (facies 5). In these latter two cases, it is conceivable that a unit consisting of facies 16 sands was originally present at the top of the interval, but was removed by a later erosion event.

Higher up in the section, strata above the pebbly horizon indicated as E6.5 tend to be dominated by "distal" offshore deposits of facies 1 and 2. These strata are only infrequently cored.

Further basinward, a different type of vertical succession is encountered. These sections represent units deposited beyond the depositional edge of the Kakwa Member (e.g. Plint *et al.* 1986; Fig. 1.1). Only four cores providing sections through these strata were available in the present study area. These are illustrated in Figure 5.20.

Figure 5.20. Measured core sections from "basinward" portions of the Cardium Formation, as described in text.

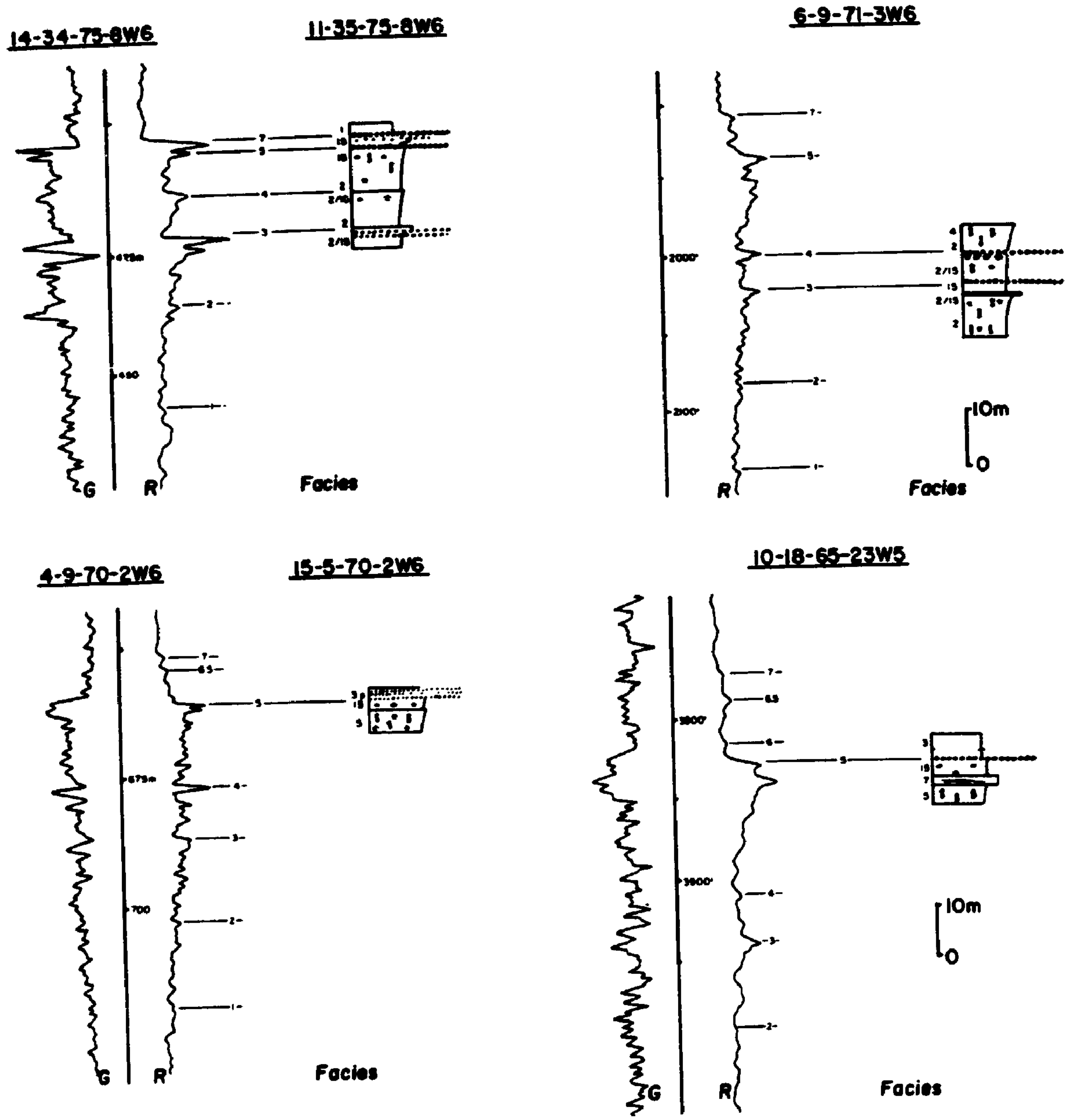
14-34-75-8W6
11-35-75-8W6
6-9-71-3W6
G
R
Facies
10m
0
4-9-70-2W6
15-5-70-2W6
10-18-65-23W5
675m
700
2000'
2100'
3800'
3900'

In these four cores, the dominant lithofacies encountered can generally be ascribed to the "distal" parts of the offshore facies association. These include facies 2, facies 15, rocks transitional between the two (laminated dark mudstones with minor thin (generally less than 1 cm thick) sandstones, indicated as 2/15), plus facies 3 and 1. Sandier, presumably more "proximal" facies (e.g. 4, 5, 7) are less abundant. These facies are generally organised into sandier upward successions, and these tend to be capped by thin pebbly mudstones or conglomerates. The conglomerates and sandier upward successions can generally be identified as distinctive markers on the accompanying well logs.

5.3.5 Summary - the Cardium Formation in core

In this section, it has been shown that the "lower" parts of the Cardium Formation in core (i.e. including the upper part of the Kaskapau Formation up to the top of the Musreau Member) are very similar to their occurrence in outcrop. In particular, the Kakwa Member is divisible into two parts, a lower portion dominated by facies 16 and an upper portion dominated by facies 17. These are generally separated by an abrupt grain size break with an irregular micro-topography (e.g. overhanging walls), which is in turn overlain by either a thin pebble layer, undulose-laminated carbonaceous sandstones, mudstones, or directly by the upper portion of the Kakwa Member. Rocks deposited in a fluvial setting replace the "upper" portion of the Kakwa Member in some cores. These strata have a distinctive gamma ray well log signature which is useful for their identification in wells for which no core is available. The Musreau Member resembles its outcrop equivalents, being dominantly fine-grained (mudstones and siltstones), but the thickness of this member decreases measurably to the northeast, finally pinching out entirely.

Overlying the Musreau and Kakwa members are lithologic units which are not observed in outcrop. These belong to the offshore facies association; thick shoreface sandstones (facies 16 and 17) or conglomerates are generally absent (but see 11-22-65-6W6, Fig. 5.18). Similar strata are also found basinward of the depositional limit of the Kakwa Member. Subsurface correlations to be presented in the next chapter will show that some of these units are temporally equivalent to the shoreface sandstones of the Kakwa Member.

5.4 Evidence for relative sea level change from early diagenetic phases: An example from the Cardium Formation

Given the importance of depositional environment in the formation of early diagenetic minerals, it seemed logical to evaluate the potential use of these phases in detecting transgressive and regressive episodes in marine to non-marine successions. In this section, I will present the results of a study of early diagenetic siderite from the Mistanusk Creek section of the Cardium Formation. Siderite was chosen because petrographic analyses indicated that it is a common early diagenetic phase in this part of the formation, and because its elemental and oxygen isotopic composition are known to be at least partially controlled by the salinity of the waters from which it precipitates.

Good samples of early diagenetic siderite (see Chapter 3) were obtained from strata representative of most of the section at Mistanusk Creek, hence that section was selected as a test site.

5.4.1 Analytical Procedure

Samples were studied petrographically to determine their mineralogical composition and general textural relationships. X-ray diffraction of powdered samples was used to further identify mineral phases. The elemental composition of diagenetic phases was established for individual samples using the electron microprobe (JEOL JXA-8600, 15 kV potential, 1-5μm beam width, 10 nA sample current, carbonate standards and ZAF correction). Textural relationships among these phases were further delineated using the backscattered electron detector with which the JEOL JXA-8600 is equipped.

Extraction of CO_2 from siderite for isotopic analysis was completed using a modification of the technique described by Rosenbaum and Sheppard (1986). The presence of dolomite in most of the samples necessitated adoption of a two phase extraction procedure to exploit the different reaction times of siderite versus dolomite in phosphoric acid. Samples were reacted at 25°C for 10 days, and the resulting $CO_2(g)$, which derived mostly from dolomite, was then discarded. The remaining material was then reacted at 150°C for 1 hour, and the accumulated CO_2 was assumed to represent siderite. For consistency, all samples, even those not containing dolomite, were analyzed using the same procedure.

Repeated tests on a pure siderite sample revealed that this two phase extraction resulted in $\delta^{18}O$ and $\delta^{13}C$ differences of less than 0.37 ‰ and 0.34 ‰ respectively. These differences are an order of magnitude less than the inter-sample variability, and hence do not affect the trends described below. The results of these analyses are presented in Table 1 and are discussed in detail below. The results here are reported in the standard δ-notation relative to the PeeDee Belemnite (PDB).

5.4.2 Results

5.4.2.1 General - sample description and interpretation

The stratigraphy of the Cardium Formation at Mistanusk Creek has been discussed earlier in this chapter. As many of the sections through the Kakwa Member suggested that the member consists of (at least) two stacked shoreface packages, I wished to test the hypothesis that the contact between the two could be a transgression (ravinement) surface, at least at this section. In Figure 5.21a, I have

TABLE 5.1

SIDERITE COMPOSITIONAL DATA

Sample	no. of analyses	siderite phase	Average Elemental Composition[1] CaO	MgO	MnO	FeO	Isotopic Composition (PDB)[2] $\delta^{18}O$	$\delta^{13}C$
MC-14	4	"pure"	1.79	0.41	0.25	57.89	-9.3	-4.4
	6	"impure"	4.81	0.77	0.15	52.55		
MC88-3	2	"pure"	3.21	0.99	0.68	54.25	-8.2	-1.9
	2	"impure"	4.01	5.90	0.44	47.73		
MC88-2	2	"pure"	1.52	1.39	0.73	57.59	-10.4	-3.3
	4	"impure"	2.98	6.78	0.66	48.41		
MC-2	3	"pure"	3.34	0.22	0.24	54.70	-11.1	-5.6
	5	"impure"	7.32	6.26	0.04	43.13		
MC-1	2	"pure"	3.07	3.03	0.98	52.93	-8.9	-2.4
	10	"impure"	7.17	5.87	0.17	43.49		

1. Elemental compositon expressed in weight percent
2. Isotopic data for all siderite in sample, as separation of phases for individual analysis was not possible

Figure 5.21. A) Stratigraphic section of Cardium Formation at Mistanusk Creek showing sample locations (arrowed). B) Relative sea level curve based on sedimentology of measured section. C) Variations in $\delta^{18}O$ (dots), and FeO content of "impure" siderite phase (solid triangles) and "purer" siderite phase (open triangles) as a function of stratigraphic position. Trends in relative sea level curve are matched by variations in $\delta^{18}O$ and %FeO.

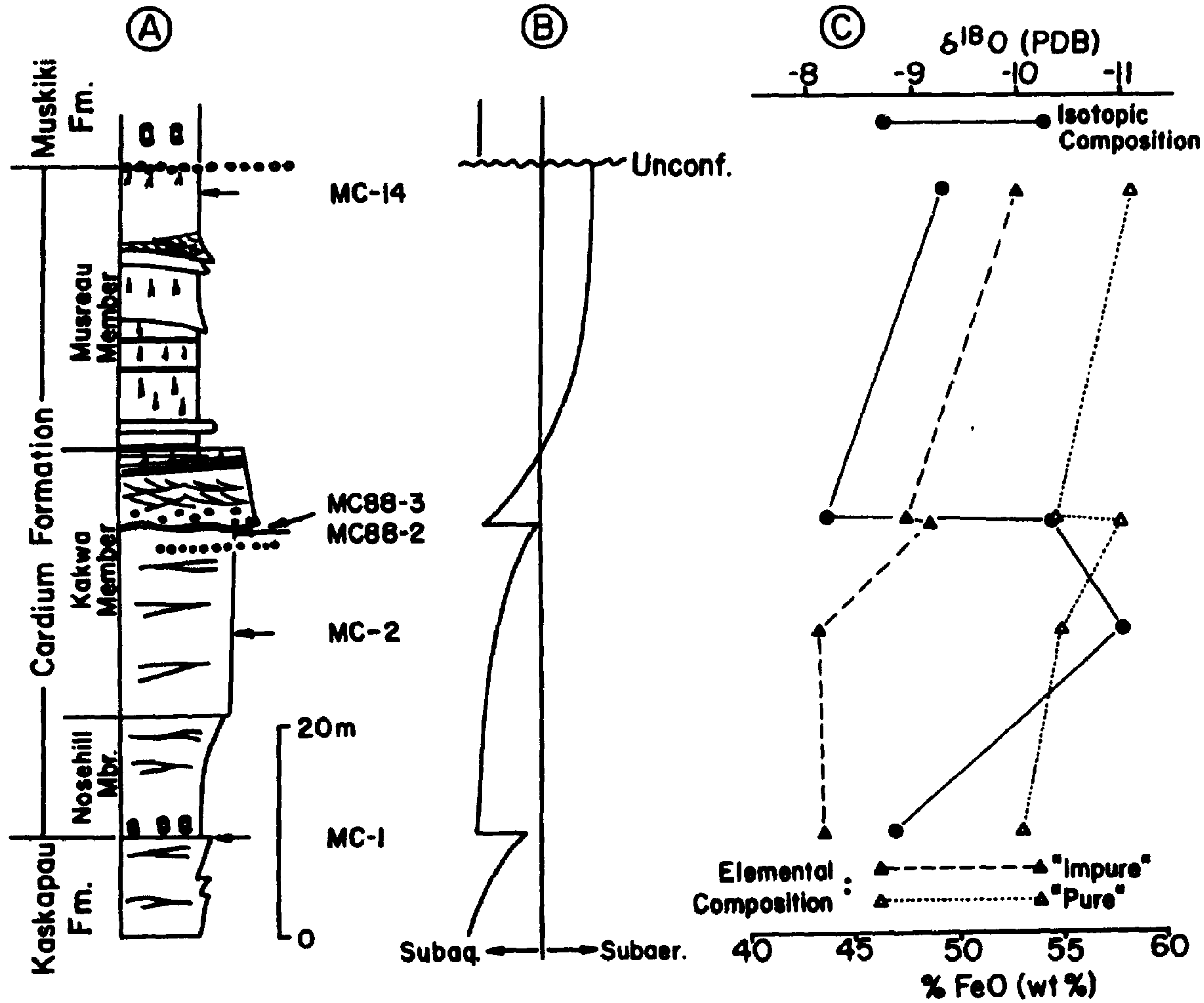

A
B
C
Muskiki Fm.
Cardium Formation
Musreau Member
Kakwa Member
Nosehill Mbr.
Kaskapau Fm.
MC-14
MC88-3
MC88-2
MC-2
MC-1
20m
0
Unconf.
Subaq.
Subaer.
δ18O (PDB)
-8
-9
-10
-11
Isotopic Composition
Elemental Composition :
"Impure"
"Pure"
40
45
50
55
60
% FeO (wt %)

redrawn the stratigraphic section to indicate the stratigraphic position of samples used in this study. For the present purposes, the formation can be divided into 5 sub-units based on sedimentologic criteria:

Unit 1, Kaskapau Formation/Nosehill Allomember. Sample MC-1 was selected from a bioturbated concretionary layer in offshore units (hummocky cross-stratified sandstones interbedded with mudstones) at the base of the formation (Fig. 5.21a). Several cross-cutting burrow phases can be identified in the siderite, which is fine-grained (generally < 10 µm; Figs. 3.2b, 5.22a) and comprises over 70 % of the rock volume. These characteristics suggest siderite formation very close to the sediment/water interface (*cf.* Gautier, 1982).

Unit 2, Lower part of Kakwa Member. Samples MC-2 and MC88-2 were chosen from the facies 16 sandstones of the lower shoreface sandstone unit of the Kakwa Member (Fig. 5.21a). In sample MC-2, selected mid-way within the unit, siderite occurs as ubiquitous silt-sized pore filling rhombs overgrown by authigenic quartz (Figs. 3.6b, 5.22b). Sample MC88-2 was collected immediately below the suspected ravinement surface at the top of the facies 16 sandstones (Fig. 5.21a). It will be recalled that this surface possesses characteristics which suggest that it formed by the erosion of an at least partially lithified substrate (Section 5.2.2). Siderite in this sample occurs both as a

Figure 5.22. A) Backscatter image of two siderite phases in burrow from sample MC-1 showing brighter ("purer") phase overgrown by darker ("more impure") phase. B) Backscatter image of siderite rhomb from sample MC-2 with core of purer siderite surrounded by more impure phase, overgrown by authigenic quartz. Note also compromise boundary to quartz overgrowths (arrow), and bright reaction rim (too small to probe) around siderite rhomb. C) Outcrop photograph showing irregular topography on erosion surface (solid arrow; sampling site for MC88-2) capping swaley cross-stratified sandstone of lower shoreface package. Note thin normally graded unit which drapes the surface (open arrow; sampling site for MC88-3). D) Backscatter image of two siderite phases in eogenic nodule from sample MC88-2. E) Backscatter image of two siderite phases in eogenic nodule from sample MC88-3. F) Photomicrograph of siderite spherulites from sample MC-14. Diameter of largest spherulites is about 0.4 mm.

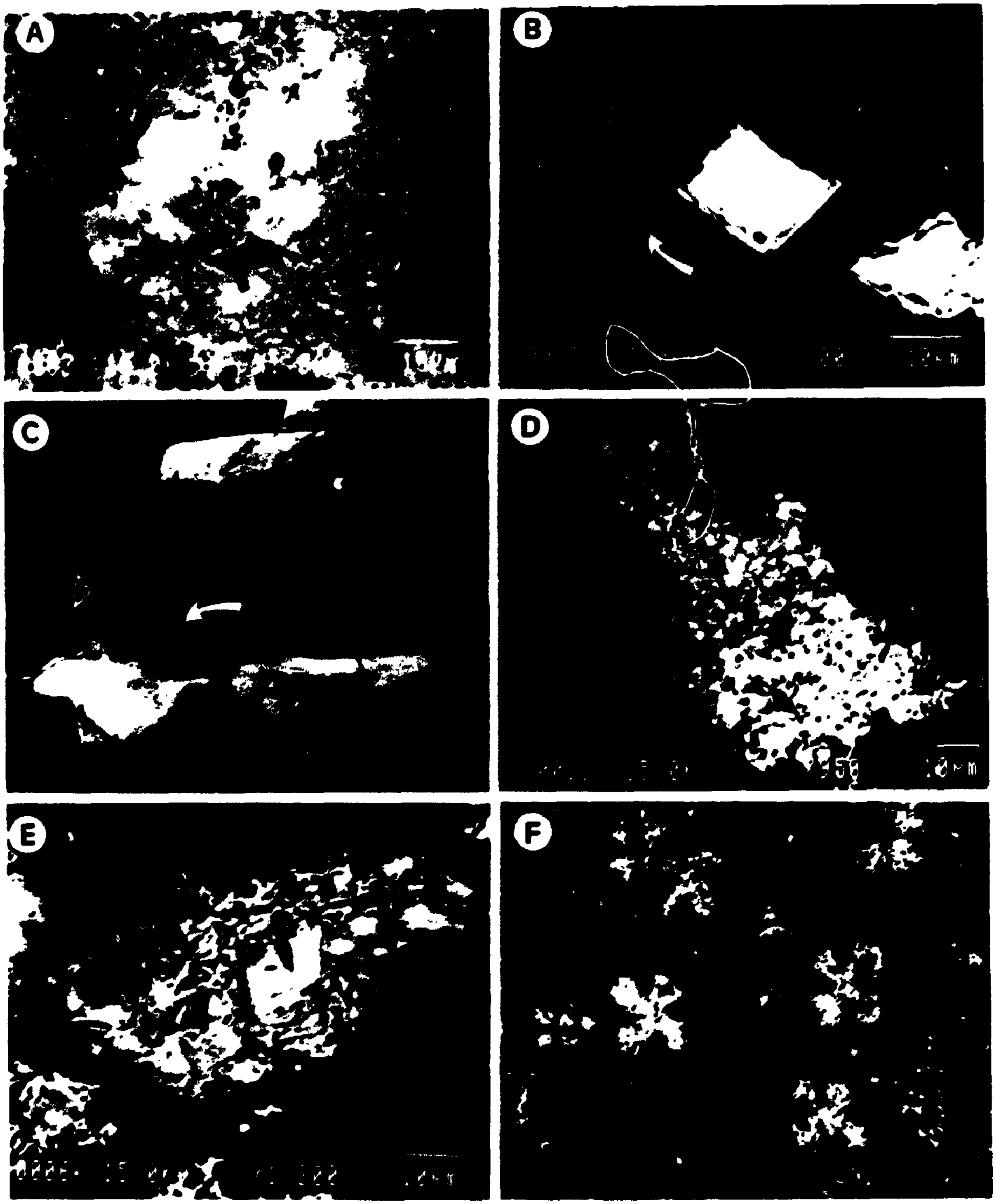
A
B
C
D
E
F

very finely crystalline (few μm) cement, and as more coarsely crystalline eogenic nodules (Fig. 5.22g). Quartz overgrowths are not common, but can be seen to post-date the siderite.

Unit 3, "Middle" part of Kakwa Member. A thin (up to 15 cm thick) normally-graded fine grained sandstone to carbonaceous mudstone unit drapes the suspected ravinement surface at the top of the facies 16 sandstones (Fig. 5.22c). Sample MC88-3 was taken from the sandstone (Figs. 5.21a, 5.22c), and siderite in it occurs both as a cryptocrystalline cement, and coarser-grained eogenic nodules (Fig. 5.22d). The presence of mudstone suggests a transition to quieter (?deeper) water conditions.

Unit 4, Upper part of Kakwa Member. This unit consists of the upper, coarser-grained shoreface unit of the Kakwa Member (Fig. 5.21a). Siderite was not observed in any of the samples of this unit from 17 localities (Chapter 3). This suggests that siderite precipitated in both the lower shoreface package (unit 2) and the graded unit (unit 3) before deposition of the upper, coarser-grained shoreface unit, a period of probably less than 10^5 years (Chapter 1).

Unit 5, Musreau Member. Sample MC-14 was chosen from a sideritic interval associated with rooted horizons in a dark grey mudstone about 2 m below the top of the formation (Fig. 5.21a). Siderite in this sample is spherulitic (spherules up to 0.5 mm in diameter; Fig. 5.22f) in a matrix of silt-sized quartz, clay minerals and lesser microcrystalline Ca-phosphate. Siderite in fine-grained non-marine successions commonly indicates reducing conditions in poorly-drained soils (Wright, 1989). Siderite spherulites are poorly documented from modern soils, but their presence in paleosols has previously been attributed to formation in lower portions of the soil profile (Tucker, 1981).

In Figure 5.21b, I have constructed a relative sea level curve for the Cardium Formation at Mistanusk Creek, based on the inferred depositional water depth of the preserved stratigraphic section. In that figure it can be seen that I interpret the vertical succession of strata to have been produced by the stacking of two progradation (upward shoaling) events. This model will now be tested against the siderite compositional data.

5.4.2.2 Elemental composition of the siderite

X-ray diffractograms suggested the presence of two compositionally distinct siderites in all of the samples. This was indicated by separate peaks at d-spacings of 2.79 and 2.81 Å or by a single broad peak at 2.80 Å. These different siderite phases could be distinguished by differences in grey tone on photomicrographs produced using the backscattered electron detector attached to the electron microprobe. The lighter grey siderite contains more Fe relative to the darker grey siderite in which Ca and Mg are more abundant (Table 4.1).

In all samples, the darker grey siderite post-dates the lighter grey siderite (Fig. 5.22a,b,d,e). In sample MC-1, the lighter grey phase is restricted to specific burrow-filling cements and comprises less than 1% of the total siderite. In sample MC-2, the lighter grey phase is found as a core to some siderite rhombs; less than 10% of the total siderite is composed of this variety. The finely crystalline siderite of samples MC88-2 and MC88-3 consists entirely of the darker grey phase, with the lighter grey phase being restricted to eogenic nodules. Finally, the spherulites in sample MC-14 have an Fe-rich siderite core, with a greater substitution of Fe by Ca occurring towards the margins.

Recent work, compiled by Mozley (1989a), suggests that the "purity" of siderite, expressed as the degree to which Fe is replaced by Ca and Mg, can be related to paleosalinity. He found that freshwater siderite is always relatively "pure", whereas there is extensive replacement of Fe in marine siderite. In Figure 5.21c the percent FeO is plotted to examine vertical trends in siderite composition. In the diagram, closed triangles represent the darker grey, more "impure" siderite in individual samples, whereas the open triangles represent the lighter grey, "purer" siderite.

Comparison of Figures 5.21b and 5.21c demonstrates that chemically purer siderite, for both phases, tends to be associated with shallower water (to non-marine) deposits. If one assumes that shallower waters received greater freshwater input, these trends are in agreement with Mozley's (1989a) earlier results. That the "pure" and "impure" siderites show sympathetic variations in Fe-content through the section is considered as evidence for the early formation of both.

5.4.2.3 Isotopic Composition of the siderite

The oxygen isotopic compositions of the siderite is a function of its crystallization temperature and the isotopic composition of water from which it precipitated. The textural evidence for early (i.e. low temperature) siderite formation leads one to interpret inter-sample variations as resulting from salinity differences in formation waters. Siderite precipitated from fully marine waters would be expected to have $\delta^{18}O$ (PDB) values close to $0°/_{oo}$, whereas increasingly negative $\delta^{18}O$ values should reflect the addition of isotopically light meteoric waters. It should be noted that studies of time-equivalent strata in Manitoba by Kyser *et al.* (*in press*) indicate that $\delta^{18}O$ values of the waters of the Western Interior Seaway were typically about $4°/_{oo}$ lower than that of the open ocean.

When taken in vertical succession (Fig. 5.21c), the oxygen isotope values of the siderites can be matched to the inferred relative sea level curve based on the sedimentology of the section. The lowering of the $\delta^{18}O$ values from MC-1 to MC-2 reflects increasing freshwater influence as the shoreline prograded. The similarity in $\delta^{18}O$ values of sample MC88-3 (the sandstone draping the ravinement surface) to sample MC-1 (at the E1/T1 surface) probably indicates a return to deeper water conditions following transgression.

The isotopic composition of siderite in sample MC88-2 is intermediate between that of the overlying and underlying samples. Sedimentological evidence suggests that MC88-2 was deposited in shallower water than the underlying sample MC-2, and siderite in it should therefore be isotopically lighter. This difference could be explained if continued siderite growth took place in deeper waters following transgression and ravinement (concomitant with siderite precipitation in MC88-3 which immediately overlies the ravinement surface), although definitive textural criteria are lacking.

The oxygen isotopic composition of the spherulitic siderite in MC-14 (from the non-marine Musreau Member) suggests a return to fresher water conditions from MC88-3. However, its $\delta^{18}O$ value is not as low as that from the shoreface sandstones of MC-2 and MC88-2. This might reflect higher salinity porewaters (indicated by higher CaO percentages towards spherulite margins) with depth in the soil profile (*cf.* Wright, 1989), although the possibility that it represents development of brackish water conditions behind a transgressing shoreline (see Chapter 7) cannot be excluded with the available evidence.

The range of $\delta^{13}C$ values (from -5.6 to -2.0 $^{o}/_{oo}$) cannot be reconciled with a significant contribution by CO_2 (isotopically very light) formed during thermal decarboxylation of organic matter at depth. Siderite with carbon isotopic compositions similar to those reported here can be found in the Viking Formation (Longstaffe and Ayalon 1987), where they are associated with early, shallow diagenesis, and CO_2 derived from dominantly inorganic sources. Similar $\delta^{13}C$ values have recently been reported by Pye *et al.* (1990) for Recent (post Second World War) marine siderites from the intertidal zone of England. They suggested that carbonate was derived partly from marine (inorganic) sources, partly from biogenic degradation of organic matter.

5.4.3 Summary of siderite compositional data

The presence of two compositionally distinct authigenic siderites in a single sample has been reported previously (e.g. Pearson, 1967; Mozley, 1989b). Given the limited data available from this study, I do not wish to speculate on the reason for the co-existence of the two phases. Rather, I will emphasise that *in the present case*, both phases appear to follow the same trends in elemental composition. These trends match that of the oxygen isotopic composition of the siderites, if it is assumed that the controlling variable for all was the salinity of the pore waters at the time of crystallization. Both trends match quite closely those which would be predicted on the basis of the sedimentology and stratigraphy of the Mistanusk Creek outcrop. This inferred relation is strengthened by the textural evidence for early siderite precipitation in all samples.

Although both of the compositional variables are dependent on a number of other factors, such as temperature of crystallization and pore water evolutionary trends (e.g. Curtis *et al.* 1986; Longstaffe 1989; Mozley 1989a), the observed relationships strongly suggest that the siderites formed early enough in the diagenetic history of the Cardium to record the influence of the depositional waters. The compositional evidence provides support for the hypothesis that two separate phases of shoreline progradation, each producing a distinct shoreface sandstone, are separated by a transgression surface at the Mistanusk Creek section. Similar trends might be expected in early diagenetic phases from other transgressive/regressive successions.

5.5 Summary

As noted in Chapter 3, most of the available outcrop and cores sections represent stratigraphic sections through the Kakwa Member. A similar vertical succession of facies is noted from both outcrop and core. Both the upper part of the Kaskapau Formation and lower part (i.e. below the Kakwa

Member) of the Cardium Formation consist of sandier- and coarsening-upward successions which suggest a hierarchial arrangement of cyclicity. The tops of some of the larger cycles are sideritic, or overlie thick sandstones. The Kakwa Member in almost all cases appears to consist of (at least) 2 stacked shoreface "packages". The lower part is dominated by a coarsening-upward unit of facies 16 sandstones (locally capped by beach laminated sandstones and, rarely, *in situ* root traces), whereas the upper part generally consists of an upward fining unit consisting of facies 17 sandstones.

Based upon the available evidence, the Kakwa Member could represent either two vertically superimposed, near-tabular shoreface sandstone units, or a series of shingled shoreface sandstone units. These two possibilities are represented in Figure 5.23 and, given only the measured sections, it is impossible to decide between the two alternatives. In the next chapter, it will be shown that in the absence of continuous outcrop exposure, the solution to this problem can only be obtained where good well coverage is present.

The results of the siderite study are incompatible with a model whereby the contact between the lower (facies 16 dominated) and upper (facies 17 dominated) shoreface "packages" at Mistanusk Creek represents a break developed by the lateral migration of rip current channels on the

Figure 5.23. Figure showing how measured sections (outcrop or core), each apparently consisting of two stacked shoreface packages (stippled), could represent either two tabular shoreface sandstones, or a series of shingled shoreface sandstone lobes. Black represents non-marine strata.

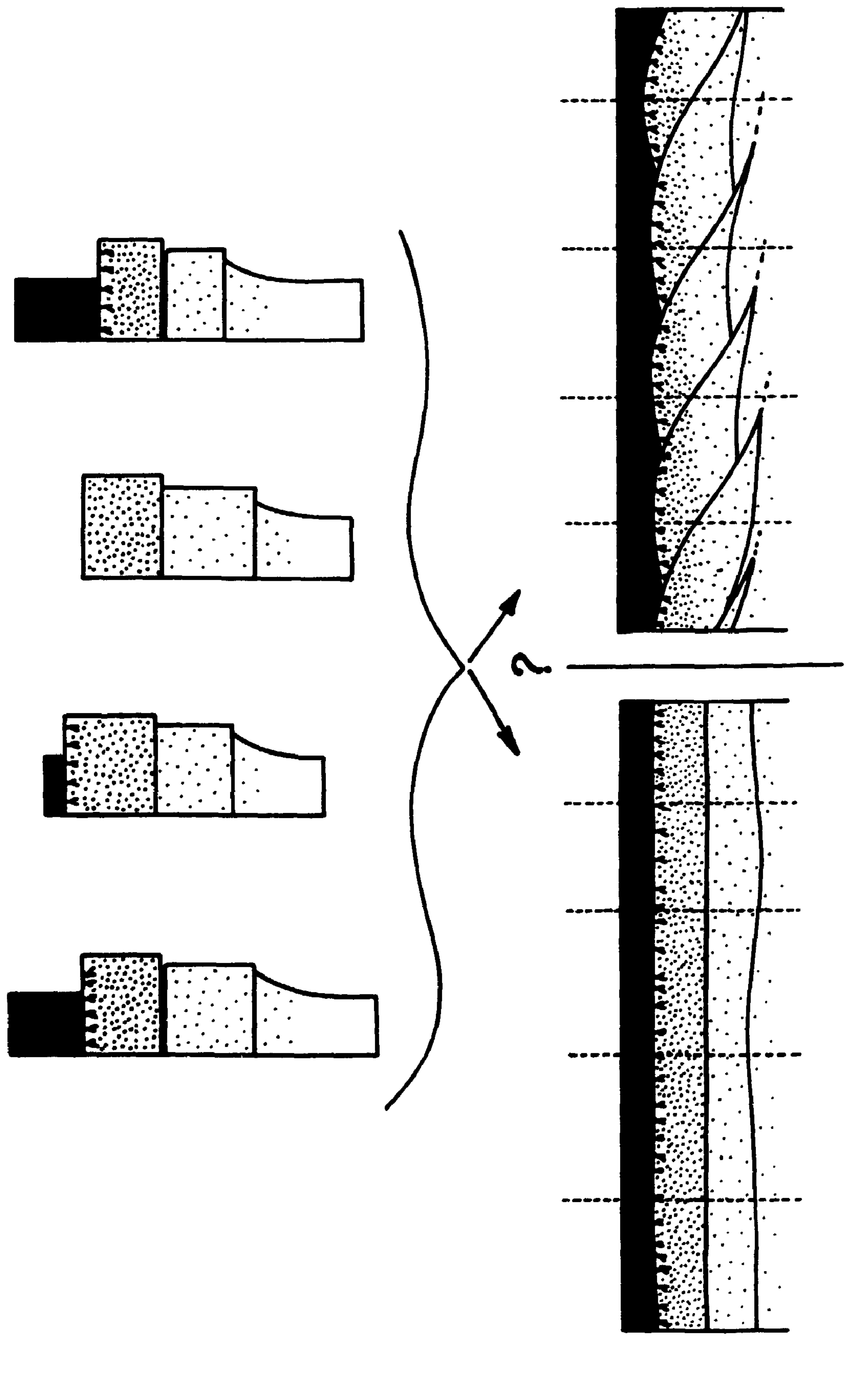

shoreface (e.g. Hunter *et al.* 1979). The differences in cementation across the contact, the local presence of mudstone, and the relative deepening of water suggested by the siderite compositional data are considered to be incompatible with the barred shoreface model. Some of these characteristics are present in other measured sections (analysis of siderites from other sections was not attempted), and beach laminations and root traces can *underlie* the contact in these sections.

The Musreau Member is dominantly fine-grained. Obvious lagoonal deposits (e.g. oyster beds) are generally restricted to the basal few meters of the member. The remainder probably (as suggested in Chapter 3) represents channel and interchannel deposits of anastomosing fluvial systems.

The strata overlying the Musreau and Kakwa members, and those which are at least partial temporal equivalents of the two, consist of sedimentary rocks of the offshore facies association. Commonly, they are arranged into sandier upward successions capped by thin conglomerates (in places a single clast thick). Thick shoreface sandstones (if they ever existed) do not appear to be preserved.

Finally, the results of an investigation of early siderite cements from the Mistanusk Creek section suggest that early diagenetic phases can develop isotopic and elemental compositional trends which reflect transgressive or regressive paleoshoreline movements. These trends arise from the varying influence of marine and fresh water during early diagenesis. While these results should be generally applicable (i.e. other formations and probably other authigenic phases), results of a similar investigation of the Marshybank Formation were not as clear (J. MacKay, pers. comm.) possibly because of more complex relationships between authigenic phases, for example mixing of "early" and "late" diagenetic siderite.

CHAPTER 6

SEQUENCE STRATIGRAPHY OF THE CARDIUM FORMATION

6.1 Introduction: Sequence stratigraphy and the Cardium Formation

In this chapter, I wish to present the details of the sequence stratigraphic framework that was developed for the Cardium Formation in the study area. The principal aim of this part of the study was to determine whether or not the Plint *et al.* (1986, 1987, 1988) stratigraphic framework (developed further south) is applicable in this more northerly study area. It will be demonstrated that, with certain modifications, the sequence stratigraphy developed by those authors *is* a workable model for the Cardium Formation in the present study area.

6.1.1 Terminology

The reader will note that the terminology employed here is slightly different from the previous authors. To begin, the "E/T" (erosion/transgression) surfaces are here labelled simply as "E" surfaces. This is because, as noted in Chapter 1, it is not always apparent that two distinct phases of erosion (subaerial Erosion and Transgressive erosion) have been preserved. Instead, it would appear that transgressive erosion has removed most evidence of subaerial exposure (roots etc.), if they were present, at the top of upward-shoaling (i.e. sandier upward) successions. In this case, the packages delimited by the *transgressive* erosion surfaces (allomembers, NACSN 1983) are more closely akin to the *genetic stratigraphic sequences* of Galloway (1989) than the *depositional sequences* of EXXON workers (e.g. Posamentier *et al.* 1988). I should also point out that although the "E" surface notation employed here implies erosion (subaqueous or subaerial), it is likely that in their more basinward portions these surfaces more probably represent hiatal surfaces. In the absence of outcrop or core, the determination of exactly how much of the surface represents an erosion surface (subaerial or submarine) and how much is a hiatal surface is considered an intractable problem.

I have also chosen to downplay reference to the names of specific allomembers, and will instead generally discuss the "intervals" (i.e. genetic stratigraphic sequences) between two erosion ("E") surfaces. There are three main choices for this approach. First, as noted in the last chapter, core is sparse to absent in the more basinward portions of the formation's extent in this area; distinguishing the upper, sandy portions of the Raven River Allomember (strictly speaking, between T4 and E5) and the Carrot Creek Allomember (between E5 and T5, if it is present) is thus not possible. By referring to the E4 - E5 interval (as defined above), both of these allomembers are included. Second, as demonstrated below, I have been able to redefine how various portions of the Kakwa Member relate to their offshore equivalents (Nosehill, Bickerdike, Hornbeck allomembers). Here, by referring to the E1 - E2 or the E3 - E4 interval, I am presenting true allostratigraphic units, and the relationship between the shoreface and offshore units is more readily apparent. Finally, there appears to be some inconsistency with the identification of the E6 and E6.5 surfaces, as the present results are not compatible with previously published interpretations (e.g. Bartlett 1988; Plint 1988; Wadsworth 1989). As shown below, the surface I have traced as the E6.5 surface seems to correlate in places with the E6 surface of earlier authors, making the definition of the Dismal Rat and Karr allomembers problematic.

6.1.2 Methodology

As noted briefly in the previous chapter, the identification of the "E" (or "E/T") surfaces of the Plint *et al.* (1986, 1987, 1988) stratigraphy has been an iterative process in the present study. In some cases it has been possible to match well logs from the present study area to well logs from the original studies (Fig. 6.1). In other cases the distinctive log signature (for example the sandier-upward nature of the Raven River Allomember, or the blocky log response of the Kakwa Member), or the stratigraphic position (e.g. E7 at the top of the formation) have allowed positive identification of the allostratigraphic subdivisions of the Cardium Formation.

Figure 6.1. Comparison of log markers from Plint et al. (1986) and present study.

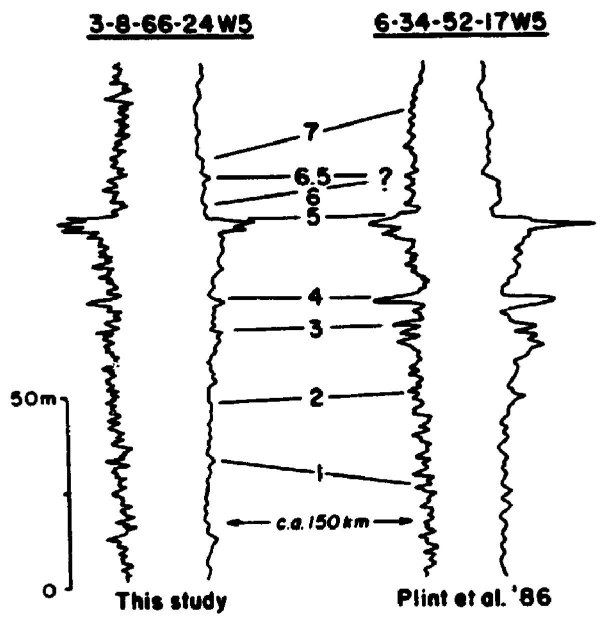
3-8-66-24W5
6-34-52-17W5
7
6.5
?
6
5
4
3
2
1
50m
0
c.a. 150 km
This study
Plint et al. '86

In addition, three correlation lines were constructed which joined the present study area to the study areas of previous authors further south (Plint 1988; Wadsworth 1989), as a further constraint on the identification of specific "E" surfaces.

In the present study, the elucidation of the internal stratal "geometry" of the Cardium Formation began with the construction of a regionally extensive grid of well log cross-sections (Fig. 6.2). Wherever possible, core data (or outcrop sections) were employed to identify facies successions and erosion surfaces, thus constraining the correlations. As the work progressed, new cross-sections were constantly checked against the existing lines. By constructing an intersecting grid of cross-sections (E-W lines and N-S lines), it was possible to "box in" individual picks. This procedure helped further constrain the new correlations and served as a check of the existing correlations. As new data became available (for example, after the second year of logging core), it too was employed to further test the validity of the existing stratigraphy.

Picks from well logs used in the cross-sections were matched to nearby wells which were not used. This procedure eliminated the necessity of using *every* well in the regional cross-section grid. Once all picks had been identified on the logs, the depth below the Kelly Bushing (as read off the well log) for each pick of each well was recorded, then

Figure 6.2. Cross-section grid employed to establish regional correlation of surfaces.

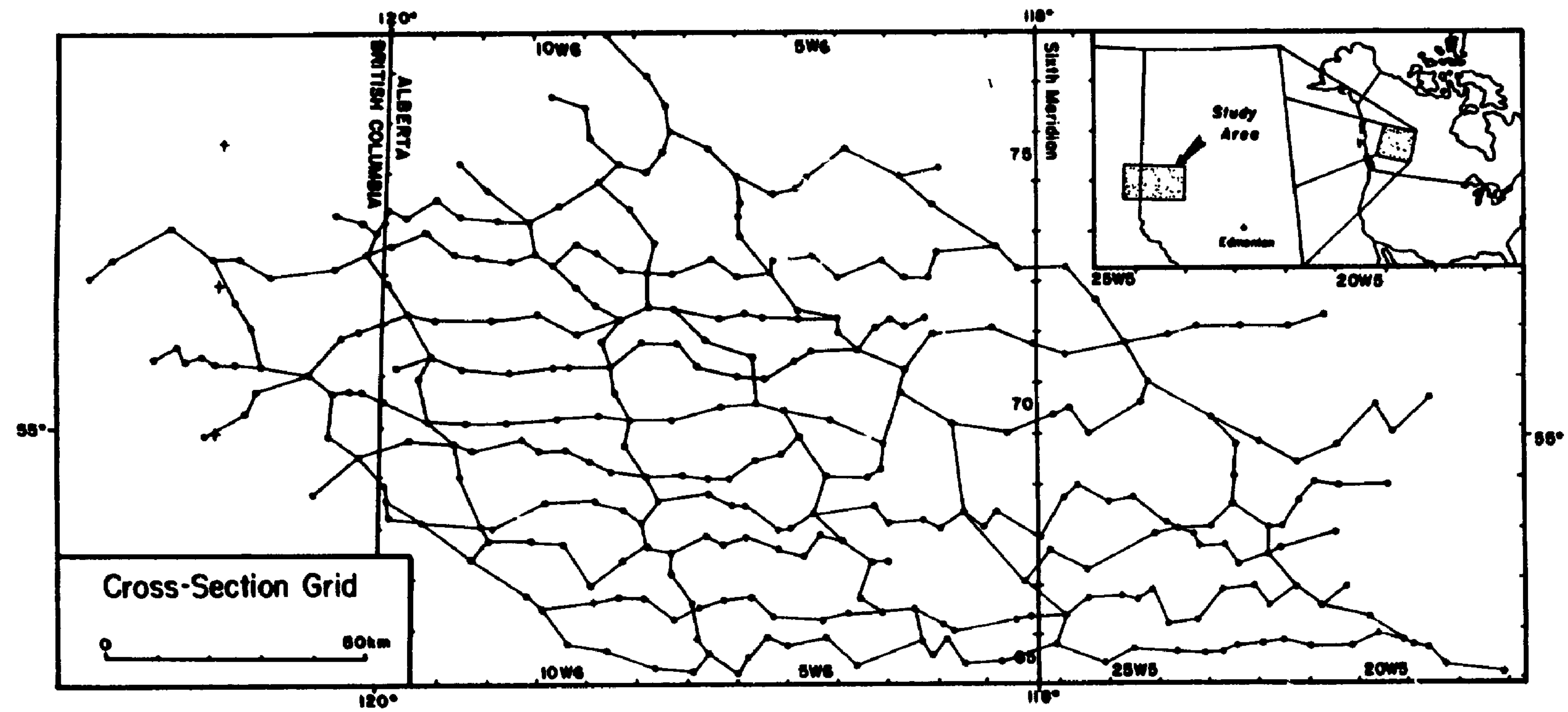

Cross-Section Grid

input into a computerized database system developed by the author (see Appendix 2). This was employed to generate data files which were input into the *Surfer 4.0* software package (produced by Golden Software) for the construction of isopach maps and surface diagrams.

In the next section, selected cross-sections through the Cardium Formation in the study area will be presented. This will clarify the two-dimensional stratal geometry of the formation. Subsequently (Section 6.3), the nature of the individual "E" surfaces and allomembers (in the sense described above) will be examined in ascending order, describing sequentially the history of sedimentation and erosion in this area. Discussion of the ultimate causative mechanisms responsible for producing the observed sedimentary succession of will be deferred until the next chapter.

6.2 Cross-sections through the Cardium Formation

A figure summarising the stratigraphic relationships of the Cardium Formation in the present study area was presented in Chapter 1. In this section I will outline the evidence for the present interpretation of stratal geometries.

To begin, I would like to present three summary E-W ("regional") cross-sections through the formation (Fig. 6.4, locations in 6.3a). Each section is based on approximately 20 data points; they represent lines "distilled" from the

Figure 6.3. A) Location of regional cross-sections presented in Figure 6.4.

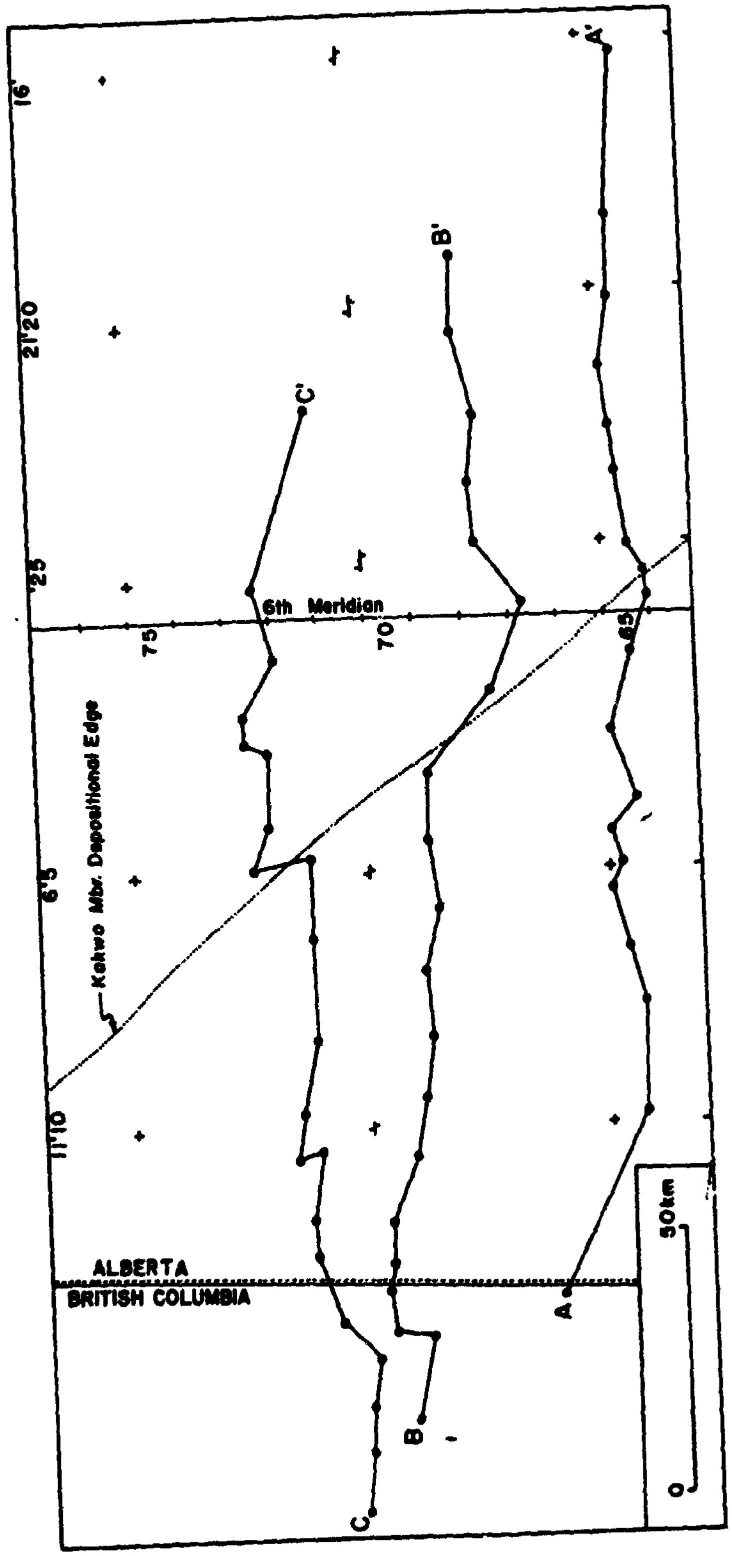

16'
21'20
25
6'5
11'10
75
70
65
6th Meridian
Kakwa Mbr. Depositional Edge
ALBERTA
BRITISH COLUMBIA
A
A'
B
B'
C
C'
0
50km

Figure 6.3 (cont.) B) Location of detailed cross-sections presented in Figures 6.5, 6.6, 6.7.

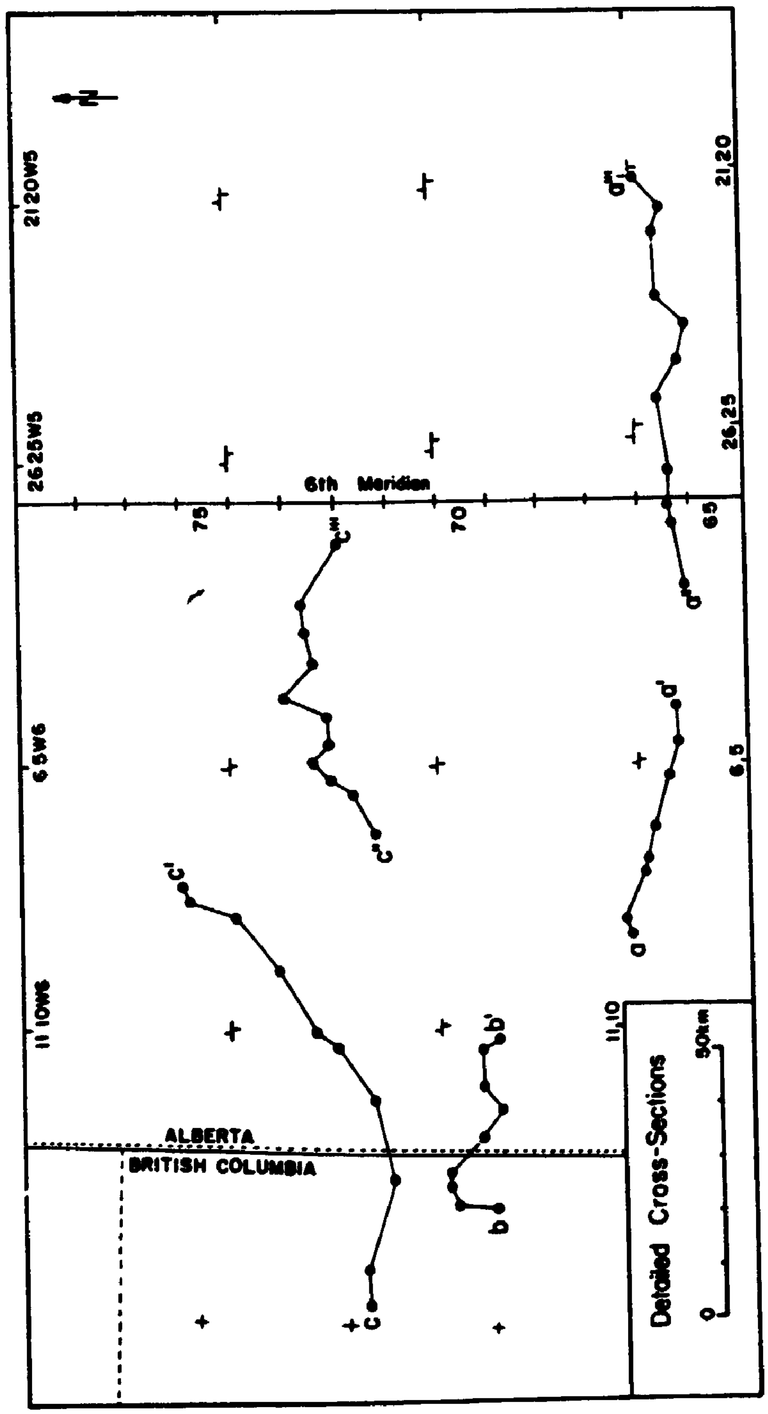
Detailed Cross-Sections
0
50km
ALBERTA
BRITISH COLUMBIA
6th Meridian
75
70
65
2120W5
2625W5
65W6
1110W6
21,20
26,25
6,5
11,10
N
a
a'
a''
a'''
b
b'
c
c'
c''
c'''

Figure 6.4 A) Regional cross-section A-A'. Location of control points indicated by open circles above Datum. See text for description.

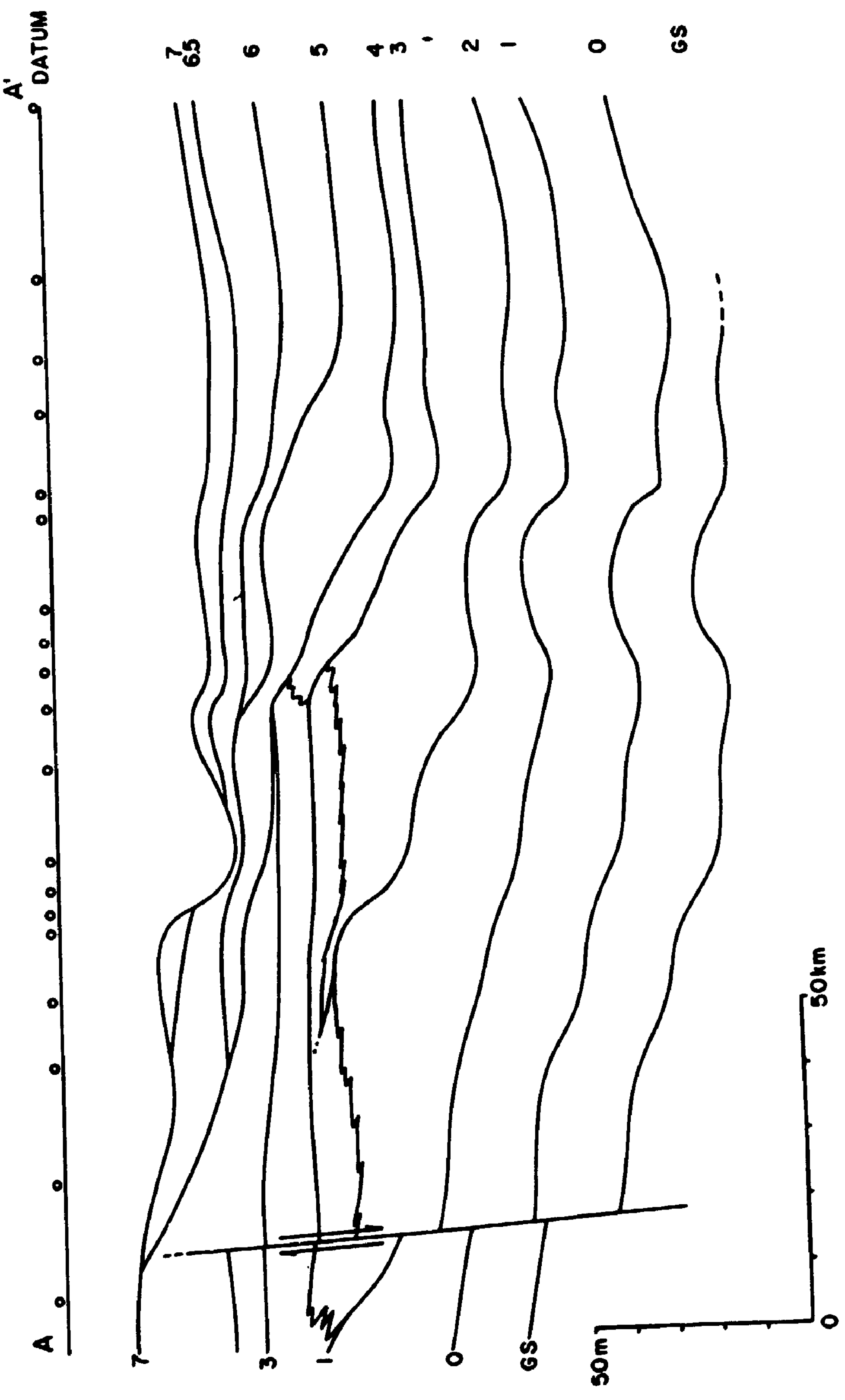

A
A'
DATUM
7
6.5
6
5
4
3
2
1
0
GS
7
3
1
0
GS
50m
0
50km

Figure 6.4 B) Regional cross-section B-B'. Location of control points indicated by open circles above Datum. See text for description.

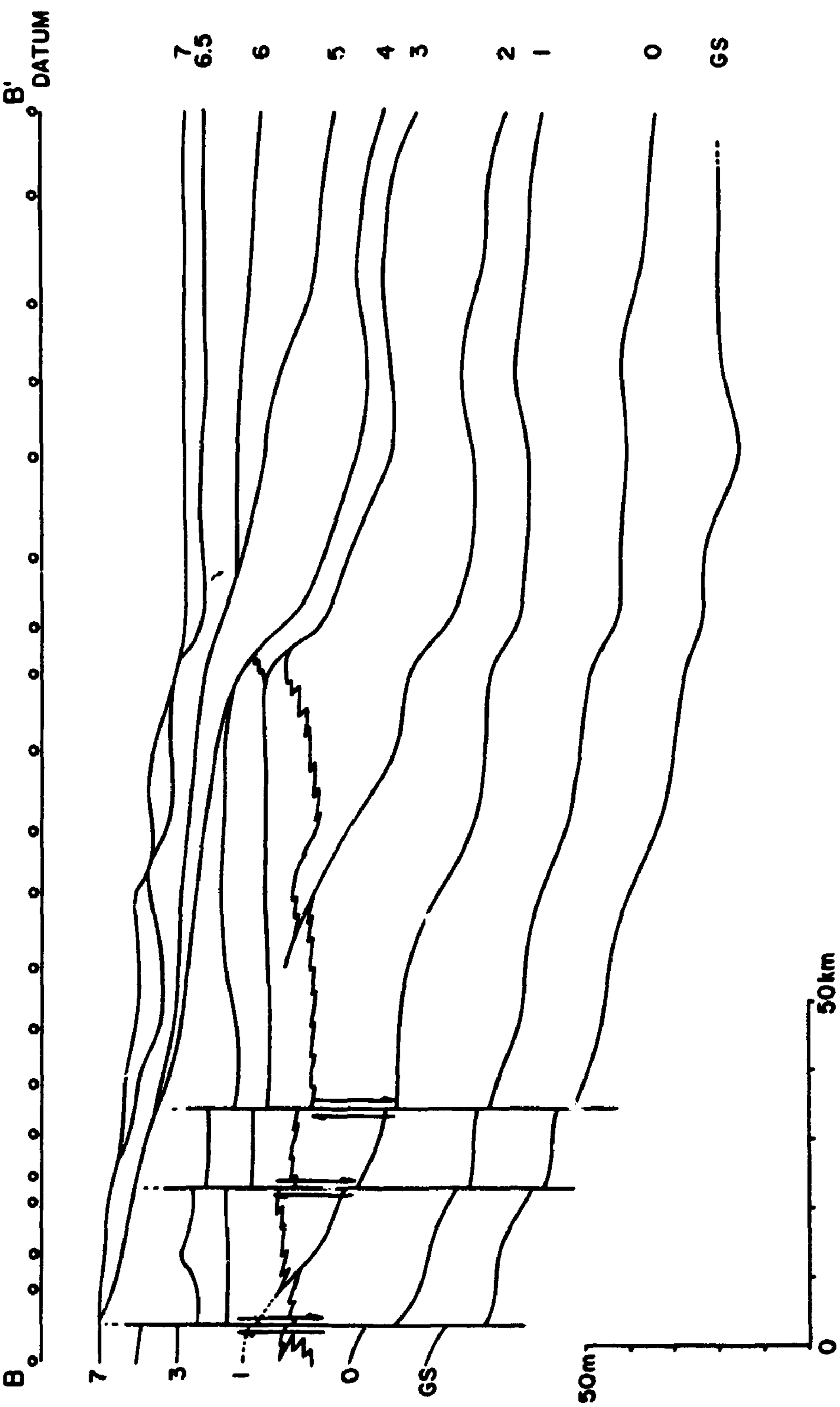
B
B'
DATUM
7
6.5
6
5
4
3
2
1
0
GS
7
3
1
0
GS
50m
50km
0

Figure 6.4 C) Regional cross-section C-C'. Location of control points indicated by open circles above Datum. See text for description.

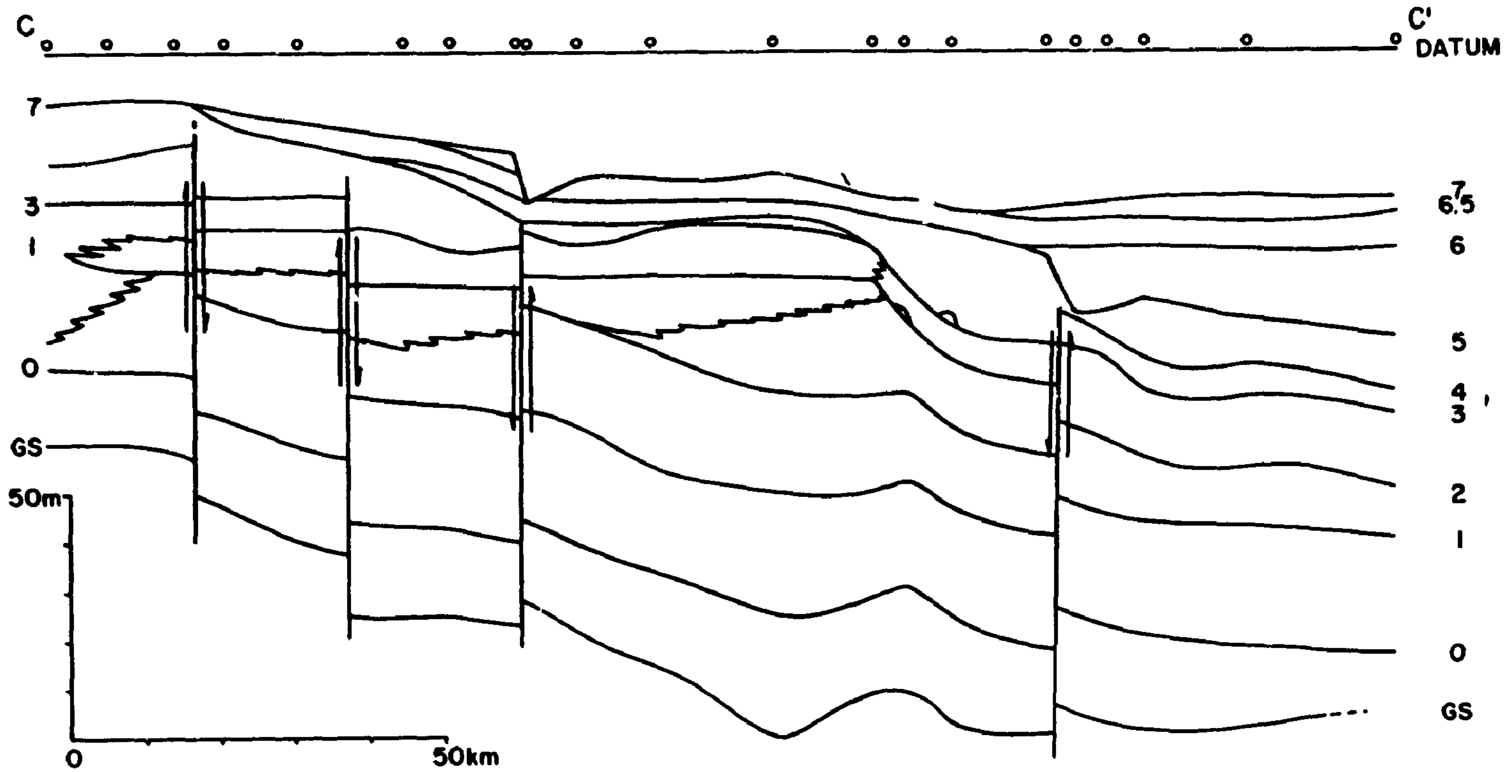
C
C'
DATUM
7
3
1
0
GS
50m
0
50km
7
6.5
6
5
4
3
2
1
0
GS

regional cross-section grid (Fig. 6.2). For clarity I have decided to present the cross-sections without the well logs, reasoning that a line consisting of 20 wells would be too long to present from a practical standpoint, and that the details of the correlations could be presented as separate figures (Figs. 6.5, 6.6, 6.7). I find that the presentation of the main cross-sections *without* the wells gives a clearer picture of stratal geometries on a regional scale (the scale of interest here).

The distances between wells in the main sections have been "normalised" by projecting the data points onto a line which runs at right angles to the edge of the Kakwa shoreface sandstones (as determined by mapping of the distribution of distinctive well log signatures; see Fig. 6.3a). In this way I hoped to be able to present sections which portray the basin margin to basin center distances more realistically. This manipulation was necessary because the orientation of the study area (N-S, E-W) is at an angle to the orientation of the depositional strike of the Cardium Formation (roughly NW-SE). In the north, the formation is generally too shallow to be logged, whereas the Rocky Mountain Foothills are found to the southwest, and well data are sparse. The area immediately south of the present study area has been examined previously (Bartlett 1987; Plint 1988; Plint and Walker 1987; Wadsworth 1989). As such, reorientation of the study area was not feasible.

The datum used in all the subsequent cross-sections is a marker in the Muskiki Formation (overlying the Cardium Formation). This datum was selected on a trial-and-error basis; it was the only marker in the Muskiki Formation that I was able to trace throughout most of the study area. Plint (1990) examined the stratigraphy of the Muskiki and Marshybank formations in a study area which is essentially equivalent to the present one. He labelled this the "M1" horizon, confirming the marker's regional extent and suggesting that it is an approximately planar surface in this region. In the northern and eastern parts of the study area, this marker is locally removed by erosion at the base of the Badheart Formation (see below). In these cases, I have been able to employ local markers found below, but running essentially parallel to the main (M1) datum.

6.2.1 Southern part of the study area: Regional cross-section A-A'

All but one of the wells used for the construction of this section (Fig. 6.4a) come from Twp 65 (Fig. 6.3a). Detailed sections in this area are presented in Figure 6.5a,b (see Fig. 6.3b for locations). The wells from the detailed cross-sections do not correspond exactly to the wells used in the construction of the regional cross-section, but have instead been chosen for illustrative purposes (clarity of well response and/or accompanying core).

Figure 6.5. Detailed cross-sections. A) a-a'. B)a''-a'''.

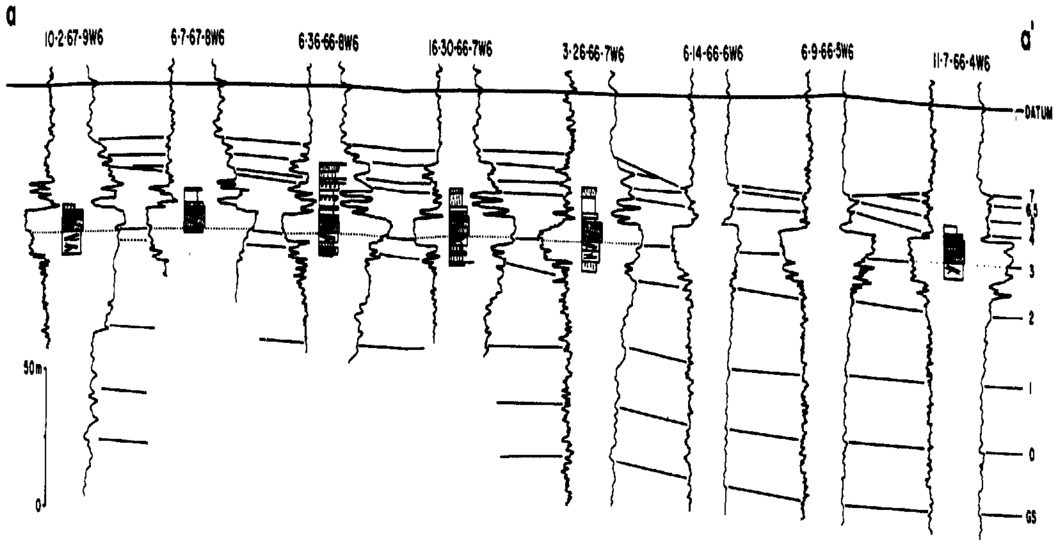
a
10-2-67-9W6
6-7-67-8W6
6-36-66-8W6
16-30-66-7W6
3-26-66-7W6
6-14-66-6W6
6-9-66-5W6
11-7-66-4W6
a'
DATUM
50m
0
7
6.5
4
3
2
1
0
GS

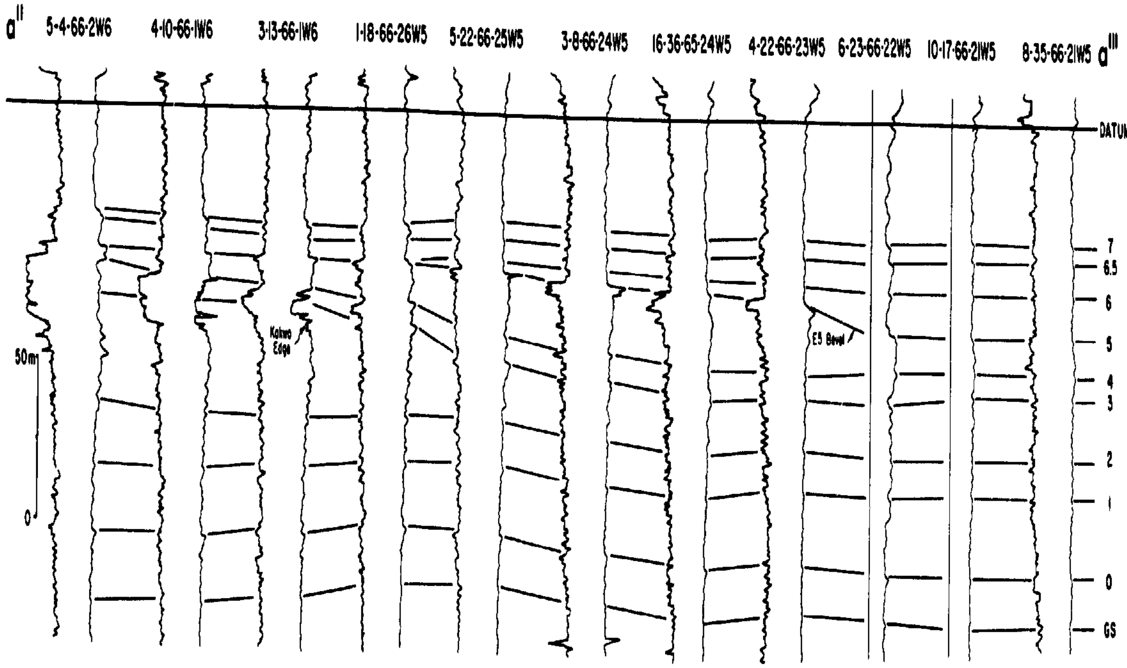
a''
5-4-66-2W6
4-10-66-1W6
3-13-66-1W6
1-18-66-26W5
5-22-66-25W5
3-8-66-24W5
16-36-65-24W5
4-22-66-23W5
6-23-66-22W5
10-17-66-21W5
8-35-66-21W5
a'''
DATUM
Kakwa Edge
E5 Bevel
50m
0
7
6.5
6
5
4
3
2
1
0
GS

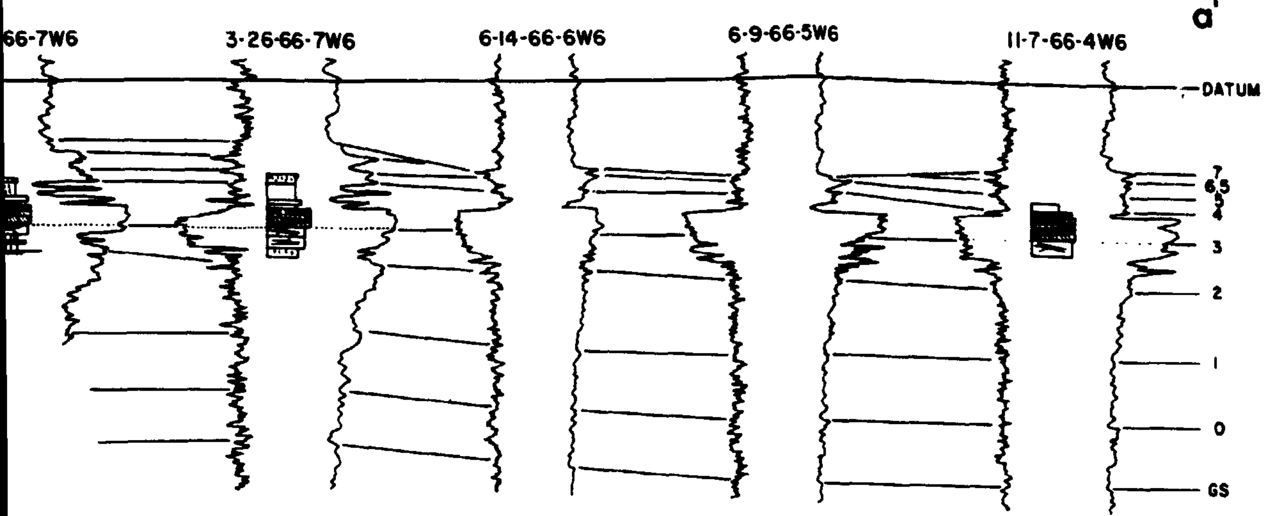
a'
66-7W6
3-26-66-7W6
6-14-66-6W6
6-9-66-5W6
11-7-66-4W6
DATUM
7
6.5
5
4
3
2
1
0
GS

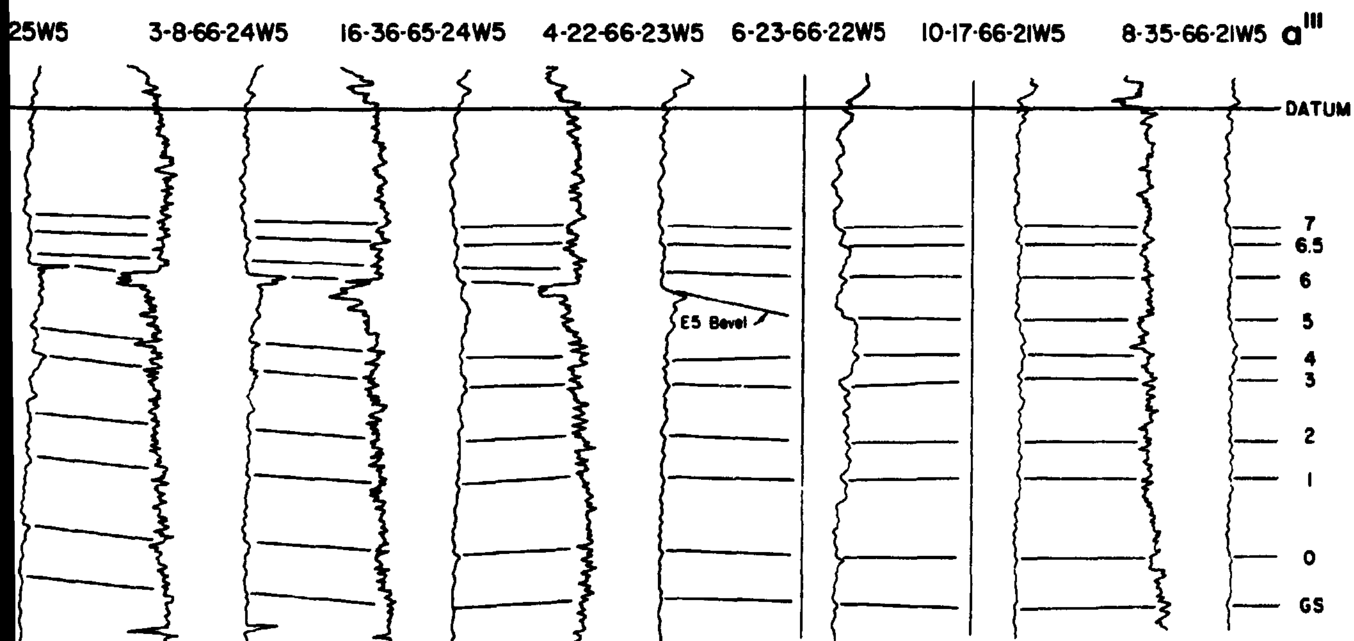
25W5
3-8-66-24W5
16-36-65-24W5
4-22-66-23W5
6-23-66-22W5
10-17-66-21W5
8-35-66-21W5
a'''
DATUM
E5 Bevel
7
6.5
6
5
4
3
2
1
0
GS

All of the "E" surfaces originally identified by Plint *et al.* (1986, 1987) can be identified in the present study area (Figs. 6.4a, 6.5a,b). An additional marker, the E6.5 surface, is continuous with the surface of the same name found further south by Wadsworth (1989) and Walker and Eyles (1988). Two surfaces underlying the Cardium Formation (the base of which is defined by the E1 surface) have also been traced throughout the present study area. The "E0" surface is a regionally extensive marker which can be correlated to the top of a 2.6 m thick facies 16 sandstone located 6 m below the main shoreface sandstones of the Kakwa Member at the Murray River section (Section 5.2.3). The "GS" surface is another regionally extensive marker which has been correlated to gritty siderite horizons at both the Murray River and Cutpick Hill sections. It is the same marker used by Stott (1967) to mark the contact between the Haven and Opabin members of the Kaskapau Formation. By continuing my correlations down into the Kaskapau Formation, I hoped to see whether any underlying structural elements (folds, faults, etc.) in that formation might have had an influence on sedimentation (or erosion) during deposition of the Cardium Formation.

There are 9 specific points I wish to make about these cross-sections. In ascending order, these are:

1) Note the "bulge" in markers GS, E0, E1 and E2 just basinward of the edge of the shoreface sandstones of the

Kakwa Member (Figs. 6.3a, 6.5b). This bulge is not due to any mispick of these markers (they are all relatively "easy" picks in this area) or of the datum. If the datum was mispicked, equivalent offsets should be evident in the overlying horizons, and this is not the case.

2) The E2 surface rises up to the west, and eventually merges into the Kakwa Member (see wells 16-30-66-7W6, 6-36-66-8W6 and 6-7-67-8W6 in Fig. 6.5a). It appears to bulge up just basinward of the point of merger. The dip on the surface here appears quite high due to the extreme vertical exaggeration, but is much less than 1°. Some of the "sharp-based shoreface" sandstones of the Kakwa Member noted by Plint (1988) are found directly above this bulge. The part of the Kakwa Member found west of where the E2 surface merges with the base of the shoreface sandstones is considered temporally equivalent to the Nosehill Allomember (strata between E1 and E2).

3) The E3 surface in the east can be traced up and into the basinward margin of the Kakwa Member (Figs. 6.4a, 6.5b). Further west, this surface is traceable as a distinct well signature throughout the Kakwa Member which corresponds to the break between the lower facies 16 dominated shoreface package and the overlying facies 17 dominated shoreface package (see cores 11-7-66-4W6, 3-26-66-7W6, 16-30-66-7W6, 6-36-66-8W6, 6-7-67-8W6 and

10-2-67-9W6 in Fig. 6.5a; other examples have been given in Chapter 5). It is an approximately horizontal surface with respect to the datum, except in the extreme west where it appears to have been displaced by fault activity. The lower part of the Kakwa east of the merger of the E2 surface is considered equivalent to the Bickerdike Allomember (strata between E2 and E3). Further evidence for these interpretations (particularly the original horizontality of the E3 surface) will be provided later in this chapter (Section 6.3.3).

4) Note how the thickness of the Musreau Member (above the Kakwa Member) decreases to the east. The thickness of this member also decreases in the extreme west. There is no evidence of "non-marine tongues" (see Fig. 1.1a) in this area, as suggested by Duke (1985) and subsequently by Plint *et al.* (1988) for the Cardium Formation further south. The E4 surface runs roughly parallel to the underlying E3 surface as it drops down basinward over the edge of the Kakwa Member. The upper, coarser-grained (typically facies 17) portion of the Kakwa Member is temporally equivalent to the Hornbeck Allomember and, when combined with the Musreau Member, these units together constitute the E3 to E4 interval.

5) The thickness of the E4 - E5 interval is greatest east of the basinward edge of the Kakwa Member (Fig. 6.4a). Further east, the thickness decreases as the E5

surface drops down. This drop is referred to as the "E5 bevel" in Figure 6.5b, and is equivalent to the bevel noted by Bergman and Walker (1986) and Walker and Eyles (1988) in an equivalent stratigraphic position at the Carrot Creek and Willesden Green fields respectively.

6) The E6 surface amalgamates with the E5 surface almost directly above the edge of the Kakwa Member. Unlike Wadsworth (1989), I was not able to trace the E6 surface further west.

7) The E6.5 surface (as defined in the eastern portions of the basin by correlation with a cross-section line provided by Jennifer Wadsworth in 1988) continues westward above the Kakwa Member, and sits above a prominent sandier-upward succession in core 6-36-66-8W6 (see section 5.3.4). This horizon appears equivalent to the "E6" horizon of Plint (1988) from just south of this area.

8) The E7 surface has a pronounced bevel in it above the Kakwa Member (wells 3-26-66-7W6 to 11-7-66-4W6 in Fig. 6.5a) where it truncates the E6.5 horizon. This is a continuation of a similar bevel ("L4") which Wadsworth (1989) was able to trace up to Twp 64. To the west of the bevel, the E7 surface truncates the E6.5 horizon and eventually merges with the erosion surface at the top of the Musreau Member.

9) A normal fault has been drawn in the extreme west of regional cross-section A-A' (Fig. 6.4a). The presence of this fault is suggested by the offsets of the top and base of the Kakwa Member, plus the E3 and underlying horizons. Although the distance between control points is fairly great in this line (due to the availability of logs in this area), tighter control on fault movement will be demonstrated in subsequent lines.

6.2.2. Central part of the study area: regional cross-section B-B'

In Figure 6.4b I present a regional cross-section through the central portion of the study area (generally Townships 69 and 70). It has been constructed in the same manner as regional cross-section A-A' (see above). A cross-section illustrating the details of the correlations in the western part of this area is presented in Figure 6.6. I did not have tight well control near the edge of the Kakwa Member (Figs. 1.5, 6.2), and so will not present a detailed cross-section of that portion of the formation.

The stratal geometries observed in this regional cross-section (Fig. 6.4b) are very similar to those observed further south in regional cross-section A-A'. Several points stand out:

1) The "bumpiness" of the lower markers (GS to E2) is subdued.

Figure 6.6. Detailed cross-section b-b'.

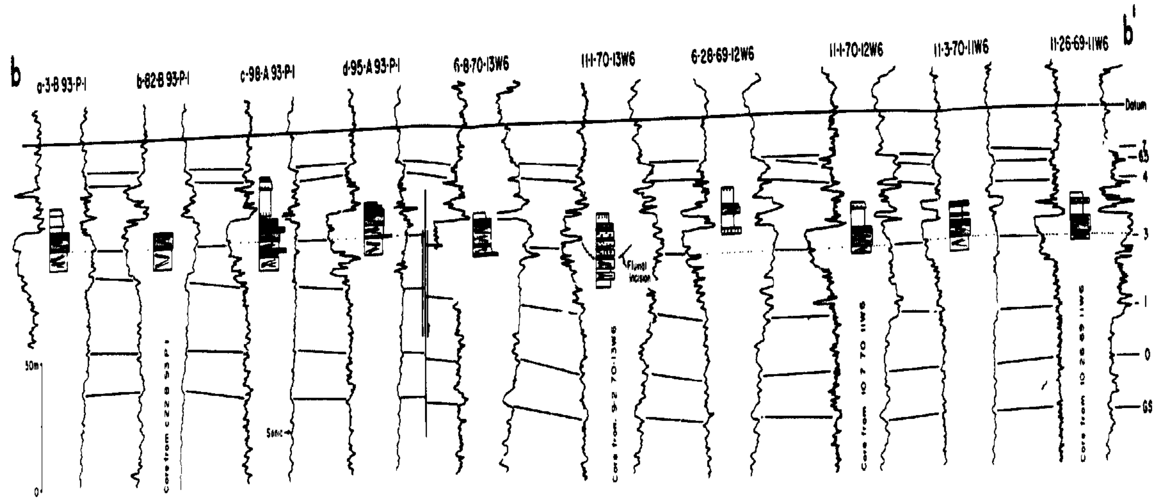
b
a-3-B 93-P-1
b-82-B 93-P-1
c-98-A 93-P-1
d-95-A 93-P-1
6-8-70-13W6
11-1-70-13W6
6-28-69-12W6
11-1-70-12W6
11-3-70-11W6
11-26-69-11W6
b'
Datum
7
6.5
4
3
1
0
GS
50m
0
Core from c-22-B 93-P-1
Sonic
Fluvial incision
Core from 9-2-70-13W6
Core from 10-7-70-11W6
Core from 10-26-69-11W6

2) Note how the E1 surface rises westward and merges with the base of the Kakwa Member in a manner similar to the E2 surface. This is shown in the detailed cross-section (Fig. 6.6). It is thus concluded that the lower part of the facies 16 dominated portion of the Kakwa Member in the far west (e.g. Murray River section - c.f. Fig. 5.5) is temporally equivalent to the upper portion of the Kaskapau Formation further east.

3) The E3 surface again appears traceable as a near-planar surface through the Kakwa Member In core, it corresponds to the break between the "lower" and "upper" shoreface sandstone packages, dominated by facies 16 and 17 respectively (Fig. 6.6). Where the E3 surface is offset, nearly equivalent offsets of the top and bottom of the Kakwa Member, and the underlying markers (GS, E0, E1) are noted (e.g. between wells d-95-A 93-P-1 and 6-8-70-13W6 in Fig. 6.6).

4) Note again how the E3 and E4 horizons drop down to the east at the Kakwa edge and then flatten out

5) The topography on the E5 bevel is subdued.

6) The horizons E6, E6.5 and E7 here behave in a manner similar to that observed in regional cross-section A-A'. A pronounced bevel on the E7 surface is lacking however.

7) There are three apparent faults in the western part of the section. Like the fault in line A-A', the

upthrown side of each is on the west. (The lateral extent of these faults will be discussed later)

6.2.3 Northern part of the study area: regional cross-section C-C'

This regional cross-section (Fig. 6.4c) represents the more northerly portions of the study area. Specific points to note include:

1) There is again (i.e. like regional cross-section A-A') an upward "bulge" in the lower markers (GS to E2) close to the eastern edge of the Kakwa Member.

2) The E1 marker rises to the west and finally merges with the base of the Kakwa Member. In the most westerly well, it appears to rest above almost 10 m of sandstone.

3) Lowstand incised shoreface units (e.g. Plint 1988) are associated with both the E3 and E4 surfaces just basinward of the Kakwa edge (Figs. 6.4c, 6.7b). The Waskahigan Member is associated with the E3 surface and the Burnstick Member is associated with the E4 surface (neither have been cored). Although these two members can be found elsewhere in the study area, this is the only location where I found them together.

4) The E5 bevel is well developed, and in places cuts down and removes *all* of the E4 - E5 interval (e.g. well 6-22-73-3W6, Fig. 6.7b).

5) The thickness of the Cardium Formation above the E5 surface is not great. The E6.5 marker is absent over

Figure 6.7. Detailed cross-sections. A)c-c'. B)c''-c'''.

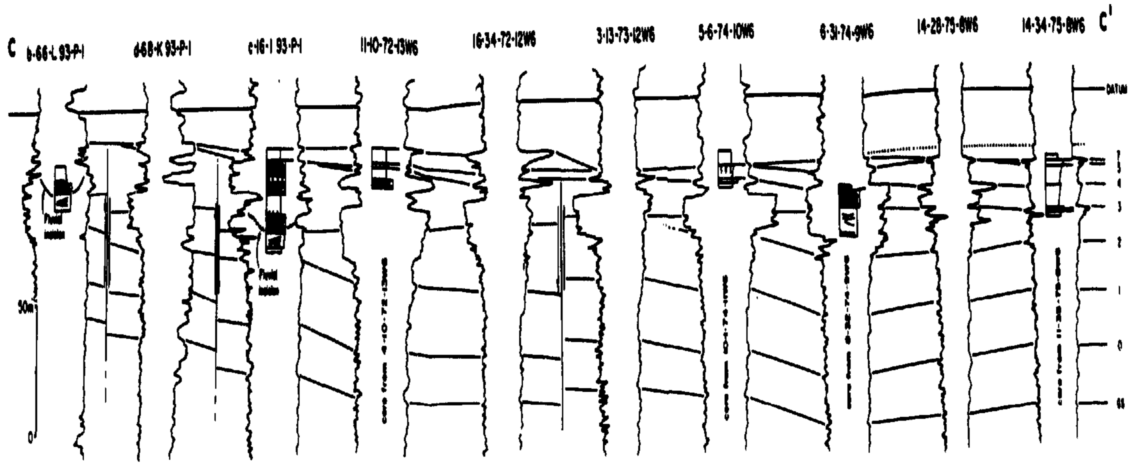

C
C'
6-31-74-9W6
14-28-75-8W6
14-34-75-8W6
DATUM
50m
0
Fluvial isolation

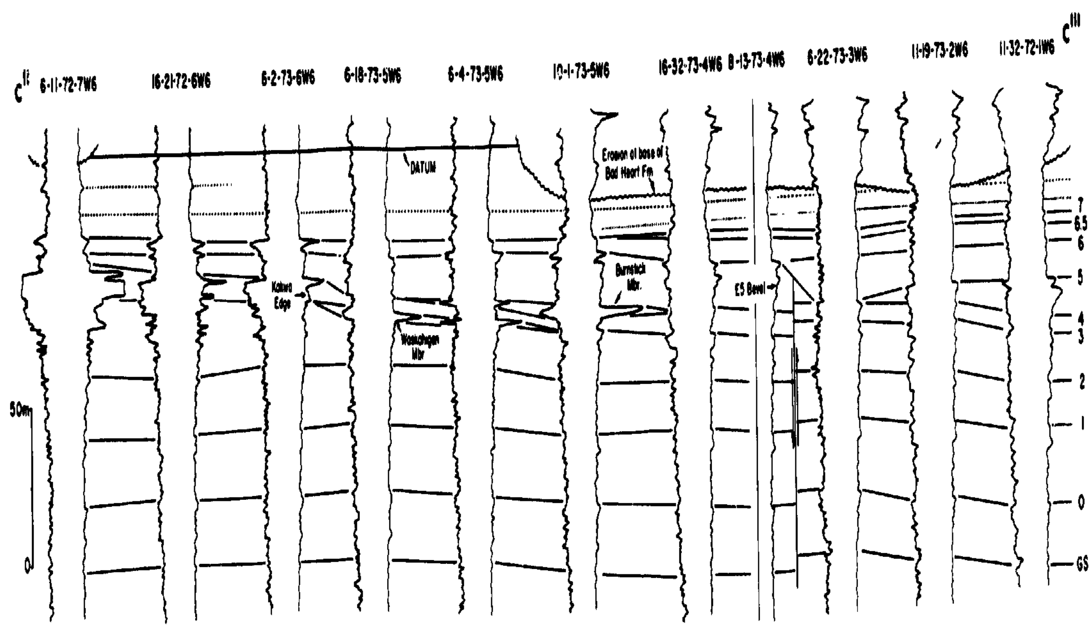

C''
C'''
6-11-72-7W6
16-21-72-6W6
6-2-73-6W6
6-18-73-5W6
6-4-73-5W6
10-1-73-5W6
16-32-73-4W6
8-13-73-4W6
6-22-73-3W6
11-19-73-2W6
11-32-72-1W6
DATUM
Erosion of base of Bad Heart Fm
Kakwa Edge
Waskahigan Mbr
Burnstick Mbr.
E5 Bevel
50m
0
7
6.5
6
5
4
3
2
1
0
GS

most of the area, being completely absent in the extreme north (Fig. 6.7a). There, the E7 surface often cuts down to the E5 surface. There is a well-developed asymmetric bevel on the E7 surface, where it cuts down and almost amalgamates with the E4 surface (well 3-13-73-12W6, Fig. 6.7a).

4) Evidence of segmentation of the Cardium Formation by fault activity is greater here than further south. In the west, two faults offset the Kakwa Member and underlying markers in the same manner as that observed further south in regional cross-sections A-A' and B-B' (i.e. the upthrown side is to the west). The two other faults indicated in the regional cross-section do not have the same geometry. They are to be found below the E7 and E5 bevels where it appears the *eastern* side has been upthrown. As in the previous cases, the fault interpretation is based on the offset of the underlying "E" surfaces (c.f. Weimer 1984, p. 15). Conceivably, the apparent fault movement could be an artifact, if the markers above the bevels all drape the bevels; by "straightening out" the Datum, the underlying markers would appear to suddenly rise up in the east. In this case however, I would expect the bevel to be buried by progressive elimination of the topography, and markers above the bevel would therefore not be nearly parallel, as observed here.

5) The M1 Datum has been removed by erosion at the base of the Bad Heart Formation in detailed cross-section c''-c''' (Fig. 6.7b). Here, the original position of the Datum has been calculated by assuming a constant distance above markers lower in the Muskiki Formation (dotted) which appear to be parallel to the M1 marker. In the next chapter, I will suggest that the occurrence of the sub-Bad Heart erosion directly above the E5 bevel is not purely coincidental.

6.2.4 Correlation of measured outcrop sections

Now that the sequence stratigraphy of the Cardium Formation has been established in the subsurface, it is possible to correlate the measured outcrop sections with greater confidence. I have chosen to proceed in this manner because it is in the subsurface that the most densely-spaced data control (well logs and core) exists, and because I believe that it is only by establishing outcrop to subsurface correlations, and then correlating between outcrop sections through the subsurface, that one can be confident of correlations of subtle surfaces or facies successions between widely-spaced outcrops.

A cross-section based on the outcrops of the Cardium Formation in the Foothills is shown in Figure 6.8 (see Fig. 5.1 for locations). Based on the results of the subsurface correlations, I have hung the sections on the E3 surface, as this seems to be a near-planar surface (except where

Figure 6.8. Correlation of measured sections from Foothills outcrops. See Figure 5.1 for locations.

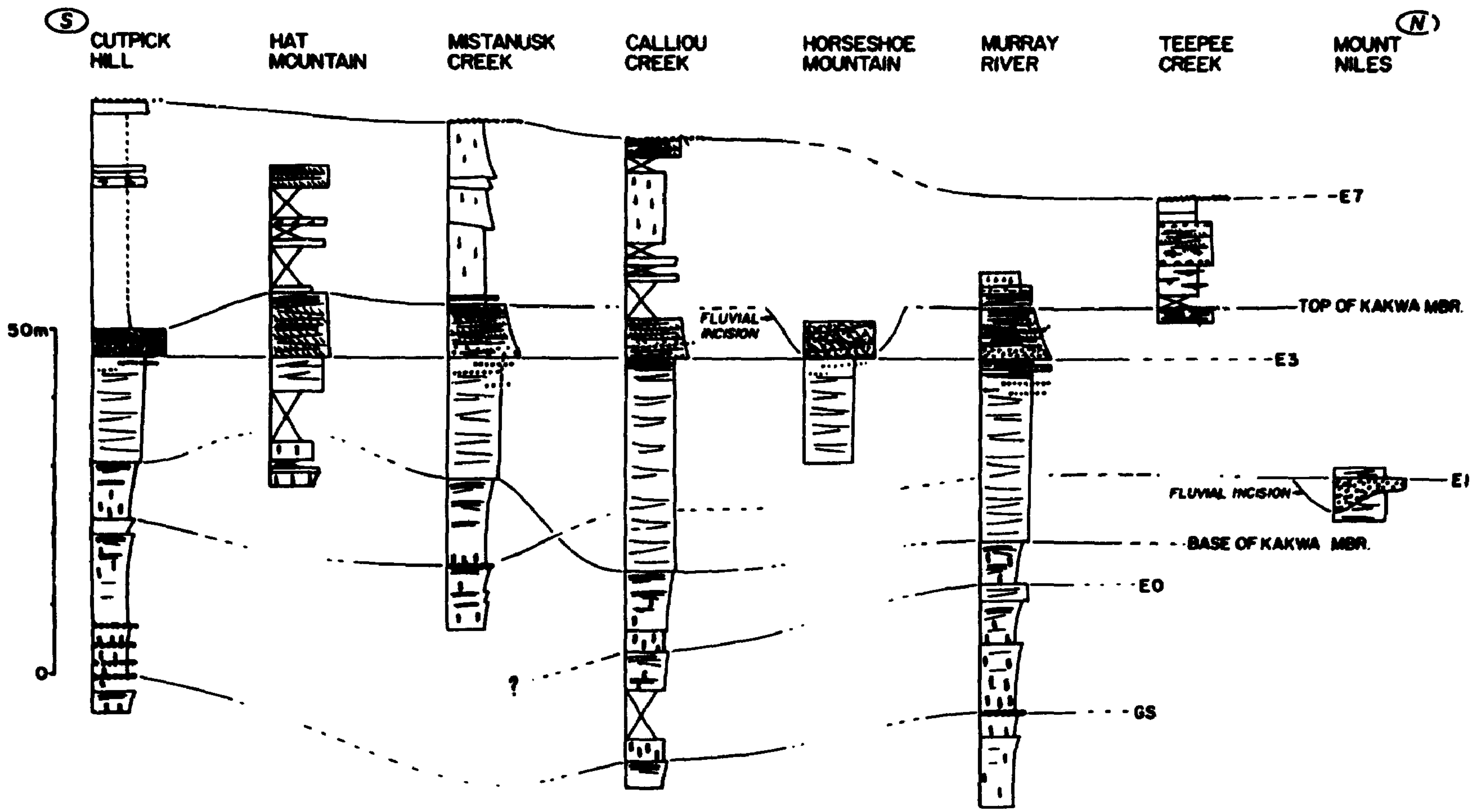

S
CUTPICK HILL
HAT MOUNTAIN
MISTANUSK CREEK
CALLIOU CREEK
HORSESHOE MOUNTAIN
MURRAY RIVER
TEEPEE CREEK
MOUNT NILES
N
50m
0
E7
TOP OF KAKWA MBR.
FLUVIAL INCISION
E3
FLUVIAL INCISION
E1
BASE OF KAKWA MBR.
E0
?
GS

offset by faults) through most of the extent of the Kakwa Member.

The GS horizon in the subsurface is so named because it was traced to a gritty siderite horizon at the Murray River section. This same horizon consists of a gritty siderite at the Cutpick Hill section, but appears to be represented by the top of a 12 m thick sandier upward succession (without siderite) at the Calliou Creek section (note that all of the measured section at Calliou Creek is not shown, the base of the section was located 29 m below the GS horizon). The E0 surface sits above 2.5 m of facies 16 sandstones at the Murray River section, and at the top of a 3.5 m thick sandier upward succession (overlain by 3 m of facies 4 and 5) at the Calliou Creek section. I was not able to trace this surface to the Cutpick Hill section.

As noted in the previous chapter, the E1 surface is represented by the top of a prominent sandier upward succession at Cutpick Hill, and by a burrowed sideritic horizon at Mistanusk Creek. In the Calliou Creek and Murray River sections, the E1 surface is located somewhere in the lower (facies 16) part of the Kakwa Member. This raises a problem concerning the definition of stratigraphic units as the E1 surface defines, according to the Plint *et al.* (1986, 1987, 1988) sequence stratigraphy, the base of the Cardium Formation. Thus in the extreme west, the lower portion of the "Kakwa Member" actually belongs to the Kaskapau

Formation. This problem was not encountered by Plint *et al.* (1988) in their outcrop to subsurface correlation, since the E1 surface appears to be found below the Kakwa Member sandstones in all outcrops shown by them. To avoid confusion (since the E1 surface does not appear to have any obvious outcrop expression in the facies 16 sandstones), I make reference to Article 58 of the North American Commission on Stratigraphic Nomenclature (1983) which states that an allostratigraphic unit "may be contiguous with a formally defined lithostratigraphic unit; a vertical cut-off between such units is placed where the units meet." Hence, I suggest that north of Grand Cache, the base of the Cardium Formation *in outcrop* should be defined as the base of the thick swaley cross-stratified sandstones of the Kakwa Member. At Mount Niles, the upper surface of the conglomerate body is covered by coarse-grained wave ripples, and is overlain by at least 3 m of facies 16 sandstones. The upper surface of the conglomerate may represent a transgression surface (see Chapter 4), probably equivalent to the E1 surface.

The E3 surface sits above parallel-laminated sandstones interpreted as beach deposits at the Calliou Creek and Murray River sections. In all sections, this horizon is characterized by a distinct grain-size break. At Horseshoe Mountain, the "upper" shoreface portion of the Kakwa Member has been replaced by conglomeratic fluvial deposits (Chapter

4). This is the only measured section where fluvially-deposited strata are exposed, although such units are sometimes found in the subsurface (Chapter 5). Unlike those other units, the Horseshoe Mountain section does not have associated shales or siltstones, thus making it more resistant to Pleistocene and post-Pleistocene erosion. Otherwise, the top of the Kakwa Member consists of beach-laminated sandstones or conglomerates (where exposed).

Oyster-bearing strata are found at the base of the Musreau Member (immediately overlying the Kakwa Member) at the Cutpick Hill, Hat Mountain, and Murray River sections. A thin (40 cm) coal directly overlies the Kakwa Member at Mistanusk Creek. The rest of the Musreau Member is typically fine-grained and poorly exposed. Rooted horizons are common in the middle to upper portions of this member. The E7 surface is represented by a thin conglomerate or "pebble veneer" (1 clast thick) wherever exposed, although it should be noted that the thickness of conglomerate is variable and Duke (1985) did not observe pebbles at this horizon at his Cutpick Hill section. It appears to drop down by about 8 m between the Calliou Creek and the Tepee Creek sections (Fig. 6.8). This is probably because the line of cross-section intersects at least one of the faults noted in the regional cross-sections. Were the outcrop cross-section to be hung on the M1 marker (not observable everywhere), then approximately 8 m of offset would have been noted on the E3 surface.

The W-E outcrop cross-section (Fig. 6.9) generally consists of partial sections through the Kakwa Member exposed along the "Cardium Escarpment". The most easterly outcrop (the Smoky River section) exposes the Raven River Allomember and higher portions of the Cardium Formation. Like the N-S outcrop cross-section, the section is hung on the E3 surface. Although the base and top of the Kakwa are not always exposed, it is apparent that neither are horizontal. The resultant thickness differences of the Kakwa Member are comparable with those noted in the subsurface (e.g. Figs. 6.4a-c).

Beach-laminated sandstones are found at the top of the lower shoreface package at Feller's Heights, Pouce Coupé (not shown in the figure, but visible at the south end of the quarry), Gundy Station and Cutbank Lake. Equivalent strata are interpreted to have been erosionally removed from the Noetai Hill, Bear Mountain and Bay Tree sections. Overlying the E3 surface at Bear Mountain, Pouce Coupé and Cutbank Lake are strata containing coarse-grained wave ripples. Other types of strata locally present at this level, in these sections and the Bay Tree section, are (pebbly) cross-bedded sandstones and undulose-laminated sandstones with laminae of carbonaceous ("coffee grounds") matter. A thin discontinuous siltstone caps this interval at the Bear Mountain section, while a shaley, sideritic

Figure 6.9. Correlation of measured sections from "Cardium Escarpment". See Figure 5.1 for locations.

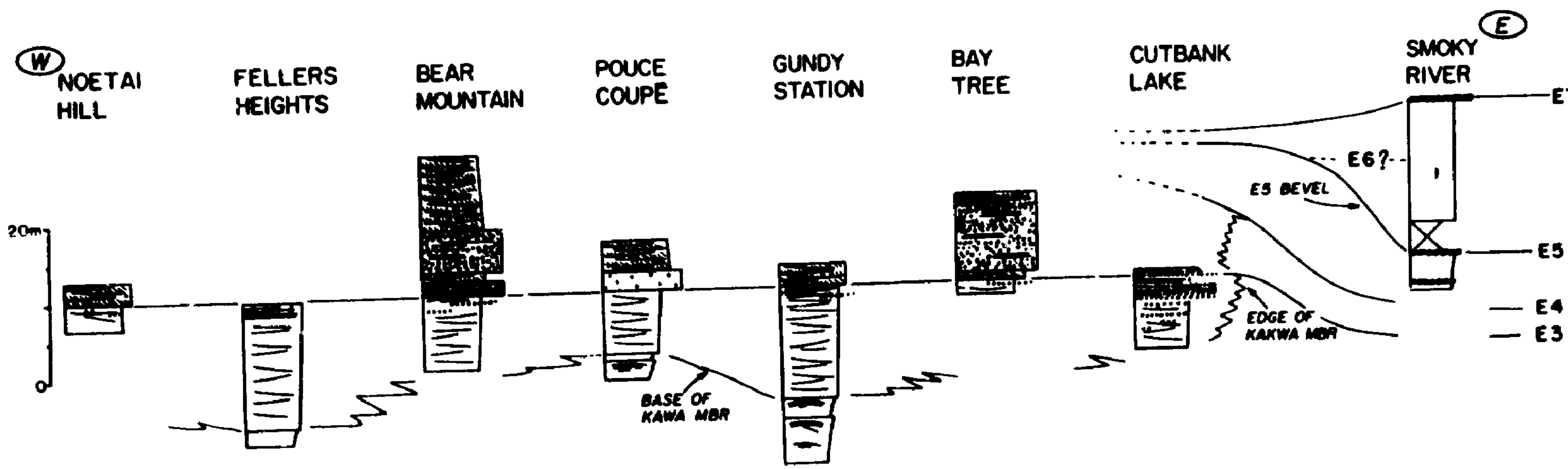

W
NOETAI HILL
FELLERS HEIGHTS
BEAR MOUNTAIN
POUCE COUPE
GUNDY STATION
BAY TREE
CUTBANK LAKE
SMOKY RIVER
E
20m
0
E7
E6?
E5 BEVEL
E5
E4
E3
EDGE OF KAKWA MBR
BASE OF KAWA MBR

interval with shell fragments overlies the pebbly sandstones at the Pouce Coupé section.

Subsurface correlations suggest that the Bay Tree and Cutbank Lake sections are both located quite close to the basinward margin of the Kakwa Member. As noted in Chapter 1, this is in agreement with the previous interpretations of Jones (1966). To the east, the Cardium Formation is not exposed again until the Smoky River section, which subsurface correlations suggest is located east (i.e. basinward) of the E5 bevel.

6.2.5 Summary of cross-sections

In this section, I have demonstrated that the event stratigraphic framework proposed for the Cardium Formation by Plint *et al.* (1986, 1987, 1988) *can*, with certain modifications, be applied in the present study area. What remains unclear, is whether the proposed modifications need to be applied to the formation as a whole, or are simply local phenomena.

Perhaps the most important alteration to the existing stratigraphy involves the recognition that the E3 surface was an originally near-horizontal surface which essentially bisects the Kakwa Member into a lower half dominated by facies 16 sandstones and an upper half dominated by facies 17 sandstones. This interpretation changes the correlations between the various parts of the Kakwa Member and the associated offshore units. As such, the lower part of the member west of where the E2 and E3 surfaces amalgamate is temporally equivalent to the Nosehill Allomember, whereas to the east of this point, the lower part of the Kakwa is correlative the Bickerdike Allomember. The upper part of the Kakwa Member is everywhere temporally equivalent to the Hornbeck Allomember.

The recognition of the E3 surface as being an originally horizontal surface has helped identify the effects of fault activity in the Cardium Formation. Fault activity appears to have been most pronounced in the western and northern parts of the study area. In at least two places, there appears to exist a relationship between the existence of a fault and the occurrence of a "bevel" in an overlying erosion surface. Other syn-Cardium vertical tectonic movements have produced a certain "bumpiness" in some of the horizons, and the origin of these will be discussed in the next chapter.

The E1 surface merges with the Kakwa Member in the extreme western portion of the study area, and eventually sits above a considerable thickness (probably at least 10 m) of facies 16 sandstones. As this occurs very close to the western outcrop belt, I suggest (following the recommendations of the NACSN) that north of Grand Cache, the base of the Cardium Formation in outcrop be defined as the base of the facies 16 sandstones, but that the E1 surface be retained as the base of the formation in the subsurface.

The subsurface and outcrop expressions of the "E0" and "GS" horizons suggests that they too could be the basinward equivalents of transgressions associated with fourth-order cyclicity. Stott (1967) has previously proposed that the GS surface (the contact between the Opabin and Haven members of the Kaskapau Formation in his cross-sections) is correlative with (or would rest on ?) the Wartenbe Sandstone, although I cannot confirm his correlations.

There are problems with the correlation of the E6 and E6.5 surfaces. Although in the eastern part of the study area my picks appear compatible with those of Wadsworth (1989) and Walker and Eyles (1988), in the west (i.e. above the Kakwa Member), I can no longer trace the E6 surface, and my E6.5 surface is correlative with the E6 surface as defined by Plint (1988) just south of the present study area. Wadsworth (1989) traced *both* the E6 and E6.5 horizons above the Kakwa Member as far north as Township 64. It should be noted that her core control was not abundant in that part of her study area, and that the core control available here not consistent with the presence of both of these surfaces in this area.

Finally, I was unable to observe non-marine "tongues", or portions of the Musreau Member which are intercalated with the "upper" allomembers of the Cardium Formation. This geometry was suggested by Duke (1985) and Plint *et al.* (1988, based on Duke's work), although these relationships were not observed in the subsurface by the latter authors. The recognition of the extent of the hiatus at the E5 surface (Chapter 1) is here considered as being incompatible with the non-marine tongue interpretation.

6.3 Sequential Description of the Depositional History of the Cardium Formation

In this section, I wish to describe the succession of events which led to the production of the observed stratal geometry in the Cardium Formation. Inasmuch as it is possible, I will limit myself to a purely descriptive account, describing the sequence of transgressions and regressions suggested by the rocks, and leaving the discussion of the ultimate controls on these T/R cycles (e.g. eustasy, tectonism, sediment supply) for the next chapter. For each erosion surface, I will present a surface diagram and isopach map (thickness of strata between it and the M1 Datum), and recall its outcrop or core expression (if observed). The intervals between erosion surfaces will be shown as isopach maps (thickness of preserved strata between successive horizons), and the observed facies successions (core and outcrop) will be recalled. As noted previously, the isopach maps and surface diagrams were produced using data files generated by the author (see Appendix 2), which were subsequently input into the *Surfer 4.0* software package.

I estimate that my picks are accurate to about ± 1 m (in the event of greater uncertainty, I did not record my pick), giving a possible spread of 2 m. As the isopach data involve two horizons, each with a possible spread of 2 m, I have chosen a 4 m contour interval for the isopach maps. In this way, I can be fairly certain that I am not trying to resolve topography which is beyond the resolution of my data (although some uncertainty remains for values which are close to the isopleth values). The figures have been reproduced several times, each time looking for features which might signal the presence of errors in the data ("bullseyes", ridges which follow township boundaries, etc.). Some small errors have undoubtably escaped detection, but they should not affect the gross trends I will be describing below.

6.3.1 Upper Kaskapau Formation

The GS to E1 interval comprises strata attributed to the upper part of the Kaskapau Formation (Opabin Member) by Stott (1967). As noted both in Chapter 3 and earlier in this chapter, these heterolithic strata tend to consist of a hierarchial arrangement of sandier upward successions, with units a few meters thick superimposed on larger (over 10 m thick) sandier upward successions. From a purely descriptive perspective, the thicker sandier upward successions can be classified as fourth order cycles (being superimposed on the third order cyclicity represented by the progradation of the Cardium Formation), whereas the smaller successions represent fifth order cyclicity.

Surface diagrams and isopachs of the Datum to GS, Datum to E0 and Datum to E1 surfaces are presented in Figures 6.10, 6.11, and 6.12 respectively. In those figures, it can be seen that all surfaces "rise" (with respect to the Datum) to the NW. A further, but more abrupt, rise in all surfaces can be seen in the extreme west. This rise coincides with the faults observed in this area in Section 6.2, and I suggest that the coherence of this trend lends further support to the interpretation of fault activity proposed in that section.

There is also a suggestion of a slight NW-SE trend, indicated by deflections of the isopleths in this direction. These irregularities are the three-dimensional expression of the "bumpiness" of the markers noted in the regional cross-sections (Section 6.2).

These surfaces probably represent the basinward expression of transgressions associated with fourth order cyclicity. The E1 surface has been shown to sit above a considerable thickness of shoreface sandstone and finally to amalgamate with the Kakwa Member in the extreme western part of the study area, whereas the E0 surface sits above a thin "tongue" of shoreface sandstone at the Murray River section, and there is a possibility that the GS surface is correlative with the transgression following progradation

Figure 6.10. Surface (mesh) diagram and isopach map of GS horizon to Datum interval. Blanked areas in upper and lower left, and upper right (title block of isopach map) have no data control. Scale in kilometers, isopleths in meters. Viewing angle for surface diagram illustrated by small diagram to lower left of that image (North towards top of page). Map area corresponds approximately to area shown in Figure 6.2.

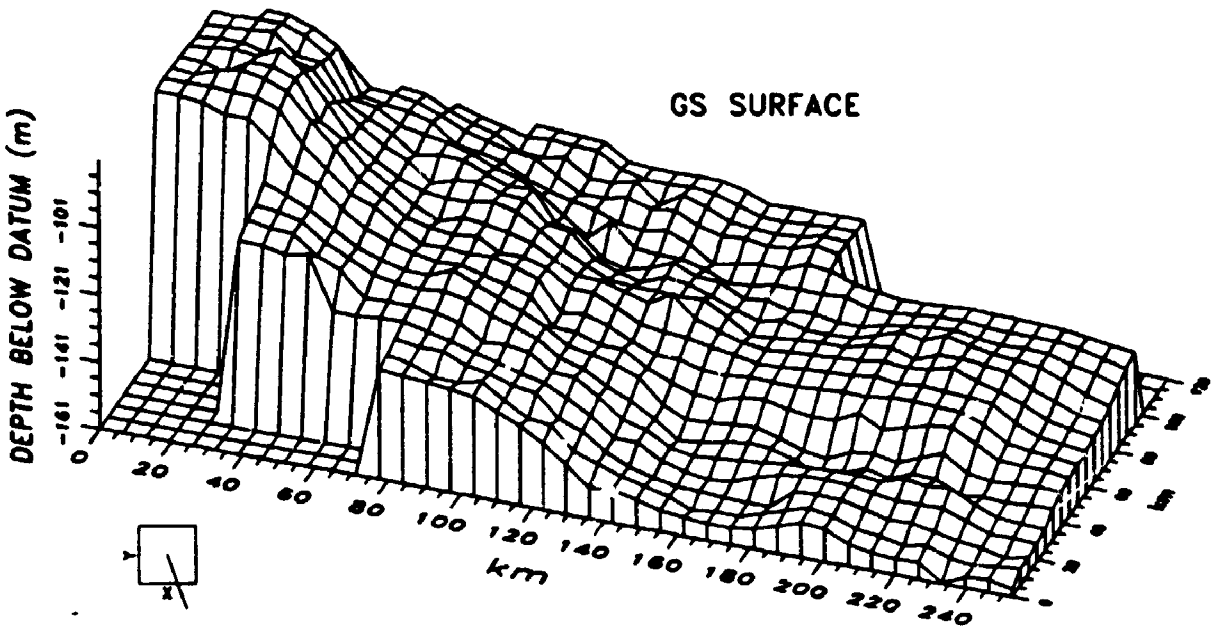
GS SURFACE
DEPTH BELOW DATUM (m)
-161 -141 -121 -101
0 20 40 60 80 100 120 140 160 180 200 220 240
km

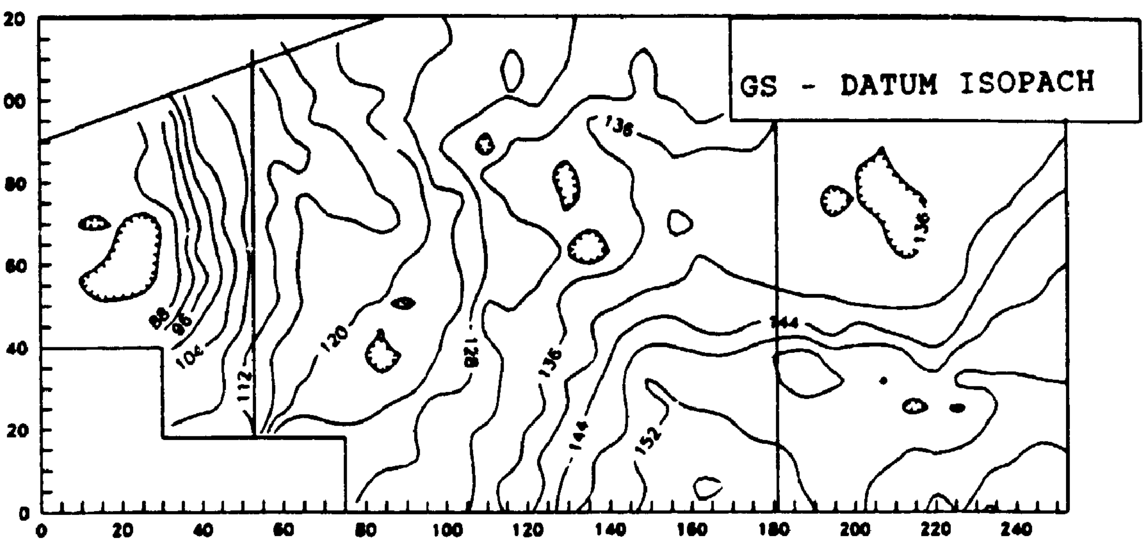
GS - DATUM ISOPACH
88
96
104
112
120
128
136
144
152
0 20 40 60 80 100 120 140 160 180 200 220 240
0 20 40 60 80 100 120

Figure 6.11. Surface diagram and isopach map of E0 to Datum interval. See Figure 6.10 for explanation.

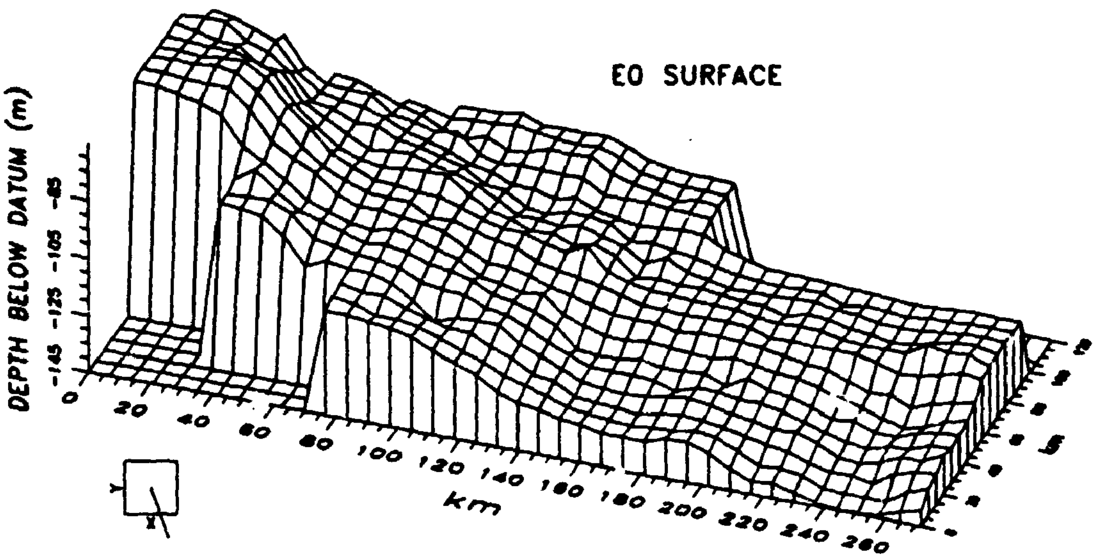
E0 SURFACE
DEPTH BELOW DATUM (m)
-145 -125 -105 -85
0 20 40 60 80 100 120 140 160 180 200 220 240 260
km
Y
X

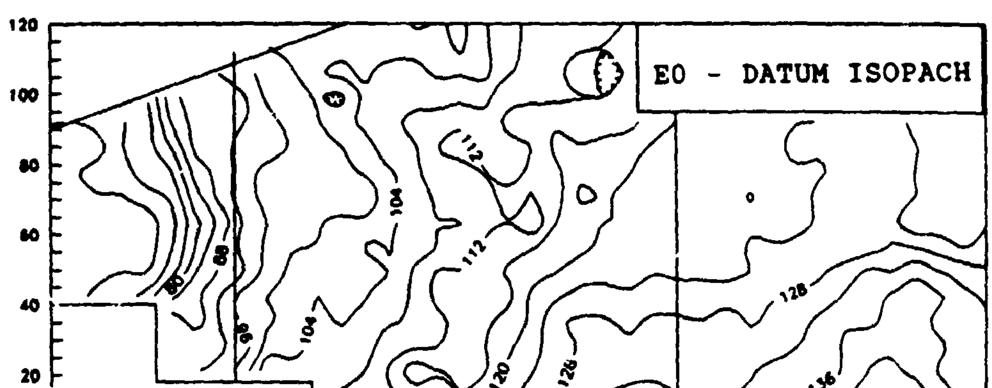
E0 - DATUM ISOPACH
88
96
104
112
120
128
136
0 20 40 60 80 100 120 140 160 180 200 220 240 260
0 20 40 60 80 100 120

5

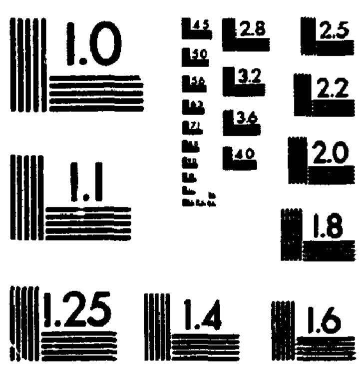

MICROCOPY RESOLUTION TEST CHART
NATIONAL BUREAU OF STANDARDS
STANDARD REFERENCE MATERIAL 1010a
(ANSI and ISO TEST CHART No. 2)

Figure 6.12. Surface diagram and isopach map of E1 to Datum interval. See Figure 6.10 for explanation.

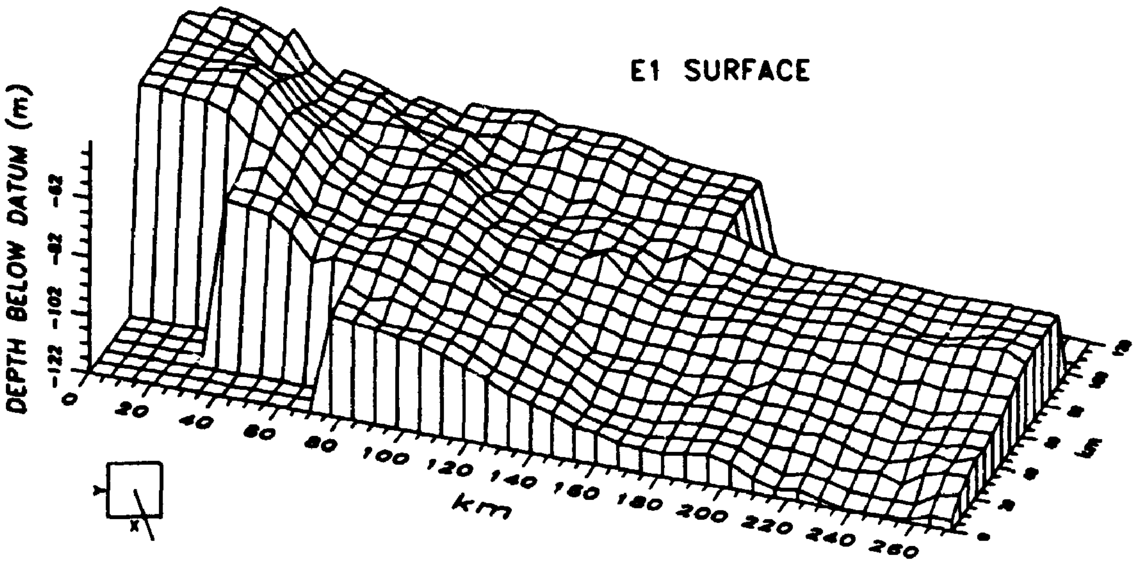
E1 SURFACE
DEPTH BELOW DATUM (m)
-122 -102 -82 -62
0 20 40 60 80 100 120 140 160 180 200 220 240 260
km
km
Y
X

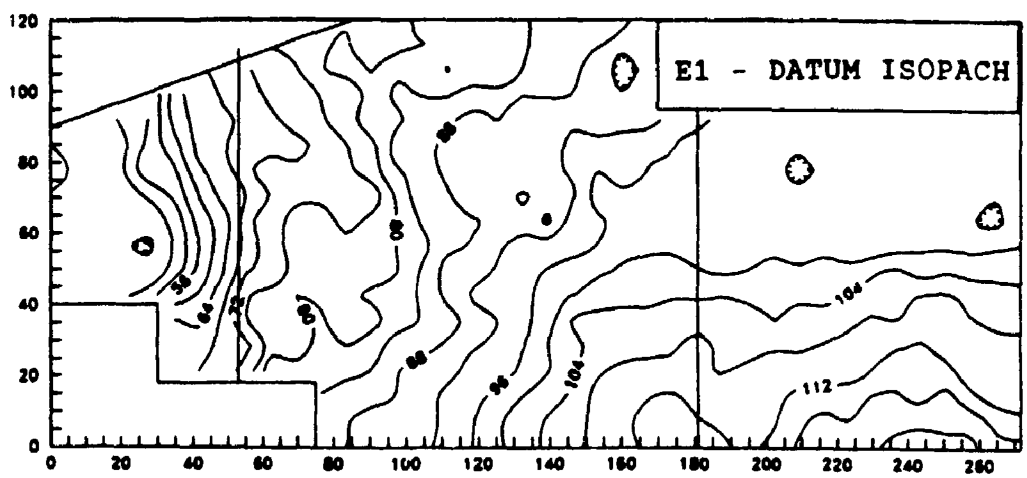
E1 - DATUM ISOPACH
120
100
80
60
40
20
0
0 20 40 60 80 100 120 140 160 180 200 220 240 260
56
64
72
80
88
96
104
112

and deposition of the Wartenbe Sandstone (Stott 1967).

6.3.2 The E1 to E2 interval

This interval consists of the Nosehill allomember and the correlative portions of the Kakwa Member. It therefore consists of facies 16 sandstones (locally capped by beach-laminated sandstones assigned to facies 17: e.g. Murray River section) and heterolithic strata assigned to the offshore facies association. Locally, pebble stringers can be found in the upper part of the shoreface sandstones (e.g. Mistanusk Creek, Murray River, Cutpick Hill).

An isopach of this interval is presented in Figure 6.13. There, it can be seen that the isopleths generally trend in a NW-SE direction, interpreted to represent the paleoshoreline orientation. In the isopach map, it can be seen that the interval forms a "sedimentary prism" with the axis of the thickest portion (contained between the 24 m isopleths) maintaining the overall NW-SE trend. The E1 to E2 interval is interpreted to represent a period of shoreline progradation (fourth order cycle), during which a sandy shoreline prograded to the NE.

The isopach map of the E2 to Datum interval, and surface diagram of the E2 horizon are indicated in Figure 6.14. It should be remembered that the E2 surface appears to amalgamate with the E3 surface in the Kakwa Member, thus it is probable that some erosion of the upper portion (in the west) of the E1 to E2 interval actually took place during

Figure 6.13. Isopach map (in meters) of E1 to E2 interval.

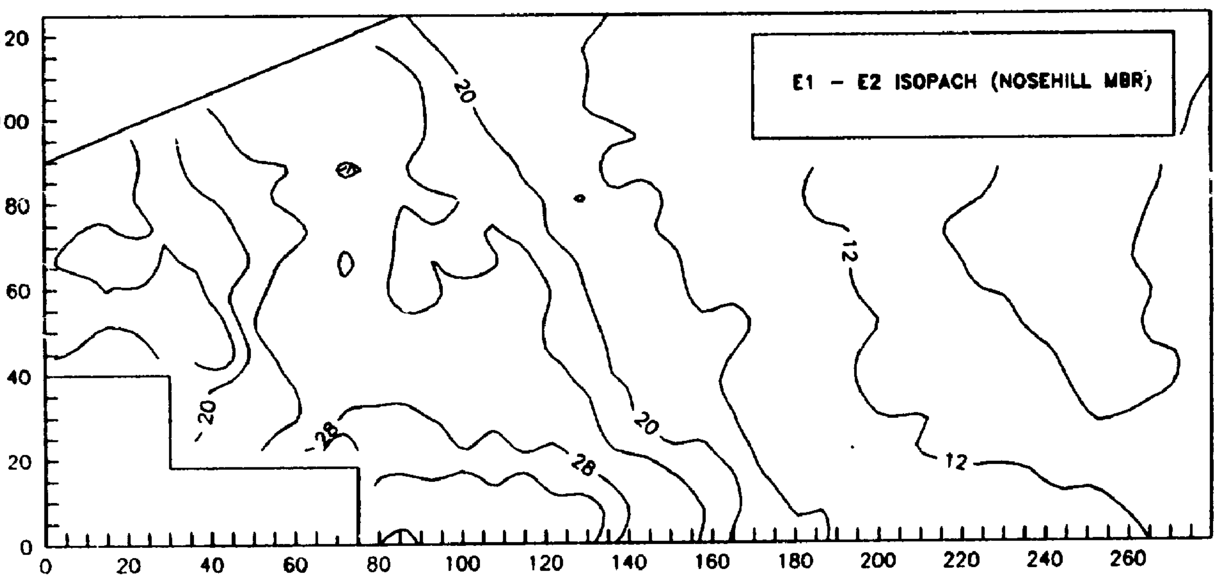
E1 - E2 ISOPACH (NOSEHILL MBR)
120
100
80
60
40
20
0
0
20
40
60
80
100
120
140
160
180
200
220
240
260
20
20
20
28
28
12
12

Figure 6.14. Surface diagram and isopach map of E2 to Datum interval. See Figure 6.10 for explanation.

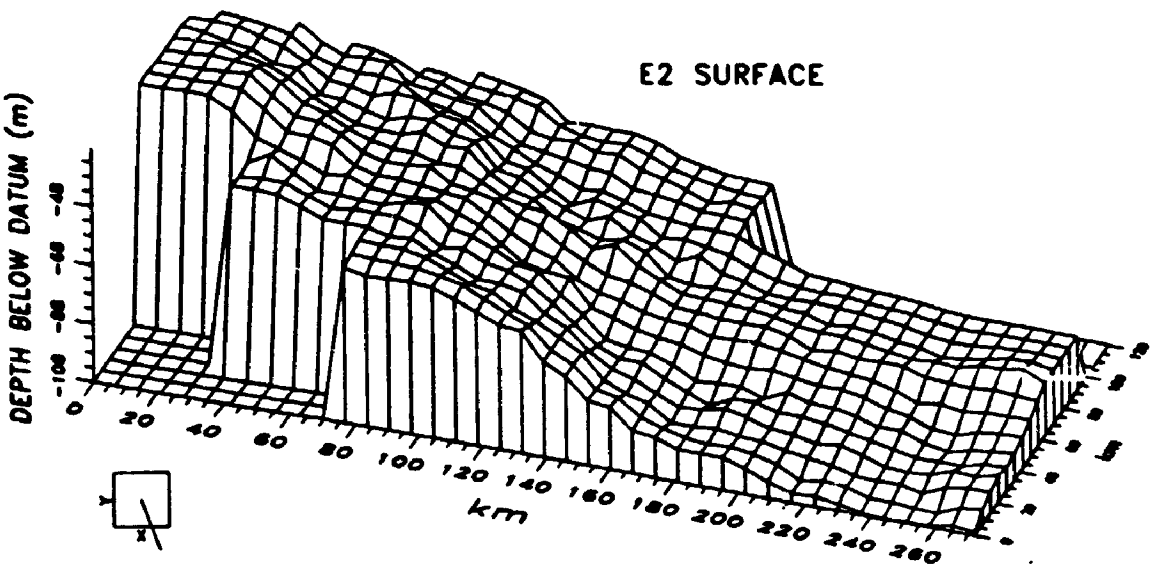
E2 SURFACE
DEPTH BELOW DATUM (m)
-100
-80
-60
-40
0
20
40
60
80
100
120
140
160
180
200
220
240
260
km

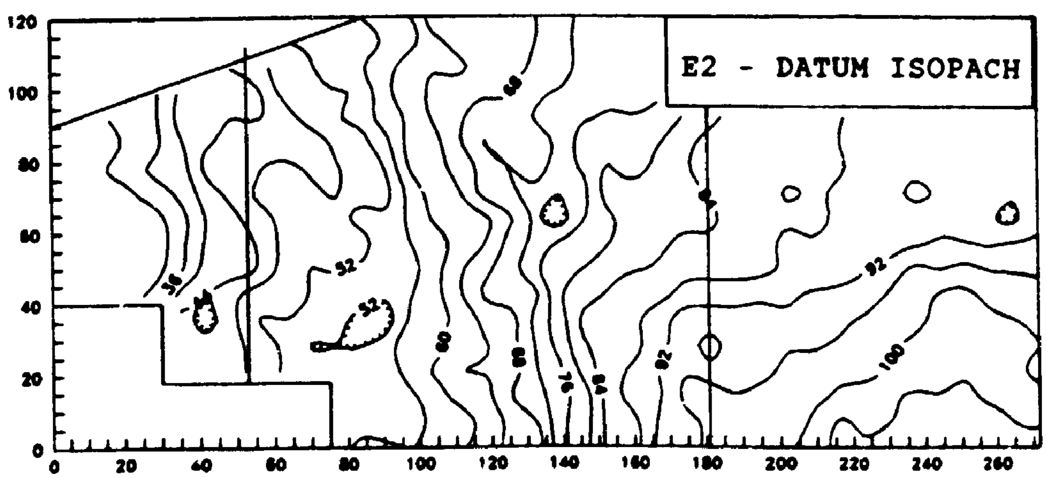
E2 - DATUM ISOPACH
120
100
80
60
40
20
0
0
20
40
60
80
100
120
140
160
180
200
220
240
260
36
52
52
60
68
68
76
84
92
92
100

the E3 transgression. The E2 surface was observed only in core, and only in the south-central portion of the study area (about Twp 66, R7W6). There (see Fig. 6.5a), it corresponds to the top of a thin facies 16 sandstone below the main part of the Kakwa Member (e.g. 6-36-66-8W6), or a layer of sideritized intraclasts (e.g. 16-30-66-7W6). The E2 surface is interpreted to have been produced during transgression following deposition of the E1 to E2 interval. A SE-NW thickness trend of the E2 to Datum interval, similar to trends associated with the GS, E0 and E1 surfaces, is apparent (Fig. 6.14), as are the faulted block in the west and subtle deflections of the isopleths representing the "bumpiness" of the surface.

6.3.3 The E2 to E3 interval

This interval consists of the Bickerdike Allomember, the correlative portions of the Kakwa Member, and minor occurrences of the Waskahigan Allomember. These strata comprise facies 16 sandstones (locally capped by beach-laminated sandstones of facies 17) and heterolithic strata of the offshore facies association. Pebble stringers and thin conglomerates can locally be found in the upper portions of the shoreface package (e.g. Cutbank Lake, Gundy Station, Bay Tree sections).

The isopach map of this interval (Fig. 6.15) shows a strong NW-SE orientation of isopleths, again interpreted as representing the paleoshoreline orientation. This is

Figure 6.15. Isopach map (in meters) of E2 to E3 interval.

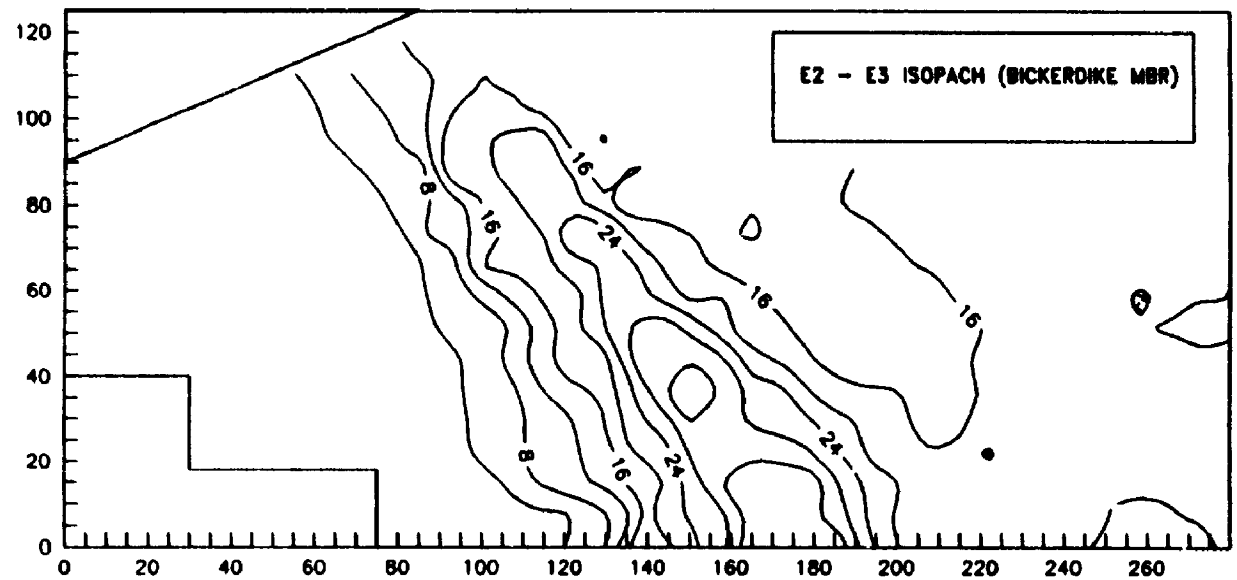
E2 - E3 ISOPACH (BICKERDIKE MBR)
8
16
24
0
20
40
60
80
100
120
140
160
180
200
220
240
260

consistent with the strike of beach-laminated sandstones observed just below the E3 surface at the Pouce Coupé section (136°-316°) and the Gundy Station section (127°-307°). The isopleths define a distinct sedimentary prism, with the western limb reflecting the rising of the E2 surface to the west, and an abrupt thinning of the interval in the east produced as the E3 surface "drops down" at the basinward edge of the Kakwa Member (c.f. Figs. 6.4a-c). East of that point, the E2 and E3 surfaces are almost parallel. The absolute value of the thickest portion of the wedge increases to the southeast, suggesting that greater accommodation was occurring there.

Some readers may contend that the data I have presented so far does not allow me to postulate that the E3 surface can be traced throughout the Kakwa Member as an essentially planar surface. Here I will address their concerns.

It will be recalled from Chapter 5 that wherever the entire thickness of the Kakwa Member can be measured in the present study area, it can be divided into a lower portion dominated by facies 16 sandstones and an upper portion dominated by facies 17 sandstones. The contact between the two is generally sharp, and may show signs of pre-lithification of the upper surface of the facies 16 sandstones (e.g. overhanging walls on erosional scours; e.g. Figs. 5.2c-e, 5.7f, 5.14). In places, beach-laminated sandstones (and more rarely, rooted horizons) underlie the contact. At the end of the last chapter, I was able to discount the hypothesis that this surface represents a grain-size break developed on a barred shoreface. I then suggested (Fig. 5.23) that the observed break could represent either one continuous surface, or be the manifestation of a series of shingled shoreface sandstone lobes.

In the subsurface, it is possible to directly test the second hypothesis. This is because the probability of "finding" the break between two shoreface units at any given distance below the datum is a direct function of the proportion of the surface situated at that level. For example, if only 5 % of the contact is found between 20 and 22 m below the datum, the odds against consistently finding the contact 21 m below the datum are rather large. Another factor involves the spacing between shingles, and the spacing between control points (core, outcrop, well logs) on the cross-sections. If the spacing between control points is similar to the spacing between shingles (or some harmonic thereof in the case of regularly spaced shingles), then it is more likely that a contact could be found at the same level in all cases.

The testing procedure involves systematically varying the lateral distance between control points, as shown in Figure 6.16. The hypothetical shingled unit shown here is the same as that illustrated in Figure 5.23. In that

Figure 6.16. Conceptual diagram illustrating testing procedure for detecting shingled shoreface sandstone bodies. See text for further description.

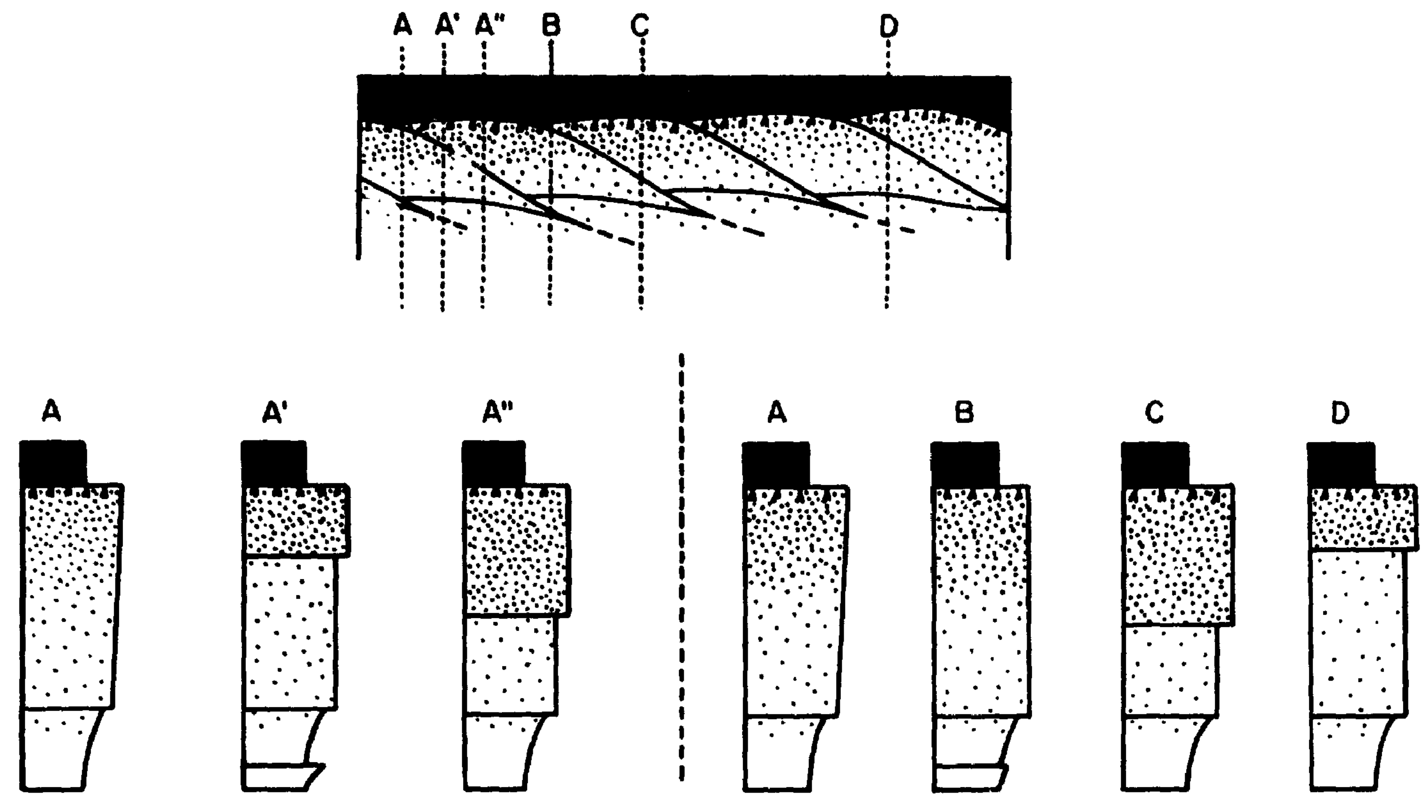
A
A'
A"
B
C
D
A
A'
A"
A
B
C
D

previous figure, the control points were fortuitously spaced so as to give the impression that one continuous surface separated two stacked shoreface packages. Here, I wish to show the effects of changing the spacing between control points. By employing very tightly spaced sections (e.g. A,A',A", Fig.6.16), such that the spacing between control points is much less than the distance between shingles, it should be possible to trace out the contact between successive shingles as it descends down. By using a more irregularly-spaced series of control points, with the lateral distance between points being much greater than the spacing between shingles (e.g. A,B,C), the laws of probability suggest that the contacts intercepted will not always appear to form one continuous planar surface. Thus, it must be concluded that the shingles *could* be detected by specifically testing for them - provided the data control is adequate (an unlikely situation if only outcrop sections are available).

In section 6.2, I presented cross-sections which demonstrate that, using irregularly- and somewhat widely-spaced control points (employing both core and well logs), the E3 surface (based on both core and well control) is essentially horizontal throughout most of the Kakwa Member's extent in the present study area. Offsets on this surface are noted only in specific areas, and these offsets are always associated with similar displacements of the top and base of the member, and the underlying erosion surfaces. On this basis, these offsets were interpreted as being due to fault movements.

In Figure 6.17, I present a cross-section using the most tightly-spaced well control available. The distance between wells is .8 km (.5 miles). In all wells shown, the contact between the upper and lower shoreface packages is clearly seen in the log responses, although no core control is available (note that these are "expanded scale" wells, and so the deflections of the Gamma Ray and Resistivity logs appear subdued). It can be seen that at this scale, the E3 surface is again traceable as a planar surface with respect to the Datum. It must therefore be concluded that the E3 surface is indeed a continuous, originally horizontal surface. I will note here that this interpretation is entirely consistent with the differences in diagenetic history noted between the upper and lower shoreface sandstone packages (Chapter 3).

The surface diagram and isopach map of the E3 to Datum interval (Fig. 6.18) illustrate the following points: a) as with the surfaces below it, the thickness between this horizon and the Datum increases to the southeast; b) the abrupt NW-SE trending break in slope on the surface represents the edge of the Kakwa Member, and the Waskahigan Member (if it were shown) rests on the steeply-dipping portion of the surface just basinward of the break (e.g.

Figure 6.17. Tightly-spaced cross-section illustrating horizontality of break (E3) between lower and upper portions of the Kakwa Member.

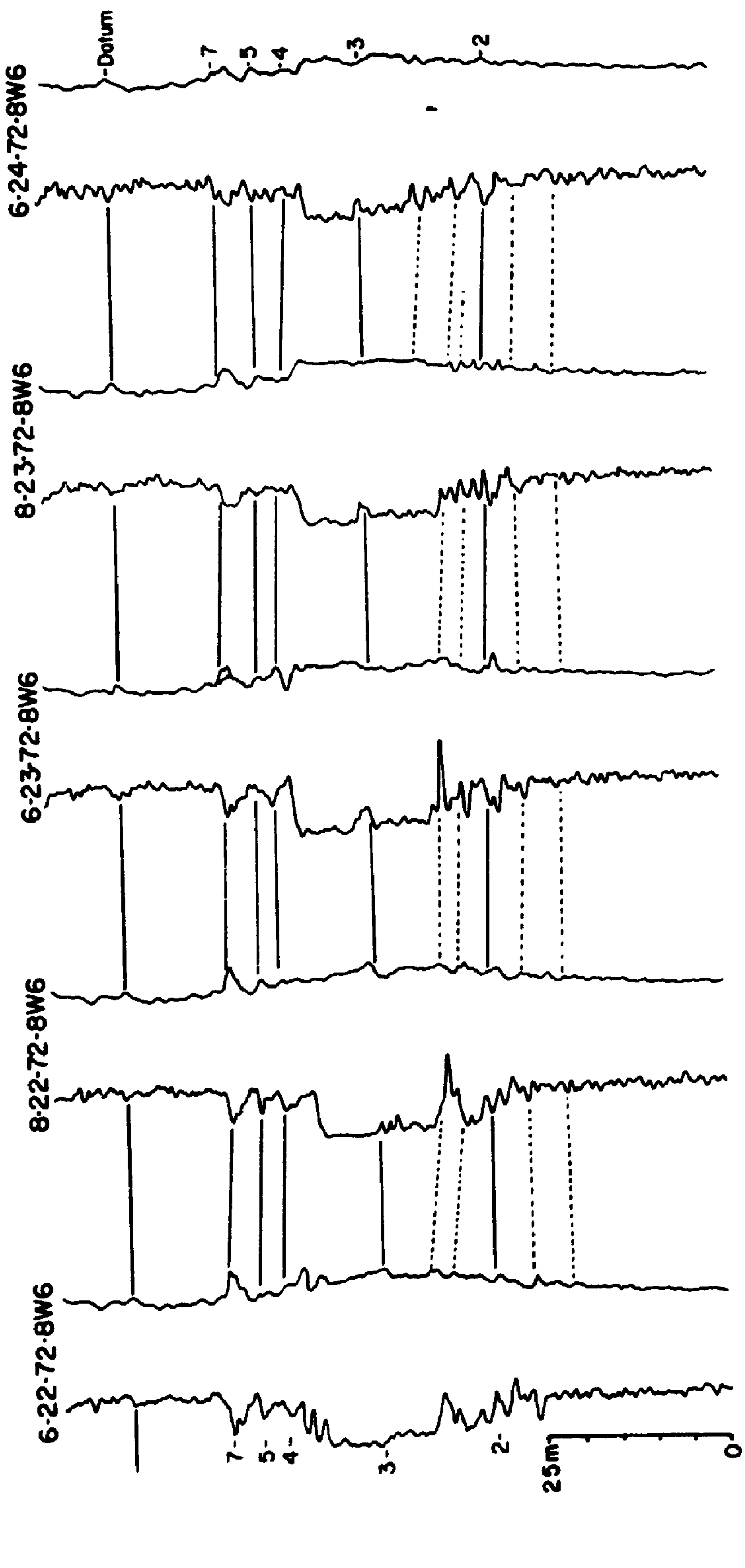
6·24·72·8W6
Datum
7
5
4
3
2
8·23·72·8W6
6·23·72·8W6
8·22·72·8W6
6·22·72·8W6
25m
0

Figure 6.18. Surface diagram and isopach map of E3 to Datum interval. See Figure 6.10 for explanation.

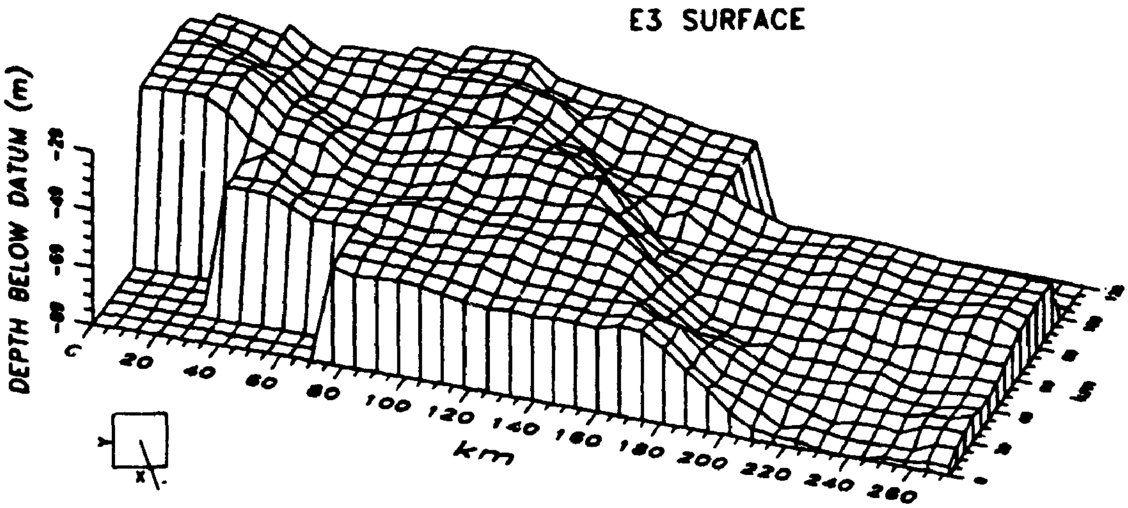
E3 SURFACE
DEPTH BELOW DATUM (m)
km
0 20 40 60 80 100 120 140 160 180 200 220 240 260

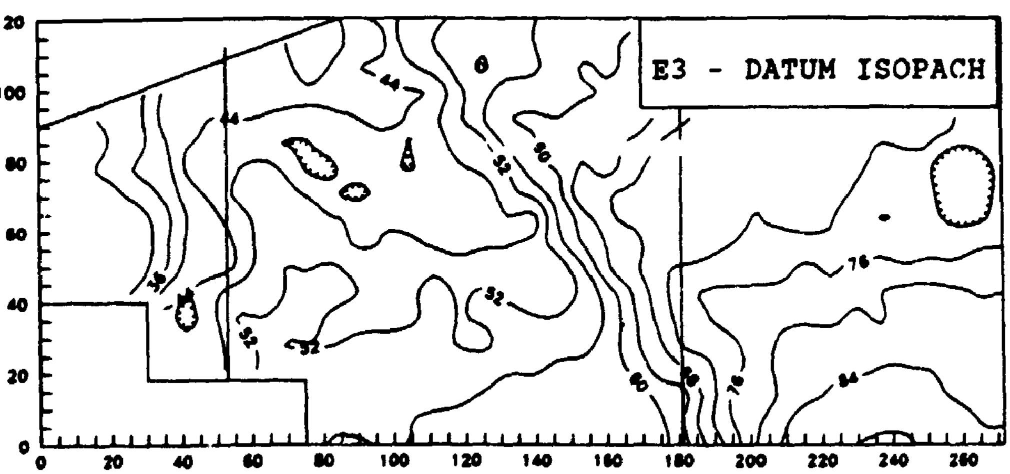
E3 - DATUM ISOPACH
0 20 40 60 80 100 120 140 160 180 200 220 240 260
0 20 40 60 80 100 120
44
52
60
68
76
84
36
32

regional cross-section C-C', Fig. 6.4c); c) note that to the west of the break in slope, the E3 surface is nearly flat, except in the west where it has been offset by fault activity in the far west.

The E2 to E3 interval represents a period of shoreline progradation followed by transgression. Swaley cross-stratified sands were deposited on the shoreface at the same time that interbedded sands and muds were being deposited in the offshore zone. Given the interpretation of the Waskahigan Allomember as a lowstand shoreface deposit (e.g. Plint *et al.* 1986; Plint 1988; I re-measured the core from the type locality (10-30-52-17W5 - see Plint *et al.* 1986) and am satisfied with the interpretation), the shoreline must have dropped below the break in slope for deposition of the Waskahigan shoreface units to occur. During the subsequent transgression, sea level rose to the top of the Kakwa shoreface sandstones and then moved at least 120 km landward (the distance from the Kakwa edge to the most westerly outcrop) over the nearly horizontal upper surface of the shoreface unit.

6.3.4 The E3 to E4 interval

This interval consists of the upper shoreface package of the Kakwa Member (typically facies 17, locally facies 8), the Musreau Member (non-marine facies association), the Hornbeck Allomember (facies 2 to 15 in cores from wells 11-35-75-8W6 and 6-9-71-3W6), and the Burnstick Allomember (never cored in this area).

The isopach map of the E3 to E4 interval (Fig. 6.19) shows that the axis of greatest deposition has shifted approximately 80 km back to the west from the same axis of the E2 to E3 interval (Fig. 6.15). The thickest part of this interval in the west is represented by strata of the non-marine facies association (the Musreau Member) as shown in the regional cross-sections (Section 6.2). As explained below (see also Chapter 7), the isopach map of this interval is not directly comparable to those of the other allomembers, as it appears that deposition of the Musreau Member occurred during relative sea level rise.

The surface diagram and isopach map of the E4 to Datum interval (Fig. 6.20) show: a) like the E3 surface, there is a discrete NW-SE trending break in slope evident which represents the basinward margin of the Kakwa Member - the Kakwa edge; b) there is a slight thickening trend to the NW; c) the E4 surface is truncated (toplap) by the E5 and then the E7 surface as one moves to the west over the Kakwa Member.

The lowest portion of the E3 to E4 interval in the Kakwa Member probably consists of palimpsest deposits in many cases. These units are represented by undulose-laminated fine sandstones with coffee grounds laminae, (locally pebbly) cross-bedded sandstones, sandstones with structures appearing to represent scour fill cross-bedding, coarse-

Figure 6.19. Isopach map (in meters) of E3 to E4 interval.

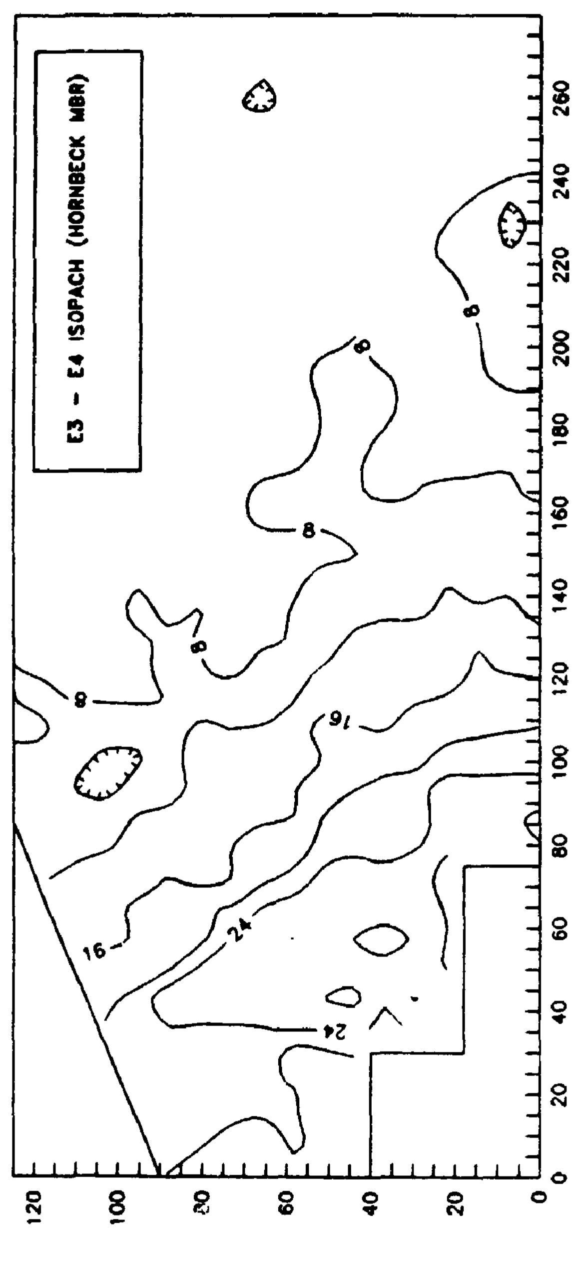
E3 - E4 ISOPACH (HORNBECK MBR)
8
16
24
0 20 40 60 80 100 120 140 160 180 200 220 240 260
0 20 40 60 80 100 120

Figure 6.20. Surface diagram and isopach map of E4 to Datum interval. See Figure 6.10 for explanation.

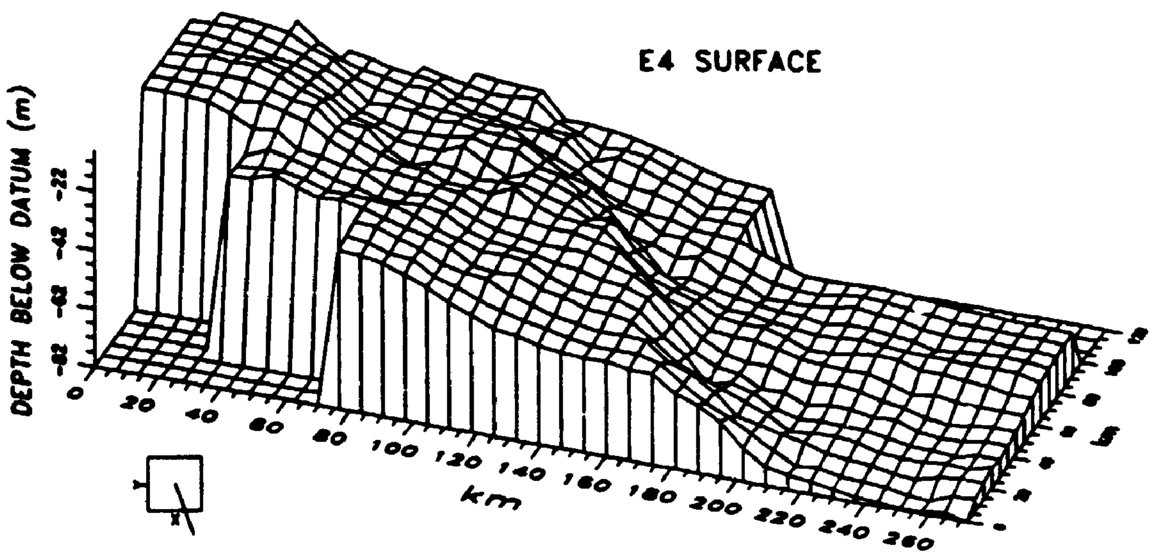
E4 SURFACE
DEPTH BELOW DATUM (m)
-22
-42
-62
-82
0
20
40
60
80
100
120
140
160
180
200
220
240
260
km
Y
X

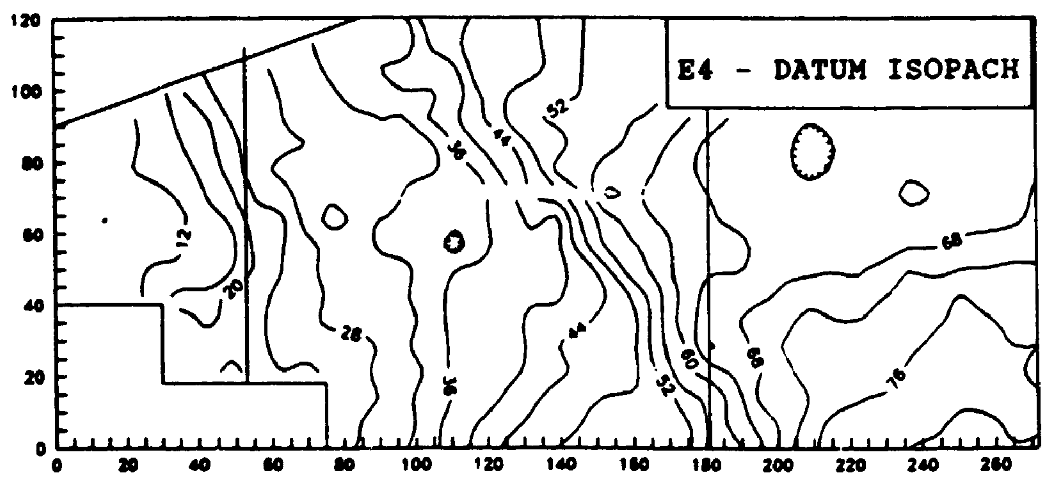
E4 - DATUM ISOPACH
120
100
80
60
40
20
0
0
20
40
60
80
100
120
140
160
180
200
220
240
260
12
20
28
36
44
52
60
68
76

grained wave ripples, thin shales, etc. They were probably initially deposited on the E3 ravinement surface during transgression (c.f. Nummedal and Swift 1987) and suffered variable amounts of reworking during both the subsequent highstand and the ensuing progradation. These deposits are not always present (e.g. Cutpick Hill). It will be recalled from Chapter 3 that some siderite cement is present in the lowest parts of this interval (i.e. the palimpsest deposits) but siderite is never present in the upper portions of this interval (i.e. the shoreface part of the package).

Progradation resulted in deposition of the upper, coarser-grained (locally conglomeratic, e.g. Bay Tree) shoreface package above the palimpsest deposits, or directly above the ravinement surface. Progradation was punctuated, with alternating episodes of faster and slower basinward shoreline displacement. During slower periods (or perhaps even minor transgressive events), barrier systems were built up. This created thicker accumulations of shoreface sandstones, in turn producing the uneven topography noted on the top of the Kakwa Member (c.f. Section 6.2). Tidal inlets (e.g. Bear Mountain section) could have developed at this time (note that the upper part of the Kakwa Member at the Bear Mountain section is also very thick), and a couple of meters (probably no more than 1 or 2 m) of lagoonal deposits, with oysters, could have formed behind the barriers (e.g. Cutpick Hill, Murray River sections).

Unlike Plint and Walker (1987), I do not believe that the majority of the Musreau Member was deposited behind a prograding barrier system. There are no conglomerate channel fills in the member, yet the evidence from Bay Tree, Cutpick Hill and elsewhere indicates that gravel was being supplied to the shoreline. The style of sedimentation in the Musreau Member suggests rapid *aggradation* (Chapter 3), yet the evidence suggests very rapid *progradation* of the Kakwa shoreline. Finally, it is not clear how a barrier coastline well over 200 km long (e.g. Plint 1988) could prograde 120 km, since fluvial input would tend to be trapped in the back barrier lagoons.

As in the case of the E2 to E3 interval, shoreline progradation again proceeded to the Kakwa edge, and sea level dropped down the break in slope. During lowstand, the linear incised shoreface deposits of the Burnstick Allomember were deposited in a position analogous to that of the Waskahigan lowstand shoreface deposits. It is also likely that the fluvial units which locally replace the upper shoreface package were incised at this time (i.e. generating a type 1 sequence boundary (Van Wagoner *et al.* 1988)).

Relative sea level rise followed, but in contrast to the E3 transgression, a thick succession of non-marine strata, the bulk of the Musreau Member, was deposited *during sea level rise* (contrast with the model of Posamentier and Vail

(1988)) on a coastal plain dominated by anastomosing river systems. The reasons for fluvial deposition and coastal plain aggradation during relative sea level rise at this stage will be discussed in the next chapter.

The E4 surface, when it separates the Musreau Member from the overlying Raven River Allomember, is often quite subtle and represented by a slight colour change of the constituent mudstones, and a transition to a marine ichnofauna (e.g. Fig. 5.19d). This suggests erosion of a relatively unlithified (i.e. "freshly" deposited) muddy substrate during transgression. This is essentially the same conclusion as that reached by Bartlett (1987) just south of the present study area.

6.3.5 The E4 to E5 interval

This interval consists of the Raven River Allomember (generally lithologies belonging to the offshore facies association, e.g. facies 3, 4, 5, 15) and the Carrot Creek Allomember (only observed as a thin pebble bed in this area - e.g. 11-35-75-8W6). Strata of the Raven River Allomember deposited east of the Kakwa edge tend to comprise two superimposed scales of sandier upwards cyclicity, the larger scale represented by the entire thickness of the member, the smaller scale by a few meter thick sandier upward cycles. Walker and Eyles (1988) showed that by correlating the smaller-scale cycles, one can delineate a series of shingled lobes in the Willesden Green area. I was not able to reproduce their results here because adequate well log coverage was not available.

Above the Musreau Member (west of the Kakwa edge), cores through the Raven River Allomember typically display a single sandier-upward succession (e.g. facies 3 to 4 to 5). Only in one core from the present study did a shoreface sandstone (facies 16) cap the succession (core from well 11-22-65-6W6).

An isopach map of the E4 to E5 interval is shown in Figure 6.21. There, it can be seen that this interval also forms a distinct sedimentary prism, with the greatest thickness of strata preserved between the Kakwa edge and the E5 bevel. Like the underlying packages, there is a suggestion that this interval thickens to the southeast. In the north-central part of the area, a "thin patch" indicated by the hachured 4 m isopleth (to the left of the title block) shows where the E5 surface nearly amalgamates with the E4 surface as seen at the base of the E5 bevel in regional cross-section C-C' (Fig. 6.4c). The long axis of this area probably delineates the underlying fault. The northern limit is unclear due to a lack of well control, and the deflection of the 8 m and 12 m isopleths to the east must be considered an artifact of the *Surfer* software, there being no data points to constrain their position.

The E4 to E5 interval represents another discrete period of progradation followed by transgression. There are

Figure 6.21. Isopach map (in meters) of E4 to E5 interval.

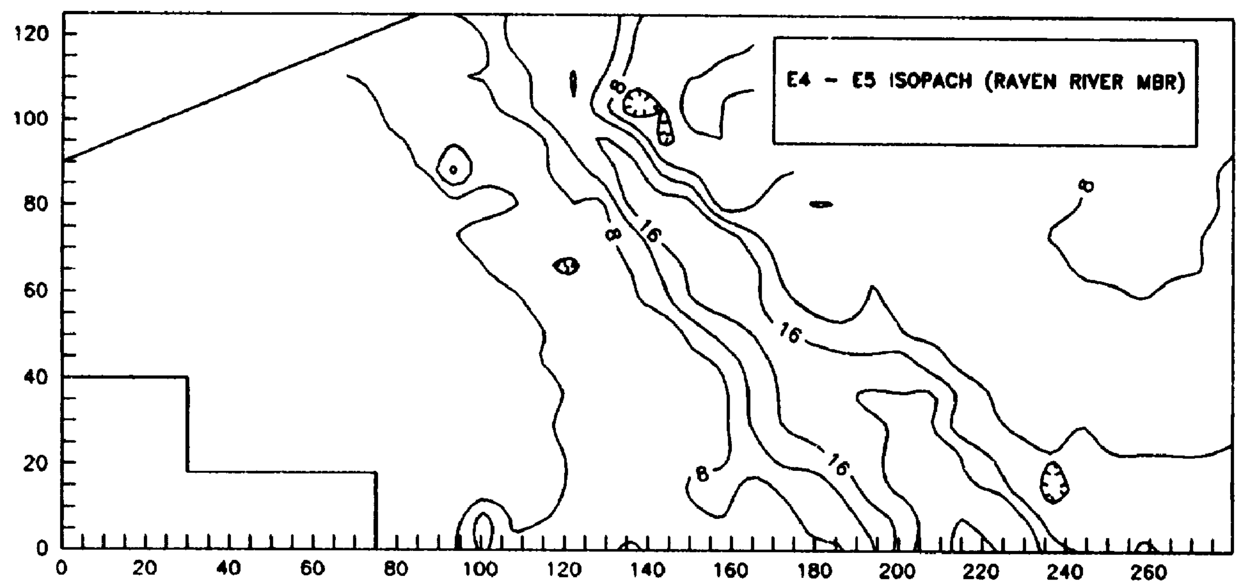
E4 - E5 ISOPACH (RAVEN RIVER MBR)
120
100
80
60
40
20
0
0
20
40
60
80
100
120
140
160
180
200
220
240
260
8
16
16
8
8
8

however, some important differences with the underlying intervals. First, it is possible (but probably unprovable) that the fine-grained basal portions of the Raven River Allomember represent clastic detritus removed from the top of the Musreau Member *during the E4 transgression* and swept over the Kakwa edge. Second, thick shoreface sandstones (facies 16 or 17) are generally not present in this interval (the only exception being 2.65 m of facies 16 preserved in 11-22-65-6W6). The shoreface deposits may have been eroded either during relative sea level fall; a similar mechanism has been observed on the Quebec North Shore, where uplifted post-Pleistocene deltaic and prodeltaic sediments (deposited during peak post-glacial submergence) have been eroding as the crust rebounds isostatically. The eroded material thus supplied has fed the prograding deltas at later shoreline positions (Dubois 1980).

The E5 lowstand is represented here only by the E5 bevel (Figs. 6.4a,c, 6.22), the position of which may have been determined structurally. Thick conglomerates of the Carrot Creek Allomember do not appear to have developed here, or at least have not been penetrated by drilling. In the west, the E5 transgression truncated the E4 surface, and strata of the E5 to E6 interval thus rest directly on the Musreau Member. The E7 surface truncates the E5 surface in the west and northwest (see below).

Figure 6.22. Surface diagram and isopach map of E5 to Datum interval. See Figure 6.10 for explanation.

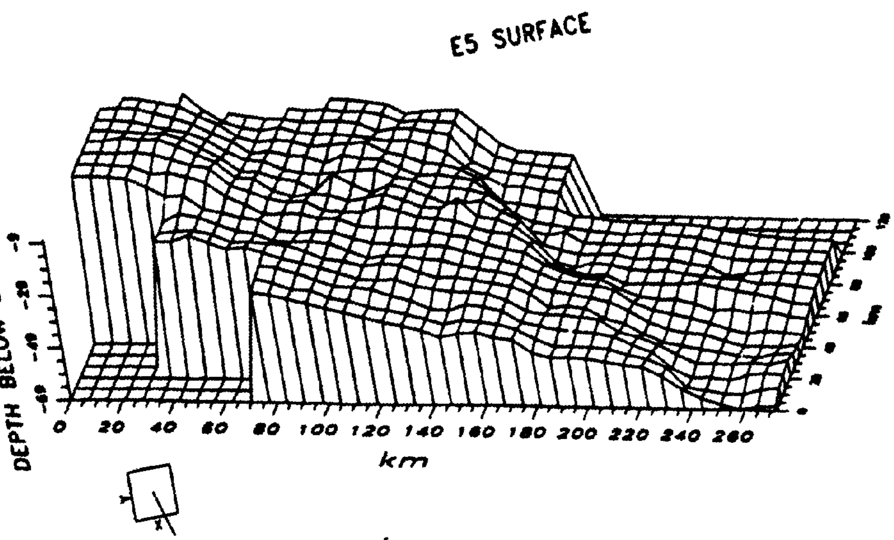
E5 SURFACE
DEPTH BELOW DATUM (m)
km
0 20 40 60 80 100 120 140 160 180 200 220 240 260

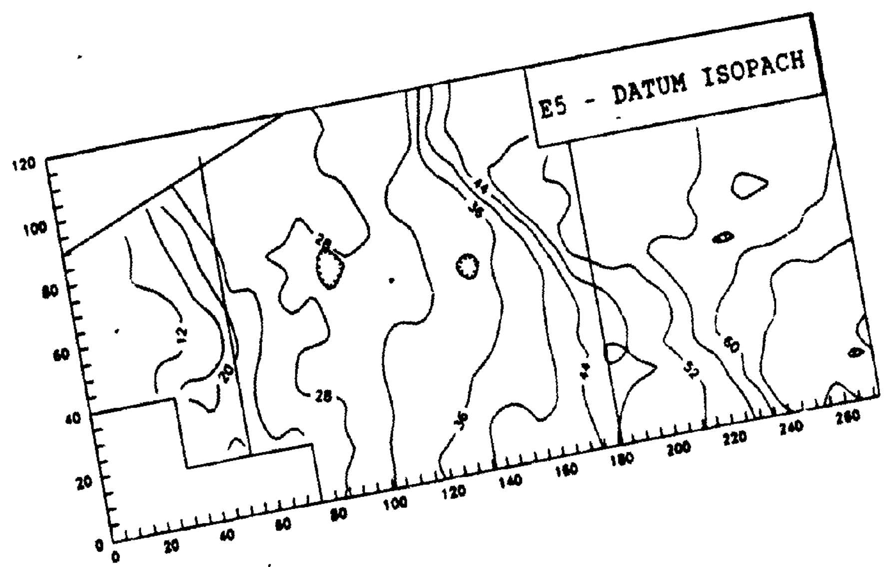
E5 - DATUM ISOPACH
12
20
28
36
44
52
60
0 20 40 60 80 100 120 140 160 180 200 220 240 260
0 20 40 60 80 100 120

6.3.6 The E1 to E5 interval - summary

As noted in Chapter 1, integration of Stott's (1963, 1967) published fossil data into the event stratigraphy of Plint *et al*. (1986, 1987, 1988) indicates that the E1 to E5 interval of the Cardium Formation is mid-Turonian in age, and that most of the E5 to E7 interval is of early Coniacian age (Plint and Hart *in prep.*). In Figure 6.23 I present an isopach map of the entire E1 to E5 interval to illustrate the overall aspect of the preserved mid-Turonian strata.

Each of the intervals appears to represent a progradational event followed by transgression. They appear similar in scale to the *parasequences* of EXXON workers (Van Wagoner *et al.* 1988), although the top of each interval *was* apparently subaerially exposed over much of its extent, and they are closely comparable to the *genetic stratigraphic sequences* of Galloway (1989). The stacking pattern is comparable with the *progradational parasequence sets* of Van Wagoner *et al.* (1988).

The isopachs of this interval essentially reiterate the two main trends of the constituent subdivisions. These are a thickening of the preserved strata to the SE, and a series of superimposed, roughly NW-SE, thickening and thinning trends. In the east, the E5 bevel is responsible for the main decrease in thickness of this interval. Note that the location of the Kakwa edge is not readily apparent, as the

Figure 6.23. Isopach map (in meters) of Middle Turonian portion (E1-E5) of Cardium Formation.

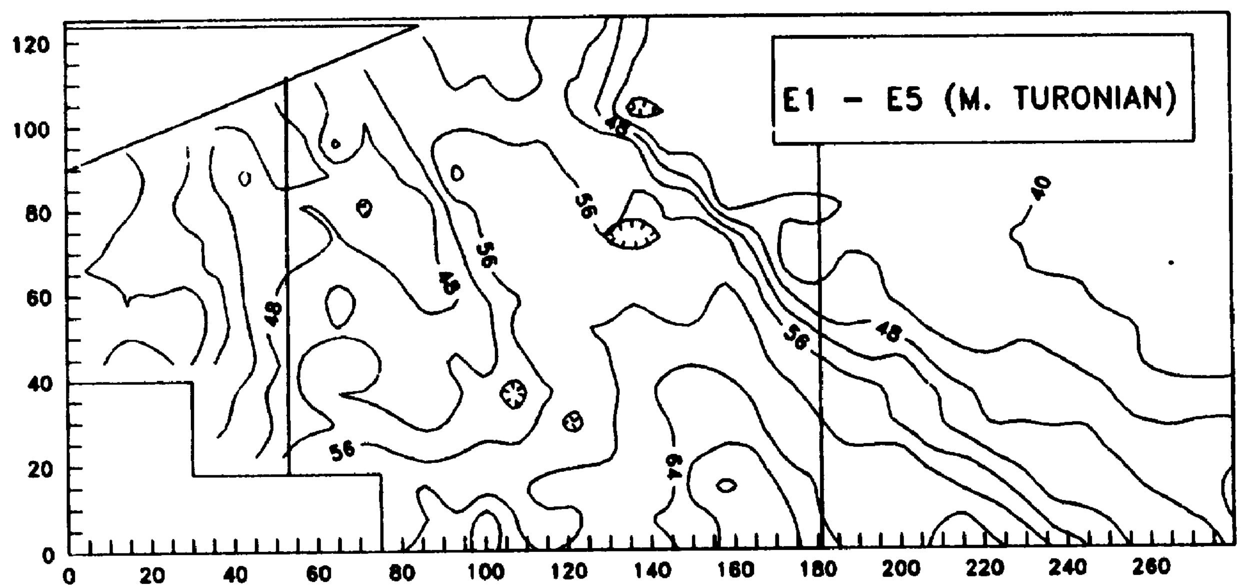
E1 - E5 (M. TURONIAN)
40
48
56
64
0
20
40
60
80
100
120
140
160
180
200
220
240
260

thickness variations of the Raven River Allomember mask the topography of the underlying E4 surface (the greatest thickness of the E4 to E5 interval lies just basinward of the Kakwa edge). In the far west, the isopleths trend in a more N-S orientation, reflecting the orientation of the faults in that area.

6.3.7 The E5 to E7 interval

I have chosen to lump all the subdivisions of this interval together in one section, as only a very limited core base (7 more or less complete cores) and only 1 measured outcrop section are available on which to base the discussion. As noted in Section 6.2, my picks for the E6 and E6.5 horizons do not necessarily coincide with those of previous workers to the immediate south (i.e. up to and including Twp 64; Bartlett 1988; Plint *et al.* 1987; Plint 1988; Wadsworth 1989). Note that the first three reports did not recognize the existence of the E6.5 surface, and that Wadsworth (1989) did not present any detailed cross-sections from the most northern part of her study area which would allow the question to be resolved (neither did she present isopach maps). The picks presented here from the basinward portions of the study area (east of the Kakwa edge) are based on data supplied by Wadsworth. These picks are internally consistent, and resemble the picks of Eyles and Walker (1988) with the E6 surface close to the E5 surface, and the E6.5 horizon close to E7.

The E5 to E6 isopach map is shown in Figure 6.24a (note that *Surfer* would not draw the "0 m" isopleth, so I have added the 1 m isopleth as a proxy). Essentially, the E6 surface is a near-planar surface (in agreement with Wadsworth 1989) which appears to onlap the E5 surface. There did not appear to be any manifestation of this surface at the Smoky River section (Section 5.2.6). There, the entire E5 to E7 interval consists of blocky-weathering black mudstones (facies 1).

The E6 to E6.5 interval isopach map is shown in Figure 6.24b. According to my correlations, it is in fact the E5 to E6.5 interval above the Kakwa Member, hence the E5/E6 designation in the figure title. Generally, the thickness of this interval is fairly uniform, except in the west (where it pinches out) and the northwest, where a NW-SE trend of the isopleths represents bevelling on the E7 surface and truncation of the E6.5 surface (see below).

Cores through this interval show a distinct succession of facies, typically with fine-grained strata of facies 2 overlain by a sandier-upward succession of facies 3, 4 and 5. The sandstones of the upper part are generally coarser (medium- to coarse-grained) than equivalent facies lower in the section (e.g. Nosehill and Raven River allomembers). They are locally pebbly in the north (e.g. 4-10-72-13W6) and in these cases I have assigned portions of them (perhaps incorrectly, although see Plint *et al.* 1986) to facies 6.

Figure 6.24. Isopach maps (in meters) of: A) E5 to E6 interval; B) E5/6 to E6.5 interval; C) E6.5 to E7 interval.

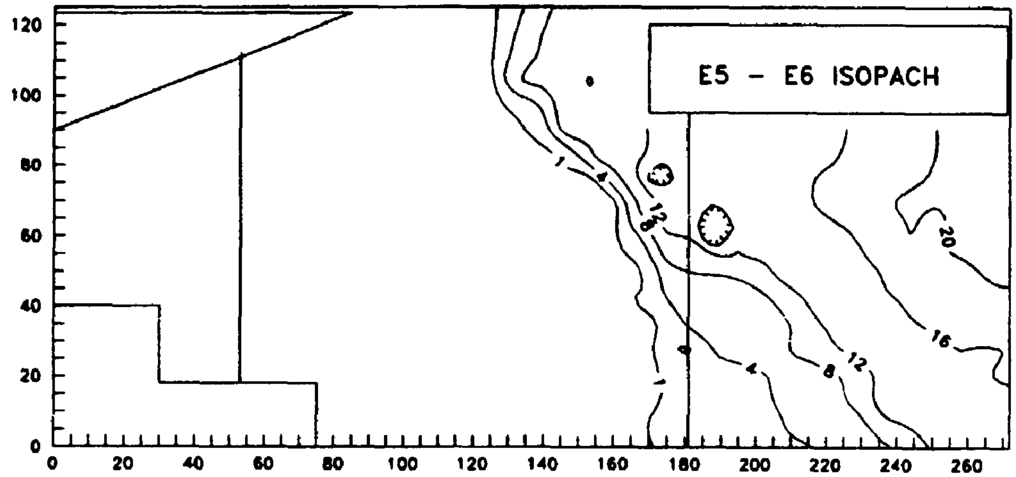
E5 - E6 ISOPACH
120
100
80
60
40
20
0
0
20
40
60
80
100
120
140
160
180
200
220
240
260
1
4
8
12
16
20

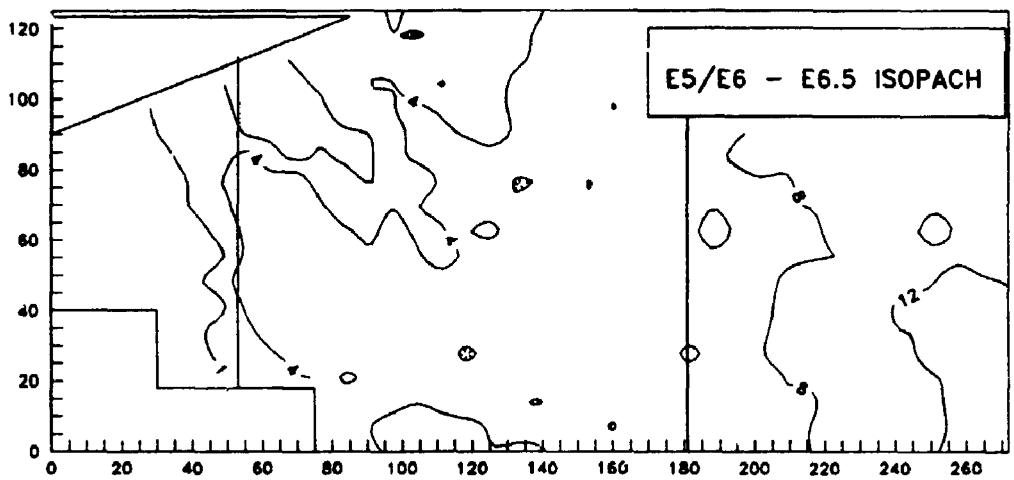
E5/E6 - E6.5 ISOPACH
120
100
80
60
40
20
0
0
20
40
60
80
100
120
140
160
180
200
220
240
260
1
4
8
12

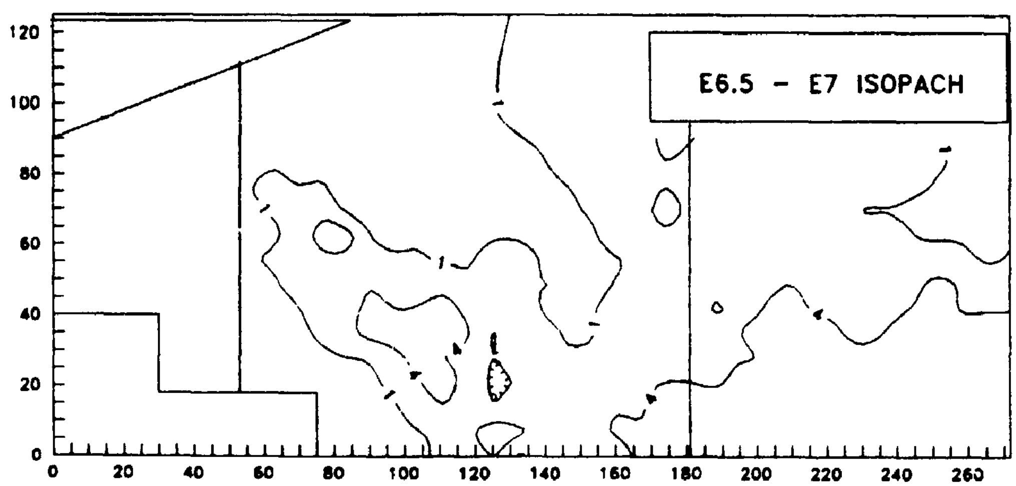
E6.5 - E7 ISOPACH
120
100
80
60
40
20
0
0
20
40
60
80
100
120
140
160
180
200
220
240
260
1
4

The thickness of either part can be variable: where best developed, both can be a few meters thick (e.g. 8-1-65-6W6), although locally either may be absent (e.g. in 10-1-74-11W6 this interval consists of a 5 m thick sandier upward succession of facies 3 to 5, whereas in 4-10-72-13W6, 2.5m of facies 2 capped by .45 m assigned to facies 6 is present).

The isopach map of the E6.5 to E7 interval is shown in Figure 6.24c. There, the extent and orientation of the truncation in the west and northwest of the E6.5 surface by E7 is readily apparent. I have only one core section through this interval (6-19-66-7W6), where 3.7 m of facies 2 separates the two horizons. This is in general agreement with the findings of Plint *et al.* (1986) and Plint (1988) which showed that this interval can be finer-grained than the underlying interval (the Dismal Rat Allomember or E5 to E6 interval of those reports, the E5 to E6.5 interval here).

A surface diagram and isopach map of the E7 to Datum interval are presented in Figure 6.25. The most prominent characteristic of the E7 surface is the presence of a NW-SE trending bevel in the western part of the area. The bevel is most abrupt in the north, loses it distinctness in the middle, and re-develops in the south of the study area.

The E7 surface is represented by a gritty siderite horizon at the Smoky River section, whereas to the west it is generally present as a thin pebble bed (Amundson

Figure 6.25. Surface diagram and isopach map of E7 to Datum interval. See Figure 6.10 for explanation.

E7 SURFACE

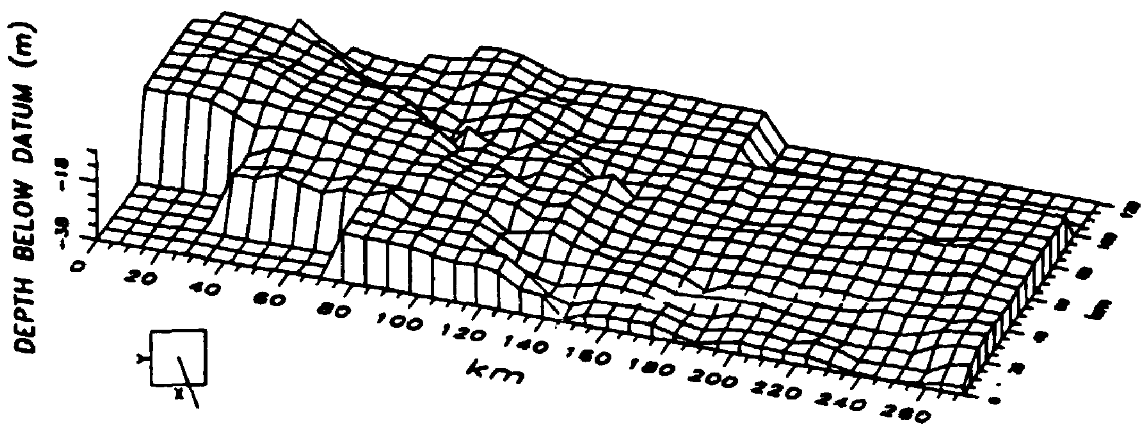
DEPTH BELOW DATUM (m)
-30
-15
0
20
40
60
80
100
120
140
160
180
200
220
240
260
km
Y
X

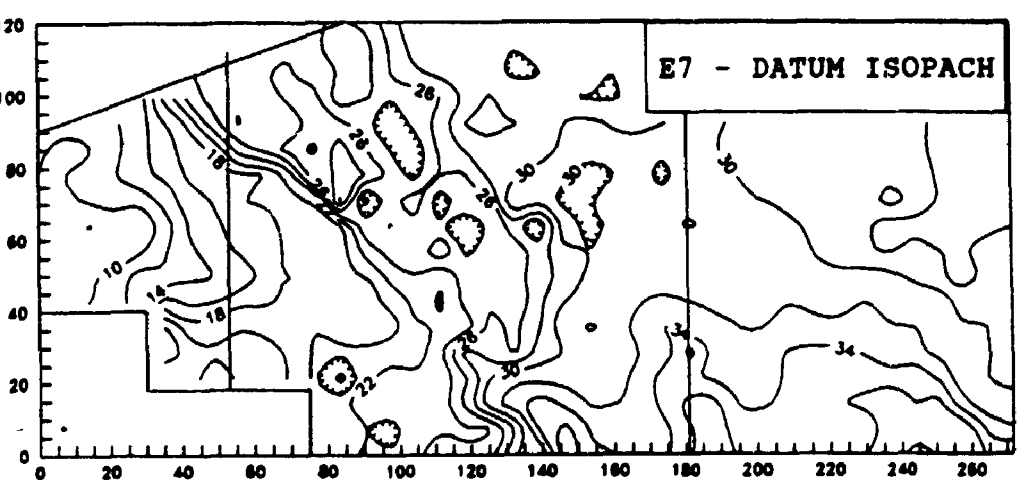
E7 - DATUM ISOPACH
120
100
80
60
40
20
0
0
20
40
60
80
100
120
140
160
180
200
220
240
260
10
14
18
22
26
28
30
34

Allomember) resting on successively lower units (stratigraphically) to the west. Thin conglomerates (pebble to cobble size clasts), and in places *Thalassinoides* or *Rhizocorallium* burrows, generally overlie this surface in the Foothills outcrops (e.g. Figs. 5.2f,g).

The isopach map of the E5 to E7 interval is presented in Figure 6.26. It can be seen that the greatest thickness of preserved strata from this interval is found east (basinward) of the E5 bevel. To the west and northwest, the interval is truncated completely, the isopleths again illustrating the NW-SE trend observed so commonly in this part of the Cardium Formation.

Peak progradation during this interval *appears* to represented by the E5 to E6.5 interval, it having the coarsest grained and thus presumably the most "nearshore" deposits. On a basin-wide scale however, the E5 to E7 interval of the Cardium Formation appears to represent another progradational parasequence set. Thick shoreface sandstones *are* found in the E6 (E6.5?) to E7 interval much further south (Plint *et al.* 1988), suggesting that their absence in the present study area represents simply a lack of preservation, or lack of deposition in a sediment-starved (i.e. dominantly erosional) system.

<u>6.3.8 The E1 to E7 interval</u>

An isopach map of the entire Cardium Formation (E1 to E7) is shown in Figure 6.27. The three most important

Figure 6.26. Isopach map (in meters) of Lower Coniacian portion (E5 to E7) of Cardium Formation.

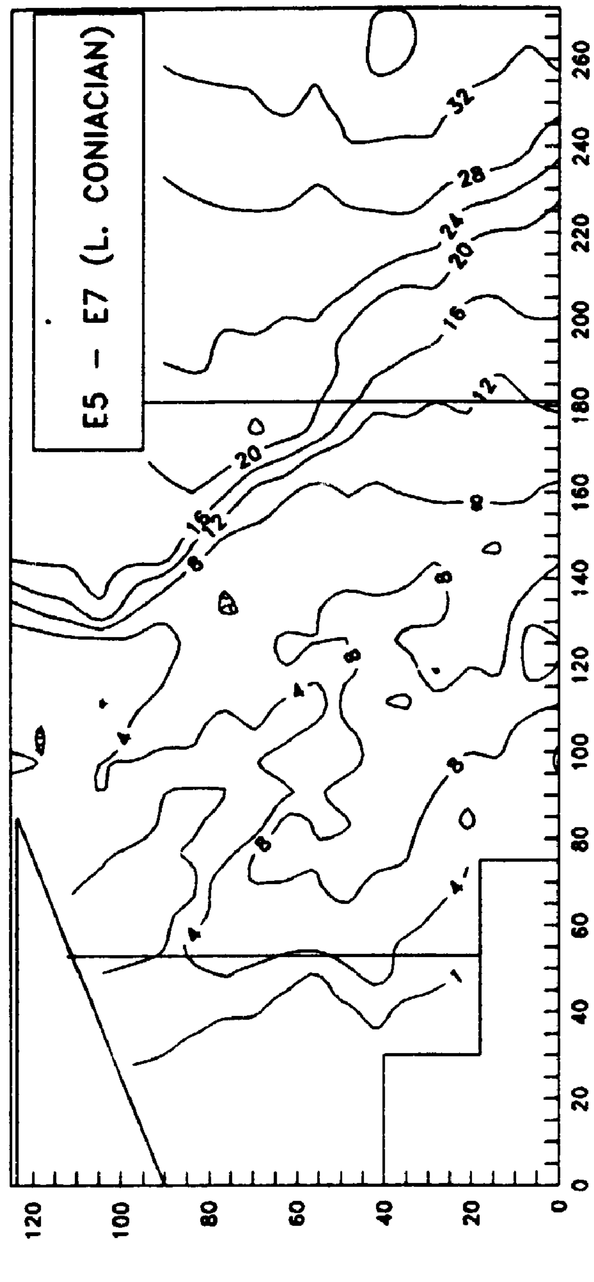
E5 - E7 (L. CONIACIAN)
0 20 40 60 80 100 120 140 160 180 200 220 240 260
0 20 40 60 80 100 120
1 4 8 12 16 20 24 28 32

Figure 6.27. Isopach map (in meters) of Cardium Formation (E1 to E7).

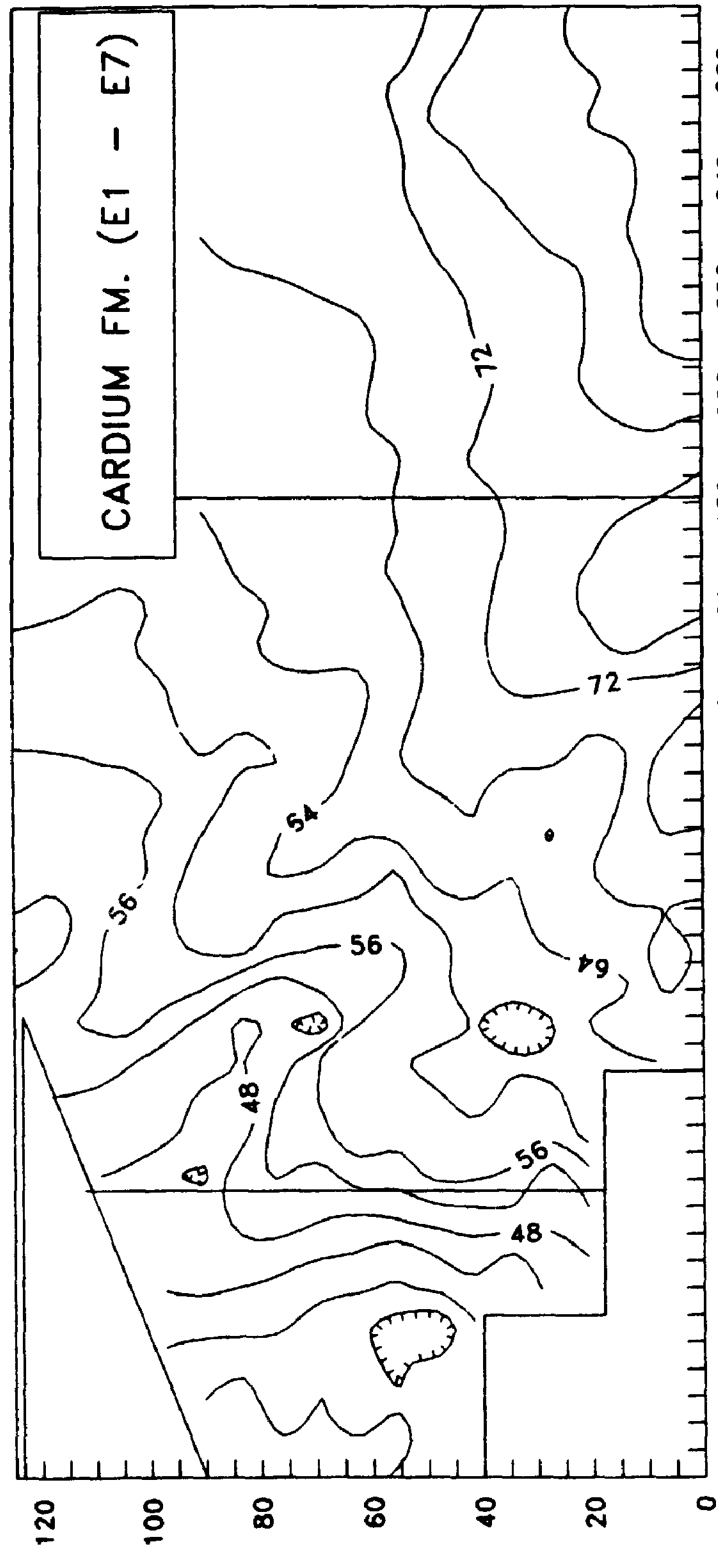
CARDIUM FM. (E1 - E7)
72
72
54
56
56
56
64
48
48
0
20
40
60
80
100
120
140
160
180
200
220
240
260
0
20
40
60
80
100
120

points about thi map are: a) a dominant SW-NE trend of the isopleths; with b) a superimposed NW-SE trend represented by substantial deflections of the isopleths in that direction; and c) the NNW-SSE trend in the extreme west. The last trend is due to fault activity, as shown in the regional cross-sections (Section 6.2). The other trends are due to basement structural elements, as will be explained in the next chapter.

6.4 Summary

The Cardium Formation is composed of two stacked progradational packages. The lower of the two is mid-Turonian in age, and consists of the E1 to E5 interval. The upper portion (E5 to E7) is mostly early Coniacian in age.

The existing event stratigraphy for the Cardium Formation (Plint *et al.* 1986, 1987, 1988) can be applied, with modifications, to the formation in the present study area. The E1 surface can be traced westward up and into the Kakwa Member, where it sits above a considerable thickness of shoreface sandstone. The non-marine strata of the Musreau Member are here considered to have been deposited shortly before or during the E4 transgression, and there is no evidence of upper non-marine tongues. These relationships are in contrast with earlier interpretations (e.g. Duke 1985; Plint and Walker 1987; Plint *et al.* 1988). The correlations of the E6 and E6.5 surfaces are internally consistent, but are not consistent with previously published interpretations. There are discrepancies between those publications however, and the matter does not appear resolvable with the core and well control available in the present study area.

The most important modification involves the correlation of the E3 surface through the Kakwa Member, dividing that member into a lower package dominated by facies 16, and an upper package dominated by facies 17. This interpretation is in contrast with previous interpretations which suggested that the Kakwa Member consists of a series of shingled shoreface sandbodies (e.g. Duke 1985; Plint *et al.*, 1986, 1988; Plint 1988). The E3 surface represents a ravinement surface, and appears to have been originally nearly planar. Knowing this, the internal geometry of the entire formation becomes clearer. A distinct break in slope is present on the E3 and E4 surfaces at the Kakwa edge, and the Waskahigan and Burnstick lowstand shorefaces are cut into the more steeply dipping portion of those surfaces in this area. Contemporaneous vertical displacements (e.g. faults, subtle warping) have been recognized here, and were not recognized by Plint *et al.* (1986, 1987, 1988) or subsequent workers in the Cardium Formation (e.g. Bergman and Walker 1987; Walker and Eyles 1988).

CHAPTER 7

MECHANISTIC CONSIDERATIONS

7.1 Introduction

In this chapter, I wish to discuss the ultimate controls on sedimentation and erosion during deposition of the Cardium Formation. As discussed in Chapter 2, the main factors which need to be considered are eustatic sea level changes, rates of sediment supply and tectonic factors, such as rates and patterns of subsidence. The possible influence of relative sea level change on deposition during deposition of the Cardium Formation will be examined first (Section 7.2). This will include a review and critique of previously published interpretations. In the next section (Section 7.3), I will suggest the possibility that tectonic elements probably had a greater influence on deposition than has previously been recognised. Finally, (Section 7.4) the interaction of sea level fluctuations and tectonic forces responsible for deposition of the Cardium Formation in this area will be reviewed.

7.2 Controls on cycle development in the Cardium Formation

7.2.1 Previous interpretations

It has long been recognised that the Cardium Formation developed as a series of regressive/transgressive (R/T) cycles. Michaelis (1957) divided the formation into 5 such cycles, and proposed using the contacts (marked by a "pebble conglomerate, a shell bed or a ferruginous siltstone with casts of numerous burrows") between cycles as time lines. As noted in Chapter 1, these ideas anticipated the proposal of a similar stratigraphic subdivision of the formation by Plint *et al.* (1986). Michaelis felt that the Cardium Formation as a whole represented a period of increased sediment supply, upon which the R/T cycles were superimposed.

Stott (1963) recognised that the Alberta and Smoky groups consisted of a nested succession of cycles. He felt that the Kaskapau (Blackstone) and Cardium formations together comprise a transgressive/regressive "megacycle" which is overlain by another megacycle consisting of the Wapiabi Formation (and equivalent units in the north). In the lower megacycle, transgression is represented by the Sunkay Member of the Kaskapau Formation, whereas regression reached its peak during deposition of the Cardium Formation. Upon these major cycles, minor shoreline advances and retreats were responsible for producing the members of the Cardium. The thin conglomerates between cycles were interpreted as transgressive lags (p. 141). Stott (1963) did not elaborate on the causes of the shoreline movements.

Most recently, the work of the "McMaster Cardium Group" (as exemplified by Plint *et al.* (1986), Bergman and Walker (1986, 1988), Plint and Walker (1987), and Walker and Eyles (1988)) has tended to suggest that short-term tectonic movements have been responsible for controlling the sequence of regressions and transgressions represented by the Cardium Formation. Progradation of many of the cycles terminated with a distinct relative sea level drop. Shoreface incision during lowstand and transgression determined the location of the lowstand shoreface units (i.e. Waskahigan, Burnstick, Carrot Creek and Amundson allomembers), with the linear shoreface trends representing incised shoreface profiles developed during temporary stillstands (e.g. Bergman and Walker 1987; Pattison 1988; Plint 1988; Walker and Eyles 1988).

Here, I wish to examine 5 specific points raised by the interpretations of the McMaster Group.

1) The first point concerns the relation between the creation of relief in the thrust belt and sediment supply. As noted in Chapter 2, it appears that periods of active thrusting (mountain building) to the west are probably represented by shales in most of the Alberta Basin. I suggest that the time frame involved in the creation of the allomembers (about 10^5 years) is too quick to have been generated by mechanisms such as periodic episodes of thrusting and isostatic rebound (uplift and erosion), or tectonic offloading of thrust sheets (followed by isostatic rebound). In the light of these arguments, I suggest that allomember development in the Cardium Formation did not occur in response to periodic warping and/or uplift in the west.

2) Concerning the origin of the erosion surfaces, it has been suggested that they were generated by either subaerial, "fully" subaqueous, or shoreface processes (e.g. E5 - Bergman and Walker 1987; E5 - Eyles and Walker 1988; E4 - Pattison 1988; E7 - Wadsworth 1989). The first two possibilities are dismissed by these authors, leaving the shoreface interpretation by default. Although I agree that *shoreline* incision *can* be invoked to account for many of the characteristics of these surfaces (but see below), I contend that the "fully subaqueous" alternative is dismissed too quickly.

Tidal currents or storm-generated currents are the only flows considered by these workers. However, there is evidence that *thermohaline* currents (generated by temperature and/or salinity contrasts) can generate significant erosion surfaces even at abyssal depths (e.g. Johnson 1972; Barusseau and Vanney 1978; Tucholke and Embly 1984). Based on faunal evidence, it has been suggested that during Cenomanian to Turonian times, cool bottom waters invaded the Western Interior Seaway from the Boreal Sea in the north (e.g. Kauffman 1984; Watkins 1986). Due to the Coriolis force, these flows would probably have been concentrated along the western margin of the seaway (as contour currents, see Kennett (1982)), where their erosive ability, if any, would have been felt. Faunal evidence for southerly flows of boreal waters along the western margin of the seaway has been presented by Eicher and Diner (1985).

Based on these considerations, I submit that an unknown amount of erosional topography might have been created on the E surfaces by thermohaline currents entering the seaway during eustatic rises (*cf.* Kauffman 1984). Realistically, their principal role may have been primarily to prevent deposition (burrowed sideritic horizons, such as the E1 surface at Mistanusk Creek) or to cause minor erosion (siderite intraclast layers, such as the E1 surface in core 6-15-65-13W6), especially in areas of pronounced bottom topography. To my knowledge, this possibility has not been previously investi.. ted, although Wallace-Dudley and Leckie (1988) have suggested that bottom currents may have played a key role in the formation of "lee side shoals" in the northern part of the present study area during a period of sea level rise in the Western Interior Seaway in Cenomanian times.

3) It has been assumed (e.g. Bergman and Walker 1988; Plint 1988; Walker and Eyles 1988) that an eroding shoreface will scour down to fairweather wave base and that this profile will be maintained as the shoreface shifts positions laterally in response to fluctuating sea levels. As noted above, although I do agree with a *shoreline* erosion model, there are certain revisions which need to be made.

To begin, I am unaware of any studies of modern shorefaces where it can be demonstrated that the shoreface profile scours down to fairweather wave base. This concept appears to be an extension of the "equilibrium shoreface profile" model as proposed by Bruun (1962; cited in Bruun 1988), and later adapted by workers such as Swift (1975). The controls on shoreface sedimentation were reviewed in Chapter 4, where it was stated that the shoreface profile is a complex function of sediment grain size (and range), sediment supply rate, wave climate, etc. Erosion of the upper shoreface is balanced by sedimentation on the lower shoreface and inner shelf (Bruun's "Ramp"; see for example Dean and Maurmeyer (1983) or Everts (1987)) during sea level rise, thus maintaining the profile. If the eroded sediment is transported far offshore (a likely scenario when eroding muds), or if the substrate is too coherent to be eroded by the available wave energy (again a possibility when eroding semi-consolidated muds), then the equilibrium profile is not maintained.

The shoreface profile is illustrated by the McMaster Cardium Group as a toboggan-shaped feature, with the horizontal part representing fairweather wave base (Fig. 7.1a). The bulk of the erosion is generated between mean sea level and fairweather wave base.

This idea runs contrary to long-established evidence that the greatest portion of coastal erosion is produced by storm wave activity in the surf zone (upper shoreface) or at the shoreline (Dietz 1963; Dean and Maurmeyer 1983;

Figure 7.1. Comparison of shoreline erosion models. A) Shoreface erosion model as envisaged by McMaster Cardium Group. Waves scour down to fairweather wave base, incising a "bevel". B) Shoreline erosion model based on modern coastal geomorphology studies. Waves erode a subaqueous shore platform (with a seaward dip) and a subaerial cliff. C) Calculated sea level rise (with respect to an arbitrary upper elevation) based on A - the shoreface incision model, B - the shoreline erosion model.

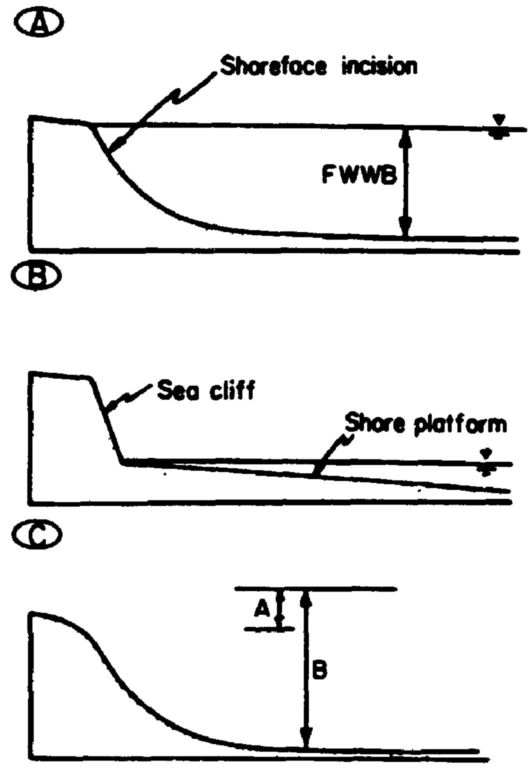
A
Shoreface incision
FWWB
B
Sea cliff
Shore platform
C
A
B

Sunamura 1983; Demarest and Kraft 1987; Bruun 1988). Eroding cliffs and shore platforms (formerly called "wave-cut platforms") are the observed morphological response of this process (Fig. 7.1b) leading to the generation of wave cut terraces. This is the process responsible for the creation of uplifted marine terraces (Sunamura 1983). The differences may appear esoteric, but they affect the calculations of the magnitude of relative sea level change (Fig. 7.1c). Significant dissection of the "bevel" by rivers would not be expected in the first model, but this process appears to have been operative at Carrot Creek (Bergman and Walker 1988, figs. 7 and 8).

4) For geometric reasons, the ability of *shoreline* erosion to generate a distinct notch (wave-cut terrace) is greatest on a steeply-dipping surface than on a flat surface. This is exemplified by the E3 surface, where shoreline erosion incised a notch on the steeply-dipping portion of the surface just basinward of the Kakwa edge, whereas there is no apparent trace of shoreline incision on the E3 surface where it is nearly planar above the lower part of the Kakwa (Chapter 6).

Tilting of the floor of the basin has been proposed by Bergman and Walker (1988) and Walker and Eyles (1988) for the E5 surface, whereas Wadsworth (1989) suggested a similar mechanism for the E7 surface. These authors have noted a tilted "staircase" type topography on the respective erosion surfaces. They suggested that, based on geometric constraints, for such a topography to be cut by shoreface incision, the "treads" (see Fig. 7.2) would have had to have been horizontal. By rotating the profile into such a position, Bergman and Walker (1988) suggested that about 200 m of relief was present on the E5 surface *in the Carrot Creek area alone* (a horizontal distance of about 20 km), Walker and Eyles (1988) added about 32 m to the E5 surface at Willesden Green, and Wadsworth (1989) proposed about 192 m of relief on the E7 surface over the entire basin. These values should be considered as absolute minima, since the "treads" (shore platforms) would originally have dipped seaward at some unknown angle.

There are several major problems with this interpretation. First, extrapolation of these rates of uplift to the western margin of preserved strata of the Cardium Formation (still probably at least several tens of kilometers east of the thrust belt) yield unrealistically high amounts of uplift. For example, taking the calculated slope (about 200 m in 20 km) of Bergman and Walker (1988) at Carrot Creek and extrapolating back to the palinspastically restored position of the Ram Falls outcrop (nearly 175 km landward of Carrot Creek; see figure 20 of Walker and Eyles (1988)), one can calculate that this locality would have been *1.75 km* above sea level during the incision of the lowest shoreline position at Carrot Creek.

Figure 7.2. Illustration of how observed "riser" and "tread" topography (top) could have been produced by shoreface erosion, providing that surface had originally been tilted so that the treads were originally horizontal (e.g. Bergman and Walker 1988; Walker and Eyles 1988). See text for further discussion.

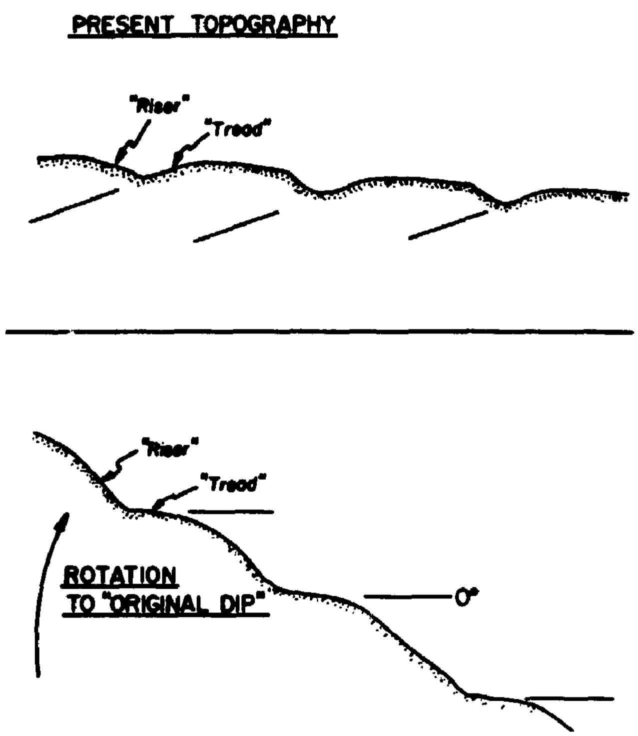
PRESENT TOPOGRAPHY
"Riser"
"Tread"
"Riser"
"Tread"
ROTATION
TO "ORIGINAL DIP"
0°

The mechanical problems of generating such relief appear not to have been addressed.

If one does admit that this amount of tilting could occur, there remain serious problems. Given this amount of uplift and tilting, one would surely expect rapid and very deep fluvial incision in the western portions of the basin. Geomorphologic studies of modern streams in California indicate that higher order streams should respond very rapidly to tectonic uplift (Merritts and Vincent 1989). I suggest that the amount of fluvial incision associated with nearly 2 km of uplift would be greater than the thickness of strata which could be removed during a subsequent transgression. One would also expect the steepening of gradients and deep fluvial incision to generate a fresh supply of coarse sediment input for the shoreline. Evidence of such a sediment influx is virtually absent for both the E5 and E7 surfaces (the Carrot Creek and especially the Amundson conglomerates being only locally developed).

5) It is generally suggested that shoreline incision will produce the deepest notches during relative stillstands of sea level. I agree that this is indeed a likely morphological response, but suggest that another process might have been active in certain cases. In particular, I would like to suggest that while uniform transgression over a planar surface will erode uniformly, shoreline erosion will tend to be intensified at "positive" topographic

irregularities in the case of an irregular surface. In Section 7.3, I will suggest how such topographic irregularities might be produced, and how the resultant shoreline notches could be distinguished from those developed during relative stillstands.

7.2.2 Cycle development - evidence from this study

In previous chapters, I have tried to emphasise that a hierarchy of cycle development exists in the Cardium Formation. Here, I wish to review the characteristics of each scale of cyclicity, and speculate about the controls responsible for the development of each. I suggest that there are three main scales of cyclicity present, the first being represented by the two main "age packages" of the formation (mid-Turonian and early Coniacian), the second by the individual allomembers, and the third by the smaller-scale sandier upward successions of the offshore units and (possibly) certain characteristics of the Kakwa Member. I will suggest that these correspond to third, fourth and fifth order cycles respectively (see Chapter 2).

Third order cyclicity

In Chapter 1, I explained how integration of existing faunal data into the Plint *et al.* (1986, 1987, 1988) stratigraphy led to the recognition of an internal hiatus at the E5 surface of the Cardium Formation. The package below the E5 surface consists of mid-Turonian strata, whereas above, the formation is mostly of early Coniacian age. As shown in Figure 1.3, the E1 to E5 package can be correlated with units such as the Ferron and Codell sandstones. The upper part of the Cardium Formation (E5 to E7) partially corresponds to the Gallup sandstone and equivalent units in the southern United States. In addition, McNeil and Caldwell (1981) have indicated that strata of Upper Turonian age, the time represented by a condensed section in the Cardium Formation, are absent from Upper Cretaceous strata of the Manitoba Escarpment. Similarly, a prominent erosion surface of this age is present throughout much of the U.S. western interior (e.g. Weimer 1984; Merewether and Cobban 1986). Thus, one can suggest that the forcing mechanism(s) was operative over the entire length of the Western Interior Seaway.

On a global basis, these periods correspond with third order eustatic sea level falls in the mid-Turonian ("90 my") and early Coniacian ("88.5 my"; Haq *et al.* 1987). As such, I suggest that the two main subdivisions of the Cardium Formation both developed in response to eustatic sea level falls. The magnitude of the early Coniacian event appears to have been smaller than the mid-Turonian excursion. The ultimate explanation for these sea level falls during a prolonged interval of high eustatic sea level (e.g. Hancock and Kauffman 1979; Haq *et al.* 1987) remains obscure.

Fourth order cyclicity

From a purely descriptive viewpoint, the allomembers of the Cardium Formation (defined in the last chapter as the intervals between successive "E" surfaces) represent fourth order cycles, with each R/T cycle representing about 90,000 to 100,000 years (Chapter 1). An overall progradational stacking pattern is evident in the mid-Turonian part of the formation, whereas the lower Coniacian portion is too poorly preserved in this area to recognise a distinct parasequence stacking pattern. Because of these limitations, I will concentrate the following discussion on the "lower" (mid-Turonian) part of the Cardium Formation.

One must begin by considering the evidence for relative sea level changes. In the last chapter (Section 6.3), I presented cross-sections which demonstrated that there existed a distinct break in slope at the basinward margin of the Kakwa Member, and that the Waskahigan and Burnstick shoreface units have been deposited in notches incised into the steeply dipping part of the E3 and E4 surfaces respectively. These relationships are shown schematically in Figure 7.3. There, it can be seen that for the shoreline position to be incised at the position of the Burnstick Allomember, a discrete relative sea level drop is required. In this case, one cannot explain the observed geometry by simply invoking changes in sediment supply, as this would

Figure 7.3. Sequence of events involved in generating lowstand shoreface deposits of Burnstick Allomember. A discrete relative sea level fall is required for shoreline position to drop below Kakwa edge. Changes in sediment supply alone cannot account for this geometry.

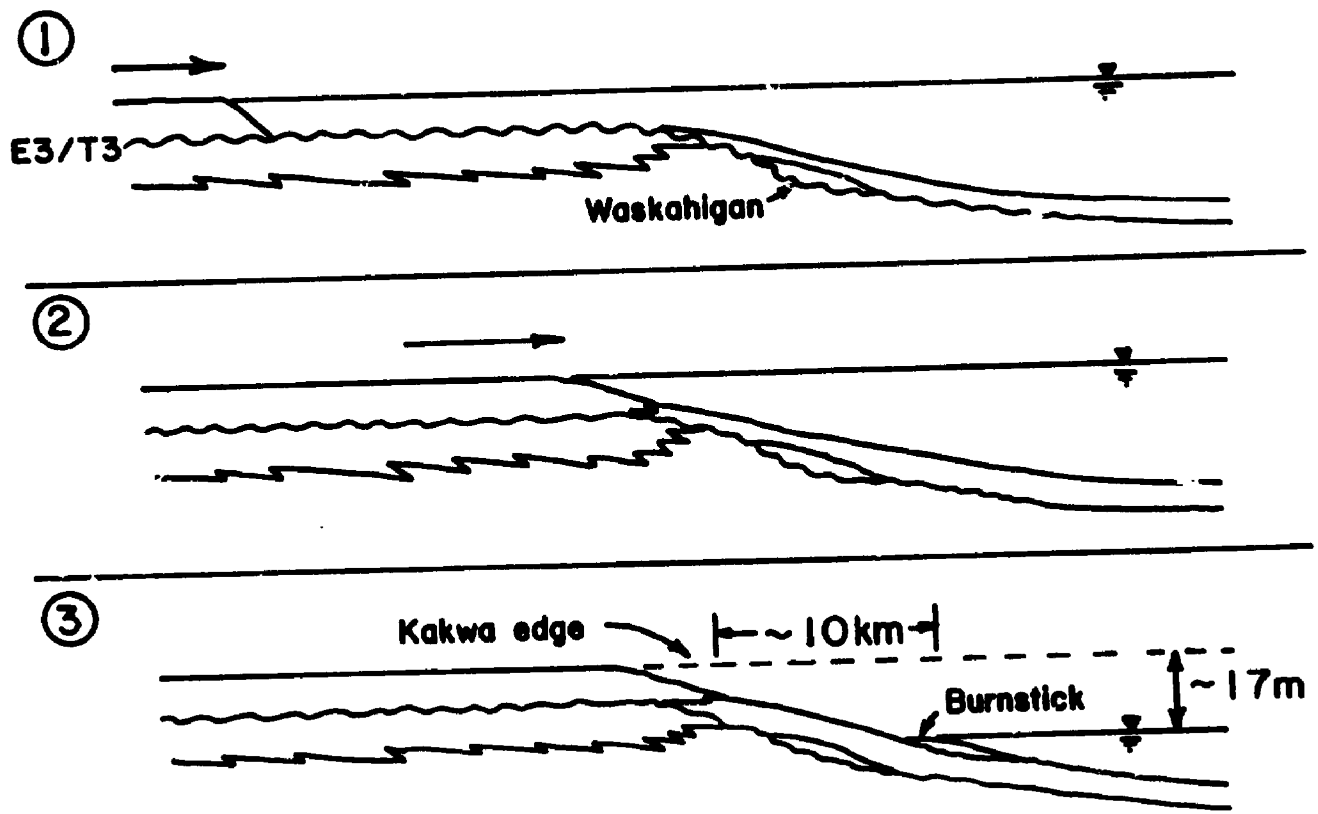
①
E3/T3
Waskahigan
②
③
Kakwa edge
~10km
~17m
Burnstick

not lead to the development of the *lower* shoreline position represented by the Burnstick Allomember. One can see that a similar argument could be made for the origin of the Waskahigan Allomember, and Bergman and Walker (1987) demonstrated that a similar case can be made for the Carrot Creek Allomember. Thus, it can be concluded that fourth order relative sea level fluctuations, superimposed on the overall Mid-Turonian regression, were responsible for the generation of individual allomembers in the Cardium Formation. This mechanism clearly explains the gradual progradation of the "sedimentary prisms" of the E1 to E2, E2 to E3 and E4 to E5 intervals observed in the last chapter (the E3 to E4 interval is an anomaly and will be discussed in Section 7.4).

Given this interpretation, the origin of these fourth order sea level fluctuations must now be addressed. Based on the discussion presented in Chapter 2, I suggest that they could represent either vertical tectonic movements or eustatic sea level changes. The bounding erosion surfaces have now been correlated for a distance of over 600 km along depositional strike (e.g. this study; Plint *et al.* 1988), suggesting an allocyclic generating mechanism.

If tectonic movements were involved, then uplift and subsidence must have been nearly uniform over most of the area covered by the Kakwa Member. In the case of tilting, if the western portion of the basin were to rise with respect to the eastern part, then one should observe evidence of substantial erosional truncation in the west. This appears not to be the case since beach laminated sandstones are preserved at the Murray River section (in the extreme west) at the top of both shoreface sandstone packages of the Kakwa Member (corresponding to the E3 and E4 surfaces). Also, in this case the rate of eustatic sea level fall at the Kakwa edge would have to be greater than the rate of subsidence there, such that the net relative sea level change would bring the shoreline down onto the steeply dipping portion of the E3 and E4 surfaces. In the opposite case, should the western part of the basin subside with respect to the eastern part, the lowered gradients above the Kakwa Member would cut off sediment supply to the shoreline. One might also expect preservation of non-marine strata in the west, and this is not observed for the E3 and E5 surfaces (the origin of the Musreau Member will be discussed later). Thus, if one wishes to invoke vertical crustal movements, these need to have operated uniformly on a regional scale. To my knowledge, such processes have not been documented.

The alternative to tectonic movements involves eustatic sea level changes. To prove this mechanism, one needs to demonstrate correlative sea level fluctuations (both timing and magnitude) in widely-spaced areas. Eustatic fluctuations of this order are considered to have been responsible for the development of fourth order cycles in the mid-Turonian Ferron Sandstone of the United States (Ryer 1983; written communication 1988), although correlation of individual Cardium and Ferron cycles cannot be demonstrated. Unfortunately, as noted in Chapter 2, it is likely that global correlation of fourth order cycles (even if synchroneity were to exist) can never be demonstrated, at least not for deposits of this age.

The main problem with this explanation is that the only known mechanism capable of creating eustatic movements of this scale (10's of meters over 10's of thousands of years) is glacioeustasy (Chapter 2). Although there is growing evidence that the Cretaceous climate was not as warm and equable as once thought (e.g. Sloan and Barron (1990) and references therein), direct evidence of continental ice masses during the Turonian is not observed. This raises the question: Does the sedimentologic and stratigraphic evidence for fourth order eustatic sea level changes from units such as the Cardium Formation (or the overlying Muskiki and Marshybank Formations - *cf.* Plint (*in press*)) force one to accept the presence of Cretaceous ice sheets? Given the present evidence, I will leave this as an open-ended question.

Fifth order cycles

Finally, I suggested in Chapter 3 that the few meter thick sandier upward successions observed in the offshore facies association were generated by climate-controlled variations in sediment supply. This interpretation of these fifth order cycles was suggested by their scale, both physical and temporal, and by comparison with similar units which have been previously so interpreted.

I suggest that climate-controlled variations in sediment supply and/or shoreline progradation rate (?storminess) may also have been responsible for the generation of linear shoreface conglomerate bodies within the Kakwa Member (e.g. Chapter 4) and beach ridge or barrier systems of the type apparently observed at the Bear Mountain locality (Section 6.3.4). If one accepts that climatic forcing can be observed in the offshore deposits, then it does not appear unreasonable to suggest that these same factors could make themselves felt in the littoral zone.

7.2.3 Summary of cycle development

In this section, I have attempted to demonstrate that the evidence of cyclicity observed in the Cardium Formation was produced by allocyclic phenomena. In particular, the two main progradational packages of the formation (E1 to E5 and E5 to E7) appear to have been the result of eustatic sea level drops. Superimposed on these third order fluctuations were fourth order relative sea level fluctuations which were responsible for the generation of individual allomembers. These may have been of glacioeustatic origin, if not, then the forcing mechanism left a sedimentary signature which strongly resembles that developed by glacioeustasy. Fifth order cyclicity in the Cardium Formation probably developed in response to climate fluctuations and the resultant effects on sediment supply.

7.3 The influence of tectonic elements

I believe that there is good evidence to suggest that tectonic elements have played an important, but previously largely unrecognised, role in controlling patterns of sedimentation and erosion during deposition of the Cardium Formation. In this section, I will attempt to defend this contention.

In the last chapter, I presented isopach maps of various intervals within the Cardium Formation, and of the entire formation. In nearly all cases, two main isopleth trends were apparent: a NW-SE thickness trend and a SW-NE thickness trend. In Figure 7.4 I have superimposed what appears to be the average trend for each onto an isopach map of the E1 to E7 interval. The value of the NW-SE trend is about 320°-140°, whereas the SW-NE trend is approximately 235°-55°. A third, more NNW-SSE trend is apparent just west of the B.C. border, is related to fault activity, and will be discussed separately.

7.3.1 Origin of the southwest-northeast trend

The SW-NE trend of the isopachs is parallel to the axis of the Peace River Arch as defined by O'Connell (1988). This relationship strongly suggests a genetic link, since

Figure 7.4. Isopach map of Cardium Formation indicating orientation of main thickness trends (A - 55°-235°; B - about 320°-140°), and known fault positions in British Columbia (C). Thickness trends are parallel to known or inferred basement structures, fault orientations do not correspond to any known basement features.

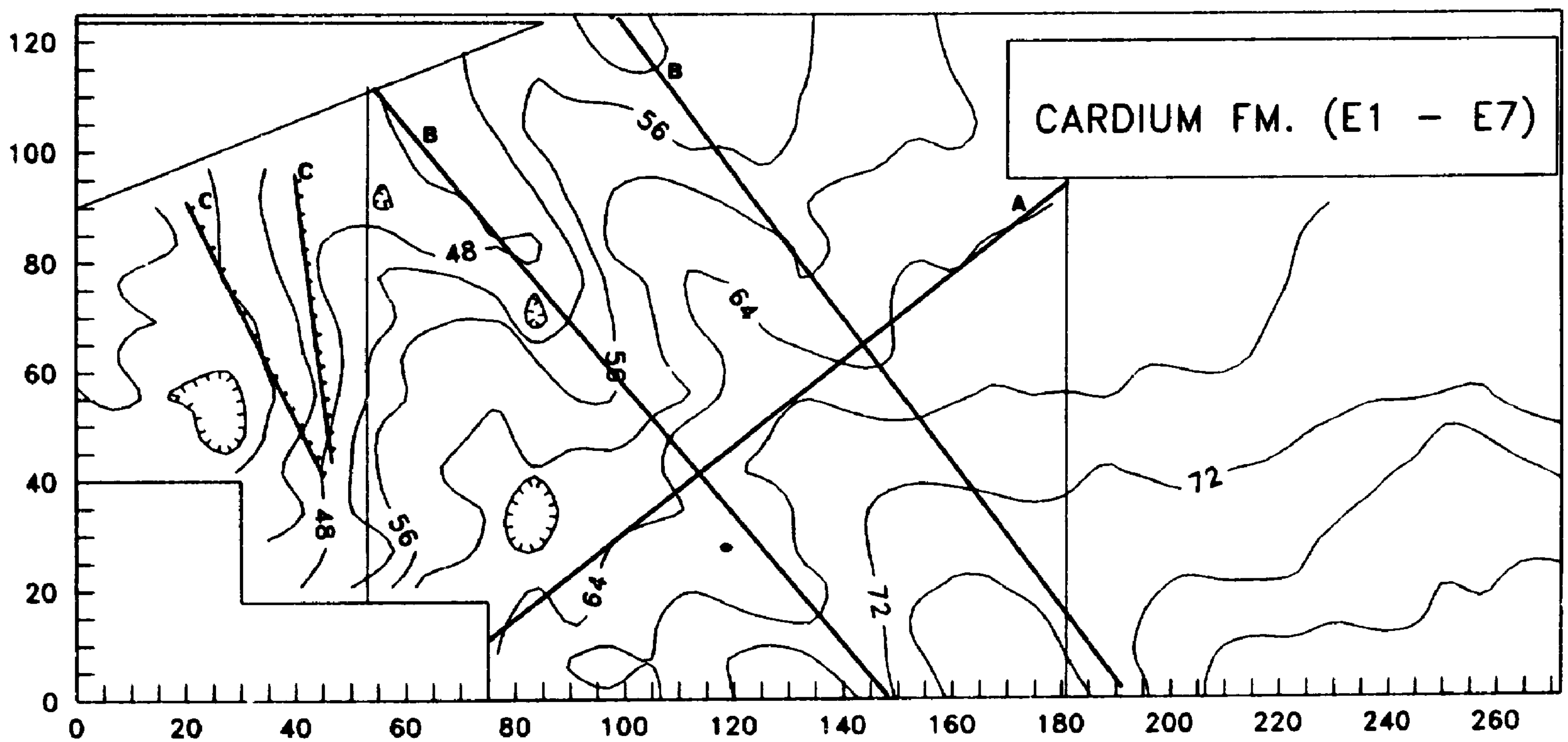
CARDIUM FM. (E1 - E7)
A
B
B
C
C
48
48
56
56
56
64
64
72
72
0
20
40
60
80
100
120
0
20
40
60
80
100
120
140
160
180
200
220
240
260

the arch is known to have started to rise sometime in the Late Cretaceous (e.g. Burk 1962; Norris 1989). The evidence from the mid-Turonian part of the Cardium Formation (Section 6.3) suggests that uplift had begun by about 90 m.a. Evidence for uplift of the Peace River Arch in Coniacian-Santonian times was presented by Norris (1989). Stott (1984) demonstrated that north of the Peace River, an unconformity is found at the top of the Cenomanian Dunvegan Formation, with (?)Coniacian marine shales of the Kotaneelee Formation (approximately equivalent to the Muskiki Formation) lying directly above. These observations suggest a possible phase of uplift of the arch during, and just after deposition of the Cardium Formation.

7.3.2 Origin of the main northwest-southeast trend

The orientation of the thickness variations which trend 320°-140° is also parallel to a number of known or inferred structural elements. These include the Fox Creek Escarpment, an erosional feature developed during the Early Cretaceous, for which a deeper, structural origin is suspected (O'Connell 1988), and a series of inferred basement faults directly under the northern part of the study area (Cant 1988). The strong correspondence between the orientation of Cardium thickness trends and the orientation of these structural elements again suggests a genetic link.

Although the orientation of this trend is close to that of the modern thrust belt, it is also approximately parallel to some much older structural trends. These include the orientation of a possible shear zone in the Proterozoic basement termed the "Chinchaga Low" (Ross and Stephenson 1989). As well, a series of major NW-SE trending basement faults (probably developed during rifting) are inferred to have existed close to this area during Middle Cambrian times (Aitken 1989). I suggest therefore, that the 320°-140° trend reflects remobilisation of these inherited basement faults during the mid-Cretaceous.

This mechanism explains the "bumpiness" of the lower markers (GS-E2) noted in the last chapter, with "highs" reflecting the approximate position of basement uplifts. I suggest that the position of the Kakwa edge was controlled structurally, with an uplifted platform to the southwest, a break in slope (reflected in the E3 and E4 horizons), and a levelling out toward the center of the basin (see Section 6.2). Finally, I would suggest that the location of the major "bevels" on the E5 and E7 surfaces was structurally controlled, for reasons I will now explain.

The E5 and E7 surfaces are different from the other horizons of the Cardium Formation in that they represent major transgressive episodes. The topography (in terms of morphology and absolute relief) on the two surfaces is quite similar. Based on the conceptual model developed in Chapter

2, it seems probable that the transgressions represented by these two surfaces occurred in response to loading in the thrust belt. According to Flemings and Jordan (1990), the forebulge would tend to migrate toward the thrust belt, "stressing" the crust. In a segmented crust, it seems reasonable to assume that a certain amount of the stress would be relieved by differential movement along pre-existing planes of weakness.

The development of erosional bevels in response to this process is illustrated in Figure 7.5. During a period of post-thrust quiescence, the decrease in both absolute rate and asymmetry of subsidence permits shoreline progradation. With renewed thrusting, the crust is stressed and reactivation of basement faults occurs, deforming the surficial units (development of a monocline). In this way, the greatest shoreline erosion thus occurs at breaks in slope. Subsequently, relaxation of the stress field ensues as thrust activity subsides, and faulted blocks return to their original position (or close). In the figure, I have shown the original topography to be nearly planar, but if a depositional break in slope also occurred at this position (a possibility with the E5 bevel), then the results could be accentuated. Also, it is unclear how far upward the fault activity would extend; in some cases, faulting does appear to have offset markers below bevels (e.g. regional cross-section C-C', Chapter 6).

Figure 7.5. Generation of asymmetric bevel by localised warping of the crust. See text for further explanation.

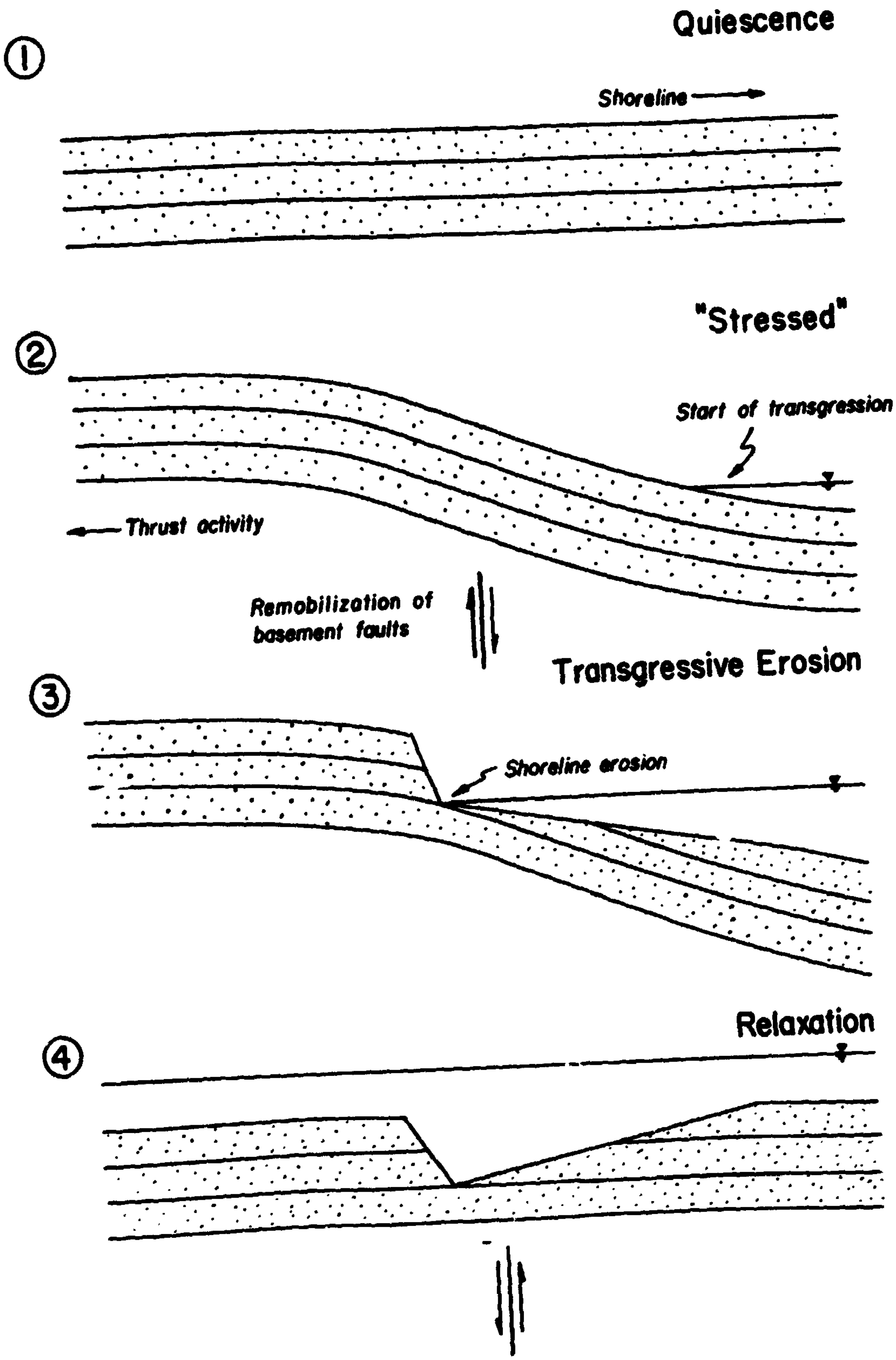
Quiescence
①
Shoreline
"Stressed"
②
Start of transgression
Thrust activity
Remobilization of basement faults
Transgressive Erosion
③
Shoreline erosion
Relaxation
④

This mechanism would explain the connection between bevels and underlying faults noted in regional cross-section C-C' (Section 6.2.3). It provides a mechanism for deforming and eroding a portion of the basin, without tilting the entire basin floor (Section 7.2). Finally, it explains why the E3 surface and the M1 Datum (the first forming just before peak regression, the second forming just after peak transgression (Plint 1990)) are nearly parallel.

To distinguish bevels generated by the tectonic mechanism described here and those related to pauses in transgression (stillstands), I suggest examining a substantial thickness of the stratigraphic record of the area in question for other possible evidence of structural activity. For example, in the case of the E5 bevel in regional cross-section C-C', there exists evidence for fault activity below that surface, evidence for substantial erosion below the Bad Heart Formation (with a trend which closely corresponds to the E5 bevel; S. Donaldson *pers. comm*), and evidence for underlying basement structures. This type of activity may not be detected if the stratigraphic interval studied is too thin.

7.3.3 Faulting in British Columbia

The faults just west of the B.C. border do not appear to have the same strike as the NW-SE trending thickness patterns. Their position is constrained by matching well log responses from wells included on cross-sections to neighbouring wells which were not. These faults may have developed prior to the development of the E5 surface, as this does not seem to be displaced where it is preserved (*cf*. regional cross-sections B-B' and C-C', Section 6.2). The mechanism responsible for their origin is unknown, but may be related to uplift of the Peace River Arch. I am unaware of any map which illustrates the position and orientation of basement lineaments in this part of the study area.

7.3.4 Application to other parts of the Cardium Formation

The evidence of syn-Cardium tectonic movements presented above leads one to ask whether similar processes might have been operative elsewhere in the Cardium Formation. In Figure 7.6 I present two cross-sections through the Cardium Formation just south of the present study area. In both cases, there appears to be an offset of the E3 horizon and the top and bottom of the Kakwa Member, with the downthrown side to the south/southwest. If these four points can be used to constrain the location of a possible fault, it orientation would have to be very close to the 320°-140° trend noted above. This location and orientation are closely related to the location of the thin sharp-based shoreface sandstones of the Kakwa Member and a greater thickness of Musreau Member (Plint 1988), the position of a major bevel in the E7 surface and concentration of conglomerate in the Amundson Allomember (Wadsworth 1989) and

Figure 7.6. Possible evidence for fault activity in the Cardium Formation from the Kakwa Field, south of the present study area. Fault is recognised by offset of E5 and lower horizons, and its trend corresponds to production trend of the Kakwa Field.

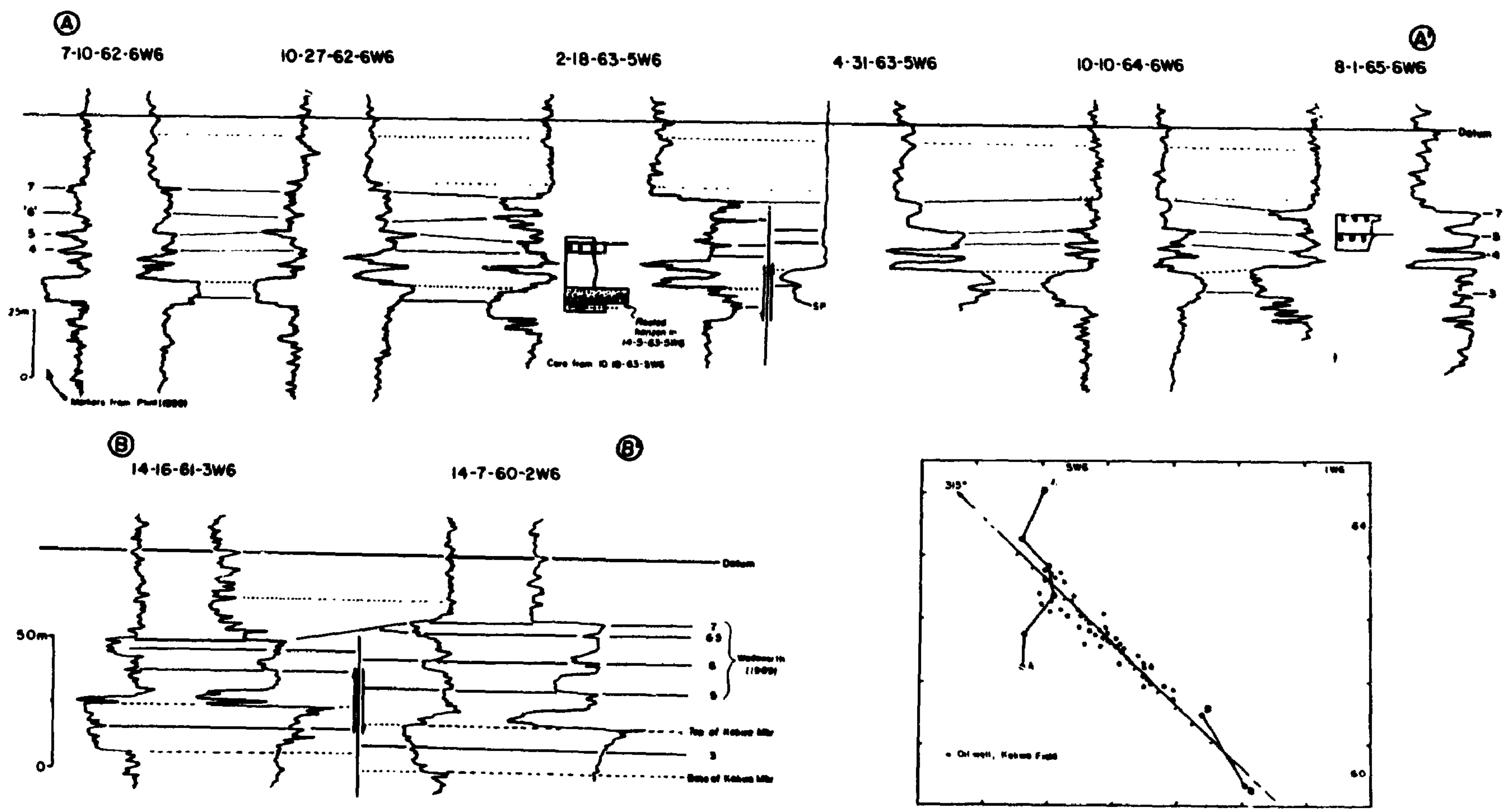
A
7-10-62-6W6
10-27-62-6W6
2-18-63-5W6
4-31-63-5W6
10-10-64-6W6
8-1-65-6W6
A'
Datum
25m
0
SP
B
14-16-61-3W6
14-7-60-2W6
B'
50m
Datum
Top of Kobes Mbr
Base of Kobes Mbr
5W6
1W6
64
60
Oil well, Kobes Field

ultimately, the production trend of the Kakwa field (unpublished map furnished by Home Oil Co. Ltd.).

Further south, the production trends of the Caroline and Garrington fields were outlined by Pattison (1988) who related them to development of linear shoreface deposits of the Burnstick Allomember; I have shown these trends in Figure 7.7. Wadsworth (1989) presented a map showing "lows" and "highs" on the E7 surface, and I have superimposed the outline of the lows from this area onto the map containing the Burnstick trends. The reader will notice the close correspondence between the two trends. Although both Pattison (1988) and Wadsworth (1989) suggested that incision of their respective surfaces was generated by stillstands, it is exceedingly difficult to conceive why two separate transgressions should slow down in exactly the same place - unless there were subtle (?structurally controlled) topographic features which controlled rates of shoreline displacement and erosion.

Jones (1980) presented a series of structural cross-sections through the Alberta Basin in which he presented evidence of the existence of widespread vertical faults. Some of these faults appear to have offset the Cardium Formation in production fields such as Pembina and Garrington, and their orientation appears to closely correspond to the trends of "bevels" in those areas. These observations suggest a genetic link, although I have not

Figure 7.7. Possible evidence for fault activity in the Caroline/Garrington area. Trends in the distribution of lowstand shoreface deposits of the Burnstick Allomember (associated with the E4 horizon) are matched quite closely by trends in topographic "lows" on the E7 surface. Data from Pattison (1988) and Wadsworth (1989) respectively.

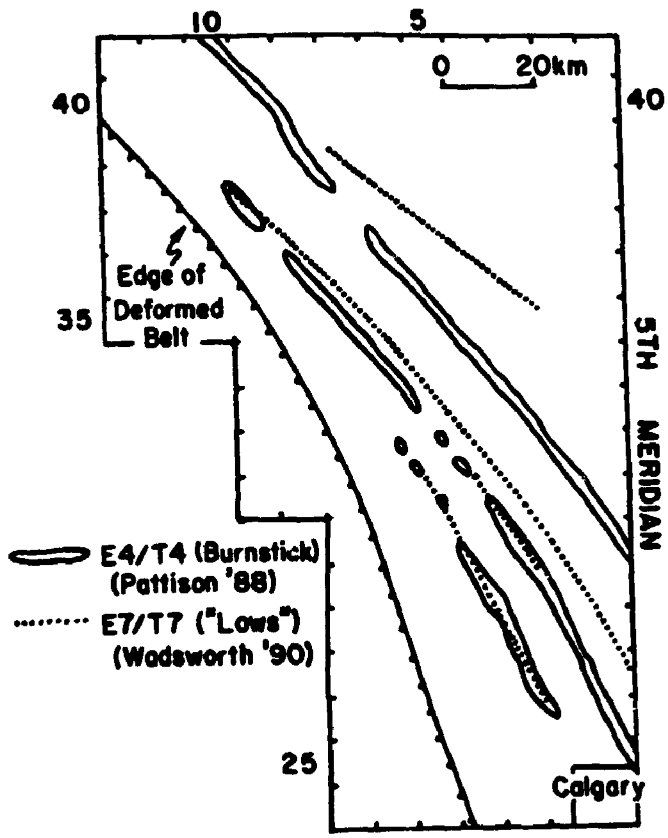

10
5
0 20km
40
40
Edge of Deformed Belt
35
5TH MERIDIAN
E4/T4 (Burnstick) (Pattison '88)
E7/T7 ("Lows") (Wadsworth '90)
25
Calgary

tested this possibility in great detail. Jones suggested that these faults represented reactivated basement faults, an idea which is supported by the interpretations presented in this study. Although I do not agree with all of Jones' interpretations, I accept his observations; these seem to have been ignored by members of the McMaster Cardium Group.

Finally, the existence of tectonically-produced breaks in slope can explain why certain erosion surfaces in the Cardium Formation have lowstand deposits whereas others do not. The E3, E4, E5 and E7 surfaces all have tectonically produced topography, and hence shoreline incision would have been concentrated along the steeply-dipping portions of those surfaces. No major breaks in slope are associated with the E1, E2, E6, or E6.5 surfaces, hence no incised shoreline positions developed. This model could help explain why incised lowstand shoreline deposits are found in units such as the Cardium Formation, whereas they are absent in units such as the Spirit River Formation (Cant 1984) or Ferron Sandstone (Ryer 1981).

7.4 Summary of the Depositional History of the Cardium Formation

In this chapter, it has been suggested that the Cardium Formation developed in response to two main third order eustatic sea level drops, upon which were superimposed fourth order relative sea level fluctuations and contemporaneous tectonic movements. The latter appear to have resulted from reactivation of basement faults underlying the study area, and there is at least some evidence that such activity may have been active elsewhere in the basin (i.e. further south) during deposition of the Cardium Formation. The fourth order sea level fluctuations can best be pictured in terms of rapid sea level rises (transgression) followed by stillstands (progradation) and relatively short-lived lowstands (see Fig. 2.2 to see how subsidence can combine with a sinusoidal eustatic curve to produce such a relative sea level curve).

In this final section, I wish to illustrate (via a series of cartoons) how these factors appear to have interacted to produce the stratal relationships observed in the present study area. Given the poor preservation and exposure of the E5 to E7 interval in this area, the depositional history of that part of the formation will not be illustrated in such great detail as the E1-E5 portion.

I have begun the series of figures with the E1 transgression, developed during relative sea level rise (Fig. 7.8a). As noted in the far west, this surface overlies at least 10 m of shoreface sandstones. Shoreline progradation followed, resulting in deposition of the Kakwa Member and the Nosehill Allomember (E1 to E2 interval; Fig. 7.8b). A lowstand and relative sea level rise ensued, with the E2 surface forming during transgression. Note that no incised shoreline was formed during lowstand, as a distinct

Figure 7.8. Reconstruction of the depositional history of the Cardium Formation in the present study area. A) Top, B) Middle, C) Bottom. See text for details.

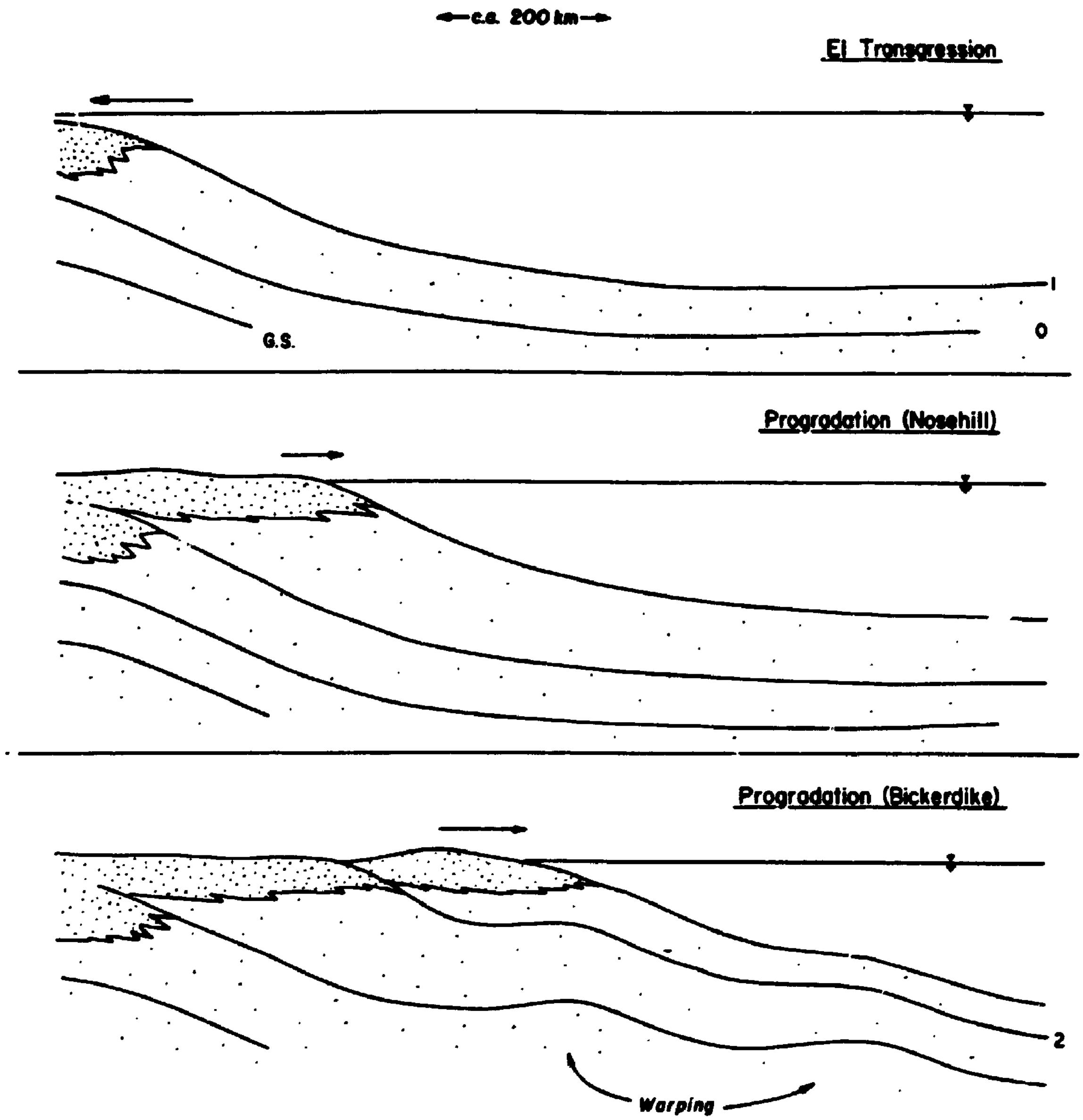

←c.a. 200 km→
El Transgression
G.S.
1
0
Progradation (Nosehill)
Progradation (Bickerdike)
2
Warping

Figure 7.8 (cont.) Reconstruction of the depositional history of the Cardium Formation. D) Top, E) Second from top, F) Third from top, G) Bottom. See text for details.

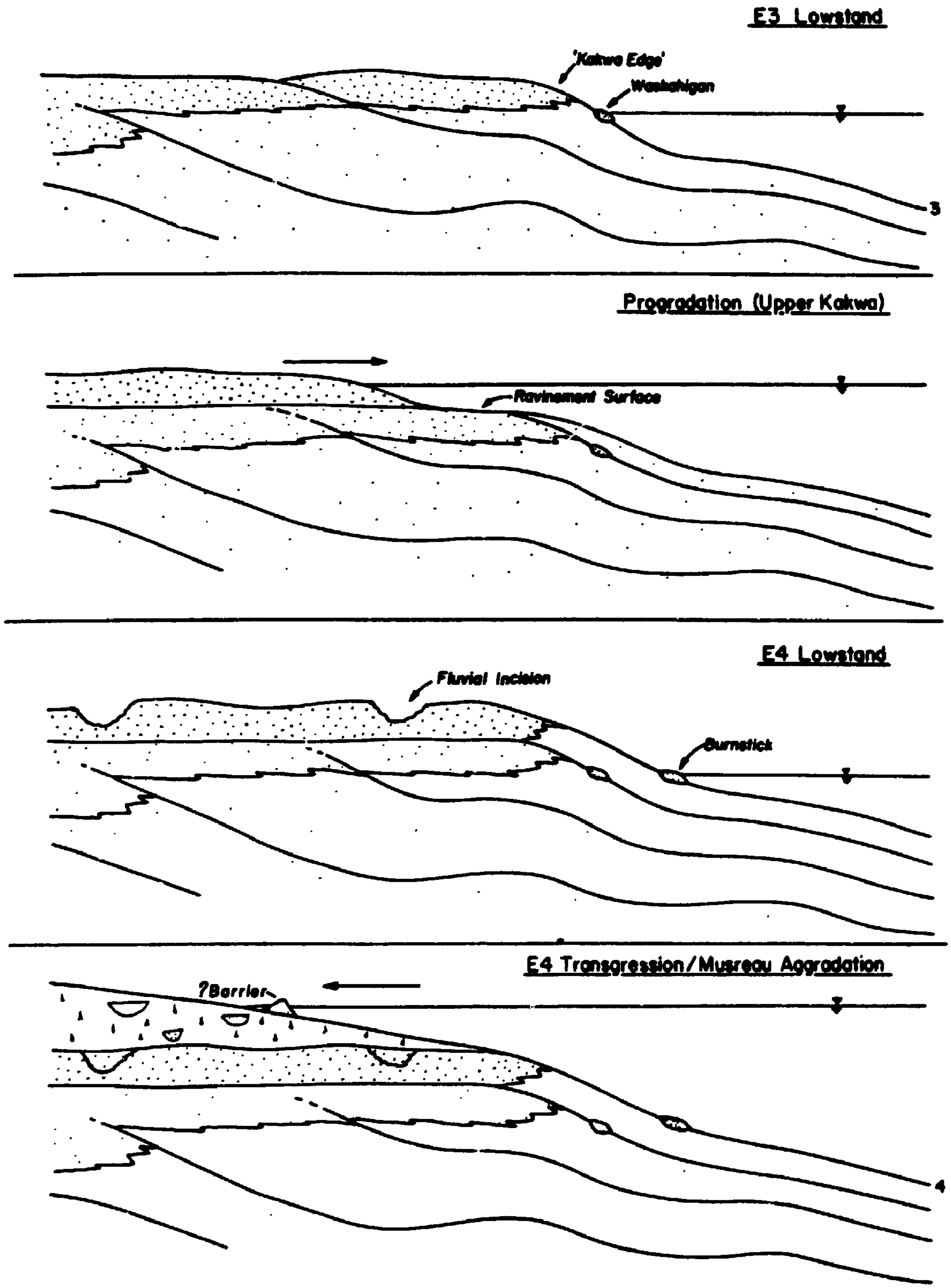
E3 Lowstand
'Kakwa Edge'
Waskahigan
3
Progradation (Upper Kakwa)
Ravinement Surface
E4 Lowstand
Fluvial Incision
Burnstick
E4 Transgression/Musreau Aggradation
?Barrier
4

Figure 7.8 (cont.) Reconstruction of the depositional history of the Cardium Formation. H) Top, I) Bottom. See text for details.

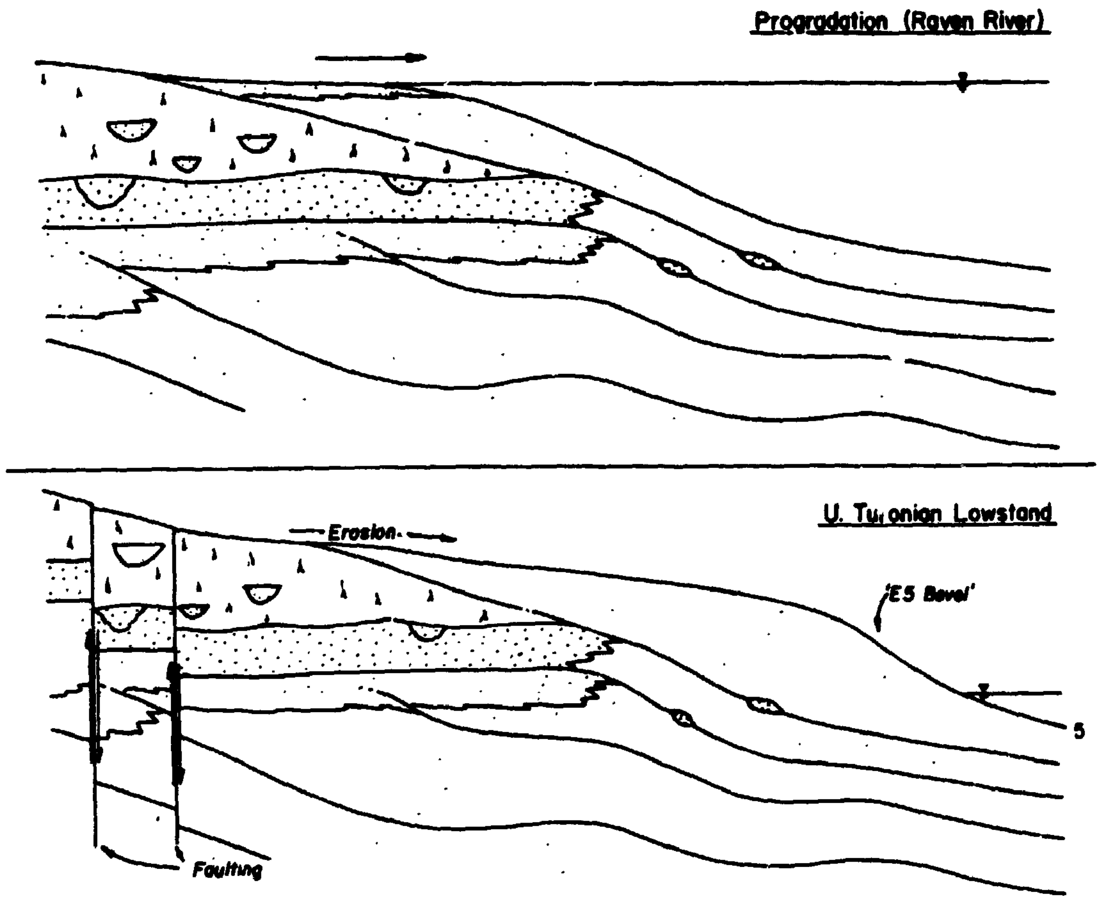
Progradation (Raven River)
U. Tu,onian Lowstand
Erosion
'E5 Bevel'
5
Faulting

Figure 7.8 (cont.) Reconstruction of the depositional history of the Cardium Formation. J) Top, K) Bottom. See text for details.

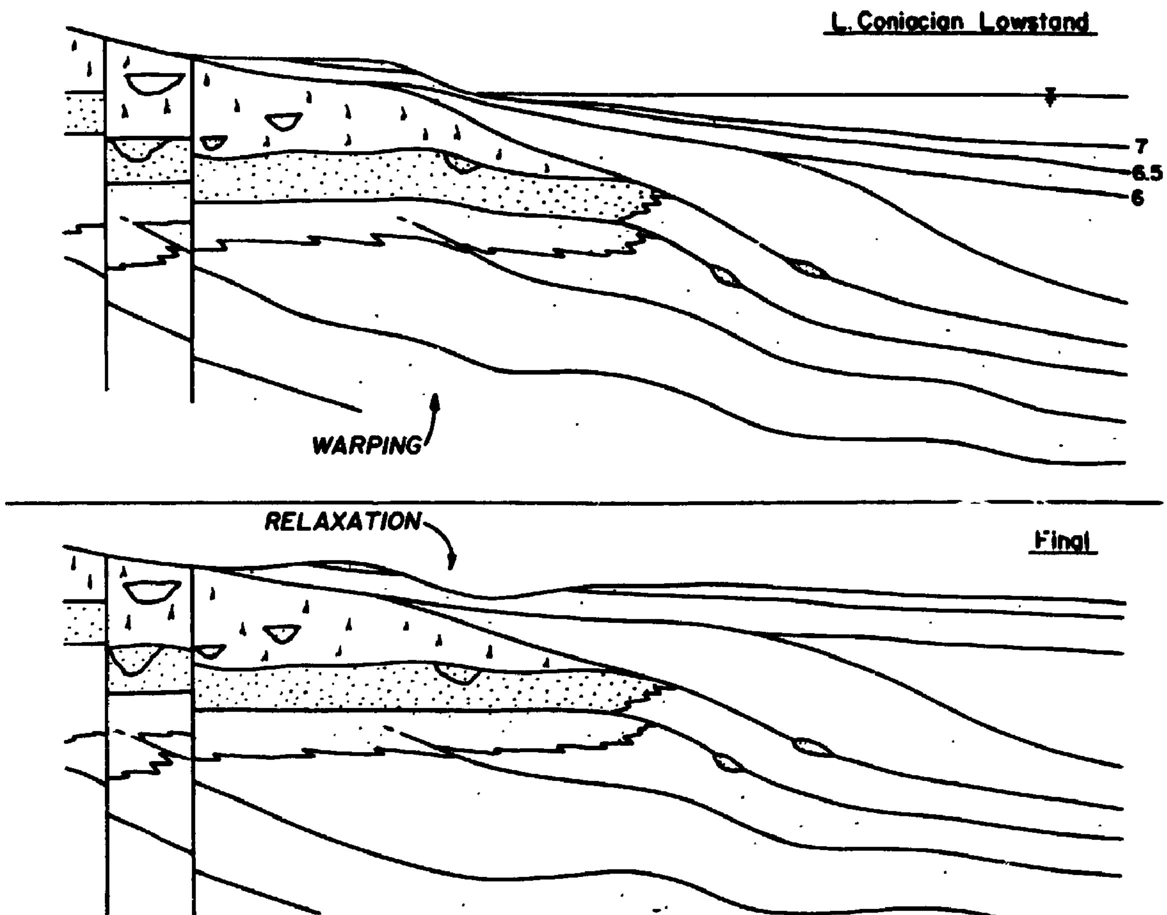
L. Coniacian Lowstand
7
6.5
6
WARPING
RELAXATION
Final

break in slope was not present.

The lower package of the Kakwa Member advanced again during the next progradational phase, while the Bickerdike Allomember developed offshore (Fig. 7.8c). Note that the top of the shoreface sandstone body, like the top of the upper shoreface package developed later, was probably not completely flat. Some prior reactivation of basement faults led to warping; one of these uplifts subsequently controlled the position of the Kakwa Edge. The shoreline position dropped down below the break in slope during lowstand, leading to shoreline incision and deposition of the Waskahigan Allomember (Fig. 7.8d). As relative sea level rose, the shoreline rose to the top of the main shoreface unit, then very quickly moved landward. Transgressive erosion eroded most beach laminated or rooted deposits from the top of the underlying shoreface unit, leaving them only in low-lying areas (explaining why they are only locally preserved). The ravinement surface (E3) developed in this way was nearly planar. Some of the sand eroded was pushed landward under the influence of shoaling waves (Chapter 4), whereas some was left on the transgression surface as palimpsest deposits to be reworked by shelf currents and during the next progradational phase.

Progradation of the upper portion of the Kakwa Member began during the ensuing relative sea level highstand (Fig. 7.8e). Sand and gravel (e.g. the conglomerate at Bay Tree) were supplied from both rivers and the palimpsest deposits of the shelf, which may have been above fairweather wave base. Shallow lagoons formed behind beach ridge/barrier systems developed during periods of slower progradation (minor transgressions?) caused climatically. Note that the shoreface could not prograde further than the Kakwa edge, since the bottom slope was too great beyond this point. During lowstand, shoreline incision below the Kakwa edge led to the formation of the Burnstick Allomember (Fig. 7.8f). Rivers crossing the coastal plain incised the upper shoreface sandstone package at this time.

The shoreline position was located far enough from the Kakwa edge (both horizontally and vertically) that as base level rose (with relative sea level rise), the coastal plain southwest of the Kakwa edge had time to respond and start aggrading (Fig. 7.8g). In the last chapter, I presented my arguments against significant fluvial deposition (Musreau Member) during progradation of the upper package of the Kakwa Member. Non-marine aggradation far from the coast during relative sea level *rise* also appears to have occurred in the Carboniferous Boss Point Formation (G. Browne, *pers. comm.*) of New Brunswick. These interpretations are not consistent with the theoretical model of Posamentier and Vail (1988), which predicts fluvial aggradation during relative sea level *fall*. Aggradation rates of 30 cm per 100 years are probably typical of floodplains of anastomosing river systems (Smith 1983). At this rate, the entire Musreau Member (about 30 m maximum thickness in this area) could have accumulated in about 10^4 years.

The establishment of fluvial deposition above the Kakwa Member in advance of the transgressing shoreline probably helped slow down the subsequent rate of shoreline displacement. Thus a positive feedback loop was established, and even more potential for non-marine aggradation was created. Transgressive erosion of the rapidly-deposited muddy sediments led to the formation of the E4 surface. Some of the material eroded may have been transported seaward and deposited as the basal portion of the Raven River Allomember.

The progradational phase of the Raven River Allomember began approximately with the next relative sea level stillstand (Fig. 7.8h). Sediment was supplied from both the thrust belt and erosion of the fine-grained deposits of the Musreau Member. Climate-induced fifth order cycles are well-developed in the upper portions of this interval. Shoreface sand deposits, if developed, were cannibalised and redeposited offshore. This relationship suggests deposition during a relative sea level fall. It may be that the rate of eustatic sea level fall began to significantly outstrip the rate of subsidence.

Normal faulting in the western part of the study area preceded the E5 transgression (Fig. 7.8i). Thrusting to the southwest led to reactivation of basement faults, warping (with minor faulting) of the mid-Turonian package, and shoreline incision during transgression (E5).

Progradation during the early Coniacian eustatic sea level fall was punctuated by 3 fourth order relative sea level fluctuations. These resulted in the deposition of the E5 to E6, E6 to E6.5 and E6.5 to E7 intervals. Subsidence rates over the Peace River Arch were lower than further south, and preservation of these intervals is less in the north. Finally, renewed thrust activity in the west again led to reactivation of basement structures and high subsidence rates leading to transgression (Fig. 7.8j, see Fig. 7.5). The topography on the E7 surface was produced at this time. Relaxation of the crust (following thrust loading) ensued, and the topography on the E7 surface was buried (Fig. 7.8k).

CHAPTER 8

CONCLUSIONS

Here, I wish to summarise my findings by listing a series of numbered conclusions.

1) The Cardium Formation consists of siliciclastic offshore, shoreface (and beach), and non-marine strata which comprise a succession of nested, cyclically deposited units developed in response to transgressive/regressive shoreline movements on various temporal scales.

2) The formation can be divided into two main progradational packages, a mid-Turonian portion and a dominantly lower Coniacian portion. They are separated by the E5 surface of Plint *et al.* (1986). They correspond to third order eustatic cycles on the Haq *et al.* (1987) global eustatic curve.

3) Fourth order relative sea level fluctuations (about 10^5 years duration) were responsible for the development of individual allomembers of the Cardium Formation. Their origin is uncertain. The stratigraphic framework proposed by Plint *et al.* (1986, 1987, 1988) for the Cardium Formation further south has been shown to be, on the whole, a workable model for the formation in the present study area. Certain modifications need to be applied however, and it is uncertain whether they need to be extended to more southerly areas.

4) Fifth order cycles are represented by few-meter thick sandier upward successions in offshore units, and possibly by certain features of the shoreface sandstones and conglomerates of the Kakwa Member. These probably are related to climate fluctuations.

5) The Kakwa Member represents the shoreface (to beach) portion of the lowest three allomembers. It consists two main portions: a) a lower part (equivalent to the Nosehill and Bickerdike allomembers) consisting principally of swaley cross-stratified very fine- to fine-grained sandstones with local preservation of beach laminated sandstones and rooted horizons at its top; and b) an upper portion (equivalent to the Bickerdike Allomember) which is usually coarser-grained (generally medium- to fine-grained sandstone) and medium scale cross-bedded to planar laminated, with a rooted horizon developed at its top. Early diagenetic siderite rhombs, quartz overgrowths and detrital carbonate grains are often present in the lower unit, but are absent in the upper portion of the member. The contact between the two parts of the Kakwa is interpreted as a ravinement surface developed during the E3 transgression, and was originally near-horizontal.

6) Aggradation of the non-marine strata of the Musreau Member probably occurred during relative sea level rise. This contrasts with the predictions of sequence stratigraphic models proposed by EXXON workers (e.g.

Posamentier and Vail 1988).

7) Conglomerates are locally present in the Kakwa Member, and generally represent shoreface or beach deposits. In agreement with previous studies, I have found that bed lenticularity decreases and clast segregation increases as the depositional influence of wave (*versus* fluvial) activity becomes more evident. Other criteria which have proven helpful in distinguishing wave-reworked from fluvial conglomerates include paleocurrent evidence, stratigraphic position, sedimentary structures (although shoreface conglomerates may have a tendency to be massive) and grain size trends. Clast shape is not a good discriminator between fluvial and shoreface conglomerates. Lenticular conglomerates may be present in shoreface deposits if they were deposited (e.g. by rip currents, or near river mouths) then buried below the influence of wave reworking.

8) I attempted to correlate the isotopic and elemental composition of early diagenetic siderite with inferred depositional water depth of the Mistanusk Creek section. Previous studies had suggested that both of these compositional variables are at least partially controlled by the salinity of the water from which it precipitates. The results match those which would be predicted based on the sedimentology and stratigraphy of the section.

9) Basement structural elements appear to have had a greater influence on patterns of deposition and erosion than

previously envisaged for the Cardium Formation. A thickening trend to the southeast probably reflects the upward movement of the Peace River Arch during deposition of the formation. Northwest-southeast trending basement features probably controlled the location of the basinward edge of the Kakwa Member, and the E5 and E7 bevels. These last two surfaces represent major marine flooding surfaces. In part, the topography on them may reflect reactivation of basement faults in response to thrust loading. The presence of a distinct break in slope at the Kakwa edge is largely responsible for the presence of incised lowstand shoreface deposits associated with the E3 and E4 surfaces. The possible role of tectonic elements during deposition of the Cardium Formation needs to be examined in greater detail to the south of my study area.

APPENDIX 1

CARDIUM FORMATION - MEASURED SECTIONS

SUMMER 1987 & SUMMER 1988

LOCALITY	NO. OF SECTIONS	MAP SHEET	ACCESS[1]	LATITUDE[2]	LONGITUDE
Mistanusk Creek	1	93-I/9	H	54°41'	120°05'
Cutpick Hill	2	83-L/3	H	54°04'	119°10'
Calliou Creek	2	93-I/16	H	54°45'	120°28'
Fellers Heights	1	93-P/10	R	55°36'	120°35'
Gundy Station	1	93-P/9	R	55°36'	120°02'
Mount Miles	12	93-P/6	H	55°25'	121°18'
Murray River	1	93-P/2	H/W	55°15'	120°43'
Pouce Coupé	1	93-P/9	R	55°39'	120°07'
Fellers Heights II	1	93-P/10	R	55°32'	120°43'
South Dawson	1	93-P/9	R	55°41'	120°21'
Bay Tree	8	83-M/13	W	55°46'	119°54'

[1] H - Helicopter; W - Walking; R - Roadside

[2] Latitude and longitude rounded to nearest minute

CARDIUM FORMATION - MEASURED SECTIONS

SUMMER 1987 & SUMMER 1988

LOCALITY	NO. OF SECTIONS	MAP SHEET	ACCESS	LATITUDE	LONGITUDE
Bear Mountain	6	93-P/9	W	55°40'	120°24'
Muskeg River Railroad	1	83-E-15	R	53°56'	118°54'
Hat Mountain	1	83-L/5	H/W	54°17'	119°40'
Coldstream Creek	1	93-P/10	R	55°34'	120°52'
Smoky River	1	83-M/9	W	55°33'	118°12'
Horseshoe Mountain	4	93-I/16	H	54°48'	120°51'
Coldstream Creek II	1	93-P/11	R	55°36'	120°51'
Noetai Hill	1	93-P/11	H	55°30'	121°05'
Cutbank Lake	3	83-M/12	W	55°43'	119°46'
Tepee Creek	1	93-P/7	W	55°19'	120°56'

MEASURED CORE SACTIONS

1988 - 1989

BRITISH COLUMBIA

d-95-A 93-P-1	c-98-A 93-P-1	a-3-B 93-P-1	c-22-B 93-P-1
b-82-B 93-P-1	c-16-I 93-P-1	b-66-L 93-P-1	c-52-A 93-P-1

ALBERTA

11-35-75-8W6	6-22-75-7W6	14-18-74-12W6	10-1-74-11W6
8-32-74-9W6	13-24-73-10W6	4-10-72-13W6	6-8-71-13W6
6-18-71-12W6	6-9-71-3W6	6-8-70-13W6	9-2-70-13W6
10-7-70-11W6	11-3-70-11W6	15-5-70-2W6	6-28-69-13W6
6-16-69-13W6	6-28-69-12W6	6-24-69-12W6	10-26-69-11W6
15-16-68-13W6	10-7-68-13W6	7-1-68-12W6	6-20-68-10W6
7-10-68-10W6	6-7-68-8W6	7-14-68-7W6	11-6-68-2W6
16-25-67-11W6	10-2-67-9W6	8-23-67-8W6	2B-11-67-8W6
6-7-67-8W6	10-1-67-8W6	13-7-67-7W6	10-31-67-4W6
6-36-66-8W6	16-30-66-7W6	3-26-66-7W6	6-19-66-7W6
11-7-66-4W6	6-15-65-13W6	10-21-65-7W6	11-22-65-6W6
8-1-65-6W6	10-18-65-23W5	10-18-63-5W6	14-5-63-5W6
10-10-52-17W5			

APPENDIX B

GW-BASIC PROGRAM FOR ISOPACH DATA ENTRY

The isopach and surface diagrams presented in Chapter 6 were constructed using databases created with and subsequently manipulated by a GW-BASIC program created by the author. These files were then employed as input into the *Surfer* package (version 4.0, by Golden Software Co.). I chose to create my own programs because I was unaware of any existing software (although it probably exists) which would allow me to perform the data manipulations I wished. My previous (albeit limited) experience with the language suggested that these manipulations could be quite readily performed with a series of simple BASIC operations.

The main advantages of using a computerized contouring program are that it allows large amounts of data to be stored, transformed and presented in a variety of fashions according to the wishes of the geologist. Once the operator is familiar with a system, output such as isopach maps can be computed and then drawn in a fraction of the time it would take to prepare the same map by hand. It should be noted however that the output of these programs must be viewed only as the software's *interpretation* of the data, and not necessarily as an objective reality. On the contrary, as the number of control points becomes greater and they become more tightly spaced, the freedom of the software to produce "errors" becomes more limited.

The original data file (here termed WELL.DAT) was made available from Home Oil Co. Ltd. in Calgary in the summer of 1988. It listed all the then available wells in the area between TWP 65 and TWP 80 from RGE 15W5 into British Columbia. For each well, the data given included: a) the well location; b) latitude; c) longitude; d) actual (A) or theoretical (T) latitude and longitude; e) well status; f) vendor code; g) total depth; h) formation at total depth; i) code for formation at total depth; j) operator; k) kelly bushing (KB) altitude; l) rig release date; m) well release date. Of this information, only items a, b, c and k were employed for this study.

The WELLDAT.BAS program which I have written can be used to create data files from which one can produce isopach maps, surface diagrams and structure maps/diagrams with the *Surfer 4.0* package. These data files can be read directly by the GRID.EXE program of that package. Upon initializing the WELLDAT.BAS program, the user will be presented with a series of options, which I will outline below. I have organized WELLDAT.BAS into a main "umbrella" portion, from which one proceeds to various subroutines according to one's selections.

```
10 REM Program "WELLDAT"
12 REM Used - to create data files
13 REM      - to select wells from WELL.DAT file & write to
a well file
20 REM       - to assign horizon picks tc well locations in
a well file
25 REM       - to edit pre-existing data in a well file
```

```
30 REM      - to generate isopach data from two well files
35 REM       - to create structure data from a single well file
40 REM
45 REM Isopach files for use as data files for "SURFER" program
50 REM
60 CLS
70 PRINT "PROGRAM WELLDAT"
80 PRINT:PRINT
90 PRINT "Choose your selection :"
91 PRINT:PRINT TAB(10) "1.     Create a data file"
92 PRINT:PRINT TAB(10) "2.       Add wells to personal database file"
100 PRINT:PRINT TAB(10) "3.    Enter new data to well file"

110 PRINT:PRINT TAB(10) "4.    Edit existing data in a well file"
120 PRINT:PRINT TAB(10) "5.     Generate isopach file from existing well files"
125 PRINT:PRINT TAB(10) "6.    Create a structure data file from a well file"
126 PRINT:PRINT TAB(10) "7.     End session"
130 PRINT:PRINT:INPUT "Your choice (1-7) : ";CHOICE
135 IF CHOICE = 7 GOTO 155
140 ON CHOICE GOSUB 1000, 2000, 3000, 4000, 5000, 6000
145 GOTO 60
155 CLS:PRINT "That's all folks !"
165 SYSTEM
```

The first step involves selecting the desired wells from the WELL.DAT file and creating a separate file to act as the personal database for the ensuing data input. This step is performed using selection #1 of the WELLDAT.BAS main menu. Once the personal database file has been created, the user *must not* re-create the file with selection #1, as any existing data in the file will be lost. It should be noted that the user must open "well files" (see below) in the same manner.

```
1000 REM Subroutine to create files for later data input
1010 REM
```

```
1020 CLS
1030 PRINT "WARNING !!!"
1040 PRINT:PRINT "Do not create a file using a pre-existing
file name"
1050 PRINT "unless you wish to lose the current contents of
that file !!"
1060 PRINT:INPUT "Prefix of file to create (______.DAT)
";PREF$
1070 FIL$ = PREF$ + ".DAT"
1080 OPEN "o",#1,FIL$
1090 CLOSE
1100 PRINT:PRINT " File ";FIL$; " has been opened "
1110 PRINT: INPUT "Enter 1 to continue, anything else to
return to main menu ";  AN$
1120 IF AN$ = "1" THEN GOTO 1030
1130 PRINT "We now return to the main menu"
1140 FOR I = 1 TO 2000: NEXT I
1150 RETURN
```

Selection 2 of the main menu allows the user to select the wells he/she desires. The well location, latitude, longitude and KB altitude are written to the personal database file. More than one session with selection #2 will probably be required to complete the selection procedure. Once the file is created, all subsequent sessions with selection #2 will simply add new choices to the existing personal database.

```
2000 REM Subroutine to add selected wells (from Well.dat
file)
2010 REM to an existing output data file
2020 REM
2030 REM
2040 CLS:INPUT "Enter prefix of output data file
(______.DAT) ";PREF$
2050 FILOUT$ = PREF$ + ".dat"
2060 OPEN "r", #1, "well.dat",113
2070 OPEN "i", #2, FILOUT$
2080 IF EOF(2) THEN GOTO 2110
2090 INPUT #2, J, W1$, LAT1, LONG1, KEL1
2100 GOTO 2080
2110 BEEP:BEEP:CLS:PRINT "Well selection, output file:
";FILOUT$
```

```
2120 PRINT:PRINT J; " wells saved to date"
2130 PRINT:PRINT "Last well saved: ";W1$
2140 CLOSE #2
2150 PRINT:PRINT "MAKE SURE CAPS LOCK IS ON NOW !!!"
2160 PRINT:INPUT "<CR> TO CONTINUE"; CR
2170 PRINT:PRINT:PRINT "SEARCHING FOR NEXT WELL"
2180 N=J+1
2190 K=J
2200 FIELD #1, 24 AS WELL$, 9 AS LAT$, 11 AS LONG$, 2 AS AT$, 3 AS STAT$, 7 AS VEN$, 7 AS TD$, 5 AS TDFM$, 8 AS FMAGE$, 11 AS OPERAT$, 6 AS KELLY$, 9 AS RIGDAT$, 11 AS WELDAT$
2210 IF J=0 THEN K=0:GOTO 2260
2220 GET #1, K
2230 IF W1$=RIGHT$(LEFT$(WELL$,18),14) THEN GOTO 260
2240 K=K+1
2250 GOTO 2220
2260 OPEN "A", #2, FILOUT$
2270 PRINT:INPUT "ALBERTA (1) OR B.C. (2) WELLS "; ANS
2280 FOR I = K+1 TO 10000
2290 IF EOF(1) THEN GOTO 2430
2300 GET #1, I
2310 IF ANS = 1 THEN GOSUB 2500 ELSE GOSUB 2600
2320 CLS:PRINT "WELL:      ";W$:PRINT:PRINT
2330 PRINT "ENTER 1 TO KEEP WELL":PRINT
2340 PRINT "ENTER 2 TO DELETE WELL":PRINT
2350 PRINT "ENTER 3 TO CHANGE WELL NAME TYPE (ALTA/BC)":PRINT
2360 PRINT "ENTER 4 TO STOP":PRINT
2370 INPUT "SELECTION ";SEL
2380 ON SEL GOTO 2390, 2400, 2410, 2430
2390 WRITE #2, N, W$, VAL(LAT$), VAL(LONG$), VAL(KELLY$):GOTO 2420
2400 GOTO 2420
2410 GOTO 2270
2420 N=N+1:NEXT I
2430 CLOSE
2440 PRINT:PRINT "We now return to the main menu "
2450 FOR I = 1 TO 2000:NEXT I
2500 W$=RIGHT$(LEFT$(WELL$,18),14)
2510 RETURN
2600 W$=RIGHT$(LEFT$(WELL$,20),16)
2610 RETURN
```

It should be noted that in some cases there are several wells listed for the same location. If accurate structure maps are to be constructed, it must be known which of these wells is the appropriate one since the kelly bushing elevation can vary slightly from well to well and the subsequent data input (program WELLDAT.BAS) employs the depth below KB as indicated on the well logs. This is not a problem if the aim is to produce isopach maps or surface diagrams, as these diagrams are based on thicknesses between markers which are not affected by changes in KB altitude.

Once the personal database file has been created, the next step involves the entry of marker depths (as read off the well logs). This manipulations is carried out with selection #3 of the main menu of the WELLDAT.BAS program. For example, one may be interested in 5 marker horizons from the imaginary Beer Formation, plus a "datum" horizon in the overlying Ale Formation. If the personal database consists of 1000 wells, the six horizons of interest will be entered for each well (i.e. 6000 separate data entries). Using the WELLDAT.BAS program, the user will need to create a "well" file for each horizon which contains only the picks (for all the wells in the personal database) for that particular horizon. In the present case, 6 well files will be created, each containing 1000 picks. From a programming perspective, I chose this approach, rather than creating a single array with all the information, both to limit the amount of data lost in the event any file is accidently "lost", and for ease of storage on floppy disks (a single array could have exceeded the storage capacity of the disk).

```
3000 REM Subroutine to enter new data to pre-existing file
3010 REM
3020 ON ERROR GOTO 3380
3030 REM
3040 PRINT:INPUT "Name of database file (______.dat) "; HOR$

3050 FILIN$ = HOR$ + ".dat"
3060 PRINT:INPUT "Name of file for data output (______.dat) "; HOR$
3070 FILOUT$ = HOR$ + ".dat"
3080 OPEN "I", #1, FILIN$
3090 OPEN "I", #2, FILOUT$
3100 CLS:PRINT "SEARCHING FOR LAST WELL SAVED"
3110 IF EOF(2) THEN GOTO 3140
3120 INPUT #2, J, WELL$, LAT1, LONG1, KEL1, H0
3130 GOTO 3110
3140 BEEP:BEEP:CLS:PRINT "Data input - file: "; HOR$:PRINT:PRINT
3150 PRINT J ;" wells saved":PRINT:PRINT
3160 PRINT "Last well saved: ";WELL$
3170 CLOSE#2
3180 PRINT:PRINT "MAKE SURE CAPS LOCK IS ON !!":PRINT
3190 INPUT "<CR> to continue"; DUMMY
3200 IF J=0 THEN GOTO 3250
3210 PRINT:PRINT:PRINT "Searching for next well"
3220 INPUT #1, I, W1$, LAT, LONG, KELLY
3230 IF WELL$=W1$ THEN GOTO 3250
3240 GOTO 3220
3250 OPEN "A",#2, FILOUT$
3260 IF EOF (1) THEN GOTO 3360
3270 J=J+1
3280 INPUT #1, I, W1$, LAT, LONG, KELLY
3290 CLS:PRINT "WELL:       ";W1$ TAB(40) "FILE: ";FILOUT$:PRINT:PRINT
3300 PRINT "ENTER S TO STOP": PRINT: PRINT
3310 PRINT "ENTER 1 FOR NO VALUE ENTRY":PRINT:PRINT
3320 INPUT "DEPTH ";H1$
3330 IF H1$="S" THEN GOTO 3360
3340 WRITE#2, J, W1$, LAT, LONG, KELLY, VAL(H1$)
3350 GOTO 3260
3360 CLOSE
3370 RETURN
3380 CLS:PRINT "You need to use pre-existing files"
3390 PRINT:PRINT "Use GW-BASIC program WELLOP.BAS to create files"
3400 PRINT:INPUT "Enter 1 to exit subroutine, 2 to try again ";ANS
3410 ON ANS GOTO 3420,3430
3420 GOTO 3360
3430 CLOSE:GOTO 3010
```

To enter the picks for the Beer and Ale formations, one must first create six data files using selection #1 of the main menu (e.g. Beer1, Beer2, etc.). Then, using selection #3 of WELLDAT.BAS, the picks for each horizon (in meters) are entered into the appropriate well file. In the event that the user does not wish to enter a value for a particular well (because, for example the well log has been truncated, or else because his/her pick is deemed unreliable), a value of "1" is entered. Note that because of the way the original database (WELL.DAT) is organized, the user will have to enter all the picks for Ranges west of the Fifth Meridian before entering picks for Ranges west of the Sixth Meridian (B.C. wells last).

It may become apparent, either during data entry or later, that erroneous values are present in the data files. *This eventuality is to be expected when manipulating a lot of data!* In this case, it will be necessary to edit the existing data file. This procedure is undertaken with choice #4 of the main menu. It is imperative that the well location to be edited be entered using the proper syntax. For Alberta wells, an example might be 02-04-067-06W6 (*not* 2-4-67-6W6), whereas for B.C. wells, a correct location might be C-029-A/093-I-16 (all letters in upper case). Again, all wells W5 will have to be edited before any wells from W6 (which are before B.C.).

```
4000 REM Subroutine to edit well depth data in pre-existing
files 4010 REM
4020 CLS
4030 INPUT "Enter horizon file to edit (________.DAT) ";NUM$
4040 IN$ = NUM$ + ".dat"
4050 OU$ = NUM$ + ".new"
4060 OPEN "i", #1, IN$
4070 OPEN "o", #2, OU$
4080 PRINT:PRINT "Editing file ";IN$
4090 PRINT:PRINT "Enter S to stop"
4100 PRINT:INPUT "Enter name of well to edit ";WELL$
4110 IF WELL$ = "S" THEN GOTO 4210
4120 IF EOF(1) THEN GOTO 4200
4130 INPUT #1, N, W$, LAT, LONG, KEL, DEP
4140 IF WELL$ <> W$ THEN 4150 ELSE 4170
4150 WRITE #2, N,W$,LAT,LONG,KEL,DEP
4160 GOTO 4120
4170 GOSUB 4300
4180 WRITE #2, N,W$,LAT,LONG,KEL,DEP
4190 GOTO 4080
4200 CLS: PRINT " FILE "; WELL$; " NOT FOUND ": GOTO 4260
4210 CLS:PRINT "Ending subroutine ":PRINT:PRINT "Writing
remaining wells to new file"
4220 IF EOF (1) THEN GOTO 4260
4230 INPUT #1, N,W$,LAT,LONG,KEL,DEP
4240 WRITE #2, N,W$,LAT,LONG,KEL,DEP
4250 GOTO 4220
4260 CLOSE
4270 KILL IN$: NAME OU$ AS IN$
4280 PRINT:INPUT "<CR> To return to main menu ";CR
4290 RETURN
4300 BEEP:CLS:PRINT "Well : ";W$
4310 PRINT:PRINT "Old depth : ";DEP
4320 PRINT:INPUT "New depth ";DEP
4330 RETURN
```

Note that this editing subroutine is for use only with the well files created using selection #3 of the WELLDAT.BAS program. Any errors in other types of files (e.g. isopach files) can be corrected either by using the MS-DOS line editor ("Edlin") or by regenerating the file.

Once the picks have been entered for all horizons (e.g. Beer1-6, Ale1), files are created using selection #5 of the main WELLDAT.BAS menu which contain the distance (in meters) between any two selected markers. This manipulation creates the files which will be employed by the *Surfer 4.0* package to generate isopach and surface diagrams. For clarity, I suggest file names such as 12.DAT for the interval between Beer1 and Beer2, 23.DAT for the Beer2 to Beer3 interval, etc. These files do not need to be generated with selection #1 of the main menu beforehand.

```
5000 REM Subroutine to read in two horizon depths from
"WELL.DAT" files
5010 REM Difference (unit thickness) written to
"_________.DAT" file
5020 REM
5030 CLS:INPUT "Enter filename prefix for lower horizon
(______.DAT)";LH$
5040 PRINT:INPUT "Enter filename prefix for upper horizon
(_______.DAT)";UH$
5050 PRINT:INPUT "Enter filename prefix for isopach data
(______.DAT)";ISO$
5060 LH$=LH$ + ".DAT":UH$=UH$ + ".DAT":ISO$=ISO$ + ".DAT"
5070 OPEN "i", 1, LH$
5080 OPEN "i", 2, UH$
5090 OPEN "o", 3, ISO$
5100 PRINT:INPUT "Anticipated maximum thickness ";MAX
5110 CLS:PRINT "Executing task"
5120 IF EOF (1) THEN GOTO 5230
5130 INPUT #1, N1,W1$,LAT1,LONG1,KEL1,H1
5140 INPUT #2, N2,W2$,LAT2,LONG2,KEL2,H2
5150 IF W1$ <> W2$ THEN GOTO 4030 5240
5160 IF H1=1 THEN GOTO 4010 ELSE IF H2=1 THEN GOTO 5230
5170 ISOP = H1 - H2
5180 IF ISOP < 0 THEN PRINT "Negative thickness at well:
";W1$ ELSE GOTO 5190:GOTO 5230
5190 IF ISOP > MAX THEN PRINT "Excessive thickness at well:
"W1$: ELSE GOTO 5200: GOTO 5230
5200 HORIZ = (120.8274 - LONG1)*63.994
5210 VERT = (LAT1 - 54.5906)*111.324
5220 WRITE #3, W1$, HORIZ, VERT, ISOP*-1
5230 GOTO 5120
```

```
5240 PRINT:PRINT "Isopach subroutine completed ": GOTO 5260
5250 CLS:PRINT "Problem at well ";W1$ TAB(40) "#";N1
5260 CLOSE
5270 FOR T=1 TO 2000: NEXT T
5280 RETURN
```

There are several points which need to be mentioned here. First, an "anticipated maximum thickness" needs to be entered before the operation begins. Any wells which exceed this thickness, or any wells having a negative thickness for the chosen interval (if the data files indicate the "upper" horizon is *below* the "lower" horizon) will automatically be listed on the screen. This helps detect bad picks or data entry errors. In the event of an error, check the data files using the edit subroutine (selection #2) to be certain that the proper values have been entered for the well. Once the mistake has been corrected, re-create the isopach file using "selection #3" of the main WELLDAT.BAS program. Note that if too small a value is chosen for the "anticipated maximum thickness", all wells exceeding this limit will be listed, even if the data are correct. On the other hand, if too large a value is entered, then there is a greater chance that mis-picks will go undetected.

A second point deals with the data output. Since my primary interest was the construction of surface diagrams, I chose to multiply the isopach value by -1. In this way, when the data is read by the GRID.EXE program of *Surfer 4.0* and then subsequently input into the SURF.EXE program, the correct topography will be shown for surfaces which have been hung on an upper datum. The Z axis in the figures will show values becoming more negative downward, and the surface can be thought of as representing the *depth below the datum*. The problem with this system is that isopach maps generated with these files (with TOPO.EXE of *Surfer 4.0*) will show negative values on the isopleths. This can be solved by multiplying the isopach values by -1 using the "Transform" function of the GRID.EXE worksheet once the data file has been read into that program.

Third, I have chosen to have the well location written to the output file. Although this data must be erased before griding the data (use the "Delete - Column" function of GRID.EXE worksheet), I thought it could be useful to quickly associate isopach values with well locations when inspecting the data.

Finally, the X and Y coordinates written by this subroutine are in kilometers. The *Surfer 4.0* package arbitrarily will select the longitude of the most westerly well and the latitude of the most southerly well and use these as the y-axis and x-axis respectively. Subsequent wells are located by calculating the distance north of the x-axis (abscissa) and east of the y-axis (ordinate). Knowing this, one can convert the distance in degrees to a distance in kilometers using the known values for the conversion as a function of latitude (available through cartography textbooks). At 55° N, 1 degree of latitude is equivalent to 111.324 km, whereas 1° of longitude equals 63.994 km. For the present study, I found the latitude of the most southerly well and the longitude of the most westerly well by inspecting the data and input these values into the subroutine as constants (line 5200 for the ordinate, line 5210 for the abscissa). Subsequent users may wish to modify these values. Thus, the X and Y coordinates will be given in kilometers east and north (respectively) of fixed lines, whereas the Z coordinate will be in meters, yielding 1000X vertical exaggeration.

The sixth option of the WELLDAT.BAS program can be used to create structure diagrams of any given horizon. The subroutine subtracts the depth below the kelly bushing (as read directly off the well log and input using selection #3 of WELLDAT.BAS) from the kelly bushing altitude. I did not end up employing any of these figures in my text, but here present a structure diagram of the M1 datum for illustrative purposes. The structure data file does not have to be created using selection #1 of the main menu. Note that the X and Y coordinates are generated in a manner identical to that in the isopach subroutine (selection #5), and the user may wish to change the formulae used (see above).

```
6000 REM Subroutine to create structure data files
6010 REM Using horizon picks (from Well.dat files) and
```

```
6020 REM Kelly Bushing elevations
6030 REM
6040 CLS
6050 PRINT "Subroutine for creating structure data files"
6060 PRINT:INPUT "Enter filename prefix for horizon
(______.dat)";H$
6070 IN$ = H$ + ".dat"
6080 OU$ = H$ + ".str"
6090 OPEN "i", 1, IN$
6100 OPEN "o", 2, OU$
6110 PRINT:PRINT:PRINT "Executing task - smoke 'em if ya got
'em "
6120 IF EOF (1) THEN GOTO 6190
6130 INPUT #1, N, W$, LAT, LONG, KEL, DEP
6140 STRUCT = DEP - KEL
6150 HORIZ = (120.8274 - LONG) * 63.994
6160 VERT = (LAT - 54.5906) * 111.324
6170 WRITE #2, W$, HORIZ, VERT, STRUCT
6180 GOTO 6120
6190 BEEP:PRINT:PRINT "File "; OU$; " created"
6200 PRINT: INPUT "<CR> to return to main menu ";CR
6210 RETURN
```

The final selection (#7) is used to exit the program. In the event that a problem arises during program execution and an error message occurs, type "CLOSE" to close any data files which have been opened, and then either press the F2 key (to run the program again) or type "SYSTEM" to exit GW-BASIC entirely.

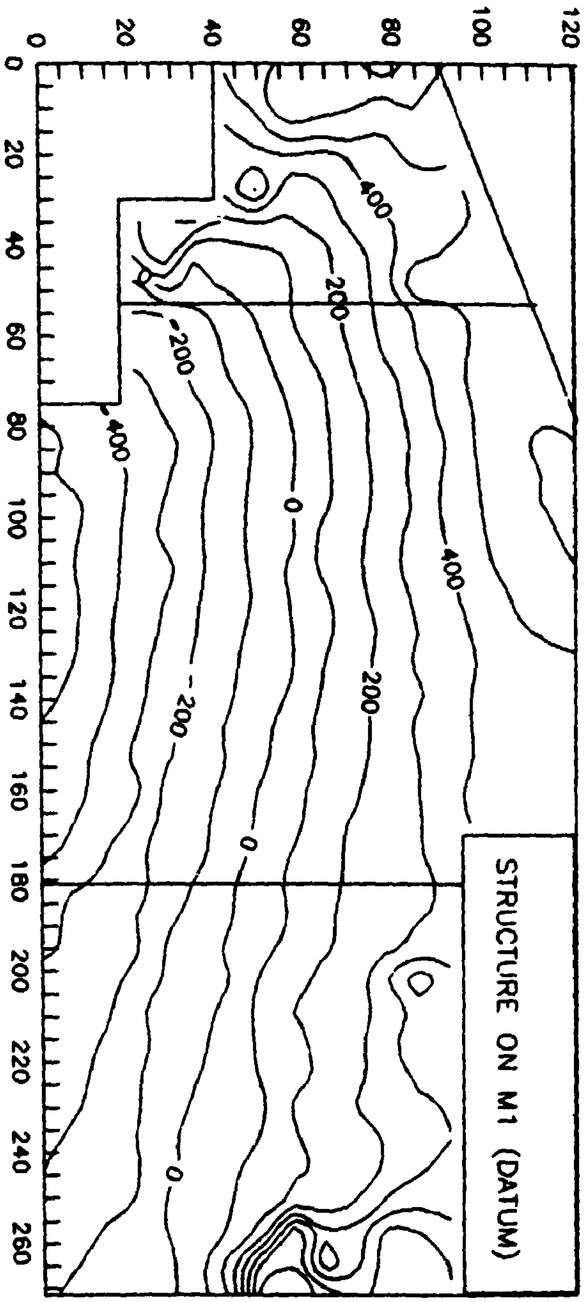

STRUCTURE ON M1 (DATUM)
0
20
40
60
80
100
120
0
20
40
60
80
100
120
140
160
180
200
220
240
260
400
200
-200
-400
0
400
200
-200
0
0

REFERENCES

Aitken, J.D., 1989. The Sauk Sequence - Cambrian to Lower Ordivician miogeocline and platform. In, B.D. Ricketts (ed.), Western Canada Sedimentary Basin, a case history. Canadian Society of Petroleum Geologists, 105-119.

Allen, J.R.L., 1982. Sedimentary structures: their character and physical basis, Volume 1. Elsevier, Amsterdam, 593p.

Allen, P.A., 1985. Hummocky cross-stratification is not produced purely under progressive gravity waves. Nature, v 313, 562-564.

__________ and Underhill, J.R., 1989. Swaley cross-stratification produced by unidirectional flows, Bencliff Grit (Upper Jurassic), Dorset, U.K. Journal of the Geological Society of London, v 146, 241-252.

______________________________, 1990. Swaley cross-stratification produced by unidirectional flows, Bencliff Grit (Upper Jurassic), Dorset, U.K., Reply. Journal of the Geological Society of London, v 147, 398-400.

Anderton, R., 1985. Clastic facies models and facies analysis. In, P.J. Brenchley and B.P.J. Williams (eds.), Sedimentology, recent developments and applied aspects. Blackwell, London, 31-47.

Arnott, R.W., *in press*. The Carrot Creek "K" pool, Cardium Formation, Alberta - a conglomeratic reservoir related to a wave-reworked distributary mouth-bar complex. Bulletin of Canadian Petroleum Geology.

__________ and Southard, J.B., 1990. Exploratory flow-duct experiments on combined-flow bed configurations, and some implications for interpreting storm-event stratification. Journal of Sedimentary Petrology, v 60, 211-219.

Ashmore, P.E., 1982. Laboratory modelling of gravel braided stream morphology. Earth Surface Processes and Landforms, v 7, 201-225.

Barron, E.J., Arthur, M.A. and Kauffman, E.G., 1985. Cretaceous rhythmic bedding sequences: a plausible link between orbital variations and climate. Earth and Planetary Science Letters, v 72, 327-340.

Bartlett, J.J., 1987. An analysis of sequence boundaries of the event stratigraphy of the Cardium Formation, Alberta.

Unpublished Master's thesis, McMaster University, Hamilton, Canada, 185p.

Barusseau, J.-P. and Vanney, J.-R., 1978. Contribution à l'étude du modelé des fonds abyssaux. Le rôle géodynamique des courants profonds. Revue de Géographie Physique et de Géologie Dynamique, v 20, 59-94.

Bates, R.L. and Jackson, J.A. (eds.), 1987. Glossary of geology. American Geological Institute, Falls Church, Va., 788p.

Baum, G.R. and Vail, P.R., 1988. Sequence stratigraphic concepts applied to Paleogene outcrops, Gulf and Atlantic basins. In, C.K. Wilgus et al. (eds.), Sea Level Changes: an Integrated Approach. Society of Economic Paleontologists and Mineralogists Special Publication 42, 309-327.

Beach, F.K., 1955. Cardium a turbidity current deposit. Journal of the Alberta Society of Petroleum Geologists, v 5, 89-98.

Beaumont, C., 1981. Foreland basins. Geophysical Journal of the Royal Astronomical Society, v 65, 291-329.

____________, Keen, C.E., and Boutilier, R., 1982. A comparison of foreland and rift margin sedimentary basins. Philosophical Transactions of the Royal Society of London, Series A, v 305, 295-317.

Berger, A.L. 1978. Long term variations of caloric insolation resulting from the earth's orbital parameters. Quaternary Research, v 9, 139-167.

Bergman, K.M., 1984. Facies and "sand body" geometry of the Carrot Creek-Cyn-Pem area, south-central Alberta. McMaster University Technical Memorandum 86-1, 50p.

Bergman, K.M., 1987. Erosion surfaces and gravel shorefaces deposits: the influence of tectonics on the sedimentology of the Carrot Creek Member, Cardium Formation (Turonian, Upper Cretaceous), Alberta, Canada. Unpublished Ph.D. thesis, McMaster University, Hamilton, Canada, 404p.

____________ and Walker, R.G., 1987. The importance of sea level fluctuations in the formation of linear conglomerate bodies; Carrot Creek Member of Cardium Formation, Cretaceous Western Interior Seaway, Alberta, Canada. Journal of Sedimentary Petrology, v 57, 651-665.

____________________________, 1988. Formation of Cardium erosion surface E5, and associated deposition of conglomerate: Carrot Creek Field, Cretaceous Western Interior Seaway, Alberta. In, D.P. James and D.A. Leckie (eds.), Sequences, Stratigraphy, Sedimentology: Surface and Subsurface. Canadian Society of Petroleum Geologists Memoir 15, 15-24.

Berner, R.A., 1981. A new geochemical classification of sedimentary environments. Journal of Sedimentary Petrology, v 51, 359-365.

Blair, T.C., and Bilodeau, W.L., 1988. Development of tectonic cyclothems in rift, pull-apart, and foreland basins: sedimentary response to episodic tectonism. Geology, v 16, 517-520.

Bluck, B.J., 1967. Sedimentation of beach gravels: examples from south Wales. Journal of Sedimentary Petrology, v 37, 128-156.

Boothroyd, J.C., 1985. Tidal inlets and tidal deltas. In, R.A. Davis Jr. (ed.), Coastal sedimentary environments. Springer-Verlag, New York, 443-532.

Bourgeois, J. and Leithold, E.L., 1984. Wave-worked conglomerates -depositional processes and criteria for recognition. In, E.H. Koster and R.J. Steel (eds.), Sedimentology of Gravels and Conglomerates. Canadian Society of Petroleum Geologists Memoir 10, 331-343.

Boyd, R., Suter, J. and Penland, S., 1988. Implications of modern sedimentary environments for sequence stratigraphy. In, D.P. James and D.A. Leckie (eds.), Sequences, Stratigraphy, Sedimentology: Surface and Subsurface. Canadian Society of Petroleum Geologists Memoir 15, 33-36.

Bromley, R.G. and Ekdale, A.A., 1986. Composite ichnofacies and tiering of burrows. Geological Magazine, v 123, 59-65.

Brown, L.F. Jr. and Fisher, W.L., 1977. Seismic-stratigraphic interpretation of depositional systems: examples from Brazilian rift and pull-apart basins. In, C.E. Payton (ed.), Seismic stratigraphy - applications to hydrocarbon exploration. American Association of Petroleum Geologists Memoir 26, 213-248.

Bruun, P., 1988. The Bruun Rule of erosion by sea-level rise: a discussion on large-scale two- and three-dimensional usages. Journal of Coastal Research, v 4, 627-648.

Burbank, D.W., Beck, R.A., Raynolds, R.G.H., Hobbs, R., and

Tahirkheli, R.A.K., 1988. Thrusting and gravel progradation in foreland basins: a test of post-thrusting gravel dispersal. Geology, v 16, 1143-1146.

Burk, C.F., 1962. Upper Cretaceous structural development of the southern flank of the Peace River Arch. Journal of the Alberta Society of Petroleum Geologists, v 10, 223-227.

__________, 1963. Structure, isopach, and facies maps of Upper Cretaceous marine successions in west-central Alberta and adjacent British Columbia. Geological Survey of Canada Paper 62-31, 10p.

Burke, K. and Sengör, A.M.C., 1988. Ten meter global sea-level change associated with South Atlantic Aptian salt deposition. Marine Geology, v 83, 309-312.

Burton, R., Kendall, C.G.St.C. and Lerche, I., 1987. Out of our depth: on the impossibility of fathoming eustasy from the stratigraphic record. Earth Science Reviews, v 24, 237-277.

Cailleux, A., 1945. Distinction des galets marins et fluviatiles. Bulletin de la Societé Géologique de la France, 5 (15), 325-404.

Cairnes, D.D., 1907. Moose Mountain district of southern Alberta. Geological Survey of Canada Report 968.

Cant, D.J., 1984. Development of shoreline-shelf sandbodies in a Cretaceous epeiric sea deposit. Journal of Sedimentary Petrology, v 54, 541-556.

__________, 1988. Regional structure and development of the Peace River Arch, Alberta: a Paleozoic failed-rift system? Bulletin of Canadian Petroleum Geology, v 36, 284-295.

__________ and Stockmal, G.S., 1989. The Alberta foreland basin: relationships between stratigraphy and Cordilleran terrane-accretion events. Canadian Journal of Earth Science, v 26, 1964-1975.

Carmichael, S.M.M., 1988. Linear estuarine conglomerate bodies formed during a Mid-Albian marine transgression; "Upper Gates" Formation, Rocky Mountain Foothills of northeastern British Columbia. In, D.P. James and D.A. Leckie (eds.), Sequences, Stratigraphy, Sedimentology: Surface and Subsurface. Canadian Society of Petroleum Geologists Memoir 15, 49-62.

Carr, A.P., 1969. Size grading along a pebble beach: Chesil Beach, England. Journal of Sedimentary Petrology, v 39, 297-311.

Carter, R.W.G. and Orford, J.D., 1984. Coarse clastic barrier beaches: a discussion of the distinctive dynamic and morphosedimentary characteristics. Marine Geology, v 60, 377-389.

Clifton, H.E., 1973. Pebble segregation and bed lenticularity in wave-worked versus alluvial gravel. Sedimentology, v 20, 173-187.

______________, 1981. Progradational sequences in Miocene shoreline deposits, southeastern Caliente Range, California. Journal of Sedimentary Petrology, v 51, 165-184.

______________, 1986. Interpreting paleoenergy levels from sediment deposited on ancient wave-dominated shelves. In, R.J. Knight and J.R. McLean (eds.), Shelf Sands and Sandstones. Canadian Society of Petroleum Geologists Memoir 11, 181-190.

______________, Phillips, R.L. and Hunter R.E., 1973. Depositional structures and processes in the mouths of small coastal streams, southwestern Oregon. In, D.R. Coates (ed.), Coastal Geomorphology. State University of New York at Binghampton, 115-140.

______________ and Thompson, J.K., 1978. *Macaronichnus segregatis* -a feeding structure of shallow marine polychaetes Journal of Sedimentary Petrology, v 48, 1293-1302.

Cobban, W.A., Erdmann, C.E., Lemke,R.W., & Maughan, E.K., 1976. Type sections and stratigraphy of the members of the Blackleaf and Marias River Formations (Cretaceous) of the Sweetgrass Arch, Montana. United States Geological Survey, Professional Paper 974, 66p.

______________, and Reeside, J.B. Jr., 1952. Correlation of the Cretaceous formations of the Western Interior of the United States. Geological Society of America Bulletin, v 63, 1011-1044.

Crickmay, C.H., 1944. Preliminary map, Pouce Coupe-Peace River, Alberta and British Columbia. Geological Survey of Canada Paper 44-31.

Cross, T.A. and Lessenger, M.A., 1988. Seismic stratigraphy. Annual Review of Earth and Planetary Science, v 16, 319-354.

Curray, J.R., 1964. Transgressions and regressions. In, R.L. Miller (ed.), Papers in Marine Geology - Sheppard Commemorative Volume. MacMillan, New York, 175-203.

Curtis, C.D., Coleman, M.L. and Love, L.G., 1986. Pore water evolution during sediment burial from isotopic and mineral chemistry of calcite, dolomite and siderite concretions. Geochimica et Cosmochimica Acta, v 50, 2321-2334.

Davidson-Arnott, R.G.D. and Greenwood, B., 1976. Facies relationships on a barred coast, Kouchibouguac Bay, New Brunswick, Canada. In, R.A. Davis and R.L. Ethington (eds.), Beach and Nearshore Sedimentation. Society of Economic Paleontologists and Mineralogists Special Publication 24, 149-168.

Davis, J.C., 1986. Statistics and data analysis in geology. John Wiley and Sons, New York, 646p.

Davis, R.A. Jr., 1985. Beach and nearshore zone. In, R.A. Davis Jr. (ed.), Coastal sedimentary environments. Springer-Verlag, New York, 379-444.

________________, Fox, W.T., Hayes, M.O. and Boothroyd, J.C., 1972. Comparison of ridge and runnel systems in tidal and non-tidal environments. Journal of Sedimentary Petrology, v 42, 413-421.

Dawson, G.M. 1881. Report on exploration from Port Simpson on the Pacific Coast, to Edmonton, on the Saskatchewan, embracing a portion of the northern part of British Columbia and the Peace River country. Geological and Natural History Survey of Canada, Report of Progress 1879-80, pt. B,1-177.

Dean, R.G. and Maurmeyer, E., 1983. Models for beach profile response. In, P.D. Komar (ed.), CRC handbook of coastal processes and erosion. CRC Press, Boca Raton, Fla., 151-165.

DeCelles, P.G., 1987. Variable preservation of Middle Tertiary, coarse-grained nearshore to outer-shelf storm deposits in Southern California. Journal of Sedimentary Petrology, v 57, 250-264.

Demarest, J.M. and Kraft, J.C., 1987. Stratigraphic record of Quaternary sea levels: implications for more ancient strata. In, D. Nummedal, O.H. Pilkey and J.D. Howard (eds.), Sea level fluctuation and coastal evolution. Society of Economic Paleontologists and Mineralogists Special Publication 41, 223-239.

Dietz, R.S., 1963. Wave-base, marine profile of equilibrium, and wave-built terraces: a critical appraisal. Geological Society of America Bulletin, v 74, 971-990.

Dobkins, J. E. and Folk, R.L., 1970. Shape d velopment on Tahiti-Nui. Journal of Sedimentary Petrology, v 40, 1167-1203.

Donovan, D.T. and Jones, E.J.W., 1979. Causes of world-wide changes in sea level. Journal of the Geological Society of London, v 136, 187-192.

Dubois, J.-M.M., 1980. Environnements quaternaires et évolution postglaciaire d'une zone cotière en émersion en bordure sud du bouclier Canadien: la Moyenne Côte Nord du Saint-Laurent, Québec. Unpublished Ph.D. thesis, University of Ottawa, 754p.

Duke, W.L., 1985. Sedimentology of the Upper Cretaceous Cardium Formation in southern Alberta, Canada. Unpublished Ph.D. thesis, McMaster University, Hamilton, Canada, 724p.

___________ 1990. Geostrophic circulation or shallow marine turbidity currents? The dilema of paleoflow patterns in storm-influenced prograding shoreline systems. Journal of Sedimentary Petrology, *in press*.

Eicher, D.L. and Diner, R., 1985. Foraminifera as indicators of water mass in the Cretaceous Greenhorn Sea, Western Interior. In, L.M. Pratt, E.G. Kauffman and F.B. Zelt (eds.), Fine-grained deposits and biofacies of the Cretaceous Western Interior Seaway: evidence of cyclic sedimentary processes. Society of Economic Paleontologists and Mineralogists Field Trip Guidebook 4, 60-71.

Ethridge, F.G. and Wescott, W.A., 1984. Tectonic setting and recognition of hydrocarbon reservoir potential of fan-delta deposits. In, E.H. Koster and R.J. Steel (eds.), Sedimentology of Gravels and Conglomerates. Canadian Society of Petroleum Geologists Memoir 10, 217-235.

Everts, C.H., 1987. Continental shelf evolution in response to a rise in sea level. In, D. Nummedal, O.H. Pilkey and J.D. Howard (eds.), Sea level fluctuation and coastal evolution. Society of Economic Paleontologists and Mineralogists Special Publication 41, 49-57.

Eyles, C.H. and Walker, R.G., 1988. "Geometry" and facies characteristics of stacked shallow marine sandier-upward sequences in the Cardium Formation at Willesden Green, Alberta. In, D.P. James and D.A. Leckie (eds.), Sequences, Stratigraphy, Sedimentology: Surface and Subsurface. Canadian Society of Petroleum Geologists

Memoir 15, 85-96.

Farrell, K.M., 1987. Sedimentology and facies architecture of overbank deposits of the Mississippi River, False River region, Louisiana. In, F.G. Ethridge, R.M. Flores and M.D. Harvey (eds.), Recent developments in fluvial sedimentology. Society of Economic Paleontologists and Mineralogists Special Publication 39, 111-120.

Fischer, A.G., Herbert, T. and Premoli-Silva, I., 1985. Carbonate bedding cycles in Cretaceous pelagic and hemipelagic sequences. In, L.M. Pratt, E.G. Kauffman and F.B. Zelt (eds.), Fine-grained deposits and biofacies of the Cretaceous Western Interior Seaway: evidence of cyclic sedimentary processes. Society of Economic Paleontologists and Mineralogists Field Trip Guidebook 4, 1-10.

Flemings, P.B. and Jordan, T.E., 1989. A synthetic stratigraphic model of foreland basin development. Journal of Geophysical Research, Series B, v 94, 3851-3866.

__________________, 1990. Stratigraphic modeling of foreland basins: interpreting thrust deformation and lithospheric rheology. Geology, v 18, 430-434.

Folk, R.L., 1980. Petrology of sedimentary rocks. Hemphill Publishing Co., Austin, Texas, 185p.

Forbes, D.L. and Boyd, R., 1989. Submersible observations of surficial sediments and seafloor morphology on the inner Scotian Shelf. In, D.J.W. Piper (ed.), Submersible observations off the East Coast of Canada. Geological Survey of Canada Paper 88-20, 71-81.

__________ and Taylor, R.B., 1987. Coarse-grained beach sedimentation under paraglacial conditions, Canadian Atlantic coast. In, D. Fitzgerald and P. Rosen (eds.), Glaciated Coasts. Academic Press, New York, 51-86.

Frey, R.W. and Howard, J.D., 1985. Trace fossils from the Panther Member, Star Point Formation (Upper Cretaceous), Coal Creek Canyon, Utah. Journal of Paleontology, v 59, 370-404.

Galloway, W.E., 1981. Depositional architecture of Cenozoic Gulf Coastal Plain fluvial systems. In, F.G. Etheridge and R.M. Flores (eds.), Recent and ancient non-marine depositional environments: models for exploration. Society of Economic Paleontologists and Mineralogists Special Publication 31, 127-156.

______________, 1989. Genetic stratigraphic sequences in basin analysis I: architecture and genesis of flooding-surface bounded depositional units. American Association of Petroleum Geologists Bulletin, v 73, 125-142.

Gautier, D.L., 1982. Siderite concretions: indicators of early diagenesis in the Gammon Shale (Cretaceous). Journal of Sedimentary Petrology, v 52, 859-871.

Gillie, R.D., 1983. Field measurements of gravel movement by wave action on the inner continental shelf. In, B.J. Holden (ed.), Proceedings of the Canadian Coastal Conference. National Research Council of Canada, 73-89.

Gleddie, J., 1949. Upper Cretaceous in Western Peace River Plains, Alberta. Bulletin of the American Association of Petroleum Geologists, v 33, 511-532.

Goodwin, P.W. and Anderson, E.J., 1985. Punctuated aggradational cycles: a general hypothesis of episodic stratigraphic accumulation. Journal of Geology, v 93, 515-533.

Graham, J., 1988. Collection and analysis of field data. In, M. Tucker (ed.), Techniques in sedimentology. Blackwell Scientific Publications, London, 5-62.

Gray, M.B. and Nickelsen, R.P., 1989. Pedogenic slickensides, indicators of strain and deformation processes in redbed sequences of the Appalachian foreland. Geology, v 17, 72-75.

Greenwood, B. and Sherman, D.J., 1986. Hummocky cross-stratification in the surf zone: flow parameters and bedding genesis. Sedimentology, v 33, 33-45.

Hammond, F.D.C., Heathershaw, A.D. and Langhorne, D.N., 1984. A comparison between Shields' threshold criterion and the movement of loosely packed gravel in a tidal channel. Sedimentology, v 31, 51-62.

Hancock, J.M. and Kauffman, E.G., 1979. The great transgressions of the Late Cretaceous. Journal of the Geological Society of London, v 136, 175-186.

Haq, B.U., Hardenbol, J. and Vail, P.R., 1987. Chronology of fluctuating sea levels since the Triassic (250 m.y. to Present). Science, v 235, 1156-1167.

______________________________________, 1988. Mesozoic and Cenozoic chronostratigraphy and cycles of sea-level change. In, C.K. Wilgus et al. (eds.), Sea Level Changes: an Integrated Approach. Society of Economic

Paleontologists and Mineralogists Special Publication 42, 71-108.

Harding, S.R.L., 1955. Regional discussion of the Cardium Formation. Bulletin of the Canadian Institute of Mining and Metallurgy, v 48, 19-24.

Harms, J.C., Southard, J.B. and Walker, R.G., 1982. Structures and sequences in clastic rocks. Society of Economic Paleontologists and Mineralogists Short Course 9, Tulsa.

Harrison, C.G.A., 1985. Modelling fluctuations in water depth during the Cretaceous. In, L.M. Pratt, E.G. Kauffman and F.B. Zelt (eds.), Fine-grained deposits and biofacies of the Cretaceous Western Interior Seaway: evidence of cyclic sedimentary processes. Society of Economic Paleontologists and Mineralogists Field Trip Guidebook 4, 11-15.

Hart, B.S., 1990. Swaley cross-stratification produced by unidirectional flows, Bencliff Grit (Upper Jurassic), Dorset, UK, Discussion. Journal of the Geological Society of London, v 147, 396-400.

Hart, B.S. and Long, B.F., 1990a. Recent evolution of the Outardes Estuary, Quebec, Canada: impact of dam construction on the river. Sedimentology, v 37, 495-507.

______________________________, 1990b. Storm deposits from the Quaternary Outardes delta, Quebec, Canada. Sedimentary Geology, v 67, 1-5.

__________ and Plint, A.G., 1989. Gravelly shoreface deposits: a comparison of modern and ancient facies sequences. Sedimentology, v 36, 551-557.

__________, Vantfoort, R.M. and Plint, A.G., 1990. Is there evidence for geostrophic currents preserved in the sedimentary record of inner to middle-shelf deposits? Journal of Sedimentary Petrology, v 60, 633-635.

Hayes, B.J.R. and Smith, D.G., 1987. Discussion on Cardium Formation 6. Stratigraphic framework of the Cardium in subsurface. Bulletin of Canadian Petroleum Geology, v 35, 363-365.

Hays, J.D., Imbrie, J. and Shackleton, N.J., 1976. Variations in the earth's orbit: pacemaker of the ice ages. Science, v 194, 1121-1132.

Hein, F.J. and Walker, R.G., 1977. Bar evolution and development of stratification in the gravelly, braided, Kicking Horse River, British Columbia. Canadian Journal of Earth Science, v 14, 562-570.

Heller, P.L., Angevine, C.L., Winslow, N.S., and Paola, C., 1988. Two-phase stratigraphic model of foreland-basin sequences. Geology, v 16, 501-504.

____________, and Paola, C., 1989. The paradox of Lower Cretaceous gravels and the initiation of thrusting in the Sevier orogenic belt, United States Western Interior. Geological Society of America Bulletin, v 101, 864-875.

Howard, J.D., 1975. The sedimentological significance of trace fossils. In, R.W. Frey (ed.), The Study of Trace Fossils. Springer-Verlag, New York, 131-146.

Hubbard, D.K., Oertel, G. and Nummedal, D., 1979. The role of waves and tidal currents in the development of tidal-inlet sedimentary structures and sand body geometry: examples from North Carolina, South Carolina and Georgia. Journal of Sedimentary Petrology, v 49, 1073-1092.

Hubbard, R.J., 1988. Age and significance of sequence boundaries on Jurassic and Early Cretaceous rifted continental margins. American Association of Petroleum Geologists Bulletin, v 72, 49-72.

Hunter, R.E., Clifton, H.E. and Phillips, R.L., 1979. Depositional processes, sedimentary structures and predicted vertical sequences in barred nearshore systems, southern Oregon coast. Journal of Sedimentary Petrology, v 49, 711-726.

Irwin, H., Curtis, C. and Coleman, M., 1977. Isotopic evidence for source of diagenetic carbonates formed during burial of organic-rich sediments. Nature, v 269, 209-213.

Jeletzky, J.A., 1978. Causes of Cretaceous oscillations of sea level in Western and Arctic Canada and some general geotectonic implications. Geological Survey of Canada Paper 77-18, 44p.

Jervey, M.T., 1988. Quantitative geological modelling of siliclastic rock sequences and their seismic expression. In, C.K. Wilgus et al. (eds.), Sea Level Changes: an Integrated Approach. Society of Economic Paleontologists and Mineralogists Special Publication 42, 47-69.

Johnson, D.A., 1972. Ocean-floor erosion in the equatorial Pacific. Geological Society of America Bulletin, v 83, 3121-3144.

Jolliffe, I.P. and Wallace, H., 1973. The role of seaweed in beach supply and in shingle transport below low tide level. Proceedings of the Annual Symposium of the Confédération Mondiale des Activités Subaquatiques, 189-196.

Jones, J.F., 1966. Geology and groundwater resources of the Peace River District, northwestern Alberta. Research Council of Alberta, Bulletin 16, 143p.

Jones, J.R. and Cameron, B., 1988. Modern coastal back-barrier environment: analog for coal basin or for carbonaceous black shale? Geology, v 16, 345-348.

Jones, R.M.P., 1980. Basinal isostatic adjustment faults and their petroleum significance. Bulletin of Canadian Petroleum Geology, v 28, 211-251.

Kachel, N.B. and Smith, J.D., 1986. Geological impact of sediment transporting events on the Washington continental shelf. In, R.J. Knight and J.R. McLean (eds.), Shelf Sands and Sandstones. Canadian Society of Petroleum Geologists Memoir 11, 145-162.

Kauffman, E.G., 1984. Paleobiogeography and evolutionary response dynamic in the Cretaceous Western Interior Seaway of North America. In, G.E.G. Westermann (ed.), Jurassic-Cretaceous biochronology and paleogeography of North America. Geological Association of Canada Special Paper 27, 273-306.

______________, 1985. Cretaceous evolution of the Western Interior Basin of the United States. In, L.M. Pratt, E.G. Kauffman and F.B. Zelt (eds.), Fine-grained deposits and biofacies of the Cretaceous Western Interior Seaway: evidence of cyclic sedimentary processes. Society of Economic Paleontologists and Mineralogists Field Trip Guidebook 4, iv-xiii.

______________, 1988. Concepts and methods of high-resolution event stratigraphy. Annual Review of Earth and Planetary Science, v 16, 605-654.

Kennett, J.P., 1982. Marine Geology. Prentice-Hall, Toronto, 813p.

Kidson, C. and Carr, A.P., 1959. The movement of shingle over the seabed close inshore. Geographical Journal, v 125, 380-389.

Kleinspehn, K.L., Steel, R.J., Johannessen, E. and Netland, A., 1984. Conglomeratic fan-delta sequences, Late Carboniferous - Early Permian, Western Spitsbergen. In, E.H. Koster and R.J. Steel (eds.), Sedimentology of

Gravels and Conglomerates. Canadian Society of Petroleum Geologists Memoir 10, 279-294.

Komar, P.D., 1976. Beach processes and sedimentation. Englewood Cliffs, N.J., 429p.

Krause, F.F., Collins, H.N., Nelson, D.A., Machemer, S.D. and French, P.R., 1987. Multiscale anatomy of a reservoir: geological characterization of Pembina-Cardium pool, west-central Alberta, Canada. Bulletin of the American Association of Petroleum Geologists, v 71, 1233-1260.

____________ and Nelson, D.A., 1984. Storm event sedimentation: lithofacies association in the Cardium Formation, Pembina area, west-central Alberta, Canada. In, D.F. Stott and D.J. Glass (eds.), The Mesozoic of Middle North America. Canadian Society of Petroleum Geologists Memoir 9, 485-511.

Krause, M.J. and Middleton, L.T., 1987. Contrasting architecture of two alluvial suites in differing structural settings. In, F.G. Ethridge, R.M. Flores and M.D. Harvey (eds.), Recent developments in fluvial sedimentology. Society of Economic Paleontologists and Mineralogists Special Publication 39, 253-262.

Kutzbach, J.E., 1981. Monsoon climate of the early Holocene: climatic experiment using the Earth's orbital parameters for 9000 years ago. Science, v 214, 59-61.

Kyser, T.K., Caldwell, W.G.E., Whittaker, S.G. and Cadrin, A.J., *in press*. Paleoenvironment and geochemistry of the northern portion of the Western Interior Seaway during Late Cretaceous time. In, W.G.E. Caldwell and E.G. Kauffman (eds.), Evolution of the Western Interior Basin. Geological Association of Canada Special Paper.

Leckie, D.A., 1988. Wave-formed, coarse-grained ripples and their relationship to hummocky cross-stratification. Journal of Sedimentary Petrology, v 58, 607-622.

____________ and Krystinik, L.F., 1989. Is there evidence for geostrophic currents preserved in the sedimentary record of inner to middle-shelf deposits? Journal of Sedimentary Petrology, v 59, 862-870.

____________ and Walker, R.G., 1982. Storm- and tide-dominated shorelines in Cretaceous Moosebar - Lower Gates interval: outcrop equivalents of Deep Basin gas trap in Western Canada. Bulletin of the American Association of Petroleum Geologists, v 66, 138-157.

Leithold, E.L., 1989. Depositional processes on an ancient and modern muddy shelf, northern California. Sedimentology, v 36, 179-202.

Longstaffe, F.J., 1989. Stable isotopes as tracers in clastic diagenesis. In, I.E. Hutcheon (ed.), Short course in burial diagenesis, Mineralogical Association of Canada Short Course Series, 15, 201-277.

_______________ and Ayalon, A., 1987. Oxygen-isotope studies of clastic diagenesis in the Lower Cretaceous Viking Formation, Alberta: implications for the role of meteoric water. In, J.D. Marshal (ed.), Diagenesis of sedimentary sequences. Geological Society Special Publication, 36, 277-296.

Longuet-Higgins, M.S., 1970. Longshore currents generated by obliquely incident waves, 1. Journal of Geophysical Research, v 75, 6778-6789.

MacDonald, W.D., 1957. The upper Cretaceous Cardium Formation between Athabasca River and the Peace River. Journal of the Alberta Society of Petroleum Geologists, v 5, 82-87.

Machemer, S.D. and Hutcheon, I., 1988. Geochemistry of early carbonate cements in the Cardium Formation, central Alberta. Journal of Sedimentary Petrology, v 58, 136-147.

Madsen, O.S. and Grant, W.D., 1975. The threshold of sediment movement under oscillatory water waves: a discussion. Journal of Sedimentary Petrology, v 45, 360-361.

Maejima, W., 1982. Texture and stratification of gravelly beach sediments, Enju Beach, Kii Peninsula, Japan. Journal of Geosciences, Osaka City University, v 25, 35-51.

Malloch, G.S., 1911. Bighorn coal basin, Alberta. Geological Survey of Canada Memoir 9.

Massari, F. and Parea, G.C., 1988. Progradational gravel beach sequences in a moderate- to high-energy, micro-tidal marine environment. Sedimentology, v 35, 881-913.

Mathews, E.R., 1980. Observations of beach gravel transport, Wellington Harbour entrance, New Zealand. New Zealand Journal of Geology and Geophysics, v 23, 209-222.

McLearn, F.H., 1918. Peace River Section, Alberta. Geological Survey of Canada Summary Report 1917, pt. C, 14-21.

_______________ and Henderson, J.F., 1944. Geology and oil prospects of Lone Mountain area, British Columbia. Geological Survey of Canada Paper 44-2.

__________ and Kindle, E.D., 1950. Geology of northeastern British Columbia. Geological Survey of Canada Memoir 259, 236p.

McNeil, D.H. and Caldwell, W.G.E., 1981. Cretaceous rocks and their foraminifera in the Manitoba Escarpment. Geological Association of Canada Special Paper 21, 439p.

Merewether, E.A. and Cobban, W.A., 1986. Biostratigraphic units and tectonism in the mid-Cretaceous foreland of Wyoming, Colorado, and adjoining areas. In, J.A. Peterson (ed.), Paleotectonics and Sedimentation in the Rocky Mountain Region, United States. American Association of Petroleum Geologists, Memoir 41, 443-468.

__________, Molenaar, C.M. and Cobban, W.A., 1983. Mid-Cretaceous Codell Sandstone Member of Carlile Shale eastern Colorado. Society of Economic Paleontologists and Mineralogists, Rocky Mountain Section Spring Field Trip Guidebook, 25p.

Merrits, D. and Vincent, K.R. 1989. Geomorphic response of coastal streams to low, intermediate and high rates of uplift, Mendocino triple junction region, northern California. Geological Society of America Bulletin, v 101, 1373-1388.

Miall, A.D., 1986. Eustatic sea level changes interpreted from seismic stratigraphy: a critique of the methodology with particular reference to the North Sea Jurassic record. American Association of Petroleum Geologists Bulletin, v 70, 131-137.

Michaelis, E.R., 1957. Cardium sedimentation in the Pembina River area. Journal of the Alberta Society of Petroleum Geologists, v 5, 73-77.

__________ and Dixon, G., 1969. Interpretation of depositional processes form sedimentary structures in Cardium Sands. Bulletin of Canadian Petroleum Geology, v 17, 410-433.

Middleton, G.V. and Southard, J.B., 1984. Mechanics of sediment movement. Society of Economic Paleontologists and Mineralogists Short Course 3, Tulsa.

Mörner, N.-A., 1976. Eustasy and geoid changes. Journal of Geology, v 84, 123-151.

__________, 1981. Revolution in Cretaceous sea-level analysis. Geology, v 9, 344-346.

Mozley, P.S., 1989a. Relation between depositional environment and the elemental composition of early diagenetic siderite. Geology, v 17, 704-706.

____________, 1989b. Complex compositional zonation in concretionary siderite: implications for geochemical studies. Journal of Sedimentary Petrology, v 59, 815-818.

Neate, D.J.M., 1967. Underwater pebble grading of Chesil Bank. Geologists' Association Proceedings, v 78, 419-426.

Nemec, W. and Steel, R.J., 1984. Alluvial and coastal conglomerates: their significant features and some comments on gravelly mass-flow deposits. In, E.H. Koster and R.J. Steel (eds.), Sedimentology of Gravels and Conglomerates. Canadian Society of Petroleum Geologists Memoir 10, 1-31.

Niedoroda, A.W., Swift, D.J.P. and Hopkins, T.S., 1985. The Shoreface. In, R.A. Davis Jr. (ed.), Coastal sedimentary environments. Springer-Verlag, New York, 533-624.

Nittrouer, C.A., DeMaster, D.J., Kuehl, S.A. and McKee, B.A., 1986. Association of sand with mud deposits accumulating on continental shelves. In, R.J. Knight and J.R. McLean (eds.), Shelf Sands and Sandstones. Canadian Society of Petroleum Geologists Memoir 11, 17-25.

Norris, B., 1989. The Upper Cretaceous Muskiki, Marshybank and Bad Heart formations (Smoky Group), Western Interior Seaway, northwestern Alberta, Canada: relative sea level control on stratigraphy and sedimentology. Unpublished M.Sc. Thesis, University of Western Ontario, London, Canada, 340p.

North American Commission on Stratigraphic Nomenclature, 1983. American Association of Petroleum Geologists Bulletin, v 67, 841-875.

Nottvedt, A. and Kreisa, R.D., 1987. Model for the combined-flow origin of hummocky cross-stratification. Geology, v 15, 357-361.

Nummedal, D. and Swift, D.J.P., 1987. Transgressive stratigraphy at sequence-bounding unconformities: some principles derived from Holocene and Cretaceous examples. In, D. Nummedal, O.H. Pilkey and J.D. Howard (eds.), Sea level fluctuation and coastal evolution. Society of Economic Paleontologists and Mineralogists Special Publication 41, 241-260.

O'Connell, S.C., 1988. The distribution of Bluesky facies in the region overlying the Peace River Arch, northwestern Alberta. In, D.P. James and D.A. Leckie (eds.), Sequences, Stratigraphy, Sedimentology: Surface and Subsurface. Canadian Society of Petroleum Geologists Memoir 15, 387-400.

Ogren, D.E. and Waag, C.J., 1986. Orientation of cobble and boulder beach clasts. Sedimentary Geology, v 47, 69-76.

Orford, J.D., 1975. Discrimination of particle zonation on a pebble beach. Sedimentology, v 22, 441-463.

Paola, C., 1988. Subsidence and gravel transport in alluvial basins. In, K.L. Kleinspehn and C. Paola (eds.), New Perspectives in Basin Analysis. Springer-Verlag, New York, 231-243.

Pattison, S.A.J., 1988. Transgressive, incised shoreface deposits of the Burnstick Member (Cardium "B" sandstone) at Caroline, Crossfield, Garrington, and Lochend; Cretaceous Cardium Formation, Western Interior seaway, Alberta, Canada. In, D.P. James and D.A. Leckie (eds.), Sequences, Stratigraphy, Sedimentology: Surface and Subsurface. Canadian Society of Petroleum Geologists Memoir 15, 155-166.

Pearson, M.J., 1967. Magnesian siderite in carbonate concretions from argillaceous sediments in the Westphalian of Yorkshire. Mineralogical Magazine, v 39, 700-704.

Pemberton, S.G. and Frey, R.W., 1984. Ichnology of storm-influenced shallow marine sequences: Cardium Formation (Upper Cretaceous) at Seebe, Alberta. In, D.F. Stott and D.J. Glass (eds.), The Mesozoic of Middle North America. Canadian Society of Petroleum Geologists Memoir 9, 281-304.

Pitman, W.C. III, 1978. Relationship between eustasy and stratigraphic sequences of passive margins. Geological Society of America Bulletin, v 89, 1389-1403.

Plint, A.G., 1983. Facies, environments and sedimentary cycles in the Middle Eocene, Bracklesham Formation of the Hampshire Basin: evidence for global sea-level changes? Sedimentology, v 30, 625-653.

__________, 1988. Sharp-based shoreface sequences and "offshore bars" in the Cardium Formation: their relationship to relative sea-level changes. In, C.K. Wilgus et al. (eds.), Sea Level Changes: an Integrated Approach. Society of Economic Paleontologists and Mineralogists Special Publication 42, 357-370.

____________, 1990. An allostratigraphic correlation of the Muskiki and Marshybank formations (Coniacian - Santonian) in the Foothills and subsurface of the Alberta Basin. Bulletin of Canadian Petroleum Geology, v 38, in press.

____________ and Hart, B.S., 1988. Field guide to the Upper Cretaceous Dunvegan (Cenomanian) and Cardium (Turonian) formations in the Dawson Creek - Fort St. John area, British Columbia. Canadian Society of Petroleum Geologists' field guide to Sequences, Stratigraphy, Sedimentology: Surface and Subsurface Technical Meeting, September 14-16, 1988, Calgary, Alberta, 51p.

____________________________, *in prep.* Integrated bio- and allostratigraphy for part of the Upper Cretaceous of the Alberta Basin: evidence for global eustatic events. Canadian Journal of Earth Science.

___________ and Walker, R.G., 1987. Cardium Formation 8. Facies and environments of the Cardium shoreline and coastal plain in the Kakwa Field and adjacent areas, northwestern Alberta. Bulletin of Canadian Petroleum Geology, v 35, 48-64.

____________ Norris, B. and Donaldson, S. 1990. Revised definitions for the Upper Cretaceous Bad Heart Formation and associated units in the Foothills and Plains of Alberta and British Columbia. Bulletin of Canadian Petroleum Geology, v 38, 78-88.

____________ Walker, R.G. and Bergman, K.M., 1986. Cardium Formation 6. Stratigraphic framework of the Cardium in subsurface. Bulletin of Canadian Petroleum Geology, v 34, 213-225.

____, 1987. Reply to discussions on Cardium Formation 6. Stratigraphic framework of the Cardium in subsurface. Bulletin of Canadian Petroleum Geology, v 35, 365-374.

___________________________ and Duke, W.L., 1988. An outcrop to subsurface correlation of the Cardium Formation in Alberta. In, D.P. James and D.A. Leckie (eds.), Sequences, Stratigraphy, Sedimentology: Surface and Subsurface. Canadian Society of Petroleum Geologists Memoir 15, 167-184.

Porter, J.W., Price, R.A., and McCrossan, R.G., 1982. The Western Canada Sedimentary Basin. Philosophical Transactions of the Royal Society of London, Series A, v 305, 169-192.

Posamentier, H.W., Jervey, M.T. and Vail, P.R., 1988. Eustatic controls on clastic deposition 1 - conceptual framework. In, C.K. Wilgus et al. (eds.), Sea Level Changes: an Integrated Approach. Society of Economic Paleontologists and Mineralogists Special Publication 42, 109-124.

_________________ and Vail, P.R., 1988. Eustatic controls on clastic deposition II: sequence and systems tract models. In, C.K. Wilgus et al. (eds.), Sea Level Changes: an Integrated Approach. Society of Economic Paleontologists and Mineralogists Special Publication 42, 125-154.

Pye, K., Dickson, J.A.D., Schiavon, N., Coleman, M.L. and Cox, M., 1990. Formation of siderite-Mg-calcite-iron sulphide concretions in intertidal marsh and sandflat sediments, north Norfolk, England. Sedimentology, v 37, 325-343.

Rahmani, R.A. and Smith, D.G., 1988. The Cadotte Member of northwestern Alberta: a high-energy barred shoreline. In, D.P. James and D.A. Leckie (eds.), Sequences, Stratigraphy, Sedimentology: Surface and Subsurface. Canadian Society of Petroleum Geologists Memoir 15, 431-438.

Reddering, J.S.V. and Illenberger, W.K., 1988. Discussion on palaeoenvironmental significance of clast shape in the Nardouw Formation, Cape Supergroup. South African Journal of Geology, v 91, 554-555.

Ricketts, B.D. (ed.), 1989. Western Canada Sedimentary Basin, a case history. Canadian Society of Petroleum Geologists, 320p.

Rine, J.M., Helmhold, K.P. and Bartlett, G.A., 1987. Discussion of Cardium Formation 6. Stratigraphic framework of the Cardium in subsurface. Bulletin of Canadian Petroleum Geology, v 35, 362-363.

Rosenbaum, J. and Sheppard, S.M.F., 1986. An isotopic study of siderites, dolomites and ankerites at high temperatures. Geochimica et Cosmochimica Acta, v 50, 1147-1150.

Ross, G. and Stephenson, R.A., 1989. Crystalline basement: the foundations of Western Canada Sedimentary Basin. In, B.D. Ricketts (ed.), Western Canada Sedimentary Basin, a case history. Canadian Society of Petroleum Geologists, 33-45.

Ross, N. and Long, B.F., 1989. Evolution morpho-sédimentaire de la barre de déferlement: un example dans le golfe du Saint-Laurent, Québec. Géographie physique et Quaternaire, v 43, 377-388.

Rust, B.R., Gibling, M.R. and Legun, A.S., 1984. Coal deposition in an anastomosing-fluvial system: the Pennsylvanian Cumberland Group south of Joggins, Nova Scotia, Canada. In, R.A. Rahmani and R.M. Flores (eds.) Sedimentology of coal and coal-bearing sequences. IAS Special Publication 7, 105-120.

Rutherford, R.L., 1927. Geology along Bow River between Cochrane and Kananaskis, Alberta. Alberta Science and Industry Research Council, Report No. 17.

Ryer, T.A., 1981. Deltaic coals of Ferron Sandstone Member of Mancos Shale: predictive model for Cretaceous coal-bearing strata of Western Interior. Bulletin of the American Association of Petroleum Geologists, v 65, 2323-2340.

__________, 1983. Transgressive-regressive cycles and the occurrence of coal in some Upper Cretaceous strata of Utah. Geology, v 11, 207-210.

Schedl, A. and Wiltschko, D.V., 1984. Sedimentological effects of a moving terrain. Journal of Geology, v 92, 273-287.

Scholle, P.A., 1979. Constituents, textures, cements and porosities of sandstones and associated rocks. American Association of Petroleum Geologists Memoir 28, 201p.

Schwab, F.L., 1986. Sedimentary "signatures" of foreland basin assemblages: real or counterfeit?. In, P.A. Allen and P. Homewood (eds.), Foreland Basins. International Association of Sedimentologists Special Publication 8, 395-410.

Sherman, D.J., 1988. Empirical evaluation of longshore current models. Geographical Review, v 78, 158-168.

_____________, Short, A.D. and Takeda, I., 1990. Sediment mixing depth and megaripple migration in rip channels. Abstracts, 13th International Sedimentological Congress, Nottingham, p.496.

Sinha, R.N., 1970. Cardium Formation, Edson area. Geological Survey of Canada Paper 68-30, 65p.

Sloan, L.C. and Barron, E.J., 1990. "Equable" climates during Earth history? Geology, v 18, 489-492.

Sloss, L.L., 1988. Forty years of sequence stratigraphy. Geological Society of America Bulletin, v 100, 1661-1665.

Smith, D.G., 1983. Anastomosed fluvial deposits: modern examples from western Canada. In, J.D. Collinson and J. Lewin (eds.), Modern and ancient fluvial systems. International Association of Sedimentologists Special Publication 6, 155-168.

Staley, G.H.S., 1987. Diagenetic alteration in the Cardium and Viking formations, western Canada. Unpublished Ph.D. thesis, University of Sheffield, U.K., 205p.

Stelck, C.R., 1955. Cardium Formation in the Foothills of northeastern British Columbia. Transactions of the Canadian Institute of Mining and Metallurgy, v 58, 132-139.

Stockmal, G.S., and Beaumont, C., 1987. Geodynamic models of convergent margin tectonics: the southern Canadian Cordillera and the Swiss Alps. In, C. Beaumont and A.J. Tankard (eds.), Sedimentary Basins and Basin-Forming Mechanisms. Canadian Society of Petroleum Geologists, Memoir 12, 393-411.

Stott, D.F., 1961. Dawson Creek map area, British Columbia. Geological Survey of Canada Paper 61-10.

____________, 1963. The Cretaceous Alberta Group and equivalent rocks, Rocky Mountain Foothills, Alberta. Geological Survey of Canada Memoir 317, 306p.

____________, 1967. The Cretaceous Smoky Group, Rocky Mountain Foothills, Alberta and British Columbia. Geological Survey of Canada Bulletin 132, 133p.

____________, 1984. Cretaceous sequences of the Foothills of the Canadian Rocky Mountains. In, D.F. Stott and D.J. Glass (eds.), The Mesozoic of Middle North America. Canadian Society of Petroleum Geologists, Memoir 9, 85-107.

Stratten, T., 1974. Notes on the application of shape parameters to differentiate between beach and river deposits in Southern Africa. Transactions of the Geological Society of South Africa, v 77, 59-64.

Sun, S.Q., 1990. Swaley cross-stratification produced by unidirectional flows, Bencliff Grit (Upper Jurassic), Dorset, U.K., discussion. Journal of the Geological Society of London, v 147, 396-397.

Sunamura, T., 1983. Processes of sea cliff and platform erosion. In, P.D. Komar (ed.), CRC handbook of coastal processes and erosion. CRC Press, Boca Raton, Fla., 233-26 .

Swift, D.J.P., 1975. Barrier-island genesis: evidence from the central Atlantic shelf, eastern U.S.A. Sedimentary Geology, 14, 1-43.

______________, Hudelson, P.M., Brenner, R.L. and Thompson, P., 1987. Shelf construction in a foreland basin: storm beds, shelf sandbodies, and shelf-slope depositional sequences in the Upper Cretaceous Mesaverde Group, Book Cliffs, Utah. Sedimentology, v 34, 423-457.

Tonnsen, J.J., 1986. Influence of tectonic terranes adjacent to the Precambrian Wyoming Province on Phanerozoic stratigraphy in the Rocky Mountain region. In, J.A. Peterson (ed.), Paleotectonics and Sedimentation in the Rocky Mountain Region, United States. American Association of Petroleum Geologists, Memoir 41, 21-39.

Tucholke, B.E. and Embley, R.W., 1984. Cenozoic regional erosion of the abyssal sea floor off South Africa. In, J.S. Schlee (ed.), Interregional unconformities and hydrocarbon accumulation. American Association of Petroleum Geologists Memoir 36, 145-164.

Tucker, M.E., 1981. Sedimentary petrology, an introduction. John Wiley and Sons, Toronto, 252p.

Vail, P.R., Mitchum, R.M. Jr., Todd, R.G., Widmier, J.M., Thompson,S., Sangree, J.B., Bubb, J.N. and Hatelid, W.G., 1977. Seismic stratigraphy and global change of sea level. In, C.E. Payton (ed.), Seismic stratigraphy - applications to hydrocarbon exploration. American Association of Petroleum Geologists Memoir 26, 49-212.

Van Wagoner, J.C., Posamentier, H.W., Mitchum, R.M., Vail, P.R., Sarg, J.F., Loutit, T.S. and Hardenbol, J., 1988. An overview of the fundamentals of sequence stratigraphy and key definitions. In, C.K. Wilgus et al. (eds.), Sea Level Changes: an Integrated Approach. Society of Economic Paleontologists and Mineralogists Special Publication 42, 39-45.

Vincent, C.E., 1986. Processes affecting sand transport on a storm-dominated shelf. In, R.J. Knight and J.R. McLean (eds.), Shelf Sands and Sandstones. Canadian Society of Petroleum Geologists Memoir 11, 121-132.

Vossler, S.M. and Pemberton, S.G., 1988. Ichnology of the Cardium Formation (Pembina Oilfield): implications for depositional and sequence stratigraphic interpretations.

In, D.P. James and D.A. Leckie (eds.), Sequences, Stratigraphy, Sedimentology: Surface and Subsurface. Canadian Society of Petroleum Geologists Memoir 15, 237-254.

Wadsworth, J.A., 1989. Morphology and origin of erosion surfaces within the Cardium Formation: Upper Cretaceous, Alberta. Unpublished M.Sc. thesis, McMaster University, Hamilton, Canada, 144p.

Walker, R.G., 1983. Cardium Formation 3. Sedimentology and stratigraphy in the Caroline-Garrington area. Bulletin of Canadian Petroleum Geology, v 31, 213-230.

____________, 1984. General introduction: facies, facies sequences and facies models. In, R.G. Walker (ed.), Facies models, 2nd edition. Geoscience Canada Reprint Series 1, 1-9.

____________, 1985. Cardium Formation at Ricinus Field, Alberta: a channel cut and filled by turbidity currents in the Cretaceous Western Interior Seaway. American Association of Petroleum Geologists Bulletin, v 69, 1963-1981.

____________ and Cant, D.J. 1984. Sandy fluvial systems. In, R.G. Walker (ed.), Facies models, 2nd edition. Geoscience Canada Reprint Series 1, 71-89.

____________ and Eyles, C.H., 1988. Geometry and facies of stacked shallow-marine sandier upward sequences dissected by erosion surface, Cardium Formation, Willesden Green, Alberta. Bulletin of the American Association of Petroleum Geologists, v 72, 1469-1494.

Wanless, H.R. and Weller, J.M., 1932. Correlation and extent of Pennsylvanian cyclothems. Geological Society of America Bulletin, v 43, 1177-1206.

Watkins, K.D., 1986. Calcareous nannofossil paleoceanography of the Cretaceous Greenhorn Sea. Geological Society of America Bulletin, v 97, 1239-1249.

Weimer, R.J., 1984. Relation of unconformities, tectonics, and sea-level changes, Cretaceous of Western Interior, U.S.A. In, J.S. Schlee (ed.), Interregional unconformities and hydrocarbon accumulation. American Association of Petroleum Geologists Memoir 36, 7-35.

Whiteaves, J.F., 1895. Some of the Cretaceous fossils collected during Captain Palliser's explorations in British North America in 1857-1860. Proceedings and Transactions of the Royal Society of Canada, 2nd series,1,110.

Whiting, P.J., Dietrich, W.E., Leopold, L.B., Drake, T.G. and Shreve, R.L., 1988. Bedload sheets in heterogeneous sediment. Geology, v 16, 105-108.

Williams, A.T. and Caldwell, N.E., 1988. Particle size and shape in pebble-beach sedimentation. Marine Geology, v 82, 199-215.

Williams, G.D. and Stelck, C.R., 1975. Speculations on the Cretaceous paleogeography of North America. In, W.G.E. Caldwell (ed.), The Cretaceous System in the Western Interior of North America. Geological Association of Canada Special Paper 13, 1-20.

Winn, R.D. Jr., Stonecipher, S.A. and Bishop, M.G., 1984. Sorting and wave abrasion: controls on composition and diagenesis in Lower Frontier Sandstones, southwestern Wyoming. American Association of Petroleum Geologists Bulletin, v 68, 268-284.

Wright, V.P., 1989. Paleosols in deltaic sequences. In, Paleosols in siliclastic sequences. PRIS Short Course Notes, 001, Reading University, 70-79.

Wright, R., Katzman, D., Montz, M.J. and Zech, R.S., 1989. Coastal and shallow marine cyclicity. In, D. Nummedal and R. Remy (eds.), Cretaceous shelf sandstones and shelf depositional sequences, Western Interior Basin, Utah, Colorado and New Mexico. American Geophysical Union Field Trip Guidebook T119, 25-33.

Worsley, T.R., Nance, D. and Moody, J.B., 1984. Global tectonics and eustasy for the past 2 billion years. Marine Geology, v 58, 373-400.

Zenkovitch, V.P., 1967. Processes of coastal development. Oliver and Boyd, London, 738p.

Zingg, T., 1935. Bertrag zur schotteranalyse. Schweizerische Mineralogische und Petrographische Mitteilungen, v 15, 39-140.